Twenty-sixth Engineering Mechanics Symposium

Twenty-sixth Engineering Mechanics Symposium

October 30 - October 31, 2023
Hotel Papendal, Arnhem

Graduate School on Engineering Mechanics
c/o Eindhoven University of Technology

PO Box 513, building Gemini-Zuid 4.133
5600 MB Eindhoven NL
Tel.: +31 40 2478306
E-mail: Engineering.Mechanics@tue.nl
http://www.engineeringmechanics.nl

Colophon:

Editor: R.A.M.F. van Outvorst

Publication date: October 2023

Contents

	Preface	5
1.	Program	6
2.	Koiter Lecture	10
3.	Introduction to the Workshops	13
4.	Introduction Presenters and Abstracts of Presentations	18
5.	Survey of Poster Presentations	51

Preface

The Graduate School on Engineering Mechanics, a joint initiative of the Eindhoven and Delft Universities of Technology, the University of Twente and Groningen, organizes on an annual basis the Engineering Mechanics Symposium. The aim of this symposium is to stimulate the communication and the exchange of information with respect to ongoing research in the field of Engineering Mechanics. To achieve this, the program contains a Koiter lecture by a leading expert in the field, topical sessions in relation to the selected research program of the graduate school, poster presentations of actual research projects by PhD-students and a meeting of the senior academic staff.

The Twenty-sixth Engineering Mechanics Symposium takes place October 30 - October 31, 2023 at Hotel Papendal in Arnhem. In the opening session, Prof. Ernst Rank will present a Koiter lecture entitled: "Immersed Boundary Methods: From Basic Principles to Efficient Inverse Modelling"

Furthermore, four workshops are organized that partly run plenary and partly run in parallel. Topics of this year's workshops are:

Trends and challenges in "Dynamics"
Organized by dr.ir. Gerard Verbiest (main organizer, TUD), dr. ing. Idoia Cortez Garcia (co-organizer, TU/e), dr. Dario Di Maio (co-organizer, UT), prof. dr. ir. Maryam Ghandchi Tehrani (co-organizer RUG)

Trends and challenges in "Green mechanics"
Organized by dr. Vanessa Magnanimo (main organizer, UT), dr. ir. Antonis Vakis (co-organizer RUG),dr. Alessandro Cabboi (co-organizer, TUD), dr. Paul Grassia (co-organizer, TUe)

Trends and challenges in "Advanced Discretization and Solution Techniques"
Organized dr. ir. Clemens Verhoosel (TU/e, main organizer), Dr. ir. Frits de Prenter (co-organizer, TUD),Prof. dr. ir. Harm Askes (co-organizer, UT), Dr. ir. Christobal Bertoglio (co-organizer, RUG)

Trends and challenges in "Mechanobiology"
Organized by prof. dr. ir. Erik van der Giessen (main organizer, RUG), dr. Dave Matthews (UT, co-organizer), prof. dr. ir. Olaf van der Sluis (co-organizer, TU/e), dr. ir. Nazli Tümer (TUD, co-organizer)

The workshop organizers provide plenary introductions on the trends and challenges of the workshops. Two of those plenary introductions have been included in the morning program on the first symposium day, whereas the other two have been included in the morning program of the second symposium day. Next, two of the actual workshops have been scheduled to run in parallel on the first symposium day, whereas the other two have been scheduled to run in parallel on the second symposium day. Each workshop consists of two parts, separated by a break. Each part consists of 2 presentations by AIOs/postdocs. The duration of each of the AIO/postdoc presentations is 20 minutes and followed by 10 minutes of discussion.

For the best AIO-presentation within each workshop a prize will be awarded. Winners will be announced directly before the closing of the symposium on Tuesday, October 31, 2023.

Additionally, there are two poster discussion sessions in which PhD-students and postdocs participating in the Graduate School on Engineering Mechanics present their current research project. In relation to these presentations a contest is organized in which a jury selects the best three contributions.

This year's members of the jury are:
Prof.dr.ir. Inna Gitman (UT, chairperson), Dr.ir. Payam Poorsolhjouy (TUe), Dr.ir. Pablo Drutetta (RuG), Dr. Iuri Rocha (TUD).

Winners will be announced directly before the closing of the symposium on Tuesday, October 31, 2023.
On Tuesday, October 31 a meeting of the senior academic staff participating in Engineering Mechanics takes place.

This report contains more detailed information on the Twenty-sixth Engineering Mechanics Symposium. Included are the following sections:

- Section 1: Detailed program of the symposium
- Section 2: Abstracts of the koiter lecture and introduction to the workshops
- Section 3: Abstracts of presentations in the workshops and a short introduction of the presenters
- Section 4: Survey of poster presentations

1

PROGRAM

Program 26th Engineering Mechanics Symposium

Monday and Tuesday, 30-31 October 2023

Monday, 30 October 2023		
10.00-10.30	**Registration and Informal get-together**	**Foyer 1 & 2**
10.30-12.40	**Opening Session**	**Athene room C**
10.30-10.40	Opening of the Symposium by **prof.dr.ir. Harald van Brummelen**	
10.40-11.40	Koiter lecture by **prof. Ernst Rank, Technical University of Munich**	
11.40-12.10	Trends and challenges in "Dynamics" **by dr.ir. Gerard Verbiest**	
12.10-12.40	Trends and challenges in "Green mechanics" **by dr.ir. Vanessa Magnanimo**	
12.45-13.45	**Lunch**	**Foyer 1 & 2**
13.50-14.50	**Workshops 1 and 2, part A**	
Workshop 1: Dynamics	**Athene room A**	**Workshop 2:** Green mechanics **Athene room C**
13.50-14.10 **Lars Janssen (TUe)** *Cut-Off Frequency Selection with Guaranteed Assembly Accuracy in Component Mode Synthesis*		**13.50-14.10** **Floriana Anselmucci (UT)** *Enhancing Soil Strength through Vegetation: Green Mechanics in Geotechnical Engineering*
14.20-14.40 **Jip van Tiggelen (UT)** *Challenges in simulating the forced vibration response of assembled space structures*		**14.20-14.40** **Robbert Nienhuis (RUG)** *Ocean Battery: the mechanics of a novel underwater energy storage technology*
14.50-15.50	**Poster Discussion Session I:** Presentation of current research projects, carried out by PhD students and Postdocs participating in Engineering Mechanics	**Athene room B**
15.50-16.20	**Break**	**Foyer 1 & 2**
16.20-17.20	**Workshops 1 and 2, part B**	
16.20-16.40 **Athene room A** **Ruben Guis (TUD)** *Confocal Atomic Force Microscopy*		**16.20-16.40** **Athene room C** **Enxhi Sulollari (TUD)** *Vibration-Induced Friction Force Modulation*
16.50-17.10 **Mahshad Farzannasab (RuG)** *Experimental Identification of Nonlinearity and Eigenvalue Assignment of a Nonlinear Electromagnetic System by the Receptance Method*		**16.50-17.10** **Shima Rezaie (TUe)** *Gold Decorated Carbon Nanotube for Molecular Hydrogen Storage- A First-Principles Study*
17.30-18.30	**Poster Discussion Session 2:** Presentation of current research projects, carried out by PhD students and Postdocs participating in Engineering Mechanics	**Athene room B**
18.30-19.00	Informal reception	**Foyer 1 & 2**
19.00-22.00	Dinner, including lecture by Karin Sluis	**Foyer 1 & 2**
22.00-24.00	Bar	**Dug Out**

Program 26th Engineering Mechanics Symposium

Monday and Tuesday, 30-31 October 2023

Tuesday , 31 October 2023		
08.45-09.45	**Plenary Session**	**Athene room C**
08.45-09.15	Trends and challenges in "Advanced Discretization and Solution Techniques" **by dr. ir. Clemens Verhoosel**	
09.15-09.45	Trends and challenges in "Mechanobiology" **by dr.Vito Conte**	
09.45-10.45	**Workshops 3 and 4, part A**	
Workshop 3: **Athene room C** Advanced Discretization and Solution Techniques		**Workshop 4:** **Athene room A** Mechanobiology
09.45-10.05 **Kevin Dijkstra (TUD)** *Local THB-Spline Bézier Projection*		**09.45-10.05** **Elmer Middendorp (TUe)** *Simulating Heart Valve Growth and Remodeling after the Ross Procedure*
10.15-10.35 **Robin Willems (TUe)** *An isogeometric analysis framework for ventricular cardiac mechanics*		**10.15-10.35** **Shari Gamaniel (UT)** *Tongue Equivalent Design for Tribological Assessment of Astringency in Plant Based Proteins*
10.45 -11.15	**Break**	
11.15-12.15	**Workshops 3 and 4, part B**	
Workshop3, cont'd: **Athene room C** Advanced Discretization and Solution Techniques		**Workshop 4, cont'd:** **Athene room A** Mechanobiology
11.15-11.35 **Hugo Verhelst (TUD)** Isogeometric Analysis of Wrinkling		**11.15-11.35** **Saber Shakibi (RuG)** Towards a Multiscale Model of the Brain ECM
11.45-12.05 **Reidmen Arostica Barrera (RuG)** Parameter estimation in fluid-solid interaction		**11.45-12.05** **Ebrahim Yarali (TUD)** Poisson's Ratio-Driven Bone Cell Growth in Meta-Biomaterials
12.20- 12.50	**Biezeno lecture by Dr. Björn Nijhuis**	**Athene room C**
12.50-13.00	**Prize ceremony and closure**	**Athene room C**
13.00-14.00	**Assembly of Project Leaders EM (lunch included)**	**Athene room A**
13.00-14.00	**Lunch**	**Foyer 1 & 2**

2

KOITER LECTURE

The Koiter lecture at the Twenty-sixth Engineering Mechanics symposium will be given by:

Ernst Rank

Previous distinguished keynote speakers at the Engineering Mechanics symposia were:

2022 Michael Ortiz
2021 Katia Bertoldi
2020 Ellen Kuhl
2019 Marco Amabili
2018 William Curtin
2017 Zhigang Suo
2016 Kurt Maute
2015 Stefanie Reese
2014 Anja Boisen
2013 Wolfgang Wall
2012 Roger Owen
2011 Oded Gottlieb
2010 Herbert Mang
2009 Charbel Farhat
2008 Gerhard Holzapfel
2007 Bernard Schrefler
2006 Alan Needleman
2005 Peter Wriggers
2004 Alan Grodzinsky
2003 Ole Sigmund
2002 Norman Fleck
2001 Edwin Kreuzer
2000 Ekkehard Ramm
1999 John Hutchinson
1998 Pieter Zandbergen,
Werner Schiehlen

Koiter Lecture

Immersed Boundary Methods:

From Basic Principles to Efficient Inverse Modelling

Prof. Ernst Rank

Technical University of Munich
Institute of Advanced Study

Immersing a structure in a larger body is a standard operation (typically associated with the term 'trimming') in geometric modelling. Immersing a computational in a 'fictitious domain' was suggested already in the 1960ies to approximate partial differential equations without the need for boundary conforming meshing. This principle has attracted greater attention in Computational Engineering since it was shown that Immersed Boundary Methods (IBM) can be implemented without compromising the computational accuracy compared to classical, boundary conforming finite element approximations.

This talk will begin with an introduction in the general principles of IBM and then concentrate on a specific variant, the Finite Cell Method, an efficient combination of IBM with Isogeometric Analysis and Higher Order Finite Element Methods. The coupling of numerical analysis to various types of geometric models for solid structures including phase field formulations will be shown. We will address an analysis of 'as-designed' versus 'as-built' lattice structures produced by additive manufacturing, discuss non-linear fracture problems based on computer tomograms and then extend the approach to inverse problems. As a field of application, we will focus on Ultrasonic NonDestructive Testing, where a numerical model is iteratively modified to identify defects inside a solid structure.

3

INTRODUCTION TO THE WORKSHOPS

Workshop 1
Trends and Challenges in "Dynamics"

G.J. Verbiest[1], Idoia Cortes Garcia[2], Dario Di Maio[3], Maryam Ghandchi Tehrani[4]

[1]Delft University of Technology, Department of Mechanical Engineering
[2]Eindhoven University of Technology, Department of Mechanical Engineering
[3]University of Twente, Faculty of Engineering Technology
[4]University of Groningen, Department of Mechanical Engineering

Dynamics is a fundamental field of physics and engineering with applications ranging from nanoscale chip fabrication to space exploration and from biomechanics to renewable energy. Recent trends in all these fields challenge current methods to measure, model, understand, and predict the dynamical behavior of such complex, multidisciplinary applications. In particular when aiming for extrema in amplitudes and frequencies across different length scales challenges remain, as they exhibit complex and often unpredictable behavior, requiring advanced mathematical tools and computational techniques such as AI. Moreover, advancements in materials science and control systems are driving the development of novel dynamical systems, such as soft robotics and autonomous vehicles, reshaping industries and pushing the boundaries of what is possible.

In the Dynamics workshop, we will see examples of a framework on how to reduce interconnected, high dimensional dynamical systems to reduce computational costs, experimental active vibration control for nonlinear systems, accurate stress analysis for structures under dynamic loads to be used in e.g. satellite launches, and an advanced Atomic Force Microscopy (AFM) based on confocal displacement sensing with application in high-speed AFMs.

Overall, these discussions shed light on the evolving challenges and innovative solutions in the dynamic analysis of complex systems, spanning from vibration control to computational modeling, nonlinear dynamics, and nanoscale measurements.

Workshop 2
Trends and Challenges in "Green Mechanics"

Vanessa Magnanimo[1], Alessandro Cabboi[2], Paul Grassia[3], Antonis Vakis[4]

[1]University of Twente, Faculty of Engineering Technology
[2]Delft University of Technology, Department of Mechanical Engineering
[3]Eindhoven University of Technology, Department of Mechanical Engineering
[4]University of Groningen, Department of Mechanical Engineering

Following the great attention on sustainability of the recent years, we propose a workshop on "green mechanics", to introduce the concept and explore its significance in addressing the pressing environmental challenges of our time. We will provide an overview of the key principles and methodologies that underpin this emerging field, multidisciplinary by nature, with a focus on innovative solutions in materials science and engineering where ***mechanics*** plays a key role.

In 2010 [1], the International Energy Agency identified the critical areas that should lead to the undelayable reduction of C02 emissions by 2050. The area that will have the largest impact (38%) is the so-called End-Use Energy Efficiency sector, where the aim is "doing more with less" [2]. The grand challenge of green mechanics would be to reduce this energy consumption in production and fabrication of materials and manufacts, and/or reduce their degradation, or at least achieve a better control of the production and final material performance.

To achieve the goals, the engineering community must embrace a broader, more ecologically conscious perspective and combine design, production and maintenance principles with factors such as material life cycle, energy consumption, waste reduction, and the impact of material choices on climate change. Such integrated approach poses new challenges yet has great potential: "traditional" Engineering Mechanics concepts can be exploited to develop materials and processes that exhibit improved performance characteristics while reducing their ecological footprint. The present workshop aims to reflect on the opportunity and foster a forward-thinking approach to green mechanics, that can lead to very advanced and environmentally responsible mechanical systems.

[1] IEA Energy Technology Perspectives 2010. Scenarios & Strategies to 2050. International Energy Agency, Paris, France, 2010.
[2] A. B. Lovins, Energy Efficiency, Taxonomic Overview, Encyclopedia of Energy, 2, 383-401, 2004.

Workshop 3
Trends and Challenges in " Advanced Discretization and Solution Techniques"

Harm Askes[1], Cristóbal Bertoglio[2], Frits de Prenter[3] and Clemens Verhoosel[4]

1University of Twente, Faculty of Engineering Technology
2University of Groningen, Faculty of Science and Engineering
3Delft University of Technology, Faculty of Aerospace Engineering
4Eindhoven University of Technology, Department of Mechanical Engineering

Computers have been used to solve mathematical problems rooted in science and engineering since their advent. In the context of engineering mechanics, the finite element method (FEM) and finite volume method (FVM) are prominent examples of computational methods that have enabled scientist and engineers to solve problems that were unsolvable before computers were invented. Following pioneering work on these methods in the 1960s and 1970s, FEM and FVM have found their way in virtually all branches of science and engineering. These developments have been accompanied by innovations in basically all aspects of computational techniques.

While the roots of discretization and solution techniques have matured, they have gradually evolved over the course of the decades. Improvements to these techniques pertain to both technical aspects, for example improving the accuracy or stability of the methods, and to workflow related aspects such as pre- and postprocessing, making the methods more powerful in solving real engineering problems. While some of these developments have improved the understanding of the techniques and their behavior, others have directly led to new capabilities. Even with the advanced capabilities of computational engineering software currently available, research on advanced discretization and solution techniques and the development of methods that are tailored to modern hardware remain driving forces for further innovation.

This engineering mechanics symposium gives a comprehensive overview of ongoing trends and challenges in advanced discretization and solution techniques. The Koiter lecture has a focus on the Finite Cell method, a higher-order finite element method for complex geometries, capable of dealing with engineering problems of tremendous complexity. In the workshop presentations, we will see other examples of innovations in discretization and solution techniques, in the form of an inverse solver for fluid-structure interaction problems, and the application of isogeometric analysis – a CAD-based finite element method – to a range of problems

Workshop 4
Trends and Challenges in " Biomechanics "

Vito Conte[1]

[1]Eindhoven University of Technology (TU/e), Department of Biomedical Engineering
[1]Institute for Complex Molecular Systems (ICMS), TU/e

Over the past few decades, we have witnessed an extraordinary transformative process of crossbreeding between the disciplines of Physics, Engineering, and Biology. This process has empowered the development of cutting-edge technologies to quantify the kinematics, rheology, and dynamics of living cells across various scales. These scales span from the molecular and subcellular levels (traditionally within the scope of Biophysics), to the cellular and supracellular levels (traditionally within the domain of Mechanobiology) and extend up to the tissue, organ, and body scales, (traditionally within the realm of Biomechanics).

At the heart of Mechanobiology lies a fundamental premise: not only do living cells function as miniature biochemistry laboratories but they also work as tiny complex mechanical machines. These machines have dynamic material properties and can move by exerting, sustaining, and transmitting forces with their microenvironment and between themselves. In this talk, I will therefore quickly touch on the core mechanobiological paradigm of "mechanoreciprocity", which embraces the concepts of cellular: i) mechano-sensing; ii) mechano-transduction; iii) mechano-response; and iv) mechano-adaptation. In the context of these fundamental concepts, I will illustrate some of the main trends and challenges that, in my view, are driving research in the field of Mechanobiology. As a relatively new field, we are just beginning to comprehend how we can leverage the ever increasing bulk of mechanobiological scientific knowledge to manipulate the kinematics and dynamics of individual cells in a controlled and predictive way. Ultimately, our aim is to be able to rationally design tissues, organs, and entire organisms as we do with constructions and machines. Simultaneously, we are also only beginning to explore ways to employ cell mechanics as a tool to hinder or halt the progression of diseases that exploit these mechanobiological processes for their development and advancement.

In this context, my talk will move to sketch an overview of the efforts ongoing in the field of mechanobiology at the four universities organising and promoting this event. By briefly showcasing the specific case studies featuring representative researchers from each of these institutions, I will set the stage for each researcher to follow up and illustrate how they are specifically spearheading their pioneering research efforts.

I will conclude with a provocative refined definition of the discipline of Mechanobiology that prescinds from history and biological scales by presenting the discipline simply as Mechanical Biology – as opposed to Biomechanics and Biophysics intended as Biological Mechanics and Biological Physics respectively.

4

INTRODUCTION PRESENTERS

AND

ABSTRACTS OF PRESENTATIONS

Workshop 1

“Dynamics”

Cut-Off Frequency Selection with Guaranteed Assembly Accuracy in Component Mode Synthesis

Lars A. L. Janssen[1*], Rob H.B. Fey[1], Bart Besselink[2], Nathan van de Wouw[1]

[1]Eindhoven University of Technology, Department of Mechanical Engineering
[2]University of Groningen, Bernoulli Institute for Mathematics, Computer Science and Artificial Intelligence
[*]e-mail l.a.l.janssen@tue.nl

Finite Element models of complex engineering systems often consist of millions of degrees of freedom which makes their usage for, e.g., design and control applications, unfeasible. In component mode synthesis techniques, the total (assembly) model is subdivided in multiple components models which are reduced in complexity and coupled to obtain a computationally feasible reduced-order assembly model.

In the structural dynamics community, it is common practice to reduce the complexity of assembly models by preserving all eigenmodes of the component models with an eigenfrequency lower than a single “cut-off frequency”. This cut-off frequency is generally selected between two or three times the maximum frequency of interest for the model’s application. However, the resulting accuracy of the reduced-order assembly model is based on the engineer's experience in selecting the cut-off frequency.

In this presentation, we introduce a mathematical approach that allows for the computation of cut-off frequencies for each component individually, given accuracy requirements on the reduced-order assembly model. We show that: 1) the required accuracy of the obtained reduced-order assembly model is guaranteed, and 2) this model contains much less degrees of freedom compared to the industrial standard approach, which results in significantly reduced computational costs associated to the usage of the model.

Abstract title: Cut-Off Frequency Selection with Guaranteed Assembly Accuracy in Component Mode Synthesis.

Workshop: Dynamics

L.A.L. Janssen (Lars)

Eindhoven University of Technology,
Department of Mechanical Engineering

Promotor: Nathan van de Wouw
Co-promotors: Rob H.B. Fey, Bart Besselink

Biography and description of research:
Graduate School on Engineering Mechanics. Graduate School on Engineering Mechanics. Graduate School on Engineering Mechanics. Graduate School on Engineering Mechanics. Graduate School on Engineering Mechanics. Graduate School on Engineering Mechanics. Graduate School on Engineering Mechanics. Graduate School on Engineering Mechanics.

Graduate School on Engineering Mechanics. Graduate School on Engineering Mechanics. Graduate School on Engineering Mechanics. Graduate School on Engineering Mechanics. Graduate School on Engineering Mechanics. Graduate School on Engineering Mechanics. Graduate School on Engineering Mechanics. Graduate School on Engineering Mechanics.

Challenges in simulating the forced vibration response of assembled space structures

UNIVERSITY OF TWENTE.

J. van Tiggelen, M.H.M Ellenbroek, B. Rosic, D. Di Maio

University of Twente, Department of Mechanics of Solids, Surfaces and Systems,
P.O. Box 217, 7500 AE Enschede
phone +31534895444, e-mail j.vantiggelen@utwente.nl

To improve the reliability of the machines we design, we need to be more accurate in performing the stress analysis for structures under dynamic loads. For example, think of satellites which need to survive the demanding launch conditions on the way to their final orbit. This requires accurate predictions of the system's dynamics for the dynamic load levels the structure will typically experience in operating conditions. One of the root causes of poor simulations can be identified in the jointed interfaces between the components of system assemblies. Every interface contributes to the forced vibration response by an intrinsic nonlinearity (i.e. friction, nonlinear stiffness, play) and the nonproportional (non-uniform) distribution of damping generated at the interfaces. Being able to model and simulate these nonlinearities is paramount for obtaining accurate, predictive models.

In this presentation an example is presented of how challenging can be the validation of system responses when a product must be certified before being commissioned for a launch or flight. Several divisions of industry dealing with dynamic models and simulations of forced vibrations are discovering how the nonlinear dynamics of joints can lead to inaccuracies in the simulated vibration responses, mainly due to the nonlinear relationships of frequency and damping with the vibration amplitude (which is high for qualification tests). Hence, the example discussed in this presentation refers to analysis of test data gathered from a satellite solar array in qualification tests. It is shown how dissimilar simulated and measured vibration data can be, and how the qualification levels enhance the nonlinear dynamics, often not predicted by dynamic models. Finally, it presents an effort to analyse a cut-out of the solar array in terms of frequency and damping nonlinearity.

Abstract title: Challenges in simulating the forced vibration response of assembled space structures

Workshop: Dynamics

Tiggelen, J. van (Jip)

University of Twente,
Department of Mechanics of Solids, Surfaces and Systems

Advisor: Prof.dr.ing. B. Rosic
Co-advisor: Dr. D. Di Maio

Biography and description of research:
Jip van Tiggelen is a first-year PhD candidate in the Applied Mechanics and Data Analysis chair at the University of Twente. His research focuses on the nonlinear effect that bolted joints have on the forced vibration response of assembled structures. In this project, both numerical and experimental approaches are employed for a better understanding of the relation between vibration amplitude, joint stiffness and friction generated in joints. The goal is to create and validate predictive models that can be used for obtaining the stress levels experienced by system assemblies under dynamic conditions.

Jip received his BSc (2020) and MSc (2022) in Mechanical Engineering from the University of Twente. He completed his MSc with a research project on the nonlinear dynamics of satellite solar arrays, which was conducted in collaboration with Airbus Netherlands.

Confocal Atomic Force Microscopy

Ruben Guis[1], M.U. Arabul[2], Z. Zhou[2], and G.J. Verbiest[1]

[1]Delft University of Technology, Mekelweg 2, Delft, 2628CD, Netherlands,
[2]ASML Netherlands B.V., De Run 6501, Veldhoven, 5504DR, Netherlands
E-mail of presenting author: R.H.Guis@tudelft.nl

Atomic Force Microscopy (AFM) has revolutionized our ability to image and manipulate matter at the nanoscale, and study the mechanical and physical properties of materials and systems at the molecular level playing a crucial role in numerous scientific fields, including materials science, biophysics, and nanotechnology. Fast and accurate measurements of small displacements in the nanometer range of AFM cantilevers is essential for such applications.

Optical detection methods have emerged as powerful tools for measuring the displacements of AFM cantilevers with high sensitivity and resolution. To measure the deflection of AFM cantilevers, usually an optical beam deflection system is used. However, optical beam deflection systems have a limited detection bandwidth of ~10MHz, because of the weighted sum taken of a 4-quadrant photodetector [1]. Another way to detect these displacements is using an interferometer [2]. However, to accurately measure quasi-static displacements with an interferometer, the position of the reference mirror and the laser wavelength should be kept extremely stable. Therefore, this method is rarely used in AFM.
To overcome the limitations of optical beam deflection systems and interferometers, we propose to use confocal displacement sensing to detect the cantilever deflection in AFM (see Figure). This method is based on purely geometrical optics. Moreover, the deflection signal can be captured on a single photodetector, hence the speed of detection is set by the photodetector bandwidth. Since confocal displacement sensing only needs a single photodetector, its detection bandwidth theoretically can go up to the GHz regime. This shows the potential for using confocal displacement sensing in high-speed AFMs as well.
In our work, we show and experimentally verify a model for the sensitivity of such a confocal system. Sensitivities similar to an optical beam deflection system or an interferometer can be reached [3]. Finally we use confocal displacement sensing in an AFM and show that it can be used to make a regular contact mode AFM image of a calibration grating.

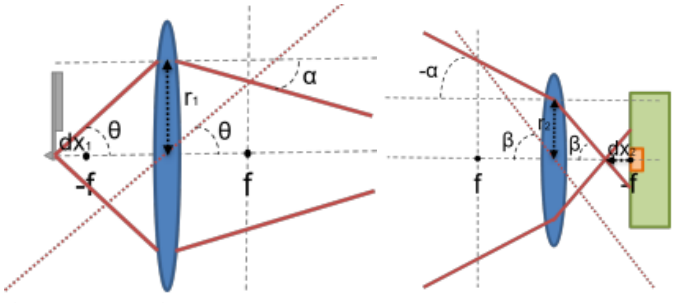

Schematic of the working principle

References:

1. https://www.zhinst.com/europe/en/blogs/what-it-takes-high-speed-afm-measurements
2. Andreeva, N. V. (2018). Atomic force microscopy with interferometric method for detection of the cantilever displacement and its application for low-temperature studies. *Ferroelectrics*, *525*(1), 178–186.
3. Siebert, M. et al. (2022). Modeling of fiber-coupled confocal and interferometric confocal distance sensors. *Measurement Science and Technology*, *33*(7).

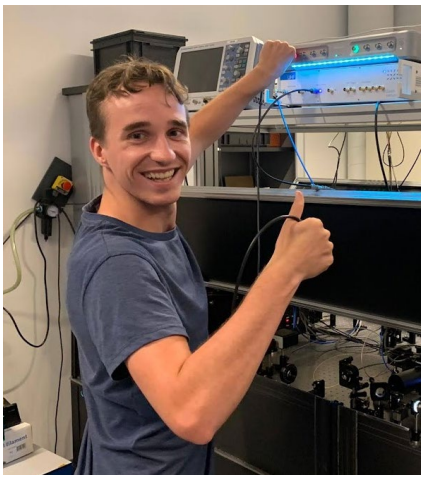

Abstract title: Confocal Atomic Force Microscopy

Workshop: Dynamics

Guis, R.H. (Ruben)

Delft University of Technology,
Department of Precision and Microsystems Engineering

Advisor: Prof.dr. P. Steeneken
Co-advisor: Dr. G. Verbiest

Biography and description of research:
Ruben Guis obtained his master's degree in Physics at Leiden University, Netherlands in 2020. For his thesis project he worked towards 3D imaging at nanoscale by attempting to measure the subsurface information using resonant hydrogen spins in Magnetic Resonance Force Microscopy.

Started in October 2020, Ruben is now doing his Ph.D. in the Precision and Microsystem Engineering department at Delft University of Technology, Netherlands, where he is further investigating 3D imaging at nanoscale; this time using ultrasound to get the subsurface information, by integrating acoustics at nanoscale into Atomic Force Microscopy.

Experimental Identification of Nonlinearity and Eigenvalue Assignment of a Nonlinear Electromagnetic System by the Receptance Method

Mahshad Farzannasab[1*] Maryam Ghandchi Tehrani[1]
[1] Engineering and Technology Institute Groningen (ENTEG), University of Groningen, Groningen, The Netherlands

In this study, active vibration control for eigenvalue assignment of a nonlinear system is presented experimentally using the receptance method. To achieve this, an experimental setup was constructed with a cantilever beam. A loudspeaker and an accelerometer were attached to the beam in order to create force and measure the acceleration of the beam. The free end of the beam was connected to a pair of identical neodymium bromide magnets, and two identical coils were placed parallel to the magnets. When the electrical current in the coils was turned on, the magnetic field created around the beam could introduce cubic stiffness into the mathematical model of the system, which was the reason for nonlinearity in the system. To identify the existing nonlinearity experimentally, a step-sine test was performed over a frequency range of 1 to 160 Hz, with steps of 1 Hz and an interval duration of 6 seconds, at four different amplitudes, both with the electrical currents switched on and switched off. In the next step, the Frequency Response Functions (FRFs) of the fundamental harmonics at all amplitudes are compared with each other. In cases of nonlinearity, the system's response would definitely change with variations in the amplitude of the input voltage.

For eigenvalue assignment, the receptance of the open-loop is first measured experimentally. Then, the Sherman-Morrison formula is used to calculate the feedback gains. During this step, the desired closed-loop poles were determined through curve fitting of the measured data. Since, unlike linear systems, the response of nonlinear systems depends on both amplitude and frequency, an iterative Sherman-Morrison algorithm is developed to calculate the feedback gains for eigenvalue assignment. Finally, the control gains obtain from the simulation are experimentally implemented in real-time, demonstrating successful pole assignment. The system remains stable at various excitation levels and different distances between the coils and magnets.

Abstract title: Experimental Identification of Nonlinearity and Eigenvalue Assignment of a Nonlinear Electromagnetic System by the Receptance Method.

Workshop: Dynamics

Farzannasab, M. (Mahshad)

Groningen University of Technology, Department of Dynamics and Vibration

Advisor: Prof.dr. Maryam Ghandchi Tehrani

Biography and description of research:
Mahshad earned both her bachelor's and master's degrees in Iran, with a particular emphasis on control techniques during her master's thesis. Currently pursuing a Ph.D. at the University of Groningen within the Department of Dynamics and Vibration, Mahshad's research centers on the active vibration control of nonlinear systems. Her work delves deeply into pole placement strategies in nonlinear structures to mitigate resonance effects.

Workshop 2

“Green Mechanics”

Enhancing Soil Strength through Vegetation: Green Mechanics in Geotechnical Engineering

UNIVERSITY OF TWENTE.

F.A.R. Anselmucci

University of Twente, Department of Construction Management and Engineering, Chair of Soil Micro Mechanics
P.O. Box 217, 7500 AE Enschede,
phone +31 534896233, e-mail f.a.r.anselmucci@utwente.nl

The interaction between vegetation and soil mechanics is gaining interest due to the demand for sustainable and eco-friendly solutions in engineering practices.
Vegetation's influence extends beyond erosion mitigation; it significantly augments the overall strength and stability of soil structures. This synergy between plants and soil offers innovative approaches to address critical challenges in geotechnical engineering, including slope stability, embankment design, and foundation engineering. As vegetation takes root in the soil, it initiates a series of transformations that affect soil structure, moisture dynamics, and mechanical behavior, ultimately influencing overall soil strength.

In the talk we will see how vegetation's impact on soil is not limited to increased shear strength; it also plays a pivotal role in delaying the attainment of peak shear strength, it increases the water retention properties of the soil, and contributes to soil consolidation. Specifically, we will elucidates how the fibrous network created by plant roots reinforces the soil matrix. Root growth can induce volumetric expansion in dense soils before shear failure, effectively redistributing stresses and delaying shear failure, ultimately contributing to improved soil stability. Finally, because vegetation's influence extends to soil moisture content through transpiration and evapotranspiration processes, experimental results will be presented to show how vegetation improves the water retention capabilities of the soil.
Understanding this eco-mechanical interaction is crucial, with implications extending to agriculture, land management, infrastructure design, and environmental conservation.

This abstract represents our exploration of green mechanics in soil mechanics, uncovering how vegetation imparts its strength to the soil mechanics and detailing the research conducted at the University of Twente.

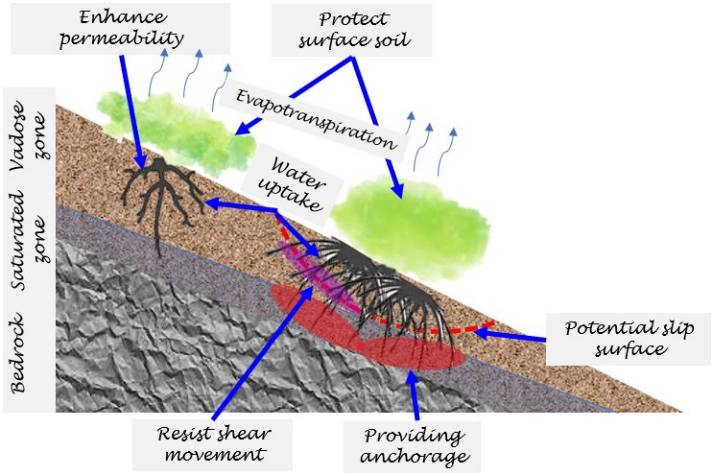

Figure 1 The research presented emphasizes vegetation's role in enhancing the hydro-mechanical strength of soil, particularly in the context of geotechnical engineering.

Abstract title: Enhancing Soil Strength through Vegetation: Green Mechanics in Geotechnical Engineering

Workshop: Green Mechanics

Anselmucci, F.A.R. (Floriana)

University of Twente,
Department of Construction Management and Engineering

Advisor: Prof.dr. Vanessa Magnanimo
Co-advisor: Dr. Hongyang Cheng

Biography and description of research:
Floriana Anselmucci is currently a Postdoctoral Researcher affiliated with the Soil Micro Mechanics group at the University of Twente. She completed her undergraduate and master's degrees at the University of Calabria in Italy, followed by her attainment of a Ph.D. from the University of Grenoble Alpes in France in 2020. Additionally, Floriana's academic journey has been enriched by international experiences as she has had the privilege of being a visiting researcher at both the James Hutton Institute in the United Kingdom and the Georgia Institute of Technology in the United States.

Her research is centered around the fields of bio-mediated and bio-inspired engineering, with a primary focus on understanding the impact of vegetation on soil hydro-mechanical responses. During her doctoral studies, Floriana pioneered a groundbreaking protocol for observing the dynamic, four-dimensional evolution of plant roots within soil using advanced X-ray tomography techniques. This allowed her to precisely quantify the influence of vegetation on soil mechanical properties.
Currently, Floriana is conducting research at the University of Twente, where she is investigating the hydro-mechanical properties of the vadose zone. Her work involves evaluating how vegetation affects the stability and properties of partially saturated soil. Additionally, she is actively engaged in research related to quantifying soil reinforcement using cutting-edge imaging processing technologies, as well as Digital Image Correlation (DIC) methods.

Ocean Battery: the mechanics of a novel underwater energy storage technology

Robbert M. Nienhuis

University of Groningen

The Ocean Battery is an underwater pumped-hydro storage (PHS) device that can be deployed in offshore and onshore energy farms to deal with the intermittency of renewable resources. While sharing many of the components and features of conventional PHS, namely the hydraulics, pumps and turbines, distinguishing features such as a buried rigid reservoir and a submerged flexible one generate interesting research challenges in the mechanics domain. Examples are the dynamic deformation of the bladder of the flexible reservoir under current and wave loading in offshore environments, the effects of biofouling on its performance, as well as the stability of the buried rigid reservoir and the soil surrounding it under cyclic loading. The presentation will give an overview of the technology as well as the research performed at the University of Groningen to address some of these challenges.

Abstract title: Ocean Battery: the mechanics of a novel underwater energy storage technology

Workshop: Green mechanics

Nienhuis, R.M. (Robbert)

University of Groningen, Faculty of Science and Engineering, Computational Mechanical and Materials Engineering

Advisor: Prof. dr. Antonis Vakis
Co-advisor: prof. dr. ir. Bayu Jayawardhana
.

Biography and description of research:
Robbert Nienhuis is a PhD candidate in the Engineering and Technology institute Groningen at the University of Groningen. He has a Master in Industrial Engineering from the University of Groningen and a background in FEM analysis and design optimization. Within the DOSTA project his work focuses on developing predictive models for a novel offshore pumped hydro energy storage system. In addition to his academic research, he is also working for the Ocean Grazer Company where he further focuses on the development of the Ocean Battery in the industrial sector.

The Ocean Battery is an underwater pumped-hydro storage (PHS) device that can be deployed in offshore and onshore energy farms to deal with the intermittency of renewable resources. While sharing many of the components and features of conventional PHS, namely the hydraulics, pumps and turbines, distinguishing features such as a buried rigid reservoir and a submerged flexible one generate interesting research challenges in the mechanics' domain. Examples are the dynamic deformation of the bladder of the flexible reservoir under current and wave loading in offshore environments, the effects of biofouling on its performance, as well as the stability of the buried rigid reservoir and the soil surrounding it under cyclic loading. The presentation will give an overview of the technology as well as the research performed at the University of Groningen to address some of these challenges.

Vibration-Induced Friction Force Modulation

E Sulollari[1], K van Dalen[2], A Cabboi[1]

[1]Mechanics and Physics of Structures, Department of Engineering Structures, Faculty of Civil Engineering and Geosciences, TU Delft, Netherlands.

[2]*Dynamics of Solids and Structures, Department of Engineering Structures, Faculty of Civil Engineering and Geosciences, TU Delft, Netherlands.*

Applying an oscillatory load is one of the most efficient ways to alter friction forces. Several theoretical and experimental studies on the influence of oscillatory loads on friction have been conducted, investigating the effect of both in-and out-of-plane oscillations for different tribological pairings and ranges of oscillation amplitudes, frequencies, and sliding velocities. However, the effect of external load on the frictional property has been studied with an emphasis on dynamic loads characterized by a high-frequency content, while a clear statement as to what is considered high-frequency is still missing. The common method of analysis for high-frequency is the method of direct separation of motion (MDMS). However, when studying the effect of a general sinusoidal excitation on friction by means of the MDMS, the analytical solutions become cumbersome or even impossible to obtain. Therefore, this study aims to show that, in case of continuous slip, a general relation, regardless of the frequency range, accounting for the induced effect of excitation on friction, can be easily obtained by utilizing the velocity response function of the system. This general relation holds for single and multi degree of freedom systems and can also be used to identify the stick-slip boundaries. Moreover, through the velocity response function, the influence of different external harmonic forces in terms of phase, excitation frequency, system characteristics and the choice of the normal contact force expression is investigated. This work also presents the effect of excitation on friction for systems with nonlinear contact properties. To analyze the nonlinear system, numerical methods and stability analysis are performed. It is shown that the application of the external excitation in a system with nonlinear contact properties can lead to both stability or instability. The effect of excitation on friction is applied to a classical mass-spring-dashpot system on a moving belt, and Amontons-Coulomb law is be considere

Picture

Abstract title: Vibration-Induced Friction Force Modulation

Workshop: Green mechanics

Sulollari, E. (Enxhi)

Delft University of Technology,
Department of Engineering Structures

Advisor: Prof.dr.
Co-advisor: Dr.

Biography and description of research:
Enxhi completed her bachelor's degree in Civil Engineering at Middle East Technical University. In 2017, she joined TU Delft to pursue her master's studies in Structural Engineering and graduated with a thesis titled "Study of nonlinear dynamic soil response to harmonic excitation using semi-analytical and numerical methods". She then worked as a structural engineer focusing on assessing the seismic performance and safety of masonry structures. In 2021, she re-joined TU Delft as a PhD candidate. Enxhi is currently studying the effect of applied oscillatory forces on altering friction forces for different types of contact configurations, including the effect of micro- and macrostructure and system dynamics. Most of the research activity consists in developing different mathematical and numerical models to quantify the effect of vibration on friction forces, combined with tailored experiments to validate such models, aiming to scale up the technique for industrial applications.

Gold Decorated Carbon Nanotube for Molecular Hydrogen Storage- A First-Principles Study

Shima Rezaie[1]*, Azahara Luna Triguero[1]

[1] *Eindhoven University of Technology, Dept. of Mechanical Engineering, Energy Technology, 5612 AP Eindhoven, Netherlands.*

** s.rezaie@tue.nl*

Abstract

The permanent use of fossil fuels has many consequences, including depletion of energy resources and negative environmental impacts. In this context, hydrogen has been introduced as a promising substitute for reducing the dependence on fossil fuels. However, using hydrogen as a fuel requires finding a convenient and cost-effective way to produce, store and deliver it. In this regard, carbon nanostructures have aroused the interest of researchers due to their high surface area, good chemical stability, low mass density, and rich pore volume. Despite these pros, bare carbon nanostructures have represented low hydrogen storage capacity at ambient temperature. Surface modification can be a promising approach to increase hydrogen adsorption capacity significantly. According to the obtained results, the addition of gold doping has a positive effect on the average binding energy, volumetric, and gravimetric capacity.

Abstract title: Gold Decorated Carbon Nanotube for Molecular Hydrogen Storage- A First-Principles Study

Workshop: green mechanics

Rezaie, S. (Shima)

Eindhoven University of Technology,
Department of Mechanical Engineering

Supervisor(s): Dr. Azahara Luna-Triguero/ Prof. David M.J. Smeulders

Biography and description of research:

Shima Rezaie received her master's degree in electrical engineering from K. N. Toosi University of Technology (KNTU), Tehran, Iran, in 2020. She is currently a PhD student in the group of Energy Technology at the Department of Mechanical Engineering at Eindhoven University of Technology (TU/e).

Her PhD topic focuses on the identification of porous materials with high potential for hydrogen storage applications. Moreover, modification of crystalline porous materials to improve their hydrogen storage capacity. She uses DFT and Monto Carlo-based simulations to investigate the operating conditions of porous materials.

Her research interests include simulation and fabrication of micro- or nanostructured materials, energy, and design and fabrication of micro- or nano-electronic devices.

Workshop 3

“Advanced Discretization and Solution Techniques”

Local THB-Spline Bézier Projection

K. Dijkstra D. Toshniwal

Delft Institute of Applied Mathematics, Delft University of Technology,
Mekelweg 4, 2628 CD, Delft, Netherlands
phone +31-610843814, e-mail k.w.dijkstra@tudelft.nl

In Isogeometric Analysis, the use of adaptive splines allows for significant savings when capturing solutions or approximating geometries with localized features. One such adaptive spline methodology that is popular for its simple implementation and attractive properties is that of Truncated Hierarchical B-splines (THB-splines) [1]. In this talk we will present a local THB-spline projector that is an extension of the Bézier projector introduced in [2].
The latter consists of two steps: an initial L2 projection on every element, and a global reconstruction step where these local projections are combined to form a final global smooth spline. The first step utilizes local linear independence of B-splines on each element. The property of local linear independence on every element is missing for THB-splines. Then, under assumptions on the mesh, we show that there exist collections of mesh elements such that the set of THB-splines with support on these collections are linearly independent over these collections. These collections are local in the sense that the elements in them are adjacent and their number depends only on the spline degree.

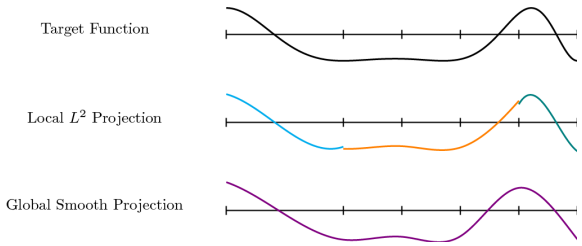

Figure 1: The THB-spline Bézier projector applied to the target. An initial local L2 projection followed by a smoothing to construct a global spline.

The above allows us to formulate a Bézier projector for THB-splines. Optimal convergence is shown and we compare our Local THB-spline Bézier projector with [3]. Lastly, an adaptive refinement strategy is introduced to produce meshes that conform to our assumptions and a comparison with [3] is made.

[1] C. Giannelli, B. Jüttler, and H. Speleers, "THB-splines: The truncated basis for hierarchical splines," *Comput. Aided Geom. Des.*, vol. 29, no. 7, pp. 485–498, Oct. 2012, doi: 10.1016/j.cagd.2012.03.025.
[2] D. C. Thomas, M. A. Scott, J. A. Evans, K. Tew, and E. J. Evans, "Bézier projection: A unified approach for local projection and quadrature-free refinement and coarsening of NURBS and T-splines with particular application to isogeometric design and analysis," *Comput. Methods Appl. Mech. Eng.*, vol. 284, pp. 55–105, 2015, doi: 10.1016/j.cma.2014.07.014.
[3] A. Giust, B. Jüttler, and A. Mantzaflaris, "Local (T)HB-spline projectors via restricted hierarchical spline fitting," *Comput. Aided Geom. Des.*, vol. 80, p. 101865, 2020, doi: https://doi.org/10.1016/j.cagd.2020.101865.

Abstract title: Local THB-Spline Bézier Projection

Workshop: Advanced Discretization and Solution Techniques

Outvorst, van R.A.M.F. (Rachel)

Delft University of Technology
Delft Institute of Applied Mathematics

Advisor: Dr. D. Toshniwal
Co-advisor: Prof.Dr. C. Vuik

Biography and description of research:
I am a first year PhD student at the TU Delft. I finished my Masters in 2022 in Numerical Analysis at the TU Delft after doing a double Bachelor in Applied Mathematics and Applied Physics.

I am researching variational multiscale stabilization for the magnetohydrodynamics equations. These equations describe electric conducting fluids which can for example be found in nuclear fusion reactors. These equations can be seen as a combination of Navier-Stokes and Maxwell, and hence are also unstable for high Reynolds numbers. In addition, in order to resolve local detail, I want to use THB-splines, such that the mesh can locally refined.

An isogeometric analysis framework for ventricular cardiac mechanics

R. Willems

University of Technology, Department of Mechanical Engineering,
Multiscale Engineering Fluid Dynamics, P.O. Box 000
phone +31-638614010, e-mail r.willems@tue.nl

The finite element method (FEM) is commonly used in computational cardiac simulations. For this method, a mesh is constructed to represent the geometry and, subsequently, to approximate the solution. To accurately capture curved geometrical features many elements may be required, possibly leading to unnecessarily large computation costs. Without loss of accuracy, a reduction in computation cost can be achieved by integrating geometry representation and solution approximation into a single framework using the Isogeometric Analysis (IGA) paradigm. In this study, we propose an IGA framework suitable for low-resolution image data of cardiac mechanics, where we show the advantageous properties of smooth splines through the development of a multi-patch anatomical model. A nonlinear cardiac model is discretized following the IGA paradigm, meaning that the spline geometry parametrization is directly used for the discretization of the physical fields. The IGA model is benchmarked with a state-of-the-art biomechanics model based on traditional FEM. For this benchmark, the hemodynamic response predicted by the high-fidelity FEM model is accurately captured by an IGA model with only 320 elements and 4,700 degrees of freedom. The study is concluded by a brief anatomy-variation analysis, which illustrates the geometric flexibility of the framework. The IGA framework can be used as a first step toward an efficient workflow for an improved understanding of, and clinical decision support for, the treatment of cardiac diseases.

Abstract title: An isogeometric analysis framework for ventricular cardiac mechanics

Workshop: Advanced Discretization and Solution Techniques

Willems R. (Robin)

Eindhoven University of Technology,
Department of Mechanical Engineering

Advisor: Dr.ir. C.V. Verhoosel
Co-advisor: Prof.dr. O. van der Sluis

Biography and description of research:
Robin Willems (1996) obtained his BSc-degree and MSc-degree (with honors) in Mechanical Engineering in 2018 and 2020 respectively, at the Eindhoven University of Technology (TU/e). During his study, his interest has been in the application of advanced numerical methods and interdisciplinary collaboration. In 2019, he did his internship at VDL ETS (Enabling Transport Solutions) in Valkenswaard, where he investigated the thermal losses during the operation of city-bus doors using turbulence models. In the subsequent year, in 2020, he did his graduation centered on the thermofluid interaction within an axial-flux permanent magnet machine. This work was conducted in collaboration with the Electrical Engineering department and it featured the utilization of isogeometric analysis techniques.

Since 2020, Robin works as a doctoral candidate at the TU/e where he collaborates with the Biomedical Engineering department to enhance the numerical computation of cardiac mechanics using advanced numerical methods. His focus is on the isogeometric analysis to facilitate a more robust connection between geometry and computation. The work is part of a multidisciplinary team (combatvt.nl) dedicated to gain an understanding of the mechanisms underlying heart rhythm disorders through the use of (data-driven) numerical models.

Isogeometric Analysis of Wrinkling

H. M. Verhelst

Wrinkling is a phenomenon all around us. Besides being well-known in the context of cosmetics, wrinkling of membranes is a structural instability studied in multiple disciplines. From nanometer scale when studying the influence of wrinkles on the properties of graphene to kilometer scale when studying the influence of wrinkling on the structural stability of very large floating structures. From the aerospace for solar sails and space antennas, to the airspace for parachutes. From biomedical sciences studying wound healing to biological sciences studying brain morphology.

Since structural instabilities such as wrinkling are highly dependent on geometry as well as geometric imperfections, the role of the geometric description in computer simulations plays an important role. Therefore, isogeometric thin shell analysis provides an important tool in the analysis of the wrinkling phenomenon. Despite the momentum in isogeometric analysis in structural mechanics, wrinkling modeling remains a challenging topic, from the aspect of multi-scale analysis and the existence of multiple solution branches in the post-wrinkling regime.

This talk highlights the latest developments in the isogeometric analysis of wrinkling. It will provide a broad overview of the state-of-the-art of wrinkling modeling and applications, and it will present novel methods related to hyperelastic wrinkling modeling with isogeometric analysis, mesh adaptivity and complex domain modelling.

Delft University of Technology, Department of Maritime and Transport Technology Engineering,
Delft University of Technology, Delft Institute of Applied Mathematics,
email: h.m.verhelst@tudelft.nl

Abstract title: Isogeometric Analysis of Wrinkling

Workshop: Advanced Discretization and Solution Techniques

Verhelst, H.M. (Hugo)

Delft University of Technology, Department of Maritime & Transport Technology and Delft Institute of Applied Mathematics

Advisor: Dr. M. Möller
Co-advisor: Dr. ir. J.H. Den Besten

Biography and description of research:
Hugo started as a student at TU Delft in 2013, and obtained his Bsc. in Maritime Technology cum laude and with honours in 2016. In 2019, he obtained a double MSc. degree in Applied Mathematics (cum laude) andin Maritime Technology (cum laude and with honours) from the same university. Between 2019 and 2023, he conducted his PhD research in the department of Maritime and Transport Technology and in the Delft Institute of Applied Mathematics, with regular research visits to Inria Sophia-Antipolis and the University of Florence. In November 2023, he will start as a post-doctoral researcher at the University of Florence, with a guest position at the Maritime Transport and Technology department at TU Delft.

Hugo just submitted his PhD Thesis on “Isogeometric Analysis of Wrinkling”. His research is about the computational mechanics of thin-walled structures, with special focus on instabilities as seen in membrane wrinkling. Through isogeometric analysis, his research relates to applied geometry and continuum mechanics of shells. From a mechanics point of view, he focused on constitutive models for thin isogeometric shells with the application to membrane wrinkling. On the other hand, from the applied geometry point of view,he focused on adaptive meshing and smooth spline basis constructions. Throughout his PhD research, Hugo contributed extensively to the “Geometry + Simulation Modules” library, where he is currently main developer for the modules related to mechanics and unstructured spline constructions.

Parameter estimation in fluid-solid interaction

R. Aróstica, D. Nolte, C. Bertoglio

University of Groningen, Bernoulli Institute for Mathematics, Computer Science and Artificial Intelligence, Nijenborgh 9, 9747AG, Groningen
phone +31-503632925, e-mail r.a.arostica.barrera@rug.nl, d.j.nolte@rug.nl, c.a.bertoglio@rug.nl

Parameter estimation in the heart has been done so far using measurement in myocardium, typically using displacement surrogates obtained from Magnetic Resonance Imaging (MRI) [1, 2]. Nevertheless, blood flow velocity measurements are routinely acquired in clinical practice and can be directly compared with the computed flow velocities if fluid-solid interaction models are used. To the best of the authors knowledge, inverse problems in cardiac mechanics using "velocity images" of the fluid flow have remained unexplored, especially since fully coupled 3D models of both solid and fluids are challenging mathematically, algorithmically and computationally.
In this talk, we will tackle this challenge by combining state of the art fluid-solid interaction forward and inverse methods to present the first results on estimating constitutive and boundary condition parameters in the cardiac muscle, using fluid flow velocity measurements. For the forward solver, we propose a semi-implicit fluid-solid coupling approach based on a unconditionally-stable fractional step method for the fluid in ALE form [3]. The inverse solver is based on a Reduced Order Unscented Kalman Filter [4] which has already been applied to vascular fluid-solid problems but only using measurements in the solid.

References:

[1] Martin R Pfaller, Maria Cruz Varona, Johannes Lang, Cristóbal Bertoglio, and Wolfgang A Wall. Using parametric model order reduction for inverse analysis of large nonlinear cardiac simulations. *International journal for numerical methods in biomedical engineering, 36(4):e3320, 2020.*

[2] Stéphanie Marchesseau, Hervé Delingette, Maxime Sermesant, and Nicholas Ayache. Fast parameter calibration of a cardiac electromechanical model from medical images based on the unscented transform. *Biomechanics and modeling in mechanobiology, 12(4):815–831, 2013.*

[3] Reidmen Aróstica and Cristóbal Bertoglio. On monolithic and chorin–temam schemes for incompressible flows in moving domains. *Applied Mathematics Letters, 112:106830, 2021.*

[4] Philippe Moireau and Dominique Chapelle. Reduced-order Unscented Kalman Filtering with application to parameter identification in large-dimensional systems. *ESAIM: Control, Optimization and Calculus of Variations, Volume 17 (2011) no. 2, pp 380-405*

Abstract title: Parameter estimation in fluid-solid interaction

Workshop: Advanced Discretization and Solution Techniques

Arostica B., Reidmen

University of Groningen, Bernoulli Institute for Mathematics, Computer Science and Artificial Intelligence

Advisor: Advisor: Prof.dr. Cristobal Bertoglio

Biography and description of research:
Currently doing a PhD at the University of Groningen, holds a master's degree from Paris Dauphine Université, France (2020) and engineering degree from the University of Chile, Chile (2019).

My research interests are numerical simulation of biomechanical systems, software development, high-performance computing and its applications in device modeling and simulation as well as parameter estimation. All my collaborations have been within multidisciplinary environments, including physicists, mathematicians as well as clinicians.

Current research involves parameter estimation in fluid-solid interaction problems from heart modeling as well as software benchmarking of such strongly nonlinear models. The question of interest: Can we estimate relevant parameters of heart models using data routinely acquired in clinical practice?

Workshop 4

“Mechanobiology”

Simulating Heart Valve Growth and Remodeling after the Ross Procedure

E. Middendorp, F. Bräu, F.P.T. Baaijens, J.D. Humphrey, C.J. Cyron, S. Loerakker

University of Technology, Department of Biomedical Engineering,
Modeling in Mechanobiology, P.O. Box 000
phone +31649607685, e-mail E. Middendorp@tue.nl

An increased understanding of growth and remodeling (G&R) of heart valves is essential to develop the next generation of living valve replacements. Yet insights in how the complex hemodynamical environment of a heart valve affects its G&R response remain rare. To obtain such insights we investigate the G&R response of the pulmonary valve after it is placed in the aortic position (Ross procedure). To model heart valve G&R, a homogenized constrained mixture model [3] was developed that consisted of elastin, glycosaminoglycans (GAGs) and collagen. In this model, turnover and production of collagen and GAGs were mediated by the stresses experienced by these constituents. Changes in constituent mass due to deviations in the constituent stress would lead to changes in tissue composition, stiffness and volume. To simulate G&R after the Ross-procedure, the homeostatic targets stresses were defined under diastolic pulmonary pressures. Then, this pressure was increased fivefold, to systemic levels, and G&R was simulated until homeostasis was re-established. This G&R response led to distinct changes in valve morphology, composition and microstructure in our model. Over the course of G&R, valves obtained a deeper, 'sagged' appearance, with thicker and longer leaflets. This increase in thickness was well in range of thickening observed in literature [4,5,6]. Once homeostasis was obtained, the composition of these valves had changed as a consequence of the deposition of GAGs and collagen fibers. Collagen was deposited more than GAGs leading to a more fibrous heart valve with a collagen dominated composition. The anisotropy of this collagenous network became less pronounced. Most fibers were still oriented in the circumferential direction, but the relative difference between the mass of circumferentially and radially aligned fibers had reduced. Altogether, these results show that mechano-mediated G&R is able to describe the adaptation of pulmonary autografts due to changes in hemodynamic loading and provides novel insights in the role the mechanical environment on the G&R of heart valves.

This project has received funding from the European Research Council (ERC) under the European Union's Horizon 2020 research and innovation program (Grant agreement No. [802967]). [1] Uiterwijk et al, PLoS One,16: e0258046,2021 [2] Szafron et al, Ann Biomed Eng 46:1938-1950,2018. [3] Cyron et al, Biomech Model Mechanobiol 14:1389-1403,2016 [4] Schoof et al, J. Thorac. Cardiovasc. Surg. 132:1426-1432,2006 [5] Mookhoek et al, J. Thorac. Cardiovasc. Surg. 139:1416-1419,2010 [6] Yacoub et al, Eur J Cardiothorac Surg, 57:977-985,2020

Abstract title: Simulating Heart Valve Growth and Remodeling after the Ross Procedure

Workshop: Mechanobiology

Middendorp, E. (Elmer)

Eindhoven University of Technology,
Department of Biomedical Engineering

Advisor: S. Loerakker
Co-advisor: F.P.T. Baaijens

Biography and description of research:

Elmer Middendorp (1995) obtained his BSc and MSc degree in Biomedical Engineering from the Eindhove University of Technology. During this period he primarily focused on the biomechanics and mechanic modeling of orthopedic tissues. Since 2019 Elmer is performing his PhD research under the supervision Sandra Loerakker where he is working on understanding the growth and remodeling behavior of (in si tissue engineered) heart valves. These in situ tissue engineered heart valves are a promising new valv replacement which is grown directly at the functional site in the body. To successfully regenerate thes valves, a thorough understanding of the biological and mechanical properties of these tissues is require during the entire regenerative process. By developing numerical models that describe the interplay betwee the mechanical environment, tissue deposition and scaffold degradation we hope to provide furth understanding of the transformation from polymeric scaffold to living valve during in situ heart valve tissu engineering.

Tongue Equivalent Design for Tribological Assessment of Astringency in Plant Based Proteins

S.S. Gamaniel, D.T.A. Matthews and E. van der Heide

University of Twente, Department of Mechanics of Solids, Surfaces and Systems (MS3),
P.O. Box 217, NL 7500 AE Enschede
phone +31-(0)53-4897025, email s.s.gamaniel@utwente.nl

Background

Consumption of plant-based food products having high composition of polyphenols leads to the sensation of astringency. For sliding oral surfaces, friction is an essential property during the oral perception of roughness and dryness which are attributes associated with astringency. Available measurement techniques have shown an existing relationship between salivary protein-polyphenol interaction and an astringent mouthfeel. This could be through the formation of insoluble aggregates (Figure 1.a) and/or disruption of the mucosal film (Figure 1.b), leading to a loss of oral lubrication.

Methods

Different factors including the chemical composition of interacting layers, structure and operation of interfaces have an effect on the astringency development process. The manner of interactions occurring at oral interfaces suggests there is a system dependence of astringency and highlights the

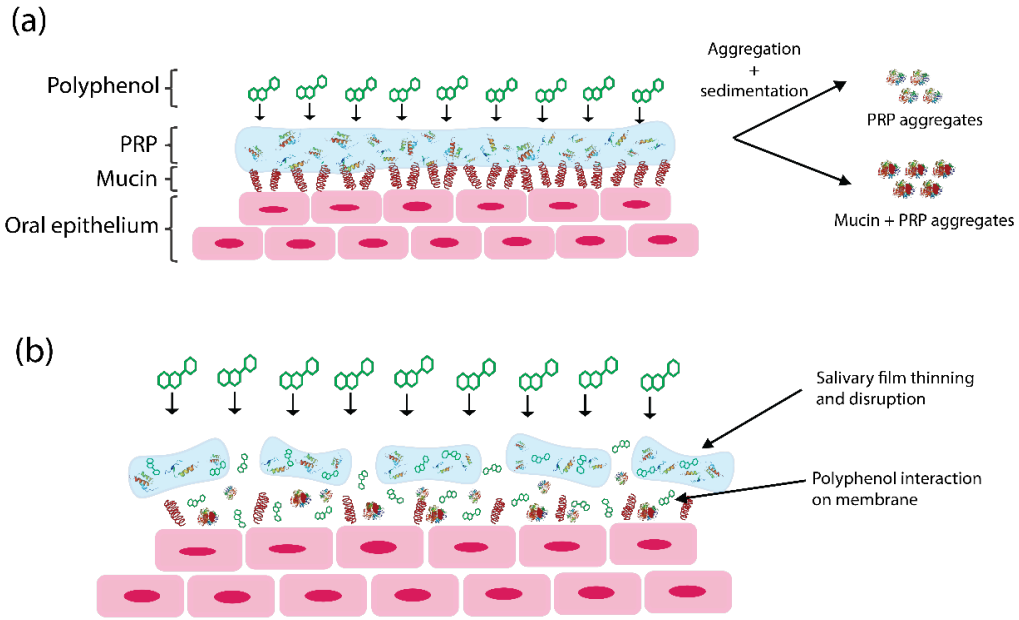

Fig. 1 *Schematic representation of the oral epithelium showing possible mode of astringency due to* ***(a)*** *aggregation of salivary proteins and* ***(b)*** *thinning and breakdown of salivary film layer due to polyphenol-saliva interaction.*

importance of adopting a tribosystems approach. This way it is possible to replicate system components, paying attention to their relations and functions within the system. We propose a tongue equivalent design that closely mimics the properties of oral surfaces which are relevant for assessing changes to oral lubrication resulting from astringency.

Results and conclusions

The final design considers the textured surface of the tongue, reproduced using an MSLA 3D printed mold. Stiffness of the tongue material was modified by introducing a double layer design consisting of a higher wear resistant surface and a low stiffness bulk. Tribological assessment of astringent compounds using the proposed tongue equivalent shows differences in measured coefficient of friction compared to saliva and also sheds insights into several aspects of astringency research needing further development.

Abstract title: Tongue Equivalent Design for Tribological Assessment of Astringency in Plant Based Proteins

Workshop: Mechanobiology

University of Twente, Department of Mechanics of Solids, Surfaces and Systems (MS3).

Advisor: Prof.dr.ir. E. van der Heide
Co-advisor: Dr. D.T.A. Matthews

Biography and description of research:

I received my Bachelor of Science (BSc) and Master of Science (MSc) degrees in Mechanical Engineering at Bilkent University in 2017 and 2020, respectively. During my Master's studies, I worked on a numerical algorithm for viscoelastic fluids in lubricated contacts where cavitation was present. This research was carried out within a project funded by the Scientific and Technological Research Council of Türkiye.

In 2023 I obtained my Engineering Doctorate degree in maintenance from the University of Twente. My work focused on designing a tongue equivalent for tribological assessment of astringency from plant-based proteins, addressing the global transition towards sustainable food sources and increasing demand for plant-based proteins as an alternative to animal protein sources. Plant protein sources such as those based on pea or faba bean contain polyphenols, which lead to an unpalatable sensation of dryness, shrinking and puckering, known as astringency. The nature of interactions at oral surfaces are considered as a tribological problem, hinting at a system dependence of oral friction resulting from astringency. I adopted a systematic method towards the design of equivalent surfaces and materials used to investigate the tribological interaction of astringent foods on oral surfaces.

Currently, I am a doctoral researcher within the Skin Tribology group of the University of Twente, where I investigate the lubrication of soft bio-tribological contacts and the friction of particle laden lubricants. For the past two years, I have lectured Statics to students in the Industrial Design Engineering Bachelor's track.

Towards a Multiscale Model of the Brain ECM

S. Shakibi, P.R. Onck, E. van der Giessen

University of Groningen, Zernike Institute for Advanced Materials,
Micromechanics, Nijenborgh 4, 9747 AG, Groningen
phone +31-(0)50-3634251, e-mail s.shakibi@rug.nl

Brain is one of the softest tissue in the body, yet its stiffness increases in the presence of cancer. Glioblastoma (GBM) is one of the most common and malignant brain tumors with a very low survival rate. Mechanical cues are known to be important in progression of GBM via a process called mechanotransduction. This process involves remodeling of the matrix around cells, i.e. extracellular matrix (ECM), and change in its mechanical properties [1]. To understand the relationship between ECM remodeling and the increased stiffness of the brain, we are developing a multiscale computational model of the brain ECM.

In contrast to the protein-based ECM of most tissues, the brain ECM is mainly based on polysaccharides with a hyaluronic acid (HA) backbone, decorated by chondroitin sulfate proteoglycans and crosslinked by tenascins. We have developed a one-bead-per-saccharide (1BPS) model for hyaluronic acid and chondroitin sulfates [2]. Despite being “super” coarse-grained from a molecular perspective, the 1BPS model makes predictions that match experimental observations in length scales relevant to the brain ECM without any fitting parameters.

Proteoglycans are brush-like polymers with a protein backbone and polysaccharide side chains. To model the conformation of proteoglycans, we have combined the 1BPS model with a one-bead-per-aminoacid (1BPA) model developed in our group [3] and an elastic network model. This model has been validated for aggrecan (a well-studied proteoglycan) in terms of radius of gyration, and is being used now for predicting the structure–property relationship of brain-specific proteoglycans, such as brevican and neurocan.

An intermediate validation of the approach is currently carried out by means of a network of HA to model the stiffness of crosslinked HA gels [4]. Subsequently, this model will be extended by including brain-specific proteoglycans and tenascin cross linking proteins, aspects of which will be highlighted in the talk. Eventually, the developed tools will allow us to predict the stiffness of brain ECM from its composition and architecture.

References

[1] J. M. Barnes et al., J Cell Sci, 2017, doi: 10.1242/jcs.191742.
[2] S. Shakibi et al., J Chem Theory Comput, 2023, doi: 10.1021/acs.jctc.3c00238.
[3] A. Ghavami et al., Biophys J, 2014, doi: 10.1016/j.bpj.2014.07.060.
[4] Credi, et al., J Mech Behav Biomed Mater, 2014, doi:10.1016/J.JMBBM.2013.09.025.

Abstract title: Towards a Multiscale Model of the Brain ECM

Workshop: Mechanobiology

Shakibi, S (Saber)

University of Groningen,
Zernike Institute for Advanced Materials

Advisor: Prof. dr. ir. Erik van der Giessen
Co-advisor: Prof. dr. ir. Patrick R. Onck

Biography and description of research:
Saber obtained his bachelor's in civil engineering at Tabriz university (Iran) and continued his masters in structural engineering at Sharif university of technology (Iran). He is interested in studying mechanical properties of materials. During his masters, he used molecular dynamics modelling to study the formation of misfit dislocations and the motion of dislocations in nickel-based superalloys.

Continuing along his interest in mechanical properties of materials, he switched focus to biomaterials in his PhD. His is currently studying mechanotransduction in brain cancer, with the aim of making a structure–function relationship between the mechanical properties of the brain ECM and its composition in healthy versus cancerous state. In this project, he is using a multiscale approach to modelling the extracellular matrix of the brain. In particular, he has developed a one-bead-per-saccharide (1BPS) coarse grained model for glycosaminoglycans in the brain. He is using the 1BPS model in combination with other coarse grained models to predict the mechanical properties of the brain ECM.

Poisson's ratio-driven bone cell growth in meta-biomaterials

E. Yarali1,2, A.A. Zadpoor1, M. Klimopoulou1, U. Staufer2, L.E. Fratila-Apachitei1, A. Accardo2, M.J. Mirzaali1

1Department of Biomechanical Engineering & 2Department of Precision and Microsystems Engineering (PME), Faculty of Mechanical Maritime and Materials Engineering, Delft University of Technology (TU Delft), Mekelweg 2, 2628 CD, Delft, the Netherlands

Stiffness of the scaffolds is a well-known mechanical cue that has a significant impact on cells, modulating their growth, focal adhesions, growth directionality, and differentiation. Moreover, other mechanical cues, such as Poisson's ratio, regulate cellular responses in terms of proliferation and differentiation of stem cells. However, from a solid mechanics standpoint, stiffness and Poisson's ratio are mutually exclusive. Therefore, to elucidate the effect of Poisson's ratio or stiffness, they should be isolated from other mechanical and morphological cues (*e.g.,* porosity and pore size). Mechanical meta-biomaterials are potential materials for decoupling Poisson's ratio from stiffness because of their intrinsic geometrical properties. Here, we aimed to determine the effect of Poisson's ratio on the responses of preosteoblast cells by isolating it from other mechanical and morphological properties of the meta-biomaterials.

The porosity and pore sizes in the design of the meta-biomaterials were selected based on the range of trabecular bone porosity (*i.e.,* 60-90%) and the size of preosteoblasts (*i.e.,*50-100 µm) (Figure 1.a.i). The size of the preosteoblasts was derived from the visualization of their cytoskeleton morphology via immunofluorescence microscopy. The rationally designed meta-biomaterials were additively manufactured via two-photon polymerization (2PP) at meso-scale (Figure 1.a.ii). The preosteoblasts initially settled on the bottom of the meta-biomaterials (*i.e.,* the pedestal), Figure 1.b, day 3) and then covered the entire meta-biomaterials within 17 days of culture (Figure 1.b, days 6 and 17). It shows that the direction of the meta-biomaterials also affects the preosteoblasts directionality. Moreover, they induced a local bending in the struts, more specifically in the meta-biomaterials with negative Poisson's ratio (=auxetic, NPR) (Figure 1.b, day 10). The metabolic activity of the preosteoblast cells not only increased over 17 days of culture, but, in the presence of the meta-biomaterials with a positive Poisson's ratio (PPRs), it was higher than that of cells cultured within NPR scaffolds (Figure 1.a.iii). The differences observed in cellular responses may be associated with the different geometry of the unit cells in the PPRs (positive-angle tilted struts) and NPR scaffolds (negative-angle tilted struts). This study showed that Poisson's ratio, as a mechanical cue should be also taken into account in the development of meta-implants.

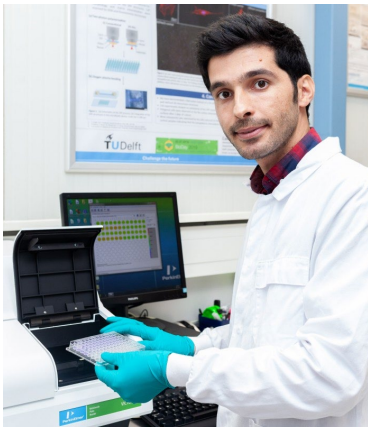

Abstract title: Poisson's ratio-driven bone cell growth in meta-biomaterials.

Workshop: Mechanobiology

Yarali, E. (Ebrahim) Ebrahim Yarali

Delft University of Technology (TU Delft), Departments of Biomechanical Engineering & Precision and Microsystems Engineering

Advisor: Dr. Mohammad J. Mirzaali & Dr. Angelo Accardo
Co-advisor: Prof. Amir Zadpoor and Prof. Urs Staufer

Biography and description of research:
This is Ebrahim Yarali, last-year PhD candidate at TU Delft, working on bone cell growth and differentiation in meta-biomaterials. More specifically, I am focused on the effect of Poisson's ratio, as a biophysical cue on the proliferation and differentiation of pre-osteoblast cells. To achieve this, we need to first decouple Poisson's ratio, from all other mechanical and morphological properties, such as porosity, pore size, elastic stiffness and permeability. This is a multi-disciplinary project involving computational mechanics, micro-fabrication (*e.g.,* two-photon polymerization), and cell mechanobiology

Graduate School on Engineering Mechanics
c/o Eindhoven University of Technology

PO Box 513, building Gemini-Zuid 4.133
5600 MB Eindhoven NL
Tel.: +31 40 2478306
Fax: +31 40 2447355
E-mail: Engineering.Mechanics@tue.nl
http://www.engineeringmechanics. nl

5

SURVEY

of

POSTER PRESENTATIONS

This section contains a survey of poster presentations of actual PhD-projects within the Graduate School Engineering Mechanics. Furthermore, poster presentations are available through: **www.engineeringmechanics.nl**

Survey of Poster Presentations Twenty-sixth EM Symposium 2023

	Name	Univ	Title Poster
1	Adly, MA	TUD	Multi-Scale Failure Modelling of Metallic Thin-Walled Structures
2	Akhtar, M	TUe	Effects of particle size on rheology and printing speed on dimensional accuracy in ceramics 3D printing
3	Alferink, D	TUe	Motion control of stages with dynamic links, a physics-guided approach
4	Arellano Ortega, L	UT	Prediction of degradation and failures of AmmoniaDrive installations
5	Arnaoutis, V	UT	Generalized Kalman filter based Reinforcement Learning
6	Asijee, T	UT	Laser Assisted Fibre Placement of Thermoplastic Composites From the theory behind Disney movies to aircraft
7	Askari, M.	RuG	Vibration Energy Harvesting via Smart Piezoelectric Structures
8	Babbepalli, P	TUe	An efficient physics-based Model Order Reduction with Optimal Selection of Reduced Basis for Geometrical Nonlinear Problems
9	Behboud, A	TUe	Experimental Study to Assess Micro-mechanical Behavior of Oil Paintings over Time
10	Basile, S	TUD	Drive System of a Resonant Flapping Wings Micro Aerial Vehicle
11	Bentalib, S	UT	Microstructure evolution during fusion bonding of thermoplastic composites
12	Berghuis, M	UT	Estimating physical parameters from simulation data with the ensemble Kalman filter
13	Bieleman, G	UT	Fibre-Matrix Distribution Evolution of Thermoplastic Composite Fusion Bonding Interfaces
14	Blümer, V	UT	Mechanical properties of Ti-6Al-4V processed by additive manufacturing
15	Brands, D	UT	Composite forming simulations: from characterization to validation
16	Bruinsma, S	UT	Rotational Speed Estimation in Vibration Spectra
17	Brunner, F	RuG	Predictive modelling of liquid metal induced fracture in Fe-based alloys
18	Buser, Y	UT	Induction Heating of Unidirectional Thermoplastic Composites Thermographic and electrical characterisation
19	Cordewener, B	TUe	A numerical framework for the electro-mechanical analysis of conductive tracks in printed electronics
20	Dijkstra, K	TUD	Variational Multiscale stabilization of the Magnetohydrodynamics equations
21	Dizman, E	TUe	Computational Modeling of Hydrolytic Degradation in Oil Paintings
22	Dodsworth, L	TUe	A road to more sustainable steel production: Understanding the effects on impurity elements on the mechanical performance of steel by bridging RVE data to micromechanical tests
23	Fallahnejad, A	UT	Physically consistent data-driven constitutive models by machine learning
24	Farzannasab, M	RuG	Experimental Identification of Nonlinearity and Eigenvalue Assignment of a Nonlinear Electromagnetic System by the Receptance Method
25	Feehilly, T	TUe	Active Metamaterials Emergent Behaviour and Design
26	Fioravanti, D	RuG	Machine Learning Interatomic Potential for Pure Zn
27	Gartner, T	TUD	Effects of Material Architecture in Elastic Impact Mitigation
28	Gödde, T	UT	Utilizing neural networks for large scale spatial domain decomposition of surrogate models
29	Gülmez, D	TUD	Computational Modelling of Chopped Tape Thermoplastic Composites

30	Gupta, S	UT	Stochastic Multiscale Analysis of Thermoplastic Composite Materials
31	Haasjes, R	UT	Towards a small-scale active anechoic chamber
32	AHashemzadeh, A	UT	Hybrid Modelling of Lateral Flow in Hot Rolling of Steel Strips
33	Hendriks, F	TUe	Graph Neural Networks with Embedded Symmetries for Robust Computational Homogenization
34	Hofman, P	TUD	Computational Modeling of Fatigue Failure in Composite Laminates
35	Hoof, van R	TUe	Digital Twin of Interacting Medical Interventional Devices and Patient Tissues
36	Huijer, A	TUD	Structural health monitoring of composite marine propellers using embedded piezoelectric sensors
37	Jalali Moghadas,	UT	Studying the real area of contact to develop a friction mode
38	Janssen, L	TUe	Top-Down Component Requirements with Guaranteed Assembly Accuracy
39	Karaca, K	TUe	Continuous non-parametric density space for a data-driven solution approach
40	Karaseva, I	UT	Multiscale analysis of reinforced elastomer-based composites
41	Keizers, L	UT	Fault Bond Graphs for Correct Prognostics
42	Kessels, B	TUe	Model Parameter Updating for Digital Twins using Gaussian Process Regression as Inverse Mapping Model
43	Kovacs, N	TUD	Physically Recurrent Neural Networks for Cohesive Homogenization of Composite Materials
44	Kuci, X	TUe	Design of a gradient locally resonant acoustic metasurface for negative reflection
45	La Rosa, L	RuG	Structure and mobility of twin boundaries in Ni-Ti Shape-Memory Alloys revealed by atomistic simulations
46	Liupekevicius, R	TUe	Sound insulation performance of labyrinthine metamaterial described by enriched homogenized continuum
47	Maga, L	TUD	Kinematic-based Mathematical and Numerical Formulation for Soft Tissues Growth and Remodeling accounting for Multiple Constituents
48	Maia, M	TUD	Physically Recurrent Neural Network (PRNN) for rate and path-dependent heterogeneous materials
49	Mesman, K	TUD	Quantum Computing for Machine Learning Interatomic Potentials
50	Mudunuru, S	TUe	Time-dependent Anisotropic Behavior of Continuous Fibre Reinforced Thermoplastics.
51	Munzone, F	UT	Comparison of artificial neural network and physics-informed neural network applied to finite deformation
52	Nazemzadeh, N	UT	Modelling of Recycled Fibre-Reinforced Polymer Composites
53	Nijhuis, B	UT	A new view on the solution of rate-independent crystal plasticity models
54	Pantoji, S	TUD	Gaps and Overlaps in Automated Fiber Placement (AFP) Composites. Why do they occur?
55	Parsa Sadr, A	TUe	A multi-scale approach for chemo-mechanical degradation of paper: insights into the governing factors
56	Pereira, A	TUD	Numerical and Experimental Study of a Butt-Joint Thermoplastic Composite Multi-Stringer Panel Under Compression
57	Pierik, E	UT	A New Setup to Measure Friction of Thermoplastic Composite Tape in Melt
58	Pirmoradi, P	TUe	Multi-Scale Study of Fiber Orientation Effect on Mechanical Behavior of Fiber-Reinforced Concrete
59	Poort, L	TUe	Reduction of Interconnected System Models: Extending Computational Limits with Abstractions
60	Poorte, V	TUD	Structural integration of a full-composite, double-walled, vacuum-insulated, cryo-compressed tank

61	Poot, A	TUD	A Bayesian Approach to Modeling Finite Element Discretization Error
62	Rezaeinejad, S	UT	Melting-Free Metal Production: Solid-State Additive Manufacturing of an Al-Mg-Si Alloy Using FSEAM
63	Rezaie, S	TUe	Gold Decorated Carbon Nanotube for Molecular Hydrogen Storage- A First-Principles Study
64	Rezazadeh, V	TUe	Unravelling air entrapment during polymer thin film lamination: A two-scale model
65	Ribeiro Marinho, N	UT	Dynamics-based impact identification method for composite structures
66	Riccioli, F	TUD	Non-Contact Acoustic Emission Monitoring of Corrosion-Fatigue Damage in Mooring Chain Links
67	Riccius, L	TUD	Bayesian Machine Learning for Multiscale Modeling of 3D-printed Materials
68	Rojas Vega, C	TUe	Computational modelling of moisture transport in paper sheets through a multi-phase flow approach
69	Saccone, C	TUD	Acoustic Emission Sensing for Informed Maintenance of Ship Structures
70	Scheeren, B	TUD	Acoustic Emission Bearing Condition Monitoring in Practice: Laboratory to Field
71	Schönthaler, J	UT	Life prediction of composite materials
72	Schuttert, W	UT	Robust Process Control for the Induction Welding of Thermoplastic Composites
73	Shakibi, S	RuG	The Brain Extracellular Matrix: A Multiscale Computational Study
74	Sikundalapuram Ramesh, S	TUe	Experimental characterization of Acoustic Metasurface and Metafoams
75	Silva, R	TUe	Bayesian estimation and uncertainty quantification of a temperature-dependent thermal conductivity
76	Storm, J	TUD	A Microstructure-based Graph Neural Network for Accelerating Multiscale Simulations
77	Sulollari, E	TUD	Vibration-Induced Friction Force Modulation
78	Tay, E	TUD	Mimicking Living Bones To Optimise Hierarchical Multimaterial, 3D Printed Auxetic Metamaterials
79	Tiggelen, van T	UT	Forced vibrations of system assemblies: An unsolved challenge
80	Tosti Balducci, G	TUD	Substructures as classifiers: predicting composites failure with classical and quantum kernel methods
81	Troost, N	TUD	Friction stir welded joints in steel maritime structures: micro-material scale characteristic fatigue properties
82	Vasconcelos, A	TUD	Design Optimization of Acoustic/Elastic Metamaterial-Based Structures for Underwater Noise Mitigation
83	Verhelst, H	TUD	Tension-Field Theory for General Hyperelastic Materials in Isogeometric Analysis
84	Visser, F	TUe	Optimised matrix and fIbre treatment for recycling composites
85	Voorthuizen, van K	UT	Fluid-conveying pipes in the floating frame of reference formulation
86	Willems, R	TUe	An isogeometric analysis framework for ventricular cardiac mechanics
87	Wong, W	TUD	Relating strain hardening, ductility and impact energy to ductile fracture toughness for steels
88	Xu, Q	TUe	Simulation of PIR pyrolysis in self-supporting sandwich panels under fire
89	Yarali, E	TUD	Poisson's ratio-driven bone cell growth in meta-biomaterials
90	Zhang, L	RuG	Efficient, Accurate, and Transferable ML Potentials: Application to Dislocation and Cracks in Iron
91	Zhang, X	TUD	Scaling Law between 3D-printed Polymer Yield Strength and Printing Parameters

92	Zijl, van C	TUD	Structural nonlinearities in marine hydroelasticity: A frequency-domain method for efficient numerical modelling
93	Zwarts, S	TUD	Finding the Evolution law of Representative Elementary Volume Convergence
94	Zwet, van der J	TUD	Prevention of enclosed voids in topology optimization
95			
96			
97			
98			
99			
100			

Multi-Scale Failure Modelling of Metallic Thin-Walled Structures

M.A. Adly, C.L. Walters

Department of Maritime and Transport Technology,
Faculty of Mechanical, Maritime and Materials Engineering,
Delft University of Technology

Background & Objective

Figure 1: Damaged ship hull [1]

Fine-scale modelling is generally successful in simulating the localization behaviour of ductile metals. However, when modelling large thin-walled structures (such as in figure 1) with shell elements, the commonly used element dimensions are not sufficiently accurate. A traction-separation law (TSL) accounting for the local phenomena in a force-separation relationship in the global structure would achieve the required balance between accuracy and computational efficiency. In order for such a TSL to be more realistic in practice, it should only be based on information known *a priori* and be initiated at the strain associated with mesh sensitivity which is generally related to necking initiation. A TSL for the uniaxial tension case is illustrated in figure 2.

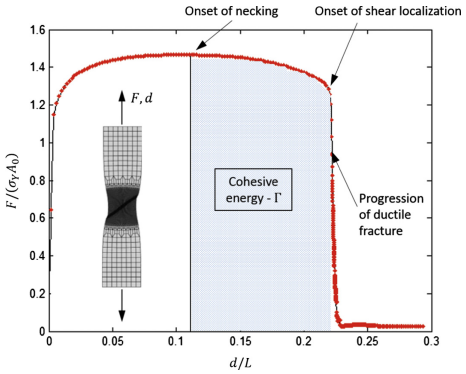

Figure 2: TSL activation zone [2]

Methodology

Obtaining a TSL for the plane strain case was the starting point. The methodology for which is illustrated in figure 3. Through assumptions on the geometry of the neck profile, internal material displacements and the localizing portion of a specimen, it was possible to obtain the local stresses and strains using finite strain plasticity theory. The TSL for a finite strain specimen can consequently be obtained from the dimensions and material model only.

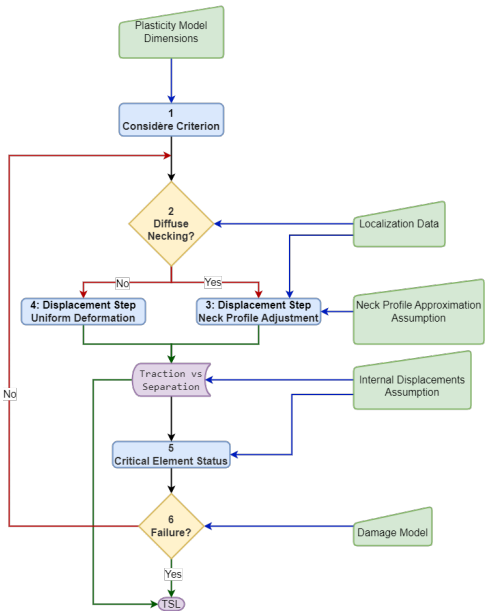

Figure 3: TSL methodology

Sample Results

In order to to verify the TSL, a comparison was made between the global displacement - local critical equivalent plastic strain obtained using the analytical TSL and FEA. A sample result for one specimen is showcased in figure 4. The results show acceptable correlation within the critical range between 0.5 and 1 equivalent plastic strain.

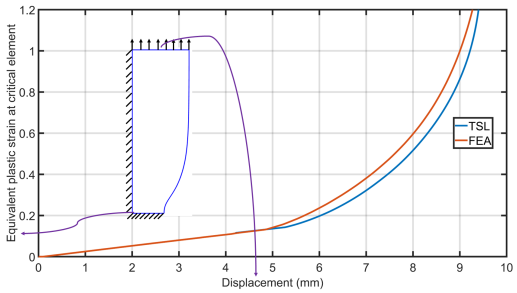

Figure 4: Sample results

Focal Research Points & Future Work

Currently the estimation of the localizing portion of the specimen is obtained from a benchmark finite element simulation and then analytically correlated to other dimensions and material models. It is desired to find a more physics informed approach to deduce this. The whole methodology is then to be extended for more general biaxial stretching cases.

References

[1] https://www.doldrumsbv.nl/en/services/damage-surveys/

[2] P.B. Woelke, M.D. Shields, J.W. Hutchinson, Cohesive zone modeling and calibration for mode I tearing of large ductile plates, Engineering Fracture Mechanics. 147 (2015) 293–305.

PhD progress: 1 | 2 | 3 | 4

Defensie Materieel Organisatie
Ministerie van Defensie

Effects of particle size on rheology and printing speed on dimensional accuracy in ceramics 3D printing

Moeen Akhtar, Diletta Giuntini, Marc Geers

[1]Eindhoven University of Technology

[2]Graduate School Engineering Mechanics

Introduction

DIW of ceramics utilizes a viscoelastic paste to create shapes through the extrusion process. Successful printing relies heavily on rheological properties (shear thinning, sufficient storage modulus (G′), sufficient yield stress (τ_y)), and extrusion parameters (printing speed and nozzle diameter). Among all parameters, printing speed holds great importance, and yet its effects on dimensional accuracy are unexplored. In our experiments, we investigated the effects of ceramic particle size on the rheological properties of the paste, the behavior of the paste during extrusion, and the effect of rheology and printing speed on dimensional accuracy.

Experimental:

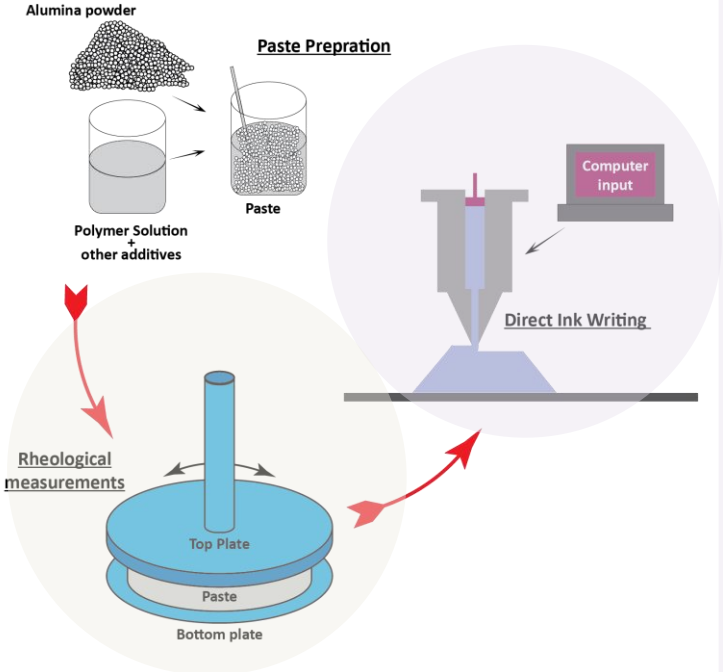

Rheological properties

Shear thinning

Storage modulus (G′) & Yield stress (τ_y)

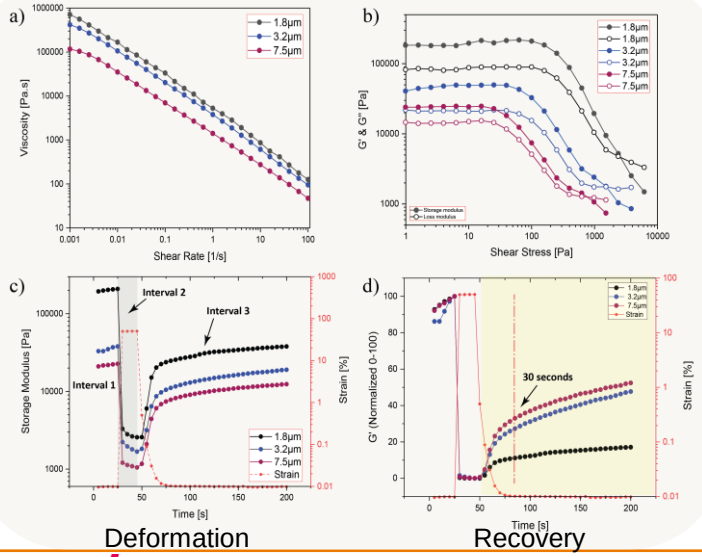

Deformation Recovery

Extrusion Dynamics

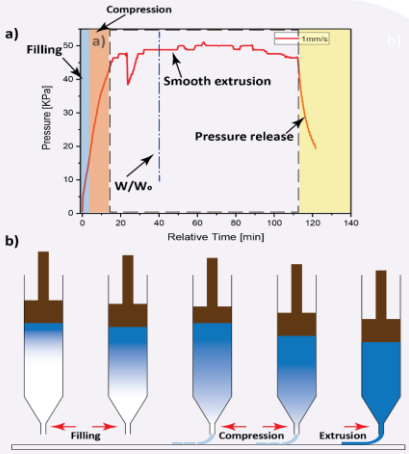

Due to the compressibility of paste, there exists a pressure gradient

Dimensional Accuracy

1D-Filaments

W/W_0 = ratio b/w filament width and nozzle dia (Ø)

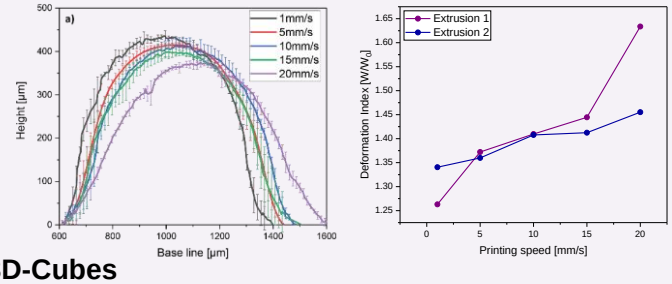

3D-Cubes

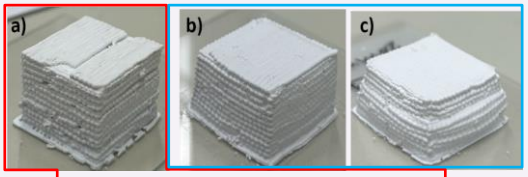

a)1mm/s
b)10mm/s
c)20mm/s
Ø - 600µm

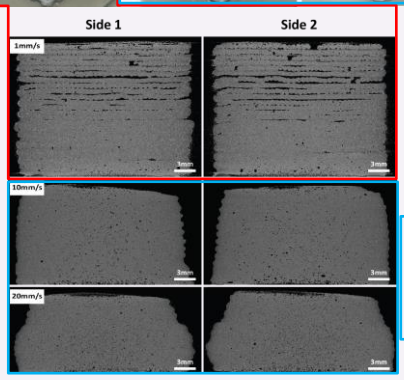

Better dimensional accuracy; cross-sectional defects

No cross-sectional defects; dimensional accuracy is compromised

Conclusions and Outlook

Printing speed affects the dimensional accuracy greatly and there exists a compromise between the accuracy and cross-sectional defects.

It therefore is important to develop the optimum relationship between rheological properties, and extrusion parameters (nozzle diameter, printing speed) to create defect-free object meeting the dimensional requirements.

Motion control of stages with dynamic links, a physics-guided approach

D.W.T. Alferink, R.H.B. Fey,
N. van de Wouw, M.F. Heertjes
Eindhoven University of Technology,
Department of Mechanical Engineering

Introduction

Wafer scanners need to become increasingly accurate and fast to fulfill the ever-increasing demands in the semiconductor industry. This results in tighter specifications on tracking performance for the moving stages in these wafer scanners, where even the smallest sources of disturbances deteriorate tracking performance. One of these sources are dynamic-links (DLs), i.e., the physical connections between two stages (or between a stage and the fixed world) that themselves show dynamic behavior. These DLs consist of cables providing electrical current, sensor signals, purging gases, etc. Figure 1 shows a dual-stroke wafer stage with cable slabs (DLs).

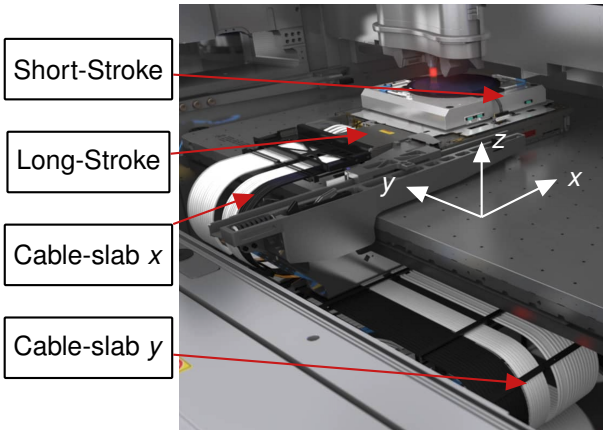

Figure 1: A dual-stroke wafer stage with cable slabs.

Problem statement

The wafer stage is a dual-stroke motion stage that consists of two main parts: the long-stroke stage for micrometer positioning accuracy, and the short-stroke stage for nanometer positioning accuracy. Positioning these stages faster and more accurately to obtain smaller microchips at higher production rates requires enhanced control techniques. Up to now, these stages are primarily modeled as a floating mass, and thus disturbance forces caused by DLs are not included. In order to support enhanced control, modeling of these stages should be extended to included DL models. A dual-stroke wafer stage has three categories of DLs and is illustrated in Figure 2. Namely,

- Flat flexible cables: for sensor signals and electrical current.
- Coolant/air tubes: for cooling fluids, purging gases etc.
- Cable slab: providing the combination of the above.

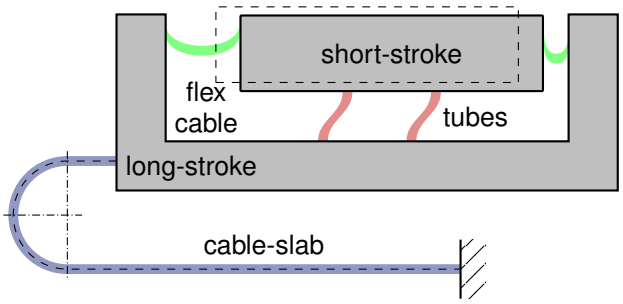

Figure 2: A dual-stroke wafer stage with the three categories of dynamic links.

Each category of DLs shows different type of dynamic behavior. Visco-elastic behavior and dry friction appears in each category and are the only effects present in the flex cables (see [1]). In addition, the tubes exhibit inertia effects. The cable slab manifest all above mentioned effects in combination with position-dependent dynamics: as the stage moves, the effective mass and geometry of the cable-slab changes.

Goal of the project

The main research question of this PhD project:

- *How to model, identify and compensate the dynamic link-induced disturbances on motion stages by (preferably) physically interpretable models that are as simple as possible?*

In order to answer this question, the following topics will be discussed:

1. Experimental analysis of hysteresis in motion control applications due to DLs and the resulting effects on tracking performance.
2. Modeling and identification of DL dynamics.
3. Developing new compensation/control strategies to deal with the detrimental effects of DLs.

Initial results

The initial research direction is quasi-linear frequency domain analysis for motion control applications including hysteretic disturbance forces induced by DLs. Motion control systems heavily rely on acceleration feedforward and current results show that hysteresis realizes a feedforward mismatch primarily in the low frequency range where the setpoint profiles have their main contribution. For this reason, one should reconsider current feedforward control architectures in obtaining smaller tracking errors in the presence of DLs.

References

[1] Vogels, A.A.A, Fey, R.H.B., and Heertjes, M.F., *"Experimental modeling of hysteresis in stage systems: A Maxwell–Iwan approach,"* Mechatronics, vol. 75, p. 102525, 2021.

Prediction of degradation and failures of AmmoniaDrive installations

L.J. Arellano Ortega[1,*], R. Loendersloot[1], T. Tinga[1,2]

[1] *University of Twente*
[2] *Netherlands Defence Academy*
[*] *l.j.arellanoortega@utwente.nl*

Introduction

The dramatic increase in energy consumption is attributed to population growth and technological developments. The main sources of energy are fossil fuels, which increase the amount of CO_2 emissions. Reducing these emissions completely is a challenge, which is why many researchers recommend switching to clean fuels as soon as possible. Ammonia (NH_3) is considered one of the most promising hydrogen carriers and clean fuels. It is the leading candidate as an alternative fuel for long-distance and other maritime, or heavy-duty applications. However, its successful application is highly challenging due to its complex combustion properties, concerns about the effects on the marine environment and human safety [1]. **AmmoniaDrive** addresses these issues by adopting NH_3 in an innovative power and propulsion system for ships utilising a combination of the state-of-the-art Solid Oxide Fuel Cell (SOFC) and Internal Combustion Engine (ICE) technology shown schematically in Figure 1.

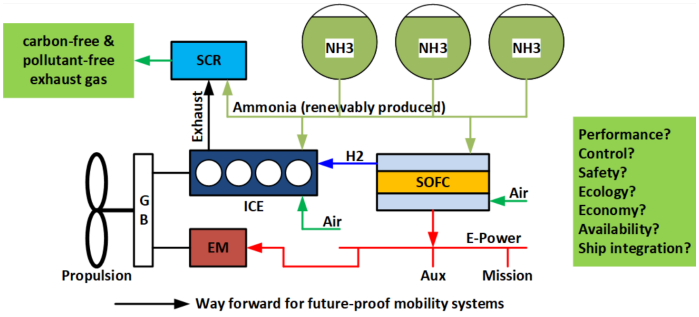

Figure 1: AmmoniaDrive system scheme [1]

NH_3 is incompatible with existing marine power and propulsion systems. It burns slowly and its use in ICE requires a promotor fuel. Therefore, the key idea behind the combined SOFC-ICE AmmoniaDrive system is to use a part of the hydrogen produced in the SOFC as a promotor fuel to reduce the need for additional engine modifications.

Scope of the research

The contribution of this research is responsible for generating knowledge about the **failure behaviour** of AmmoniaDrive installations, identifying the **parameters to be monitored** and translating these into **maintenance policies** that guarantee high system availability.

Main challenges

The power and propulsion system investigated in AmmoniaDrive contains many non-proven subsystems in new configurations introducing the following challenges:

- It is a completely new system configuration, so there is little experience/knowledge on performance, reliability, failure behaviour of (sub)systems and components.
- There is a limited amount of available experimental/field data and accurate physical models.

Research questions

The associated research questions are:

- What are the expected failure modes and underlying failure mechanisms of the interacting installations and how can this failure behaviour be modelled/predicted and monitored?
- How can the current and future overall system condition be quantified and be estimated or predicted and how can the control system be utilized to extend the expected time to failure?

Methodology

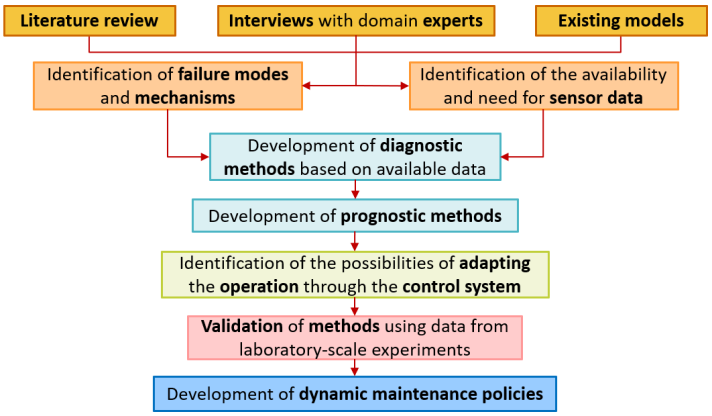

Figure 2: Flow diagram of intended project methodology

Current objective

In order to accurately understand the failure behaviour of a system, some methodologies are proposed in the literature [2]. Failure mode and effects analysis (FMEA) and fault tree analysis (FTA) are two commonly used methods for failure analysis. A combination of both results in a more advanced method which is used to prioritize between failure modes [3].

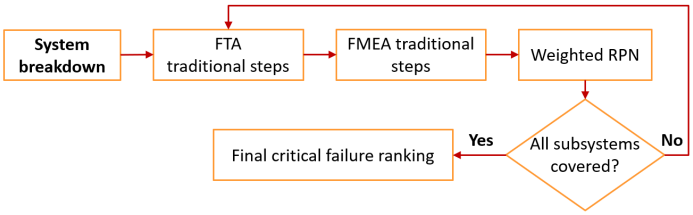

Figure 3: FTA-FMEA integration algorithm. Adapted from [4]

References

[1] AmmoniaDrive. AmmoniaDrive website: About. 2022. `https://ammoniadrive.tudelft.nl/` (accessed 19 September 2023).
[2] Tinga T. Principles of loads and failure mechanisms: Applications in maintenance, reliability and design. Springer London; 2013.
[3] Peeters JFW, Basten RJI and Tinga T. Improving failure analysis efficiency by combining FTA and FMEA in a recursive manner. *Reliab Eng Syst Saf* 2018; 172: 36–44.
[4] Shafiee M, Enjema E, Kolios A. An Integrated FTA-FMEA Model for Risk Analysis of Engineering Systems: A Case Study of Subsea Blowout Preventers. *Applied Sciences*. 2019; 9(6):1192.

Generalized Kalman filter based Reinforcement Learning

Vasos Arnaoutis, Bojana Rosić

University of Twente, Netherlands

Introduction

Temporal Difference is a well-known model-free method used in reinforcement learning. An ongoing challenge with this type of learning is to incorporate as much information into the learning process as possible. In this work this is done through probabilistic learning strategy.

Cumulative return

Cumulative return is defined as a collection of rewards R_k taken at state s_k and action a_k, i.e:

$$G_t = \sum_{k=t+1}^{T} \gamma^{k-t-1} R_k(s_k, a_k). \tag{1}$$

The known value metrics of reinforcement learning, state-value (V) and action-value (Q) can be derived by taking the expectation of the cumulative return, conditioned on a discrete event.

$$V(s) = \mathbb{E}[G_t | S_t = s] \tag{2}$$
$$Q(s,a) = \mathbb{E}[G_t | S_t = s, A_t = a] \tag{3}$$

A priori G_t from eq.(1), and respectively $V(s)$ and $Q(s,a)$, is not known, and thus can be modelled as uncertain i.e. a random variable $G_t(\omega)$. By use of theoretical formulations shown in [1], one may infer the knowledge on G_t by using a generalised Kalman filter equation:

$$G_t^a(\omega) = G_t^f(\omega) + K(R_t^o - \hat{R}_t^f(\omega)) \tag{4}$$

where superscripts a, f, o stand for assimilated, forecast, and observation respectively.

Parameterization and Discretization

The value functions from eqs.(2-3), defined collectively as V, can be further parameterized. An example is to use linear parameterization such that

$$V \approx V_\theta = \theta\Phi \tag{5}$$

where Φ is a known "optimal basis" function and θ is the unknown parameter.

Being unknown, θ is modelled as uncertain by assuming some prior knowledge. Hence, both the value function and the cumulative return are implicitly defined as random variables. In this way we define a priori parameter $\theta(\omega)$ as a polynomial chaos expansion

$$\theta(\omega) \approx \hat{\theta}(\omega) = \sum_{\alpha \in \mathcal{J}} \theta^{(\alpha)} \Psi_\alpha(\xi(\omega)) \tag{6}$$

in which $\xi(\omega)$ are known random variable of standard type.

Application

The common control problem of the inverted pendulum (Figure 1 is considered as a use case with dynamics defined as

$$\ddot{\phi} = \frac{g\sin(\phi) - \beta ml\dot{\phi}\sin(2\phi)/2 - 50\beta\cos(\phi)\alpha}{4l/3 - \beta ml\cos^2(\phi)},$$

where ϕ is the angular position, α is the control input, l is the length of pendulum, m and M are the mass of the pendulum and cart, and $\beta = \frac{1}{m+M}$.

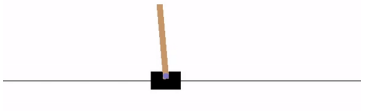

Figure 1: Inverted Pendulum

Results

Figure 2 is based on a variation of SARSA, that implements the generalized Kalman Temporal Difference equation for the action-value function. The polynomial expansion in eq.(6) is constructed with a basis of Hermite polynomials up to third-order.

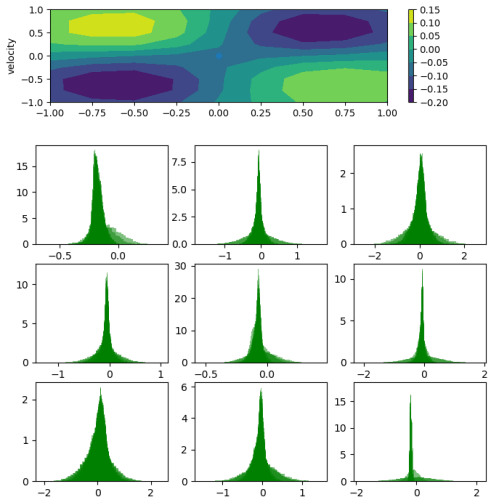

Figure 2: Value function and variance over nine states

Conclusion

The presented algotihm is generalisation of Kalman temporal learning, and is approximate Bayesian learning. Instead of sampling we use functional representation that can be used to improve sample efficiency, expressiveness and stability of a stochastic system.

References

[1] Matthies, H. G., Zander, E., Rosić, B. v., & Litvinenko, A. (2016). Parameter estimation via conditional expectation: a Bayesian inversion.

Laser Assisted Fibre Placement of Thermoplastic Composites

From the theory behind Disney movies to aircraft

T.J. Asijee[1,2], W.J.B. Grouve[2], E.T.M. Krämer[1], M.I. Abdul Rasheed[3]

[1]*Thermoplastic composites Research Center*
[2]*UT - Production Technology*
[3]*UT - Applied Mechanics and Data Analysis*

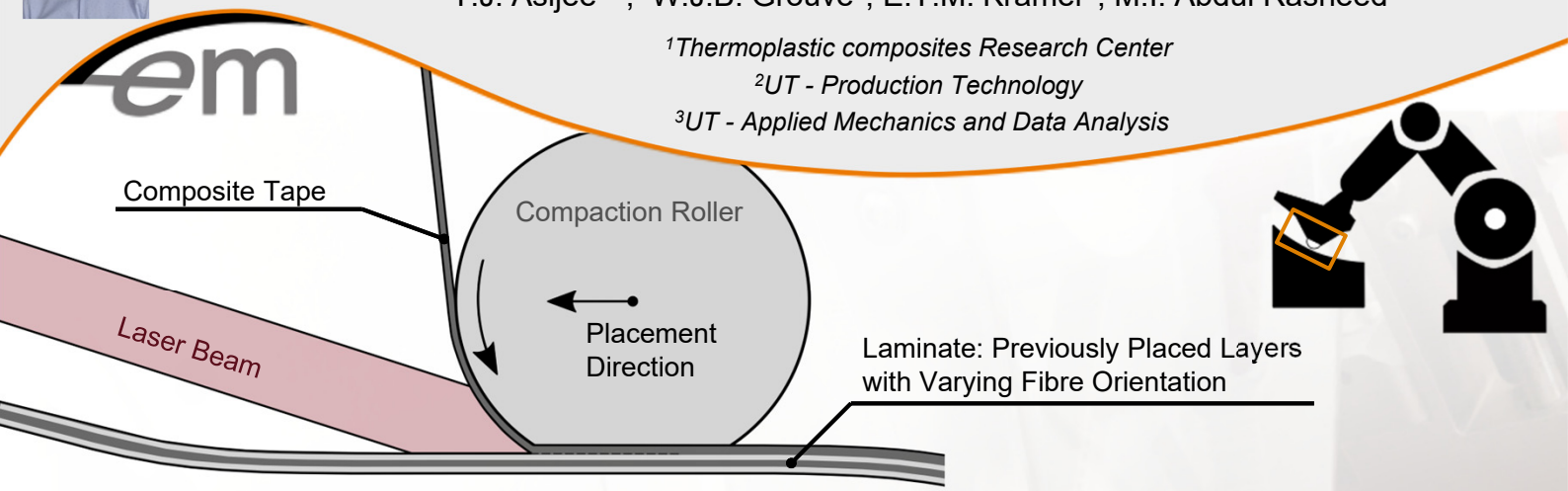

'3D Printing' of Large Composite Panels

Laser assisted fibre placement (LAFP) is an additive manufacturing process for thermoplastic composites. The process relies on a laser to melt a thermoplastic matrix.
By better understanding the interaction of the laser light with the material, the reliability of this manufacturing process can be improved.

Figure 1: Robot system to produce an 8-meter-long thermoplastic composite fuselage section [1].

Effect of Laser Light on a Composite Tape

The scattering behaviour of laser light is characterized experimentally using the setup below. Multiple images are processed into a radiance map using exposure fusion.

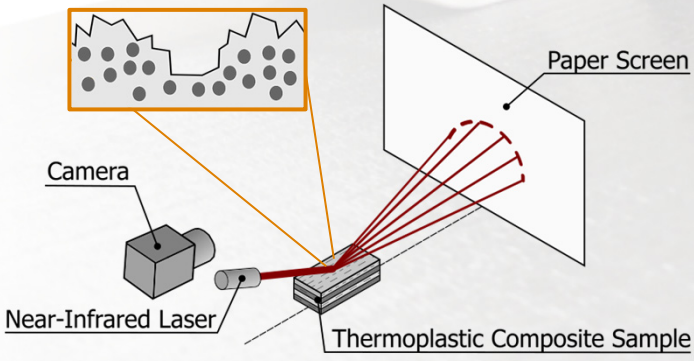

Figure 2: Schematic representation of the light scattering setup with a fibre-reinforced composite sample.

The scattering of light depends on:

(1) surface roughness
(2) fibre-matrix distribution
(3) optical properties of the material

Measurement of Light Scatter

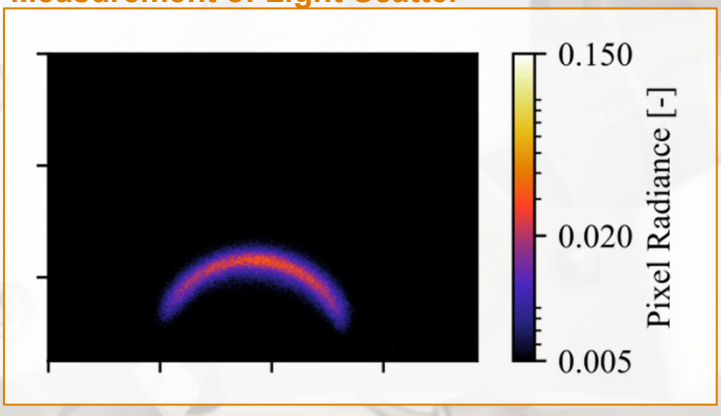

Figure 3: Radiance map for a composite sample with the laser direction aligned with the direction of the fibres.

The intensity and direction of the scattered light shows the anisotropic nature of carbon fibre reinforced composites. Numerically, these effects can be captured using Bidirectional Reflectance Distribution Functions (BRDFs), which are widely used in graphics rendering for e.g. animated Disney movies.

Conclusions & Future Work

The measured patterns will be parametrized using a BRDF. This information can then be used to improve simulations of the laser assisted fibre placement process, where this BRDF can be used.

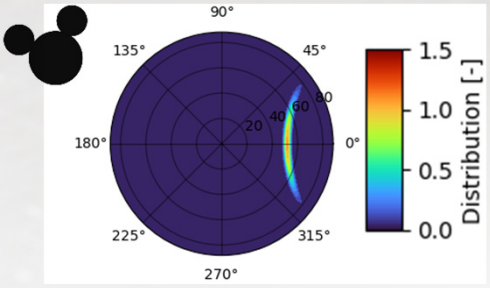

Figure 4: Example polar plot representing the intensity of a BRDF over the hemisphere

[1] G. Nehls, STUNNING project develops 8.5-meter thermoplastic fuselage skin, CompositesWorld, 2021

More information:

Vibration Energy Harvesting via Smart Piezoelectric Structures

M. Askari, M. Ghandchi Tehrani

Dynamics and Vibration Group

University of Groningen (RUG)

Introduction

Ambient mechanical vibration can be converted into electricity through the use of piezoelectric energy harvesters (PEHs), resulting in the generation of electrical energy at the microwatt to milliwatt scale [1]. This generated electricity can be used for autonomous operation of low-power electronics such as wireless sensor networks (WSNs), biomedical implants, as well as embedded, and portable electronics. PEHs represent viable and practical alternatives to conventional energy sources, such as batteries, as they do not require maintenance or replacement and can be used in applications where the use or replacement of batteries is prohibitively expensive or even impossible [2].

Single- and Multi-DOF PEHs

In this study, we propose single-DOF and multi-DOF layouts for vibration energy harvesting (shown in Figure 1). The primary aim is to introduce novel and effective configurations for harvesting energy from low-frequency vibrations commonly found in various engineering applications. Each layout consists of three fundamental components: a substrate structure (Aluminium), piezoelectric patches (PZT-5A), and proof masses (Steel). Electric voltage/power is generated by piezoelectric patches when the PEH is subjected to vibration at their resonance frequency(s). It is therefore necessary to match the resonance(s) of the PEHs with that of the external vibration source.

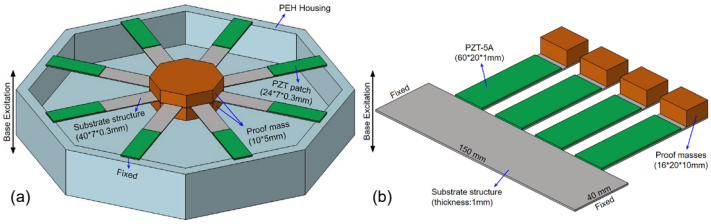

Figure 1: The proposed (a) single-DOF vibration harvester placed on its housing and (b) multi-DOF vibration harvester

Note that both parallel and series configurations are used to electrically connect the electrodes of piezoelectric patches to each other. A simple electrical circuit consisting of an electric resistor is then considered for measuring electrical outputs.

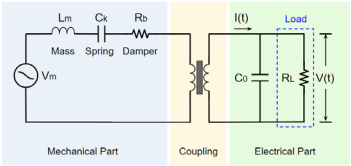

Figure 2: Electromechanical representation of the proposed PEHs

Methodology: FE Simulation

The performance of the proposed layouts is preliminarily investigated using FE simulation in COMSOL Multiphysics, including eigenfrequency and frequency-domain studies. Our goal is to also show the capability of the proposed PEHs experimentally. To ensure the accuracy of the FE simulations at this stage, the modal analyses of both layouts are conducted using Altair HyperWorks Suite as well. For illustration, the FE model of the single- DOF harvester is given in Figure 3. PEHs' response to 0.4g harmonic base excitation is measured and presented in the next section.

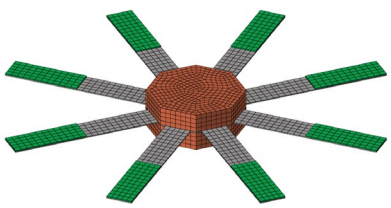

Figure 3: FE model of the single-DOF harvester

Numerical Results

The mode shapes of both PEHs have been extracted and are presented in Figure 4(a-f). Since d_{31}-type PZT patches are employed, only bending-type mode shapes are relevant for energy harvesting here, as the base excitation is also applied to the PEHs through thickness direction (i.e., z-axis). Note that the strain plot in Figure 4(b) indicates the existence of a strain node through the length of the Beams, where the induced strain changes sign. It is therefore not efficient to cover the entire length of the beams with continuous PZT patches, to avoid any voltage cancellation (see Figure 5(a)). Interestingly, Figures 4(c-f) indicate the possibility of power generation from the first four mode shapes of the proposed multi-DOF PEH. This enables such PEH to generate electric voltage or power over a frequency bandwidth. The plots in Figures 5(b-d) illustrate power generation of the single-DOF PEH against the excitation frequency and electrical load resistance for parallel and series configurations. Obviously, the harvester generate the maximum power when the excitation frequency matches the PEH resonance frequency. Also, an optimal load resistance value results in maximum power, with both parallel and series configurations delivering equal power despite the higher resistance in the series setup.

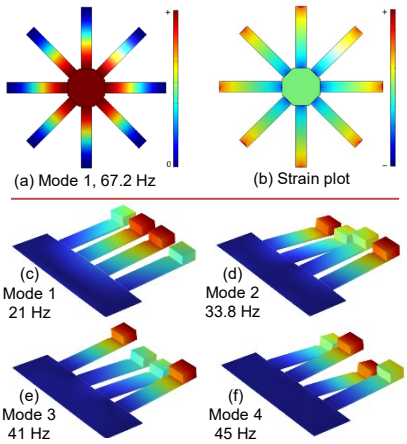

Figure 4: (a,b) The first mode shape and strain plot of the single-DOF PEH, and (c-f) The first four mode shapes of the multi-DOF PEH

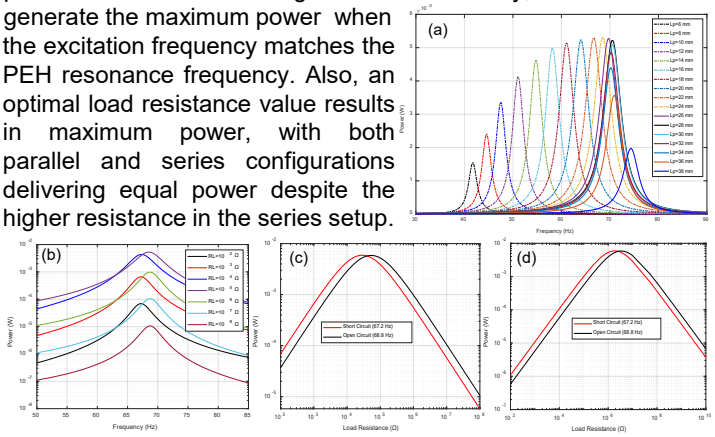

Figure 5: Power output of the single-DOF PEH against (a) the PZT length (b) excitation frequency, (c) load resistance in parallel, and (d) load resistance in series setup

Conclusion

Novel piezoelectric structures are proposed for vibration energy harvesting. The numerical results indicate sufficient performance of the proposed harvesters, generating few milliwatts of electric power under harmonic base excitation of 0.4g. However, long-term goals of this project include experimental validation of the proposed PEHs that is still ongoing. Additionally, it is desired to perform optimization studies for maximizing the electric power generated by our proposed PEHs. Nonlinearity will also be introduced to the PEH systems for enhancing their performance.

References

[1] Safaei, M., et al. (2019). *Smart Materials and Structures*, 28(11), 113001.

[2] Yang, Z., et al. (2018). *Joule*, 2(4), 642-697.

An efficient physics-based Model Order Reduction with Optimal Selection of Reduced Basis for Geometrical Nonlinear Problems

Phani Ram Babbepalli[1] Joris J.C Remmers[1], Olaf van der Sluis[1,2]

[1]Eindhoven University of Technology
[2]Philips Research Laboratories

Model Order Reduction

Model Order Reduction **(MOR)** is any endeavour that reduces the computational complexity of the High-Fidelity Model **(HFM)** by constructing a simple model called Reduced Order Model **(ROM).** Generally, projection-based MORs are used, they can be represented as

$$\boldsymbol{u \approx \Psi q \; ; \; \Psi = [\Psi_1, \Psi_2, \cdots, \Psi_i, \cdots \cdots, \Psi_n]}$$

$$\boldsymbol{\Psi \in \mathbb{R}^{N \times n} \; ; n \ll N}$$

Need Optimal Reduced Bases (RBs) $\boldsymbol{\Psi_i}$ from **physics-based** approaches such that

1. **Limits the Size n for the projection function Ψ**
2. **Enhances the Accuracy with FE simulation**

Physics-based MOR for Nonlinear problems

Computation of Vibration Modes (VMs)

$$\left[\mathbf{K_0} - \omega_i^2 \mathbf{M}\right] \phi_i = 0$$

Computation of Modal Derivatives (MDs) [2]

$$\mathbf{K_0} \frac{\partial \phi_i}{\partial q_j} + \frac{\partial \mathbf{K}}{\partial q_j} \phi_i = 0 \; ; \theta_{ij} = \frac{\partial \phi_i}{\partial q_j}$$

Construction of Linear Manifold (LM)

$$\boldsymbol{\varphi = [\phi_i, \cdots \phi_m, \theta_{11}, \cdots \theta_{1m}, \cdots \theta_{ii}, \cdots \theta_{im}, \cdots \theta_{mm}]}$$

Example : Comparison with POD and LM

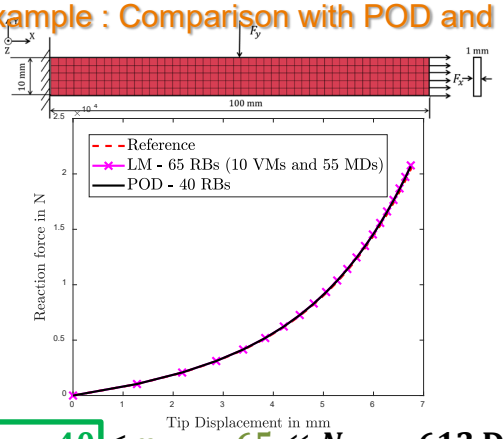

$n_{POD} = 40 < n_{LM} = 65 \ll N_{FE} = 612$ DoFs

Data-based Proper Orthogonal Decomposition (POD) is a better technique to physics-based MOR, LM without any improvements

1) Orthogonalization of RBs in LM by Gram-Schmidt Process

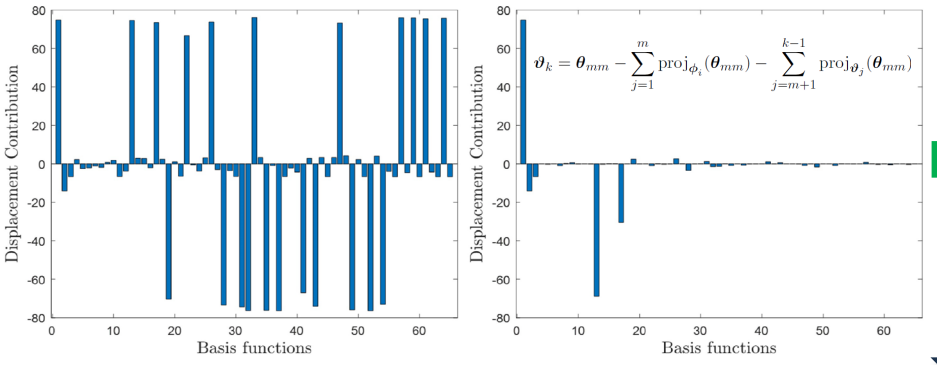

Original Linear Manifold | **Orthogonal Linear Manifold**

2) Greedy Selection of RBs in LM

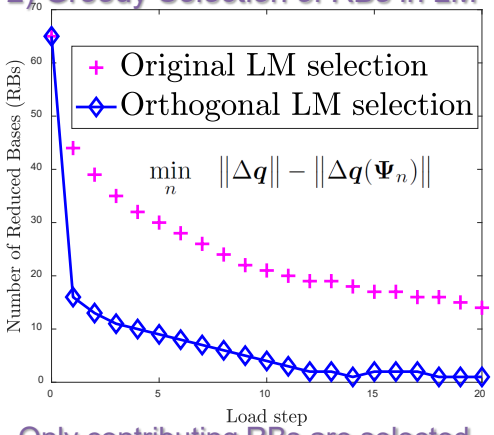

Orthogonalization reduces the contributing RBs in LM

Less Error with FE simulation

Only contributing RBs are selected

and Simulation Time

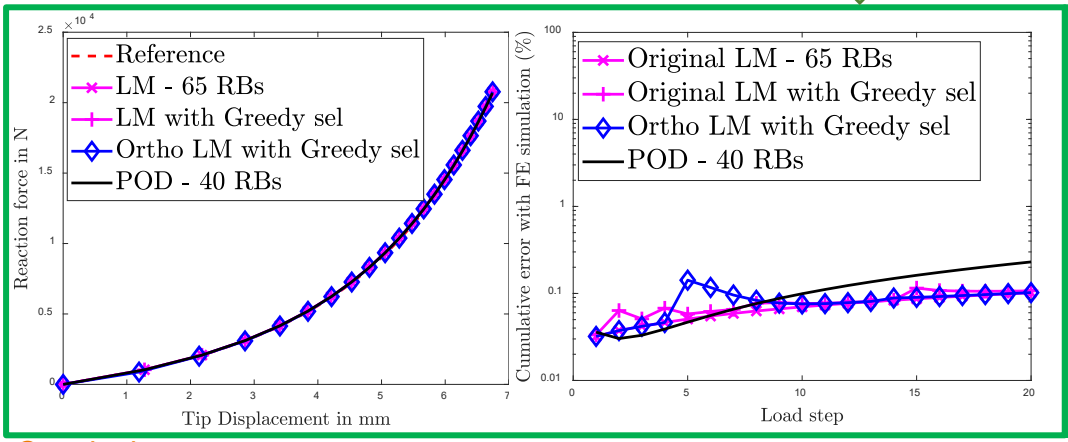

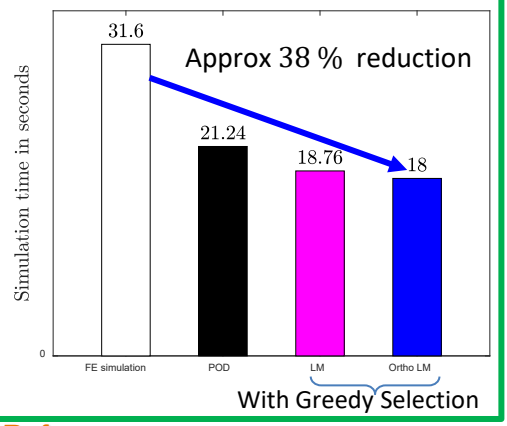

Conclusions

Two improvements to physics-based MOR, LM have been proposed : Orthogonalization of RBs and Greedy selection of RBs which have shown promise in reducing the error and simulation time

References

[1] Hernández, J. A., et al (2017), Computer Methods in Applied Mechanics and Engineering, 313, 687–722.
[2] Jain, S., et al (2017), Computers & Structures, 188, 80–94

TU/e EINDHOVEN UNIVERSITY OF TECHNOLOGY

PhD progress: 1 | 2 | 3 | 4

UPSIM

Experimental Study to Assess Micro-mechanical Behavior of Oil Paintings over Time

Ali B.Behboud[1], Johan Hoefnagels[2], Joen Hermans[3], Emanuela Bosco[1]

[1]Eindhoven University of Technology, Department of the Built Environment

[2]Eindhoven University of Technology, Department of Mechanical Engineering

[3] University of Amsterdam, Conservation Science and Chemistry

Introduction

The majority of oil paintings in museum collections suffer from various chemo-mechanical degradation phenomena. Oil paint is generally made up of layers of a drying oil (binder) and metal-based pigment particles. One of the most important degradation mechanisms in historical oil paintings is metal soap formation. Metal ions released by the pigments interact chemically with the saturated fatty acids present in drying oils to form metal soaps. Metal soaps can develop into big aggregates, which deform paint layers and may cause mechanical damage like flaking and cracking of the paint [1,2]. Figure 1 depicts metal soap protrusions that extend through various sample painting surfaces and cross-sections.

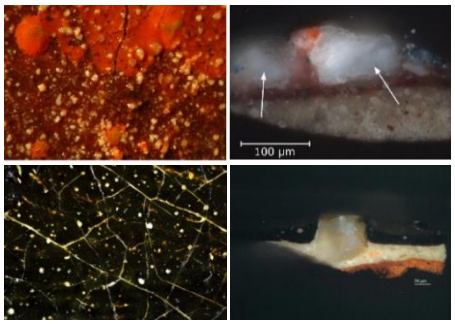

Figure 1. Metal soap protrusions in historical paints [1,2].

Additionally, the mechanical response of oil paint shows a strong dependence on the age, influencing mechanical properties such as toughness, stiffness, and ductility [3]. The interaction between metal soap formation and the ageing response of oil paintings ultimately affects their degradation response – see Figure 2.

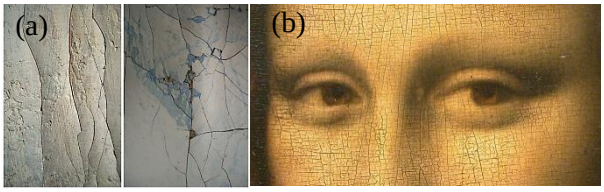

Figure 2. (a) Cracking and delamination of paint layers caused by metal soap formation [4]. (b) Craquelure pattern in the Mona Lisa painting.

Motivation and Research Plan

With the help of cutting-edge micro-mechanics experimental techniques, this study aims to identify the causes of changes in the chemo-mechanical response of oil paintings over time. This is done by developing a methodology to experimentally characterize the stress-deformation response of micro- and nano-sized samples (historic samples and model systems) using a variety of techniques, including tensile, compression, tests etc. To the best of our knowledge, this has never been explored in the literature.

Experimental Details

Departing from the tensile testers previously manufactured at the multiscale lab TU/e, in the initial phase of our work, we plan to use the fiber tensile tester [5] shown in Figure 3(a) to perform tensile tests on samples from model systems. A high-magnification 3D surface evaluation combined with Digital Image Correlation (DIC) will be used to determine the local strains [6]. In the second step, tensile tests will be performed on micro-sized historical samples utilizing a very accurate micro-mechanical setup [7], as shown in Figure 3(b). We propose to combine the micromechanical testing with in-situ, real-time microscopic inspections in order to accurately analyze the deformation occurring in the paint samples during the tests.

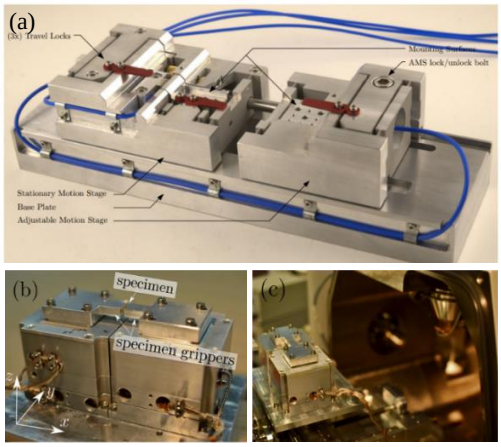

Figure 3. (a) A custom-made fiber tensile tester [5]. (b) and (c) Micro-mechanical testing setup [7].

Future Work

As a potential future work, we propose to further investigate the deformation mechanisms (both plastic and elastic deformation) by conducting other micro-mechanical tests such as bending and compression tests on micro-sized paint samples.

References

[1] G. J. A. M. Eumelen, E. Bosco, A. S. J. Suiker, A. Van Loon, and P. D. Iedema, Journal of the Mechanics and Physics of Solids **132**, 103683 (2019).
[2] G. J. A. M. Eumelen, E. Bosco, A. S. J. Suiker, J. J. Hermans, A. Van Loon, K. Keune, and P. D. Iedema, SN Appl. Sci. **2**, 1310 (2020).
[3] G. dePolo, M. Walton, K. Keune, and K. R. Shull, Herit Sci **9**, 68 (2021).
[4] M. F. Mecklenburg, SN Appl. Sci. **2**, 2182 (2020).
[5] B. Huisman., BSc Report, Eindhoven University of Technology (2023).
[6] S. Maraghechi, E. Bosco, A. S. J. Suiker, and J. P. M. Hoefnagels, Cellulose **30**, 4225 (2023).
[7] A. P. Ruybalid, O. Van Der Sluis, M. G. D. Geers, and J. P. M. Hoefnagels, Exp Mech **60**, 713 (2020).

TU/e EINDHOVEN UNIVERSITY OF TECHNOLOGY

PhD progress: 1 | 2 | 3 | 4

NWO RIJKS MUSEUM

Drive system of a resonant Flapping Wings Micro Aerial Vehicle

S. Basile

Delft University of Technology

The Atalanta project

Goal

The goal of this project is to develop bio-inspired FW-MAVs for indoor application, to support greenhouse growers in monitoring pest/disease onset detection and localization.

- Autonomous flight
- Hovering capability
- Communication with the fleet and the base station
- Management of power storage for minimal flight time
- Payload capacity

Nature – inspired micro drones

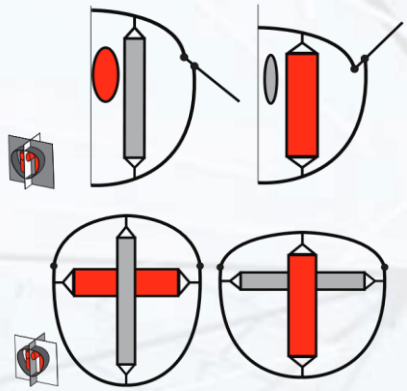

Insects are amongst the most nimble winged animals in nature. By taking inspiration from them, the aim is to:

- Scale favourably the energy usage when hovering and flying slowly
- Combine propulsion and control
- Reduce the noise

Actuating FWMAVs

Key indicators:

- Specific energy and available power
- Power-to-weight ratio

Choosing an energy carrier means having to compromise between the three essential characteristics of **flight time**, **maneuverability** and **payload capability**.

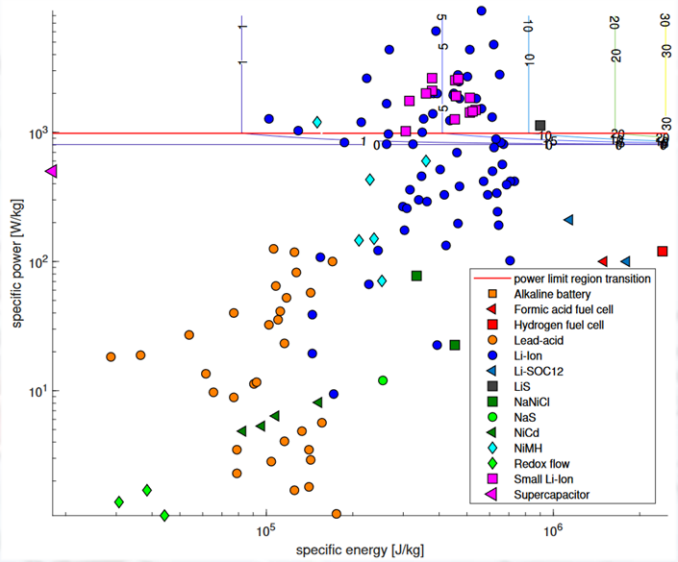

- Electrochemical energy carriers
- EM actuator
- Piezoelectric
- Compliant bellow for chemical actuator

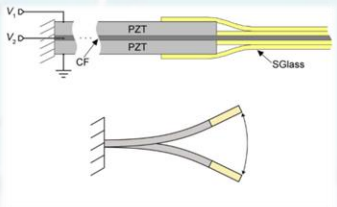

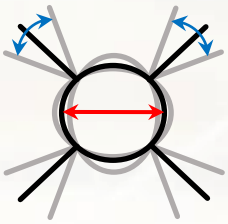

References

[1] C. T. Bolsman, Flapping wing actuation using resonant compliant mechanisms: An insect-inspired design, 2010
[2] G. Mous, The challenges of using actuators in FMWAV a review and technical analysis, 2020
[3] J. A. Roll, D. T. Bardroff, and X. Deng, Mechanics of a scalable high frequency flapping wing robotic platform capable of lift-off, Proceedings - IEEE International Conference on Robotics and Automation 2016- June, 4664 (2016).
[4] R. J. Wood, The first takeoff of a biologically inspired at-scale robotic insect, IEEE Transactions on Robotics 24, 341 (2008)

Microstructure evolution during fusion bonding of thermoplastic composites

S. Bentalib[1,3], R. Akkerman[1,3], L. Govaert[1,2], E. Klompen[3], M. van Drongelen[1]

1 University of Twente
2 Eindhoven University of Technology
3 Thermoplastic Research Center

Introduction

Aerospace and automotive manufacturers are pursuing ways to make vehicles lighter without compromising performance or safety. Thermoplastic composites (TPC) are among the leading solutions, as they possess a light-weighting potential and a good set of mechanical properties. The most suitable joining method for TPC parts is fusion bonding, whose applicability largely depends on time-consuming trial and error procedures.

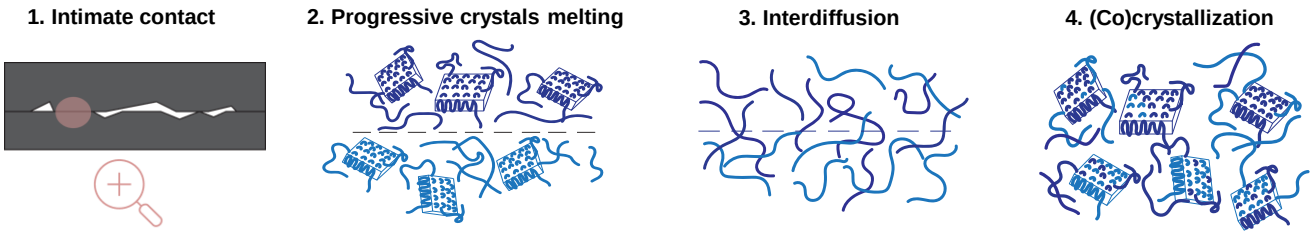

Research objective

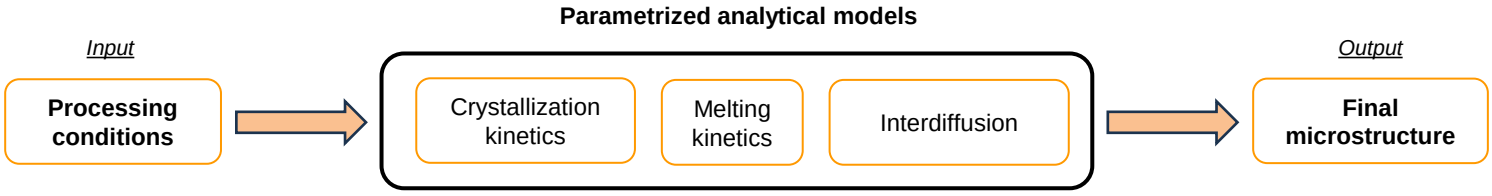

Approach

- Crystallization is modelled via Schneider rate equations
- The influence of fillers/fibres on crystallization is investigated via DSC and Flash-DSC
- Polarized optical microscopy is used to measure (at high temperatures) the growth rate of crystals

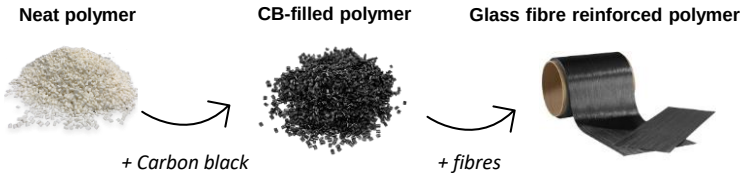

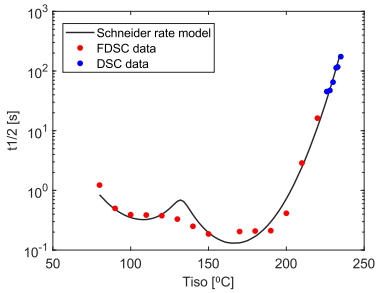

Fig.1 Measured half-time and as determined by the model

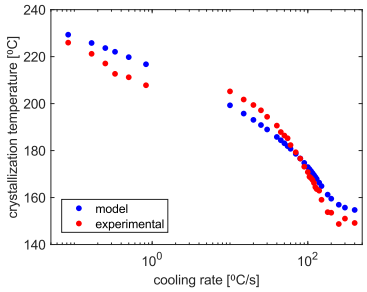

Fig.2 Experimental and predicted crystallization temperature

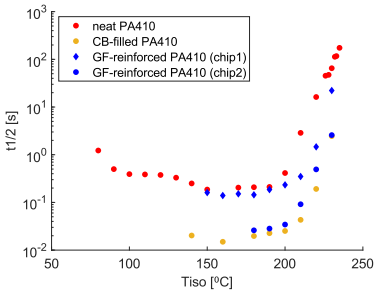

Fig.3 Crystallization half-time for neat, CB-filled and GF-reinforced PA410

Future work

- Experimentally investigate the relation between melting temperature and crystallization temperature
- Establish the relation between fibre volume fraction and resulting crystallization kinetics
- Experimentally investigate the co-crystallization between different grades of a polymer

Estimating physical parameters from simulation data with the ensemble Kalman filter

M.W. Berghuis[1], A. Stanić[1], A. Sadeghi[2], B. Rosić[1]

[1]Chair of Applied Mechanics & Data Analysis, University of Twente
[2]Department of Biomechanical Engineering, University of Twente

Objective

This project aims at simulating the behaviour of a **soft hyperelastic segment** using **physics based models** and experimental data obtained by **digital image correlation**. Assimilating the model with the data, i.e. estimating the physical parameter values, is done using probabilistic interference [1,2]. This is implemented using a **sequential Ensemble Kalman Filter** (EnKF [3]). Some challenges that are tackled with this assimilation method are:

- the discrete model is **high dimensional**. The observation forecasts given prior knowledge are therefore computationally expensive.
- the parameter-observation map is **nonlinear** (hyperelasticity, geometric nonlinearity)
- Sequential estimation requires **restarting** of simulations with updated estimates. This is disproportionally expensive for FEM models

These problems are addressed by adopting a two-stage forecast-assimilation method [4].

Simulation model

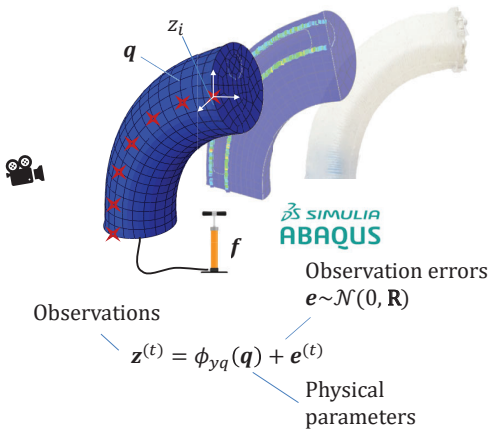

Ensemble Kalman filter [3]

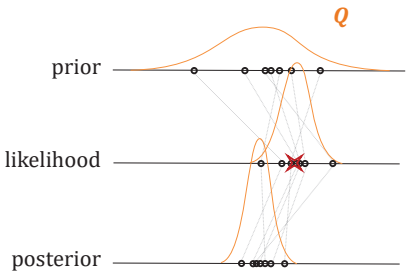

Observation forecasting [4]

Offline

- Propagate prior ensemble $Q^{(0)}$ trough FEM simulation to obtain forecasted evolution of the observations $Y_{fe}^{(t)}$ for $t = 0, \dots, N_t$.

Online

- Assemble parameter $Q_a^{(t)}$ from $Y_f^{(t)}$ and $Z_*^{(t)}$

$$Q_a^{(t)} = Q_f^{(t)} + \hat{K}^{(t)}\left(Z_*^{(t)} + E_f^{(t)} - \phi_{yq}\left(Q_f^{(t)}\right)\right)$$

with the Kalman gain $\hat{K}^{(t)} = C_{qy}\left(C_{yy} + R\right)^{-1}$

- Predict the observation $Y_f^{(t+1)}$ from $Y_{fe}^{(t+1)}$ and $Q_a^{(t)}$

$$Y_f^{(t+1)} = Y_{fe}^{(t+1)} + B^{(t)}(Q_a^{(t)} + E_{rf}^{(t)} - Q^{(0)})$$

with B is the pseudo-Kalman gain relating $Y_{fe}^{(t+1)}$ and $Q^{(0)}$

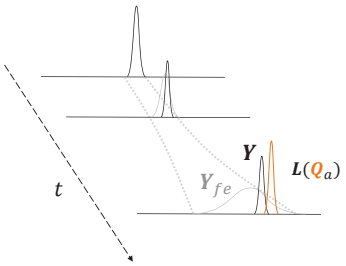

Numerical experiments

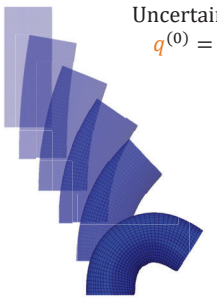

Uncertain Neo-Hookean material model

$q^{(0)} = C_{10} \sim lN(0.006115, 10\%\ \mu_{C_{10}}{}^2)$

Observations:
surface nodal displacement
$z_i = [u_{xi}, u_{yi}, u_{zi}]^T$
for $N_t = 10$ timesteps

Measurement noise
$v \sim \mathcal{N}(0, R), \sigma_z = 1\%\ \mu_z$

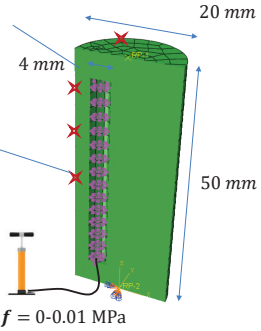

Results

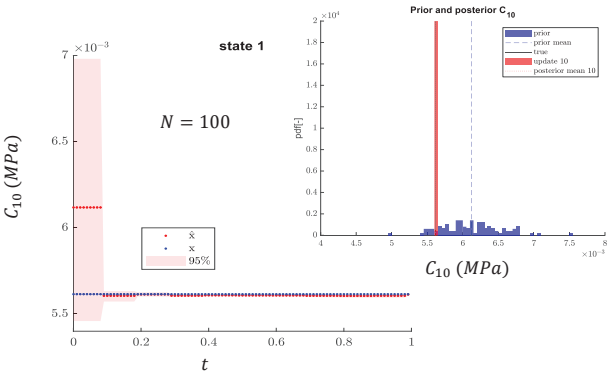

Contact details

m.w.berghuis@utwente.nl
www.linkedin.com/in/minke-berghuis

Conclusion

- Offline surface displacement observation forecasts enable online (material) parameter updates
- Succesful reduction of uncertainty for static NH material parameter

Future work

- Nonlinear arc-length solver in forecast simulation with synchronization procedure
- Experimental data from DIC as observations
- Higher dimensional parameter vector

References

[1] Matthies, H. G., et al. "Bayesian parameter estimation via filtering and functional approximations." *arXiv preprint arXiv:1611.09293* (2016).
[2] Rosić, B., et al. "Parameter identification in a probabilistic setting." *Engineering Structures* 50 (2013): 179-196.
[3] Evensen, G. "The ensemble Kalman filter: Theoretical formulation and practical implementation." *Ocean dynamics* 53 (2003): 343-367.
[4] Dobrilla, Simona, et al. "Bayesian inference of mesoscale mechanical properties of mortar using experimental data from a double shear test." *Computer Methods in Applied Mechanics and Engineering* 409 (2023): 115964.

UNIVERSITY OF TWENTE.

PhD progress

1 | 2 | 3 | 4

Fibre-Matrix Distribution Evolution of Thermoplastic Composite Fusion Bonding Interfaces

G. Bieleman[1,2], W.J.B. Grouve[1,2], E.T.J. Klompen[2]

[1]Production Technology, University of Twente
[2]ThermoPlastic composites Research Center

Motivation

Weight reduction of air and road transport vehicles is vital to reduce greenhouse gasses emitted by the transportation sector. Thermoplastic composite (TPC) materials are ideal for weight reduction. TPC parts can be fusion bonded into larger structures, allowing for energy and time-efficient assembly by excluding the weight of foreign material at the interface.

Problem statement

The performance of fusion bonded structures is governed by the interface, which is affected by the fibre-matrix distribution. Hence, performance prediction of fusion bonded TPC structures requires knowledge of process-induced fibre-matrix redistribution. This work aims to develop predictive tools for the fibre-matrix redistribution of fusion bonding interfaces.

One-step overmoulding process

Fusion bonding process of initial focus

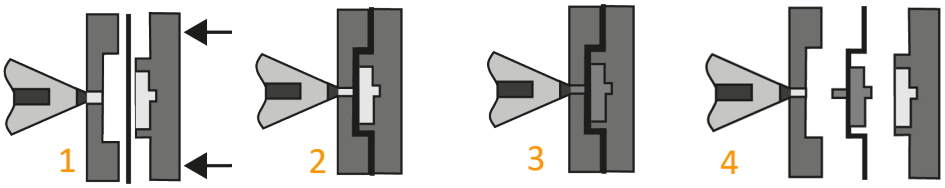

1) Starting conditions
2) Mould closure (blank forming)
3) Injection secondary structure
4) Part ejection

Mechanisms

Transverse squeeze flow
Ply movement (tool-ply, ply-ply friction)
Percolation

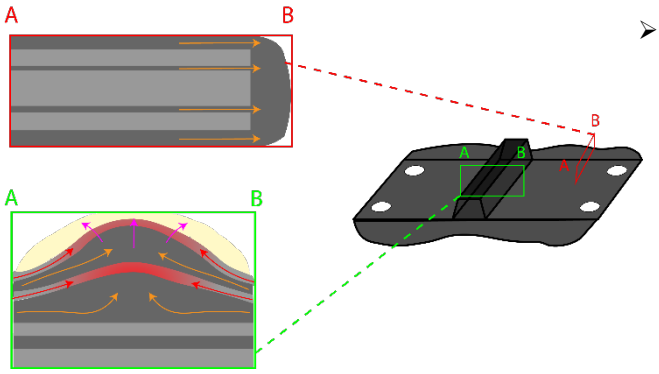

Identification of fibre-matrix redistribution mechanisms

- Focus on mould closure step of the one-step overmoulding process
- Perform forming experiments, with flat moulds containing cavities, which resemble injection moulding cavity
- Study micrographs around the cavity and edges to identify fibre-matrix redistribution mechanisms

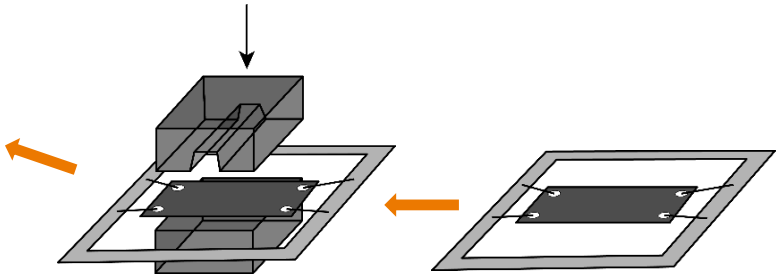

Characterisation Transverse squeeze flow

- Compress a molten UD pre-consolidated block of TPC between two compression platens
- Set compression speed, log force and local displacement
- Two materials
  - UD G/PA4.10 (50x50x1,7mm^3)
  - UD C/LMP (50x50x9,2mm^3)

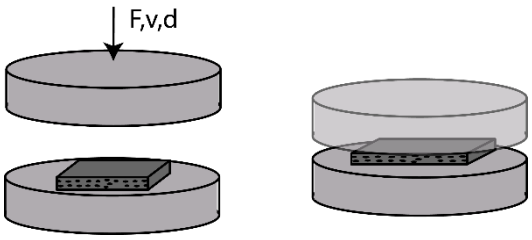

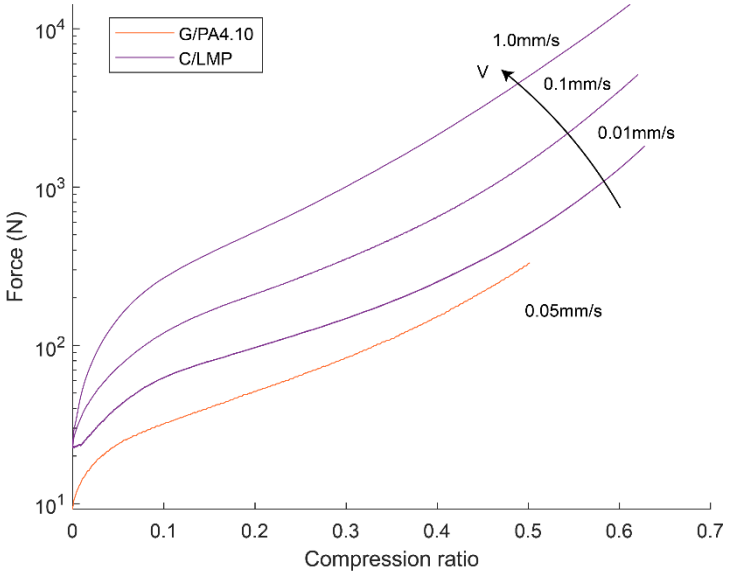

Future work

- Characterisation tool-ply friction, ply-ply friction, percolation
- Modelling framework containing characterised mechanisms

UNIVERSITY OF TWENTE.

PhD progress: 1 | 2 | 3 | 4

TPRC THERMOPLASTIC COMPOSITES RESEARCH CENTER

NWO

M2i materials innovation institute

Mechanical properties of Ti-6Al-4V processed by additive manufacturing

Vincent Blümer, Celal Soyarslan,
Ton van den Boogaard
Nonlinear Solid Mechanics, University of Twente

Content

- AM-processed Ti-6Al-4V is scanned in EBSD microscope
- EBSD images are processed into simulation domains
- Yield points are identified using DAMASK [1]
- Code framework is provided

1. EBSD imaging

- EBSD microscope provides coordinates, material phase information and crystal lattice orientation at datapoints
- Euler angles around ZX′Z″ in Sample coordinate system
- Coordinates in XY of Acquisition coordinate system
- Coordinate systems not generally coincident

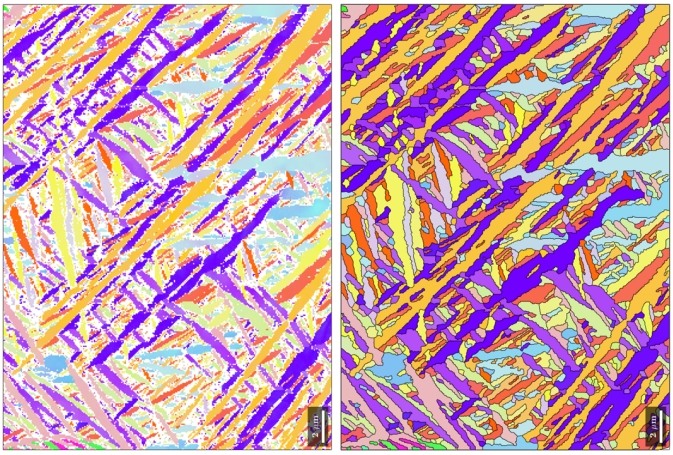

Figure 1: Grain reconstruction from the EBSD-micrograph of martensitic Ti-6Al-4V in Matlab MTEX. A typical α'-HCP microstructure within a prior-β grain region is observed.

2. Image processing in Matlab MTEX

- Grains are reconstructed using Euler angle threshold
- Small grains are removed
- EBSD image is filled to avoid zero stiffness regions

3. Crystal plasticity formulation

- Rate dependent crystal plasticity is used
- Phenomenological power law formulation for slip rates:

$$\dot{\gamma}^i = \dot{\gamma}_0 \left| \frac{\tau^i}{\tau_c^i} \right|^n \operatorname{sgn}(\tau^i)$$

- Plastic velocity gradient is obtained by summing the slip rates over all slip systems:

$$\boldsymbol{L}_p = \dot{\boldsymbol{F}}_p \boldsymbol{F}_p^{-1} = \sum_{i=1}^{N_{\text{sys}}} \dot{\gamma}^i (\boldsymbol{s}^i \otimes \boldsymbol{n}^i)$$

- Material constants and hardening rule from [2] are used

4. Load cases

- The applied stress P_0 is decomposed along x- and y-direction in stress space:

$$\overline{\boldsymbol{P}} = \begin{bmatrix} P_0 \cos(\alpha) & \text{x} & \text{x} \\ 0 & P_0 \sin(\alpha) & \text{x} \\ 0 & 0 & 0 \end{bmatrix}; \quad \overline{\boldsymbol{F}} = \begin{bmatrix} \text{x} & 0 & 0 \\ \text{x} & \text{x} & 0 \\ \text{x} & \text{x} & \text{x} \end{bmatrix}$$

- Load case is defined through macroscopic 1st Piola-Kirchhoff stress $\overline{\boldsymbol{P}}$ and deformation gradient $\overline{\boldsymbol{F}}$
- $\overline{\boldsymbol{F}}$ is constrained minimally to avoid rotations

5. Numerics

- Maximum FFT iterations are reduced from the standard 250 to 15
- Increment cutbacks reduced from standard 3 to 0

6. Macroscopic yield criterion

- Volume averaged, equivalent stress and strain measures are computed from the tensorial 2nd Piola-Kirchhoff stress $\boldsymbol{S}$ and Green-Lagrange strain $\boldsymbol{E}$:

$$\overline{S}_{eq} = \sqrt{\overline{\boldsymbol{S}} : \overline{\boldsymbol{S}}}; \quad \overline{E}_{eq} = \sqrt{\overline{\boldsymbol{E}} : \overline{\boldsymbol{E}}}$$

- From the equivalent measures the 0.2% offset yield strength $R_{p0.2}$ is computed

7. Results

- $R_{p0.2}$ yield strength is computed for all stress paths
- Von Mises and Hill48 yield criteria are fitted to datapoints

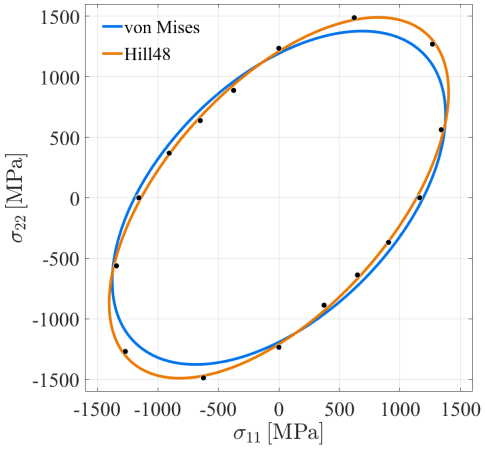

Figure 2: Computed datapoints and fitted yield criteria.

8. Code Availability

https://github.com/vblumer/em-ti-yield-points

References

[1] Roters, F, et al. "DAMASK-The Düsseldorf Advanced Material Simulation Kit for modeling multi-physics crystal plasticity, thermal, and damage phenomena from the single crystal up to the component scale." Computational Materials Science 158 (2019): 420-478.

[2] Somlo, K, et al. "Anisotropic yield surfaces of additively manufactured metals simulated with crystal plasticity." European Journal of Mechanics-A/Solids 94 (2022): 104506.

Composite forming simulations: from characterization to validation

D. Brands[1,2], W.J.B. Grouve[1], S. Wijskamp[2], R. Akkerman[1]

[1]University of Twente, Group of Production Technology

[2]ThermoPlastic composites Research Center (TPRC), Enschede

1 Characterization: Mechanical behavior in melt

Comparison of the bias extension method and torsion rheometry to measure in-plane shear deformation resistance of unidirectional thermoplastic composite materials at forming conditions.

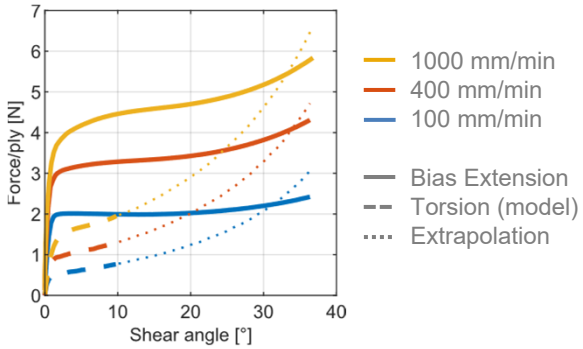

Figure 2: Bias extension response Toray TC1225 at 365°C

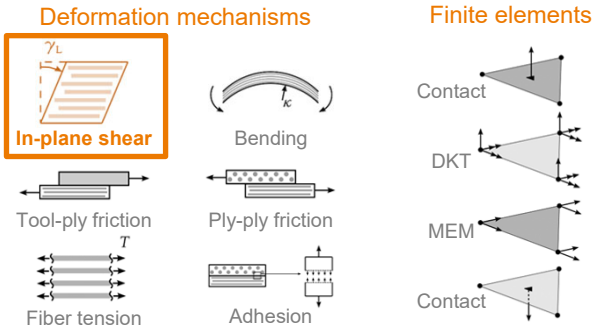

Figure 3: Overview from characterization to simulation

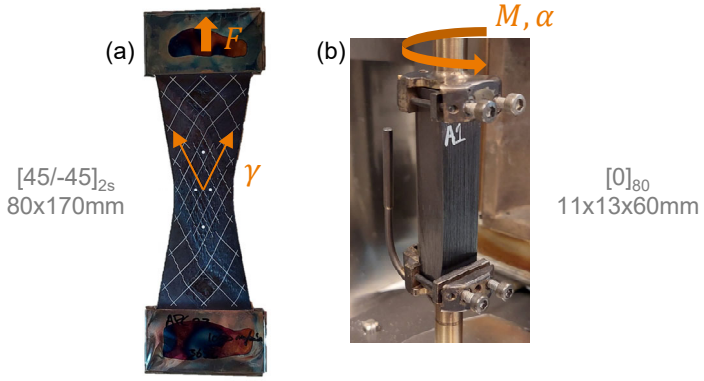

Figure 1: a) Bias Extension, b) Torsion Rheometry

2 Simulation technology

In-plane shear is one of several mechanisms used to describe the deformation of a composite laminate in the simulation. Separation of membrane and bending and the use of layered shell meshes are unique to composite forming simulations.

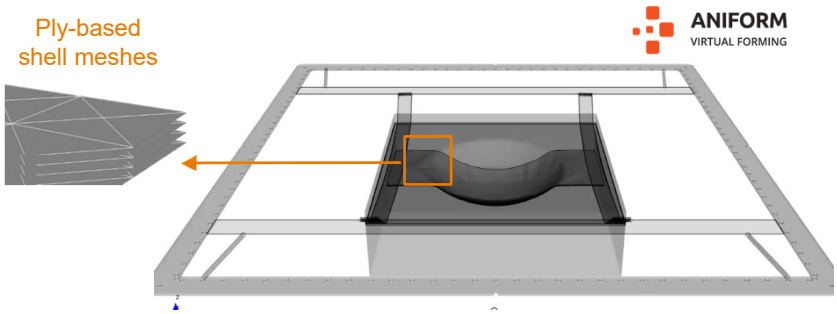

3 Validation: Wrinkling defects & in-plane deformation

A truncated hemisphere geometry is used to deliberately create wrinkling defects in laminates with various dimensions and layups. Deformations are quantified using photogrammetry analysis. Original and revised material cards are considered in simulations, featuring various modifications alongside the changes to in-plane shear.

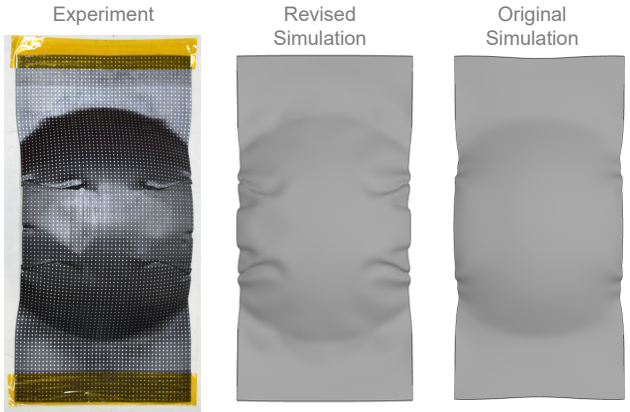

Figure 4: Wrinkling defects, experiment-simulation comparison. Toray TC1225, $[0/90]_{2s}$, 140x295mm, Press formed

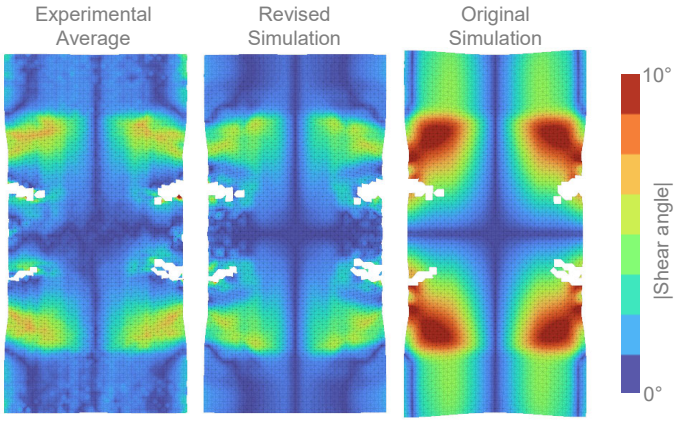

Figure 5: In-plane deformation, experiment-simulation comparison

4 Conclusion

The material cards for forming of unidirectional thermoplastic composites need to be revisited to improve the correlation with experimental wrinkling and deformations. Novel bias extension characterization experiments seem to be a part of a solution, but more research is required into the remaining mechanisms.

Rotational Speed Estimation in Vibration Spectra

S. Bruinsma[1,2], T. Tinga[1,3], R.D. Geertsma[3], R. Loendersloot[1]

[1]University of Twente
[2]Royal Netherlands Navy
[3]Netherlands Defence Academy

Introduction

- Continuous condition monitoring for increased availability
- Full spectrum analysis requires knowledge and experience
- **Feature selection** from spectra towards **AI application**
- Most features depend on rotational speed
- Tacho/speed sensors often not present/preferred

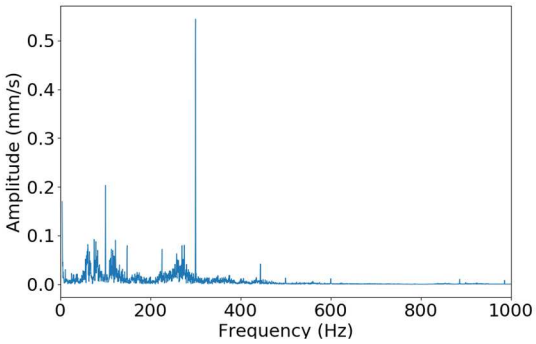

Figure 1: Example velocity spectrum, low 1X, 2X

Aim

Determine rotational speed from the spectrum alone, with minimal a priori knowledge of the measured system.

Method

Final estimate formula:

score = max(sum(amplitude ∗ harmonic) ∗ #points)

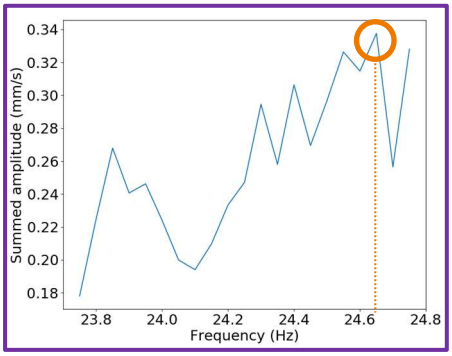

Figure 3: Method first estimate

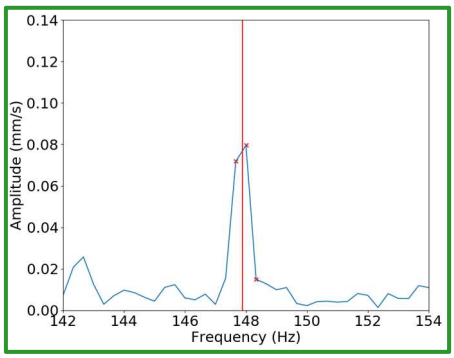

Figure 4: Method parabolic interpolation

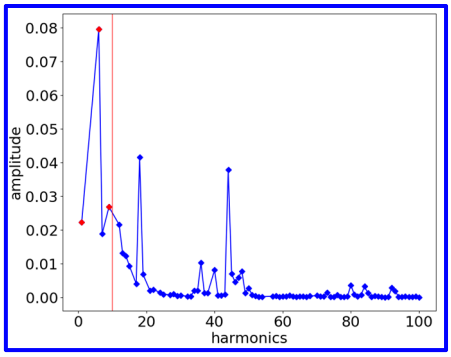

Figure 5: Method 3 highest below 10th

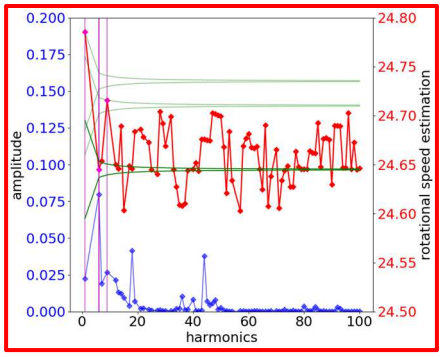

Figure 6: Method final estimate

Challenges

- Well balanced & aligned system
- High degree of accuracy vs. High degree of confidence

Challenges (examples)

- $4\ f_r \neq 2\ f_{LF}$
- $4 * 24.65\ Hz \neq 2 * 50\ Hz$
- $3\ f_r \neq 3.04\ f_r\ (BPFO)$
- $24.6\ Hz * 40 = 984\ Hz$
  $24.7\ Hz * 40 = 988\ Hz$

Results

Table 1: Results per motor, per speed

Motor:	2			4	
Speed:	100%	75%	50%	70%	overall
Accuracy:	82%	94%	86%	91%	88%

Estimation correct if error < 0,0165 Hz
→ within 2 bins at 44th harmonic (RBPF)

Method Flowchart

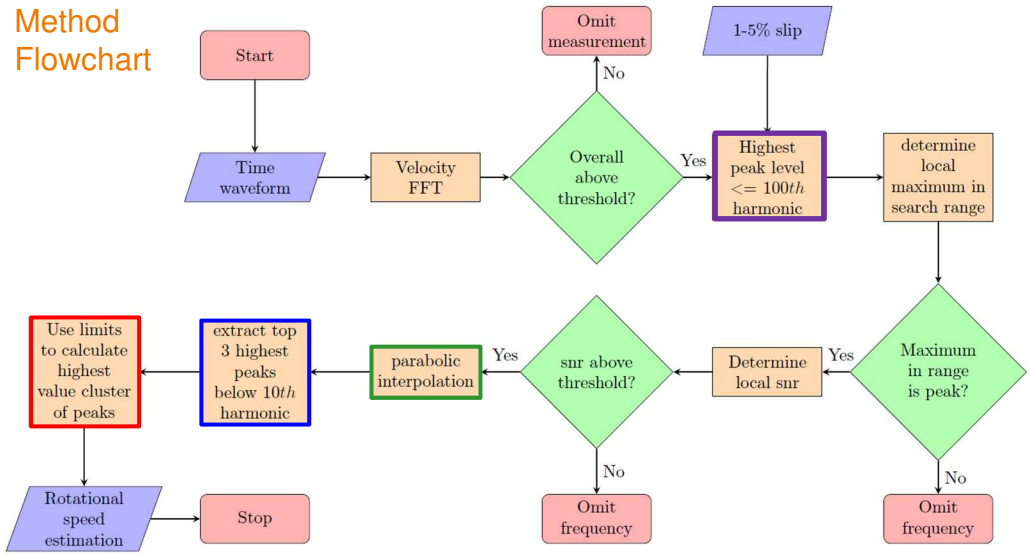

Figure 2: Method flowchart

Next steps

- Test on CWRU[1] bearing dataset
- Compare to other methods
- Finalize paper

References

[1] Loparo, K. Bearings Vibration Data Set; Case Western Reserve University: Cleveland, OH, USA.

Sietze Bruinsma
sj.bruinsma.01@mindef.nl
s.j.bruinsma@utwente.nl

UNIVERSITY OF TWENTE.

PhD progress: 1 | 2 | 3 | 4

Koninklijke Marine

NLDA

Predictive modelling of liquid metal induced fracture in Fe-based alloys

F. Brunner and F. Maresca

Computational Mechanical and Materials Engineering,
University of Groningen

f.brunner@rug.nl

Introduction & Motivation

- **What is liquid metal embrittlement (LME)?**
  Reduction in ductility and toughness of a solid metal in contact with a liquid metal (see Fig. 1 left).
- **LME is crucial for multiple applications** in the automotive and nuclear power industry, soldering, brazing and welding.

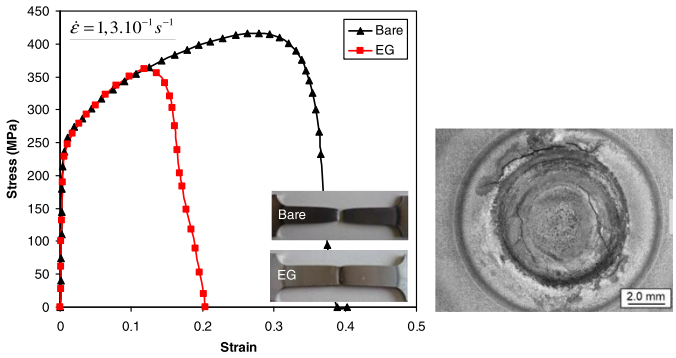

Figure 1: Left: Tensile curves of bare and electrogalvanized (EG) TWIP steel specimens at 700°C [1] Right: Spot weld with surface cracks due to LME [2]

- **Automotive Industry:** Advanced high strength steels (AHSS) have a good combination of strength and ductility. For corrosion protection they are Zn-coated. AHSS parts are joined via spot welds (several thousand in each car body), which can exhibit LME [2] (see Figure 1 right)

→ **great interest in understanding and preventing LME**

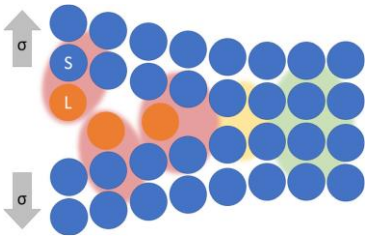

Figure 2: Schematic model of a crack tip in contact with liquid metal [3]

Project Description & Goals

- **Project aim:** Development of a predictive LME model for steels, with main focus on Zn-induced fracture.
- **LME can manifest** through e.g. interatomic bond weakening, micro-plasticity, grain boundary penetration or a combination thereof in the vicinity of crack tips [4] (see Fig. 2) → **LME predictions must account for atomistic processes** like crack tip plasticity and:
  - composition and phase of the solid metal
  - grain boundaries (GB's)
  - environmental factors: temperature, strain-rate, stress
- **Goals:** Contributing to the development of LME-free AHSS and the elucidation of LME in general

Methodology & Current Work

Methodology:

- Study of the intrinsic brittleness/ductility of the solid metal with a combination of molecular dynamics (MD) and linear elastic fracture mechanics (LEFM)
- Simulation of dislocation motion and crack propagation with a combination of MD and density functional theory (DFT)

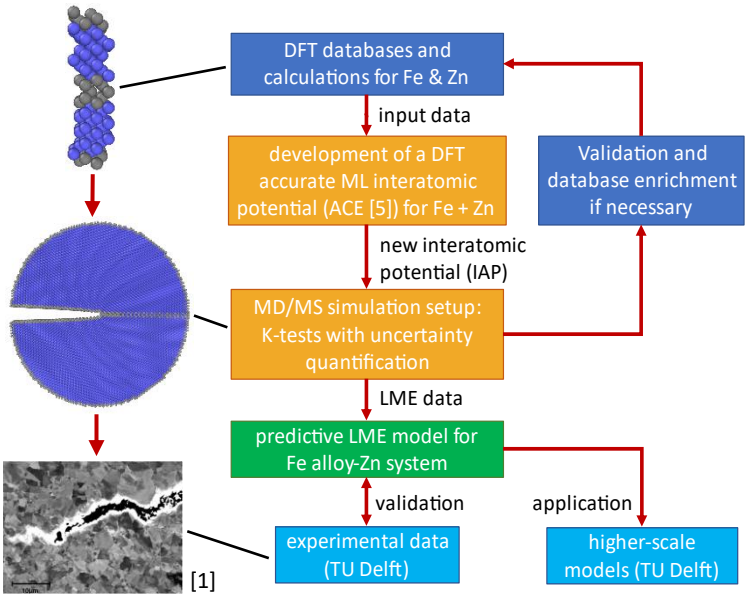

Figure 3: Flow diagram of project methodology

Current Work & Challenges:

- Establishment of a suitable K-test framework for general grain boundaries
  → challenges: predicted oscillations of field quantities
- Development of the intended ML IAP for Fe-Zn
  → challenges: treatment of changing magnetic behaviour at higher temperatures

Research Questions

- What is the intrinsic ductility/brittleness of Fe and fcc and bcc Fe dilute alloys (Zn, Mg, Si, Al, Mn)? To which degree is it altered due to the presence of a liquid metal?
- Which GB's in fcc and bcc Fe-alloys are most susceptible to LME and why?
- What are the main (nano-scale) criteria for design of LME-resistant steels?

References

[1] C. Beal, X. Kleber, D. Fabregue, M. Bouzekri; Scr. Mater. **66**, 1030-1033
[2] WorldAutoSteel. *Combined reports - AHSS implementation solution: liquid metal embrittlement study*. 2020
[3] J.E. Norkett, M.D. Dickey, V.M. Miller; Metall. Mater. Trans. A **52**, 2158–2172
[4] X. Gong. *Liquid Metal Embrittlement of a 9Cr-1Mo Ferritic-martensitic Steel in Lead-bismuth Eutectic Environment under Low Cycle Fatigue*. PhD thesis. 2015
[5] R. Drautz; Phys. Rev. B **99,** 014104

Induction Heating of Unidirectional Thermoplastic Composites

Thermographic and electrical characterisation

Y. M. Buser[1,2], W.J.B. Grouve[2], E. Krämer[1], R. Akkerman[1,2]

[1]ThermoPlastic composites Research Center (TPRC)

[2]University of Twente

Introduction

Induction welding is an attractive technology for the fusion bonding of carbon fibre reinforced thermoplastic composites. In this process, **eddy currents** are induced in the carbon fibre network by an alternating electromagnetic field, which heats up the parts (→). In **unidirectional ply-based composites**, the formation of eddy currents relies on the ply interfaces to create efficient closed-loop pathways. A deeper understanding of how this fibrous architecture governs heat generation is required to improve control and/or predictability for large scale application of the welding process, enabling lightweight aircraft construction.

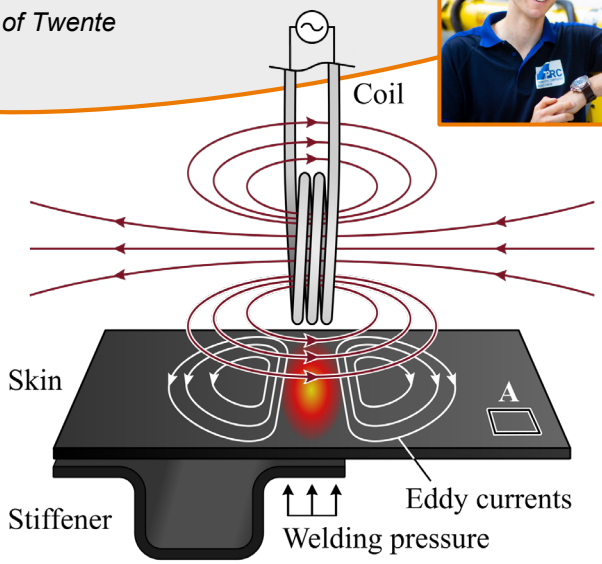

Electrical conductivity characterisation

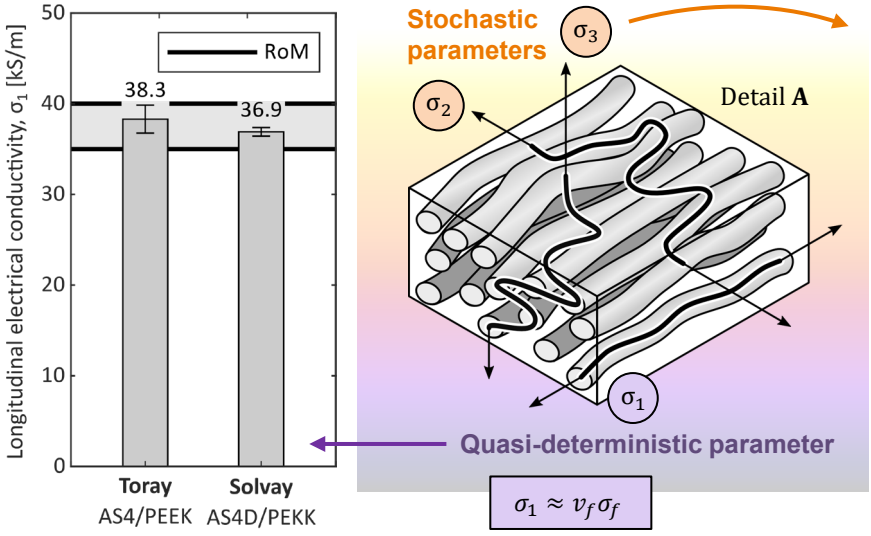

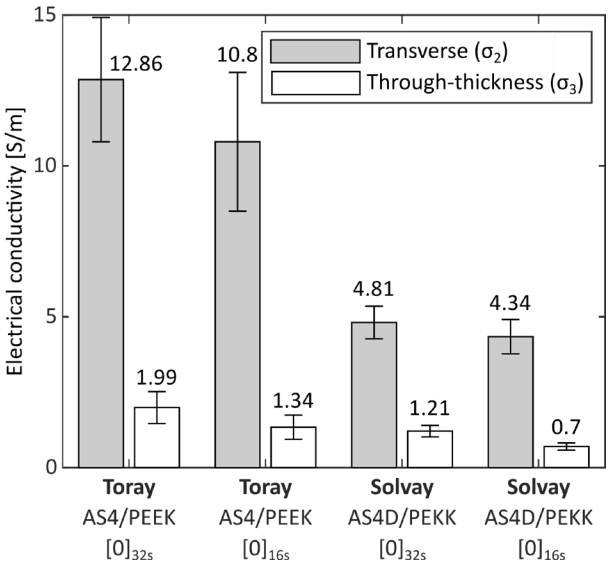

Induction heating simulations

AS4/PEEK laminates where heated with a **stationary coil** (⟮⟯), while monitoring the heating response with an **IR camera**. The experiment is reproduced in **thermo-electrical simulations** (↓), adopting the characterised electrical conductivity data (↑).

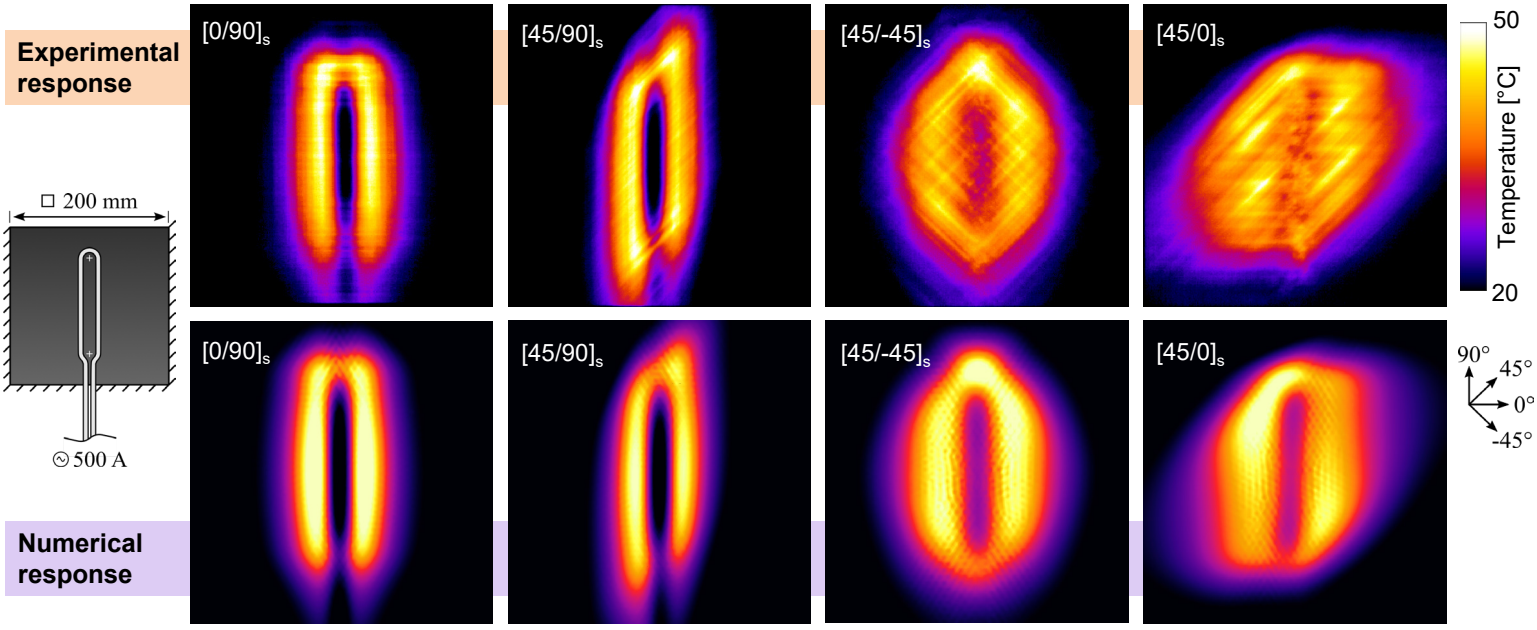

PhD progress

1 2 3 4

UNIVERSITY OF TWENTE.

A numerical framework for the electro-mechanical analysis of conductive tracks in printed electronics

Britt Cordewener, Marc Geers, Joris Remmers

Eindhoven University of Technology

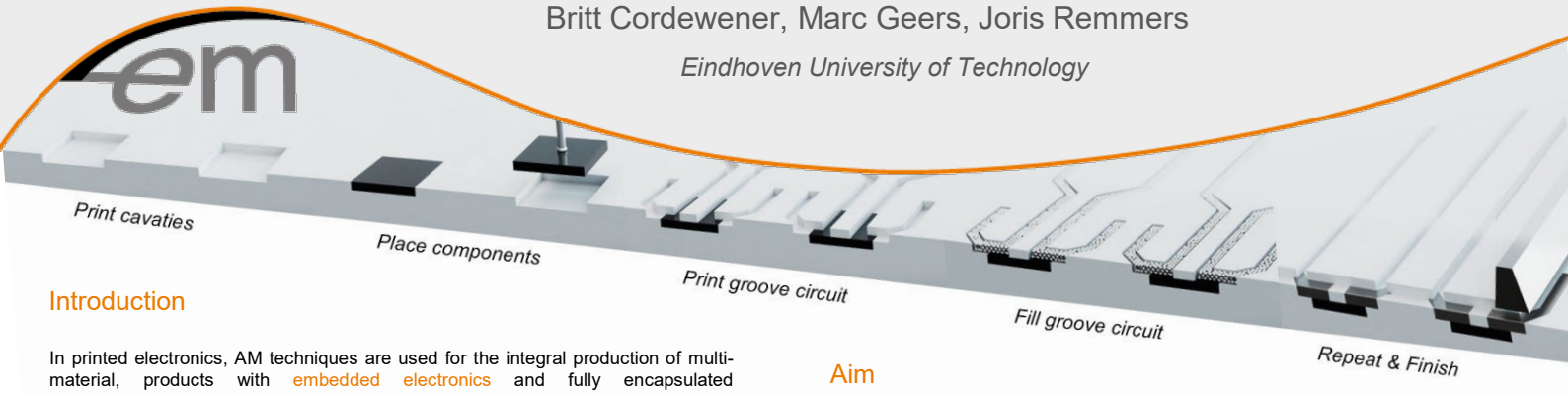

Introduction

In printed electronics, AM techniques are used for the integral production of multi-material, products with embedded electronics and fully encapsulated interconnecting conductive tracks. The electro-mechanical performance of the printed conductive tracks is strongly depending on the composition of the conductive inks and the microstructure obtained after processing of the inks. To analyze this performance in terms of the resistivity, a multi-physics model is created that allows for the analysis of the effects of strains imposed on the microstructure of a track and the prediction of the electro-mechanical performance of given ink compositions.

Aim

- Prediction of performance for given ink compositions
- Analyze & predict malfunctioning/failure tracks
- Improved strategies for printing of conductive materials

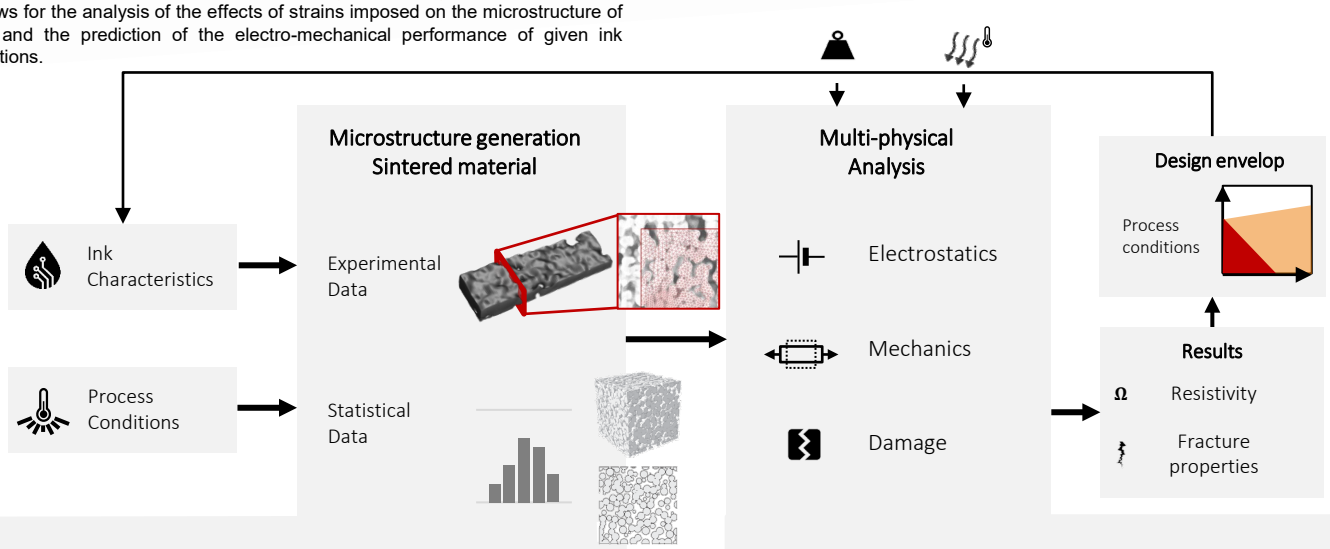

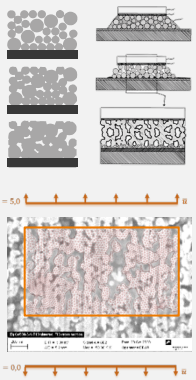

Microstructure generation

Why |

An adequate geometrical representation of the microstructure is required as an input for the multi-physics model. Microstructure of sintered track depends on process conditions and Ink characteristics and governs the Electro-mechanical performance.

How |

Experimental Data
- 2D → FIB SEM images
- 3D → CT scans

Statistic generation
- Particle size distribution
- Sintering

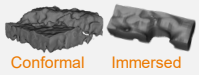

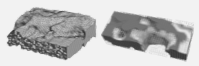

Numerical Framework

What |

Modelling electro-mechanical fracture with two successive mechanisms:

I. Mechanical fracture of the solid
II. Decrease of conductivity as a direct result

How |

Multi-field approach:

- $\boldsymbol{u}$ Displacement
- ϕ Electric potential
- d Crack phase-field

Solver |

The system is implemented in a finite element framework and solved using a staggered procedure in combination with a dissipation based solver.

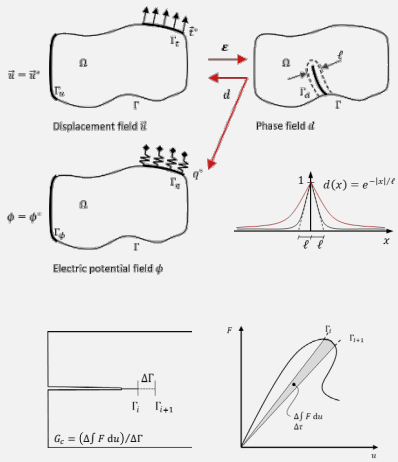

Results |

The effective resistivity of simplified representations of conductive tracks under mechanical loading is analyzed. The contour plots show the development of damage and its consequence on the potential field distribution.

- An increase in resistivity is observed, which is caused by crack formation in the conductive material, that resembles the trends observed in experimental research.
- Besides the porosity, the percolation path is identified as a relevant geometric feature for the fracture properties.
- Parameter studies with synthetic RVE's will give insights in the effects of sintering times and particle size distributions.

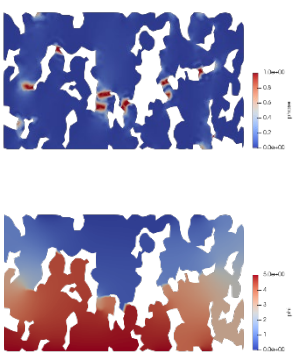

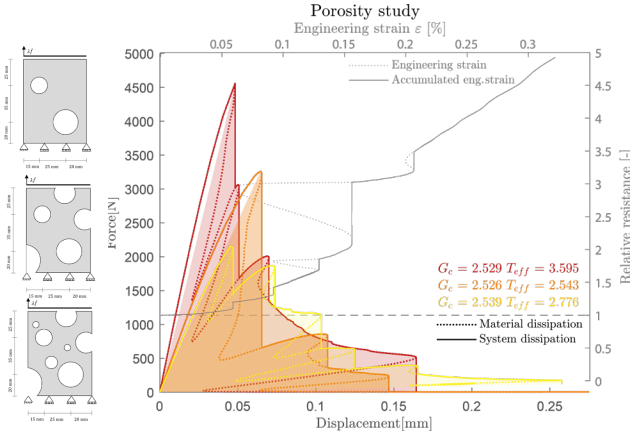

Variational Multiscale stabilization of the Magnetohydrodynamics equations

K.W. Dijkstra[2], D. Toshniwal[2],

[2] *Delft University of Technology*

Introduction

The incompressible resistive Magnetohydrodynamics (MHD) equations are a model that describes electrically conducting fluids. Examples of these include solar flares, but also the magnetically confined plasma in fusion reactors.

This model is a combination of the incompressible Navier-Stokes equations and the reduced Maxwell equations. Because of this, the same instabilities arise for the high Reynolds number case. Because of this, for the same reason, we can use stabilization techniques for Navier-Stokes for MHD. We have chosen for variational multiscale (VMS), which incorporates the effect of the fine sub-scales that cannot be captured by the finite element space. In addition, we make use of compatible B-spline space discretizations to investigate the usefullness of Finite Element Exterior Calculus for the incompressible resistive MHD equations.

Magnetohydrodynamics

The incompressible resistive Magnetohydrodynamics model is given by:

$$\partial_t \mathbf{u} + \mathbf{u}\cdot\nabla\mathbf{u} - \mathrm{R_e}^{-1}\Delta\mathbf{u} + \nabla p - \mathrm{S}\mathbf{J}\times\mathbf{B} = f\,, \tag{1a}$$

$$\mathbf{J} - \mathrm{R_m}^{-1}\,\mathrm{curl}\,(\mathbf{B}) = 0\,, \tag{1b}$$

$$\partial_t \mathbf{B} - \mathrm{curl}\,(\mathbf{E}) = 0\,, \tag{1c}$$

$$\mathrm{div}\,(\mathbf{u}) = 0,\ \ \mathrm{div}\,(\mathbf{B}) = 0\,. \tag{1d}$$

Where $\mathbf{J} = \mathbf{E} + \mathbf{u}\times\mathbf{B}$ is the current density, $\mathrm{R_e}$ and $\mathrm{R_m}$ are respectively the fluid / magnetic Reynolds numbers and S is the Lundquist number. The MHD equations can be seen as the combination of the incompressible Navier Stokes equations and Maxwell equations, where the fluid is electrically charged, and hence experiences a lorentz force $\mathbf{J}\times\mathbf{B}$.

Variational Multiscale

Within VMS, the fine scales that are not captured by the coarse scales (associated to a finite element space $V_h \subset V$) are incorporated to stabilize the method. Given a general weak form

$$(\mathbf{u}, \mathbf{v}) = \langle f, \mathbf{v}\rangle \ \ \forall \mathbf{v} \in V\,. \tag{2}$$

Here $(\cdot,\cdot)$ is some bilinear form. Let $u_h = \mathbb{P}u$ be the solution of (2) projected onto the finite element space V_h. Then, using the orthogonal decomposition $V = V_h \oplus V'$, the general weak form of (2), can be split into:

$$(\mathbf{u}^h, \mathbf{v}^h) + (\mathbf{u}', \mathbf{v}^h) = \left\langle f, \mathbf{v}^h\right\rangle \qquad \forall \mathbf{v}^h \in V^h\,, \tag{3a}$$

$$(\mathbf{u}^h, \mathbf{v}') + (\mathbf{u}', \mathbf{v}') = \langle f, \mathbf{v}'\rangle \qquad \forall \mathbf{v}' \in V'\,. \tag{3b}$$

By solving / approximating problem (3b) for $\mathbf{u}'$, and using this expression to eliminate $\mathbf{u}'$ from (2), we obtain the VMS formulation.

VMS stabilization of MHD

The MHD equations are stabilized in a similar approach as in [1] while using compatible B-spline spaces. Two fine-scale components are introduced, the fine-scale pressure p' and the fine-scale velocity $\mathbf{u}'$. In the steady state case, the latter is approximated as follows

$$\mathbf{u}' = \tau_M\left(f - \mathbf{u}_h\cdot\nabla\mathbf{u}_h + \mathrm{R_e}^{-1}\nabla\mathbf{u}_h - \nabla p_h - \nabla p' + \mathrm{S}\mathbf{J}\times\mathbf{B}\right)\,, \tag{4}$$

while ensuring that this fine-scale velocity is divergence free. In contrast to the velocity fine-scales, the fine-scale pressure is not eliminated from the equations, but instead is sought in a finite element space which at least contains the coarse-scale pressure space.

Further outlook

As the preliminary results look promising, we aim to investigate

- fine-scale for **E** and **B** components (and if these are needed)
- local refinement with THB-splines (potentially driven by fine-scale components)

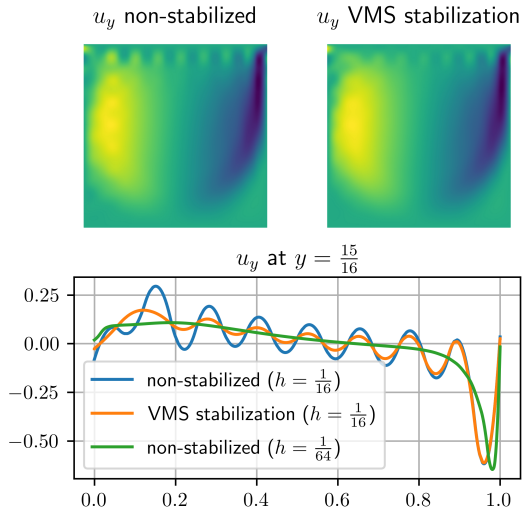

Figure 1: The velocity y-component of a lid driven cavity problem for $\mathrm{R_e} = \mathrm{R_m} = 1000, \mathrm{S} = 0.3$ with $h = \frac{1}{16}$ over the unit square. The right most figure shows the same velocity y-component for the slice $y = \frac{15}{16}$ and compares both to the non-stabilized and the VMS stabilized with a non-stabilized high resolution $h = \frac{1}{64}$ simulation.

References

[1] J. A. Evans, D. Kamensky, and Y. Bazilevs, "Variational multiscale modeling with discretely divergence-free subscales," Computers & Mathematics with Applications, vol. 80, no. 11, pp. 2517–2537, Dec. 2020, doi: 10.1016/j.camwa.2020.03.011.

Computational Modeling of Hydrolytic Degradation in Oil Paintings

E.A. Dizman[1], A.S.J. Suiker[1], E. Bosco[1]

[1] *Eindhoven University of Technology*
Department of the Built Environment

Introduction

Oil paintings are highly susceptible to chemical and physical degradation processes over time, triggered by the effects of environmental conditions, such as humidity and temperature fluctuations. These ageing phenomena may result in visible changes, namely cracks and delaminations. As a result, the paint surface may lose its integrity, which affects the expected lifespan of the painting.

(a) (b)

Figure 1: Examples of cracking mechanisms in oil paintings. (a) and (b) are taken from [1] and [2], respectively.

As far as chemical changes are concerned, moisture diffusion leads to hydrolysis processes in the oil paintings, which result in the cleavage of the ester bonds in the cross-linked polymer. This process is described as

$$\text{ESTER BONDS} + H_2O \rightarrow \underbrace{\text{R–COOH}}_{\text{carboxylic acid group}} + \underbrace{\text{R'–OH}}_{\text{hydroxyl alcohol group}}$$

where R and R' denote the remaining parts of the polymer chain. Hydrolysis has consequences for the mechanical response of the painting, as it is linked to a reduction in the tensile strength of the paint. The study aims to predict the degradation of oil paintings by formulating a thermodynamically-consistent model coupling a diffusion-reaction model and a mechanical model. This model will provide insight for art conservators to counteract further deterioration.

Thermodynamical Framework

In order to develop a model for degradation of oil paintings by hydrolysis processes, a thermodynamic framework is constructed. For this purpose, the Helmholtz free energy ψ is split into elastic, plastic and diffusion parts as commonly done in the literature.

$$\psi(\boldsymbol{\varepsilon}_e, c, \mathbf{I}) = \psi_e + \psi_p + \psi_m \tag{1}$$

which can be used to obtain

$$\boldsymbol{\sigma} = \frac{\partial \psi}{\partial \boldsymbol{\varepsilon}_e} \quad \text{and} \quad \mu = \frac{\partial \psi}{\partial c} \tag{2}$$

where $\boldsymbol{\sigma}$ and μ refer to the Cauchy stress and chemical potential, respectively. Damage due to hydrolysis for cross-linked polymers is defined in [3] via a decay in the material fracture strength

$$D^{hydr} = 1 - \frac{\sigma_t}{\sigma_0} \quad \text{and} \quad \sigma_t = \sigma_0 \, e^{-ut} \tag{3}$$

$$u = kec \tag{4}$$

u = hydrolytic degradation rate of the material
k = rate of hydrolysis
e = ester content
c = water content

Numerical Modelling

A sequentially coupled finite element framework is adopted for the numerical implementation of the multi-physics problem, coupling moisture diffusion to the mechanical response. For this purpose, the UMATHT subroutine provided by the commercial software Abaqus is tailored to model the moisture diffusion part of the numerical framework using the analogy between heat transfer and mass diffusion.

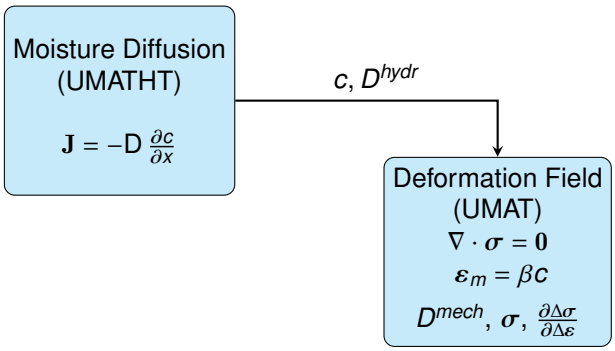

Outlook

In the future, the numerical framework described above can be enhanced by adapting the constitutive model developed for cross-linked polymers [4] to model hydrolytic degradation.

References

[1] Elkhuizen, W.S., Callewaert, T.W.J., Leonhardt, E. et al. (2019). Comparison of three 3D scanning techniques for paintings, as applied to Vermeer's 'Girl with a Pearl Earring'. Heritage Science 7(89).

[2] Canadian Conservation Institute (2017). Government of Canada. https://www.canada.ca/en/conservation-institute/services/conservation-preservation-publications/canadian-conservation-institute-notes/know-your-paintings-deterioration.html

[3] Vieira, A. C., Vieira, J. C., Ferra, J. M., Magalhães, F. D., Guedes, R. M., & Marques, A. T. (2011). Mechanical study of PLA–PCL fibers during in vitro degradation. Journal of the Mechanical Behavior of Biomedical Materials, 4(3), 451-460.

[4] Bahrololoumi, A., Morovati, V., Poshtan, E. A., & Dargazany, R. (2020). A multi-physics constitutive model to predict hydrolytic aging in quasi-static behaviour of thin cross-linked polymers. International Journal of Plasticity, 130, 102676.

A road to more sustainable steel production:

Understanding the effects on impurity elements on the mechanical performance of steel by bridging RVE data to micromechanical tests

L.R. Dodsworth[1]

[1]*Mechanics of Materials (MoM) group, Mechanical Engineering, Eindhoven University of Technology*

Introduction

This project is part of the DEPMAT project, which aims at reducing the carbon emissions of steel production, currently responsible for around 7% of global carbon emissions, by increasing the amount of recycled steel used in steel production. The inherent elemental and hence mechanical property inconsistencies of recycled steel, limit the applications and the amount of recycled steel used today. DEPMAT aims to address these inconsistencies by compensating the fluctuation in properties, by live adjustments of the processing parameters, as shown in Fig.1.

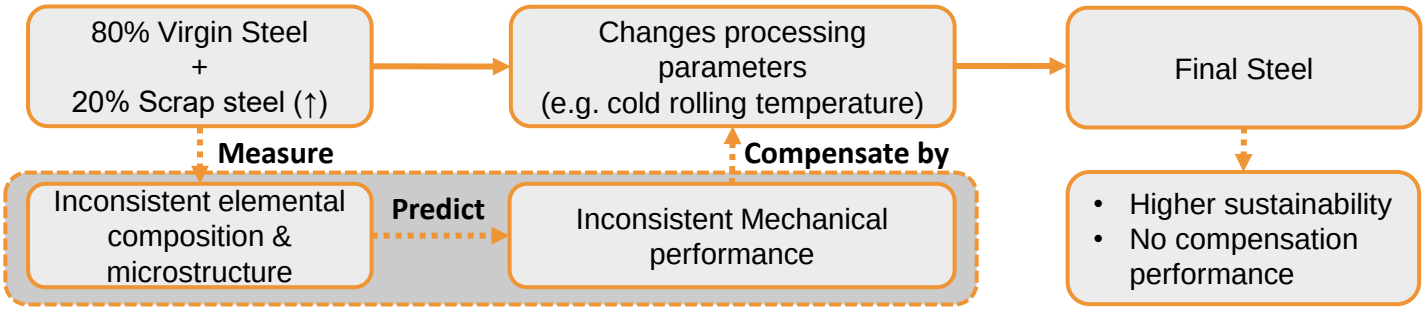

Fig. 1: Proposed greener steel workflow DEPMAT

The fast prediction of mechanical performance from inconsistent elemental composition and microstructure, highlighted in gray in Fig.1, will be done through neural network or model-free methods. Because these require a lot of data, not only experimental but also simulated RVE data will be required. My PhD project focusses on comparing the experimental and simulated data at different impurity concentrations, and if necessary improve the simulations to include the effects of these impurity elements. From literature, based on their concentration and effect on the microstructure and by extend mechanical performance, it was concluded that Cu, Ni, Sn, Mo & Cr are the most impactful elements for recycling.

Proposed workflow

Experimental micromechanical tests

Specimen preparation:
Twin-jet polishing → Ultra-thin samples allow for quasi 3D (2.5D) microstructural analysis

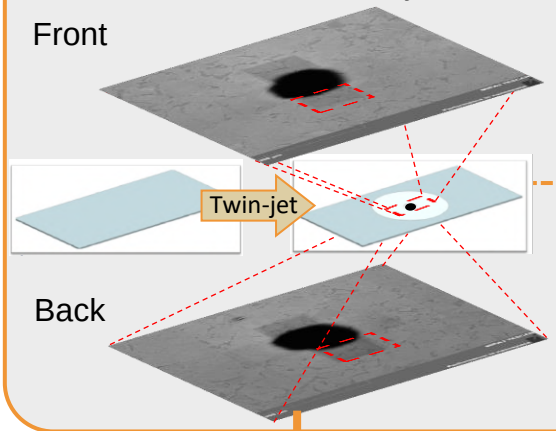

Structural analysis

BSE EBSD

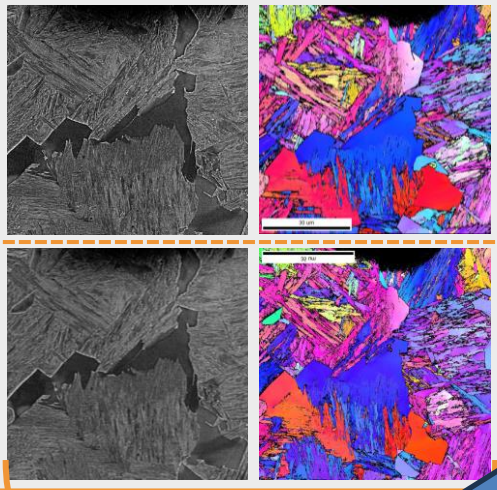

Tensile response analysis

Tensile test

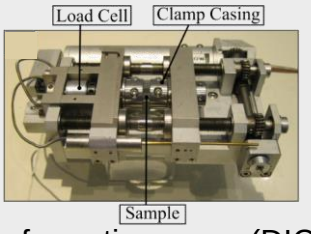

Deformation maps (DIC)

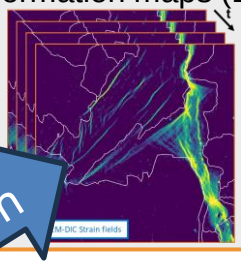

+Thickness map

3D mesh

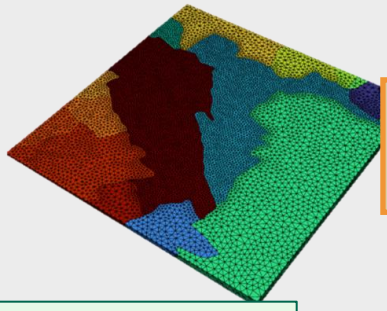

Crystal plasticity simulation

Tensile response

Comparison

Comparison exp. & num.

How good for different impurity concentrations?

↓

Are addition mechanisms in simulations required?

- Precipitates in grain
- Grain boundary precipitates
- Solid solution hardening

Vermeij & Wijnen *et al.* (2023)

PhD progress

1 2 3 4

Physically consistent data-driven constitutive models by machine learning

A. Fallahnejad, E.S. Perdahcioglu, T. van den Boogaard

Chair of Non-linear Solid Mechanics, Department of Mechanics of Solids, Surfaces & Systems (MS3), University of Twente

Email: a.Fallahnejad@utwente.nl

LinkedIn profile

Problem Statement

- Blast furnaces are the biggest emitters of CO_2 due to the iron extraction from ore.
- A really high load on the environment because of the huge amounts of unused scrap.

Challenges

More Scrap → More Impurities (Al, Mn, Cr,…) → More scatter in material composition

Lack of accuracy and pace at the same time in the present models through the steel manufacturing

The crucial need for models capable of capturing **higher orders of details**

Project Scheme

Microstructure Information

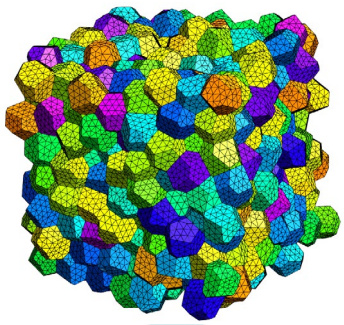

- Investigating multiple RVEs under different loading directions and discovering the correlations between parameters.
- Investigating and building the ML model and making sure to obey the physics principles.
- Building the base UMAT model for isotropic material.
- Modifying and enhancing the UMAT with extra microstructure features.

Crystal Plasticity Simulations → **ML** → **Fully functioning Constitutive Model**

Goals and Outcomes

- More flexibility, a wider range and better control over the desired properties.
- More competitive products.
- A substantial decrease in CO_2 emissions.
- A novel ML model that can fully replace the intermediate stages and be trained with crystal plasticity simulations.

UNIVERSITY OF TWENTE.

PhD progress: 1 | 2 | 3 | 4

materials innovation institute

Experimental Identification of Nonlinearity and Eigenvalue Assignment of a Nonlinear Electromagnetic System by the Receptance Method

Mahshad Farzannasab1* Maryam Ghandchi Tehrani1

1 Engineering and Technology Institute Groningen (ENTEG), University of Groningen, Groningen, The Netherlands

Introduction

Control of nonlinear structures is challenging because of the complex mathematical model [2].
Receptance method is beneficial technique in order to prevent resonance [1]. In this study, active vibration control for eigenvalue assignment of a nonlinear system is presented experimentally using the receptance method. To identify existence of nonlinearity experimentally, a step-sine test was performed. In cases of nonlinearity, the system's response would definitely change with variations in the amplitude of the input voltage. At the final step, in order to perform eigenvalue assignment, the desired closed-loop poles were determined through curve fitting of the measured data.

Experimental Setup

For this study, an experimental setup was constructed with a cantilever beam. A loudspeaker and an accelerometer were attached to the beam in order to create force and measure the acceleration of the beam (Figure 1). The free end of the beam was connected to a pair of identical neodymium bromide magnets, and two identical coils were placed parallel to the magnets. When the electrical current in the coils was turned on, the magnetic field created around the beam could introduce cubic stiffness into the mathematical model of the system, which was the reason for nonlinearity in the system.

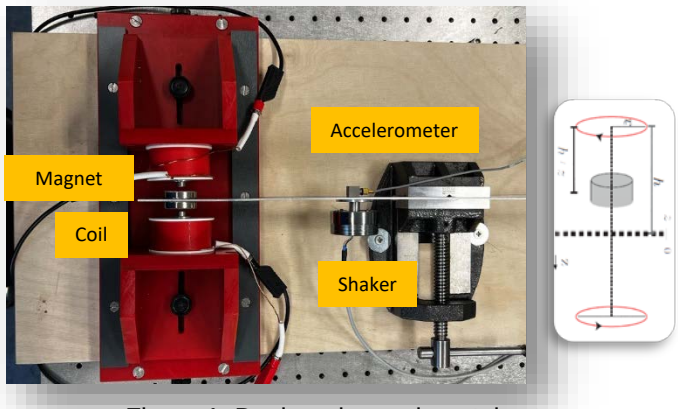

Figure 1: Designed experimental setup

Method

To identify the existing nonlinearity experimentally, a step-sine test was performed over a frequency range of 1 to 160 Hz, at four different amplitudes, both with the electrical currents switched on and switched off. In the next step, the Frequency Response Functions of the fundamental harmonics at all amplitudes are compared with each other. In cases of nonlinearity, the system's response would definitely change with variations in the amplitude of the input voltage. For eigenvalue assignment, the receptance of the open-loop is first measured experimentally. Then, the Sherman-Morrison formula is used to calculate the feedback gains.

Since, unlike linear systems, the response of nonlinear systems depends on both amplitude and frequency, an iterative Sherman-Morrison algorithm is developed to calculate the feedback gains for eigenvalue assignment. Finally, the control gains obtain from the simulation are experimentally implemented in real-time, demonstrating successful pole assignment. The system remains stable at various excitation levels and different distances between the coils and magnets.

Results

Figure 2, shows the effect of changing the displacement between the coils in the constant electrical current, numerically and experimentally.

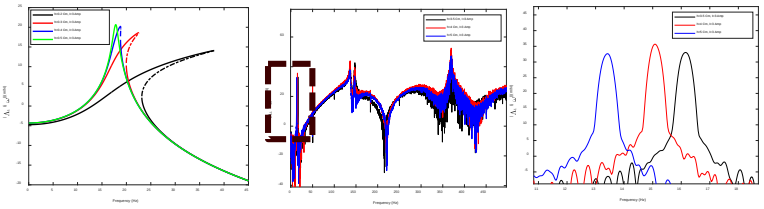

Figure 2: Effect of changing the displacement in the constant electrical current

Figure 3, shows the result of pole-placement numerically.

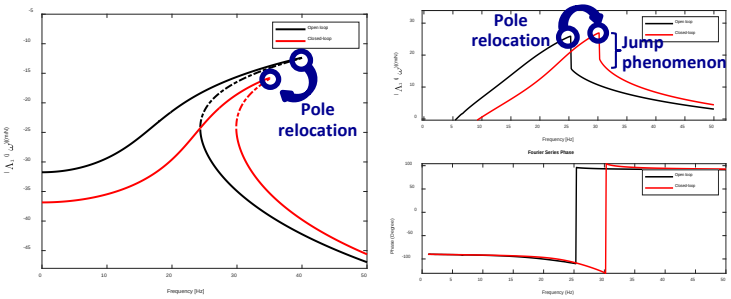

Figure 3: Eigenvalue assignment of the nonlinear system

Conclusion

This paper presents the application of the receptance method to control the poles of a nonlinear system experimentally using a nonlinear electromagnetic cantilever beam that designed and built for this purpose. By increasing the distance and decreasing the electric current between the two coils, the system behaves similarly to a linear system.
The nonlinear system's poles were assigned using the linear feedback control method and the iterative Sherman-Morrison formula. The jump phenomenon of the nonlinear FRF was shown, and pole placement was performed for only one mode of a single degree of freedom nonlinear system.

References

[1] J. E. Mottershead, et al., "Active vibration suppression by pole-zero placement using measured receptances," doi: 10.1016/j.jsv.2007

[2] B. Zaghari, et al "Dynamic response of a nonlinear parametrically excited system subject to harmonic base excitation" doi: 10.1088/1742

Active Metamaterials
Emergent Behaviour and Design

T. Feehilly[1], R. Peerlings[1], M. Geers[1], O. Rokoš[1]

[1]*Eindhoven University of Technology*
Department of Mechanical Engineering, Mechanics of Materials
5612 AZ Eindhoven, Netherlands
t.s.feehilly@tue.nl

Meta-materials

Meta-materials have opened up the possibility for exotic behaviour and improving manufacturing techniques are allowing more and more complicated designs to be realised.

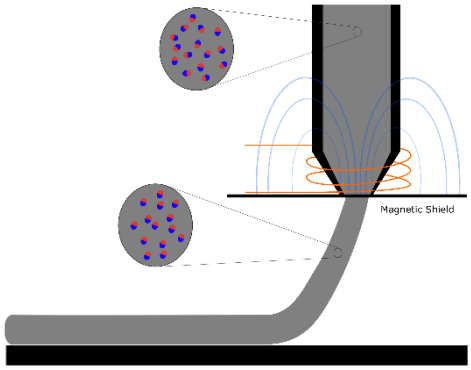

Figure 1: Schematic of 3d printing hard magnetic soft material by Kim et. al. [1]

Control

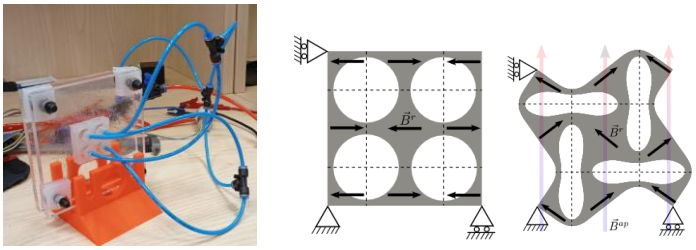

Figure 2: a) Pneumatically actuated circular stack.[2] b) Magnetically actuated material[3]

Active Property Changes

Control over the deformation gives control over material properties from mechanical to acoustic

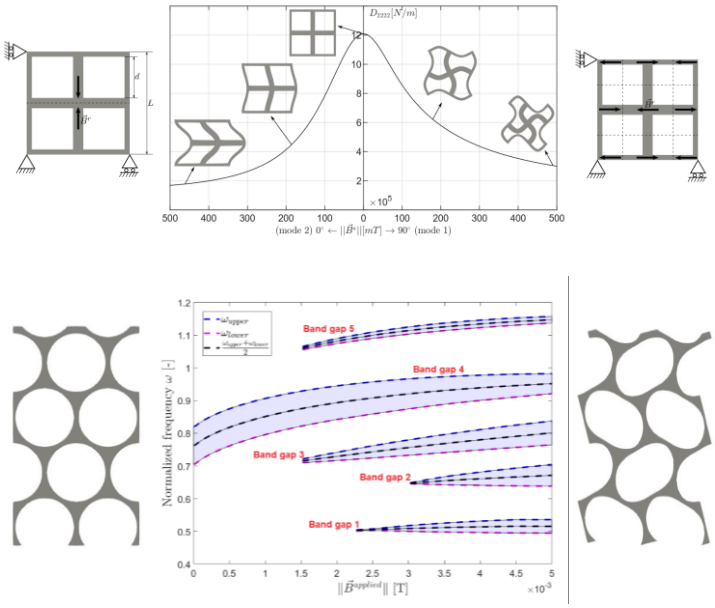

Figure 3: a) Stiffness in the vertical direction of the material changes with the strength of magnetic field.[3] b) Frequency band gaps of the material changes with magnetic field strength[4]

Design

Forward design of material properties is quite challenging. With behaviour that is highly dependent on the fine structure of the material for example different buckling modes.

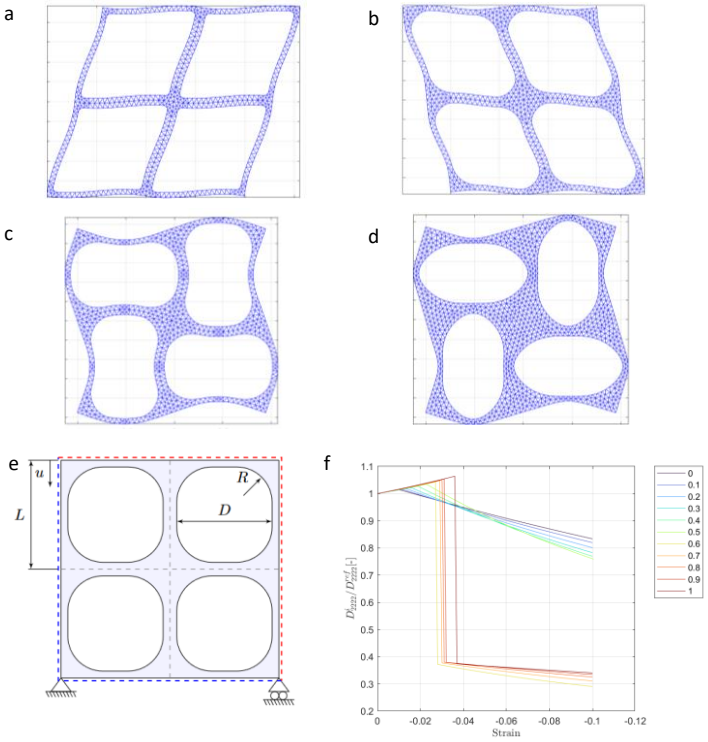

Figure 4: a-d) Buckling behaviour of holes with 2R/D=0,0.5,0.6,1 respectively e) schematic representation of material structure f) Homogenised stiffness in the y direction for different values of 2R/D

Topology Optimisation

With such a large design space and mixed physics inverse design methods are needed.

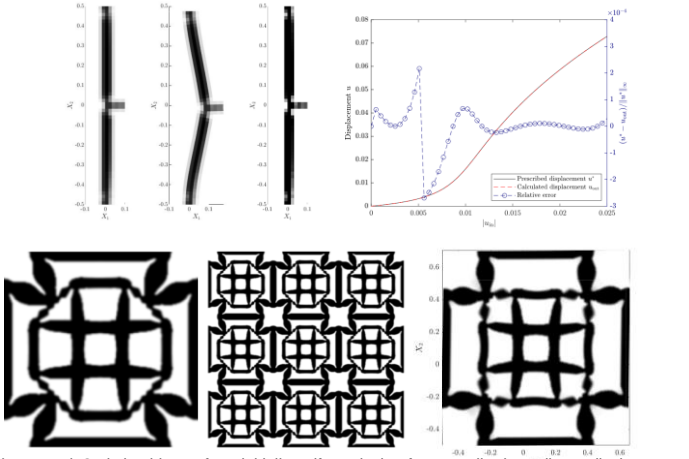

Figure 5: a) Optimised beam from initially uniform design for prescribed non-linear displacement path. b) Homogenised design from initially uniform design for Poisson's ratio -0.77. c) The expanded unit cell. All from [6]

References

1. Kim Y., Yuk H., Zhao R., Chester S.A., Zhao X., 2018. Printing ferromagnetic domains for untethered fast-transforming soft materials. Nature 558, 274–279.

Machine Learning Interatomic Potential for Pure Zn

D.Fioravanti[1], J.Hoefnagels[2], E. van der Giessen[1], F.Maresca[1]

[1] *University of Groningen*
[2] *Eindhoven University of Technology*

Introduction

Zinc-based coatings are widely used in steel industry but their deformation mechanisms are still unclear.
Atomistic modelling can help us understand what are the phenomena that control plasticity and fracture at larger scales.
To perform Molecular Dynamics the main ingredient is an interatomic potential, but for Zn a reliable and accurate interatomic potential **does not exist**.
We use Atomic Cluster Expansion (ACE), a recently developed machine learning model, in combination with HyperActive Learning algorithm to develop a Density Functional Theory (DFT) accurate interatomic potential for Zn.

DFT database e ACE training

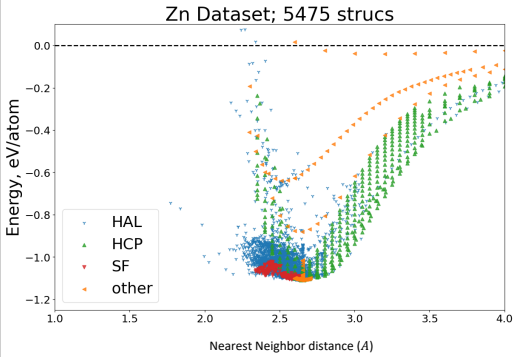

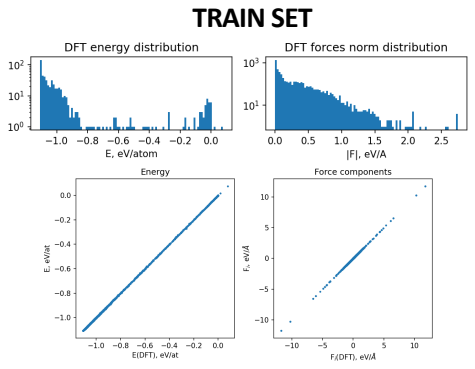

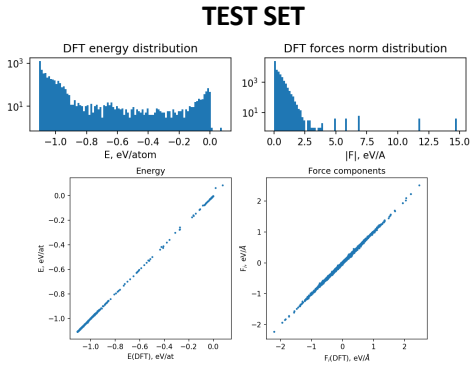

Validation of the potential

	a (Å)	c(Å)	C_{11} (GPa)	C_{12} (GPa)	C_{13} (GPa)	C_{33} (GPa)	C_{44} (GPa)	$E_{coh}(eV)$	$E_{vac}(eV)$
DFT	2.652	5.023	160	43	50	50	26	-1.107	0.445
ACE	2.652	5.036	157	53	53	58	26	-1.107	0.420

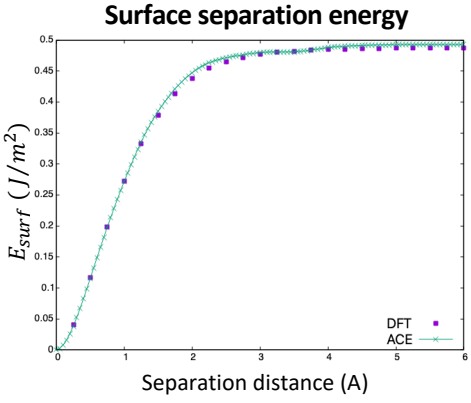

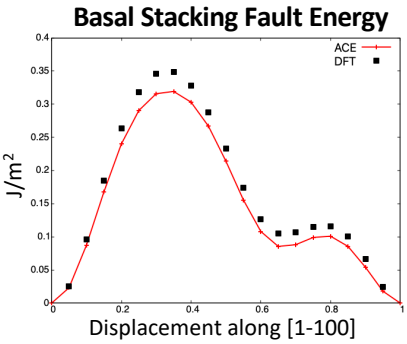

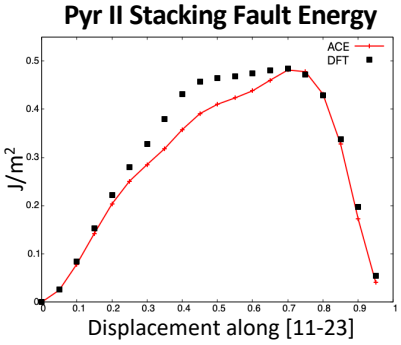

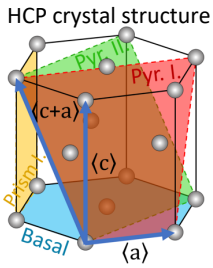

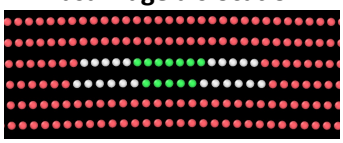

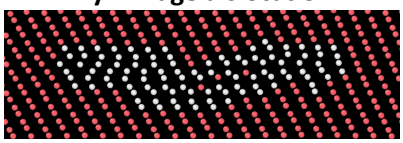

Conclusions

A new Zn ACE potential has been developed. This potential is **the first potential that can be used to study dislocations and crack propagation in Zn.**
The fundamental understanding achievable with the potential will be cast in a predictive theory of strength and failure of coatings for a wide range of alloy concentrations, to guide the design of next-generation coatings with unprecedented strength, damage and wear resistance.

References

- Drautz, Ralf. "Atomic cluster expansion for accurate and transferable interatomic potentials." *Physical Review B* 99.1 (2019): 014104.
- van der Oord, Cas, et al. "Hyperactive learning (HAL) for data-driven interatomic potentials." *arXiv preprint arXiv:2210.04225* (2022).
- Bochkarev, Anton, et al. "Efficient parametrization of the atomic cluster expansion." *Physical Review Materials* 6.1 (2022): 013804.

PhD progress: 1 | 2 | 3 | 4

Effects of Material Architecture in Elastic Impact Mitigation

T. Gärtner[a,b], S. van den Boom[b], J. Weerheijm[a], L.J. Sluys[a]

[a] *Delft University of Technology*
[b] *Netherlands Institute for Applied Scientific Research (TNO)*

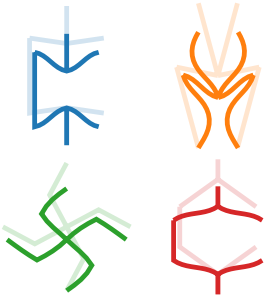

Figure 1: unit cells at $E_y^\star = 300\,\text{MPa}$, $\rho_{\text{rel}}^\star = 0.1$

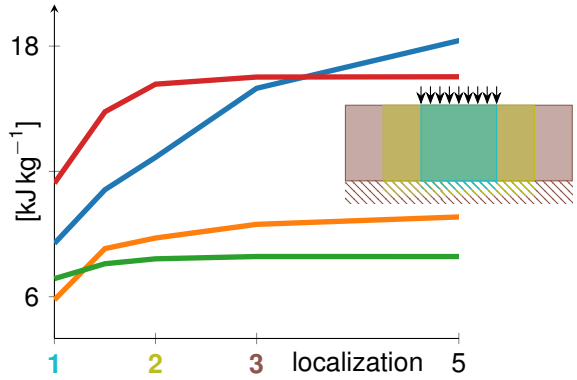

Figure 2: energy intake at 20 % compression and 10 ms^{-1} compression rate

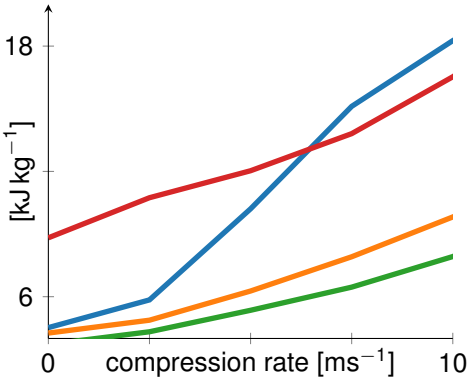

Figure 3: energy intake at 20 % compression and a localization of 5

Introduction

Metamaterials are materials architected to exhibit unique properties based on the architecture of their microstructure, rather than their constituents (examples in Figure 1). Auxetic (negative Poisson's ratio) metamaterials, demonstrate in the quasi-static regime mechanical properties favorable for impact protection, given these properties are preserved in the dynamic regime. In this regime, it remains uncertain to what extent mechanical properties can be preserved by architecture adjustments, since impact is typically accompanied by rate and inertial effects with geometrical nonlinearities.

Impact Mitigation

At low localizations and compression rates, the regular honeycomb shows the highest energy adsorption. Only the re-entrant honeycomb is able to absorb more at high localizations (> 3, Figure 2) and compression rates ($> 7.5\,\text{ms}^{-1}$, Figure 3). Thus, structures do not exhibit benefits solely based on their auxeticity. Especially the chiral and arrowhead do not generate an advantage. The evolution of elastic properties over deformation modes dominating impact (confined compression and shear) is a better indicator for the impact mitigating qualities of architected materials.

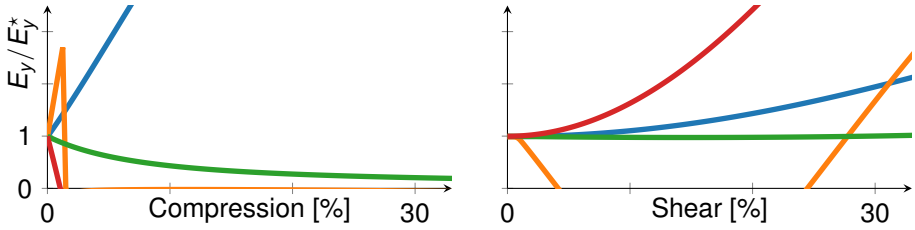

Figure 4: Young's modulus under confined compression and shear

Property Evolution

Laterally folding materials (re-entrant honeycomb and arrowhead) under compression are orienting their beams towards stretching-dominated behavior. This increases the Young's modulus. They are however prone to buckling, leading to diminished stiffness (e.g. arrowhead). The honeycomb structures (re-entrant and regular) show the highest Young's modulus upon confined compression and shear, respectively (Figure 4). This also holds for the pressure wave velocities c_{P_x} (Figure 5). It can be observed, that the velocities of lateral shear waves c_{S_x} are small compared to the pressure waves.

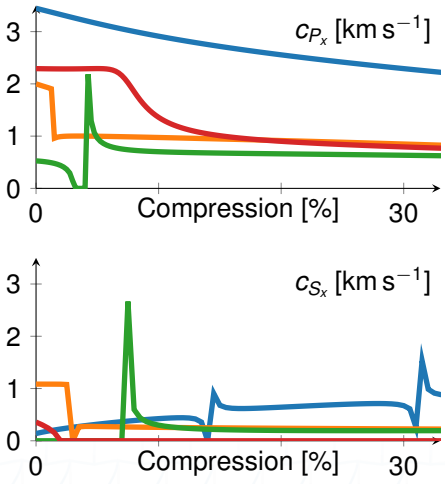

Figure 5: c_{P_x}, c_{S_x} under confined compression

Utilizing neural networks for large scale spatial domain decomposition of surrogate models

Timm Gödde, Bojana Rosić

Chair of Applied Mechanics & Data Analysis, Faculty of Engineering Technology, University of Twente

Introduction

The goal of this project is to utilize neural networks as fast predictive models for design optimization. A problem with neural network models is their high dimensionality when applied to spatially dependent problems. To reduce the number of parameters, in this work, a domain decomposition method to make predictions only dependent on local parameters is suggested.

Domain decomposition

An arbitrary function $f(x)$ with $x \in \Omega$ can be approximated by a neural network $\hat{f}_\theta(x)$ by minimising the mean squared error with respect to parameters θ.

$\hat{f}_\theta(x)$ could also be defined over two separate non-overlapping domains:

$$\hat{f}_\theta(x) = \sum_{i=1}^{2} I_i \hat{f}_{\theta_i}(x), \qquad I_i = \begin{cases} 1, & x \in \Omega_i \\ 0, & x \notin \Omega_i \end{cases},$$

where I_i is the indicator function and $\hat{f}_{\theta_i}(x)$ are separate neural network approximations on Ω_i. Under appropriate smoothness assumptions, one may decompose the function $\hat{f}_\theta(x)$ into the corresponding subdomain functions by solving the constraint optimization problem:

$$L_i(\theta_i, x_i) = \left\| f(x_i) - \hat{f}_{\theta_i}(x_i) \right\|_2^2,$$

$$\text{s.t.} \quad \hat{f}_{\theta_i}(x_l) = f_\mu,$$

$$\text{s.t.} \quad \frac{\partial \hat{f}_{\theta_i}(x_l)}{\partial x} = \frac{\partial f_\mu}{\partial x}.$$

x_l is the spatial point on the interface between two domains, and f_μ and $\frac{\partial f_\mu}{\partial x}$ are the function value and gradient on the interface between the two neural network approximations, respectively.
By the method of Lagrange multipliers $\boldsymbol{\lambda}$, the previous problem can be reformulated as unconstrained optimization problem:

$$L_i(\theta_i, x_i) = \left\| f(x_i) - \hat{f}_{\theta_i}(x_i) \right\|_2^2 + \boldsymbol{\lambda}^T \boldsymbol{C}$$

with

$$\boldsymbol{C} = \begin{bmatrix} \hat{f}_{\theta_i}(x_l) - f_\mu \\ \dfrac{\partial \hat{f}_{\theta_i}(x_l)}{\partial x} - \dfrac{\partial f_\mu}{\partial x} \end{bmatrix}$$

Given this objective function, a dual decomposition algorithm [1] is used to parallelize the training process. To enable a stable algorithm, the constraints are linearized.

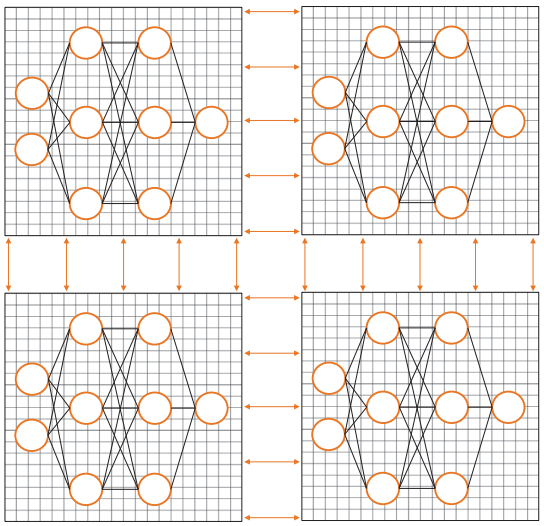

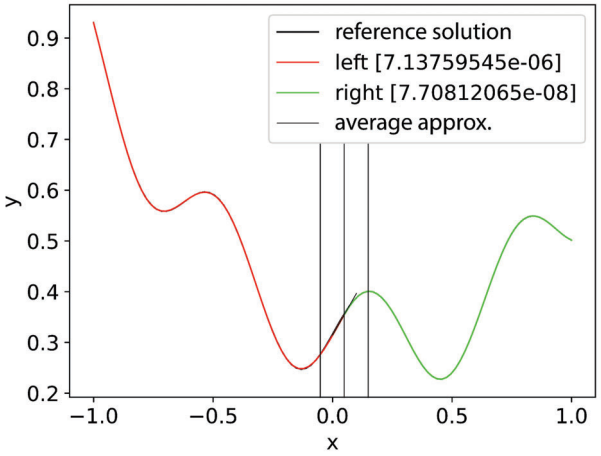

Conclusions

The domain decomposition method described here has the potential to greatly improve accuracy and training speed of spatial neural networks.
The exact improvement in training speed is to be determined. At its current state, implementation of the algorithm are quite simplistic. In addition to that, the improvement effect of splitting into multiple domains should be investigated.

References

[1] T. Gödde, B. Rosić. 2023. Neural Networks for large scale spatial Domain Decomposition. In preparation.

Contact details

t.godde@utwente.nl

UNIVERSITY OF TWENTE.

PhD progress: 1 2 3 4

materials innovation institute

TATA STEEL

Computational Modelling of Chopped Tape Thermoplastic Composites

D.E. Gülmez, S. Turteltaub, R. De Breuker

Delft University of Technology
Faculty of Aerospace Engineering
Department of Aerospace Structures and Materials

MOTIVATION

Chopped Tape Thermoplastic Composites (also known as Discontinuous Tape, DT) have been proposed for recycling, reuse and zero-waste manufacturing of structural components.

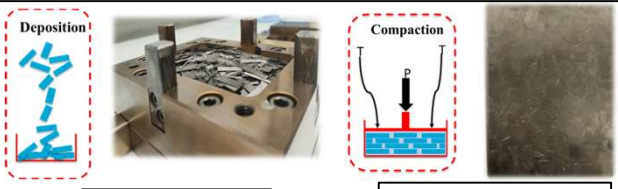

Discontinuous tapes → Chopped Tape Thermoplastic Composites

GOALS

1. Improving a representative structure according to geometrical boundaries
2. Hybridisation of continuous-discontinuous tapes
3. Formulating anisotropic cohesive laws for a microstructural damage model a modelling technique to understand the mechanical properties and failure behaviours

INTRODUCTION

recyclable

mouldable

tailorable

[1]

RESULTS (1)

Generation of the structure

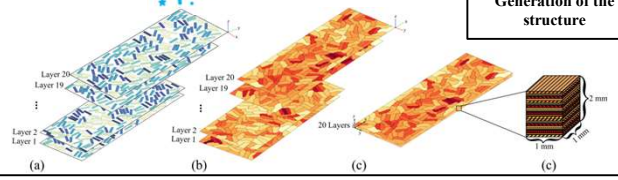

(a) Virtual layers of non-overlapping distributions, (b) Ply-wise mesoscopic variability for each virtual layer (c) Assembled equivalent CTTC laminate, and (d) Partition scale laminated structure.

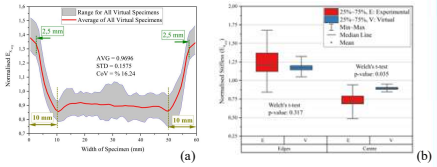

(a) Deviation of normalised stiffness for all virtual CTTC specimens with respect to the edge (b) Statistical comparison of experimental (E) and virtual (V) specimens.

Hybridisation of continuous-discontinuous tapes (CT-DT)

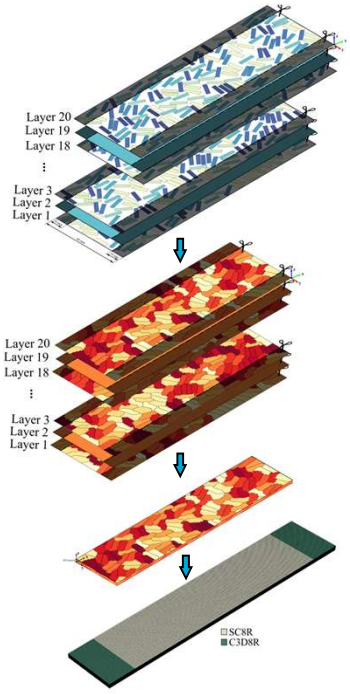

Microscale modelling of path-dependent damage onset and propagation

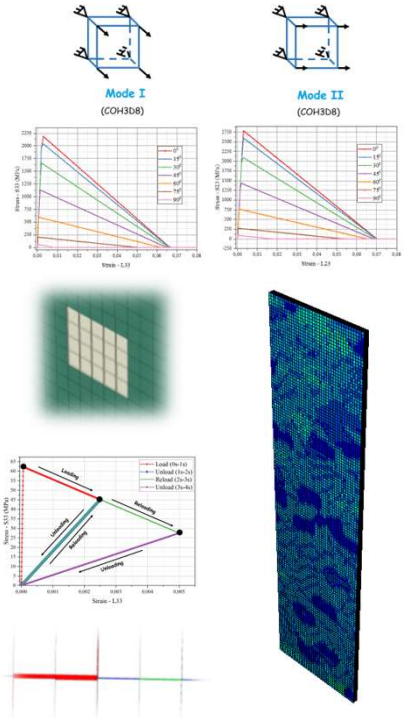

RESULTS (2-3)

Investigation of hybridised CT-DT composites to quantify ratio and sequence of CT-DT based on mechanical performance: Bending and tensile response

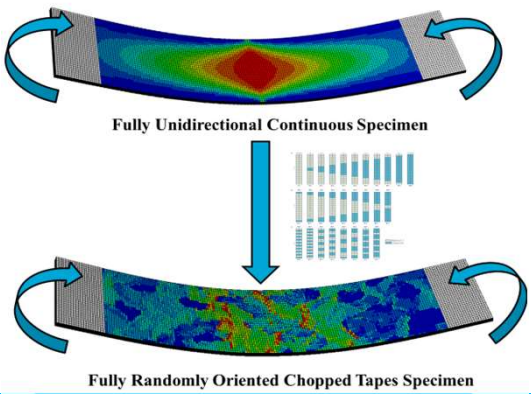

Fully Unidirectional Continuous Specimen

Fully Randomly Oriented Chopped Tapes Specimen

CONCLUSIONS: The results showed that stiffness at the edges of specimens is higher than in their centre due to the high alignment of DTs. The modelling technique enables the analysis of hybridization of discontinuous-continuous tapes and anisotropic cohesive laws for a microstructural damage model formulated.

REFERENCES:
[1] D. E. Gulmez, J. Madonado, K. Masania, J. Sinke, C. Dransfeld, Quantification of structural response and edge orientation of Chopped Tape Thermoplastic Composites in net-shaped specimens, Composite Structures, 321 (2023) 117302.

PhD progress

1 | 2 | 3 | 4

Stochastic Multiscale Analysis of Thermoplastic Composite Materials

Srideep Gupta, Dr. M.I. Abdul Rasheed, Dr. Ing. B. Rosić

Chair of Applied Mechanics & Data Analysis, Faculty of Engineering Technology, University of Twente

Introduction

Project ENLIGHTEN aims is to develop data-driven technologies based on machine learning approaches for simulating the fusion bonding process of thermoplastic composites. These real-time models then can be efficiently used in the process optimization and control.

Challenges

- Mesoscale deformation caused by a non-affine motion of fibres and matrix in the microscale (Fig. 1).
- The problem description is highly complex due to presence of variations at multiple scales, for e.g., matrix voids & cracking, fibre waviness, interfacial debonding.

Therefore, the focus of this work is to stochastically describe various scales in both process and performance models, and to transfer the information from one scale to another by the help of probabilistic upscaling (Fig. 2).

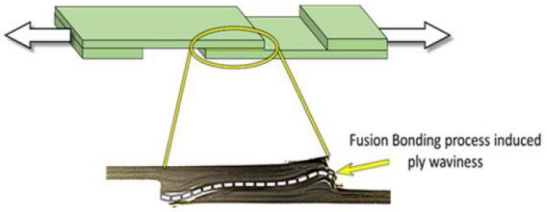

Figure 1: Mesoscale Deformation in single lap joint with measured strength of twice the nominal value. [1]

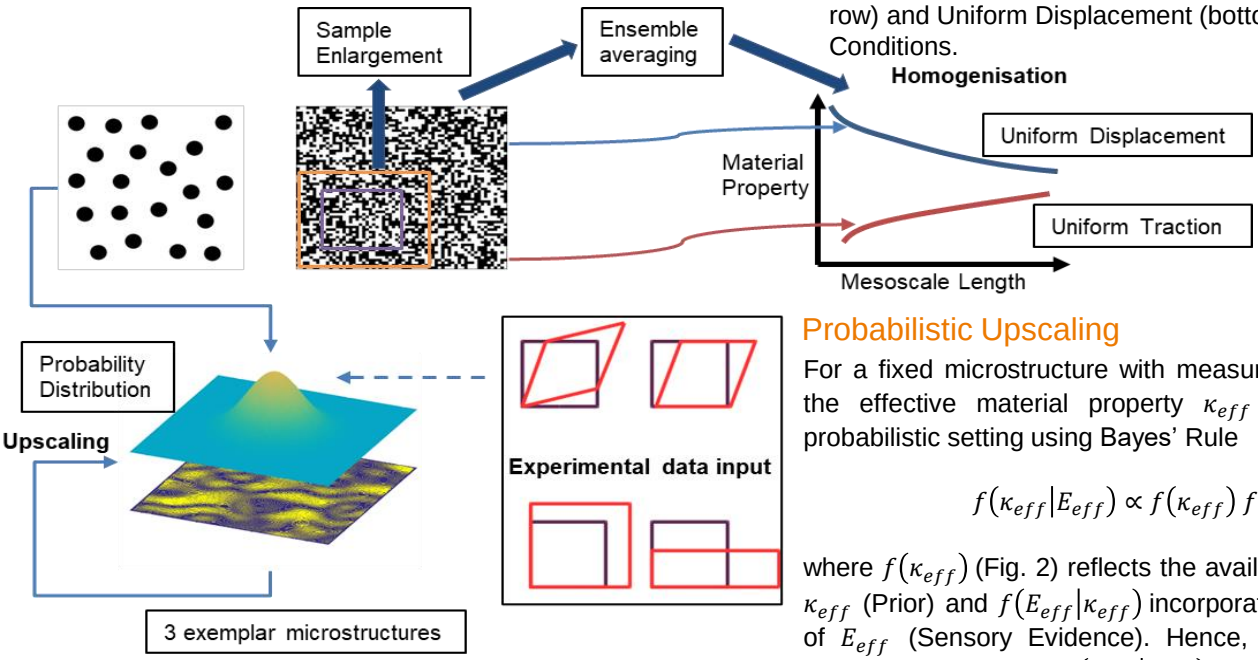

Figure 2: Homogenisation & Upscaling. ([2] & [3])

Classical Homogenisation

One example of upscaling procedure is the homogenisation approach by Hill-Mandel Condition, which considers equality of total mechanical work done from microscopic quantities and effective (macroscopic) quantities. This condition gives rise to the possible types of boundary conditions which bounds the effective material properties (Fig. 3).

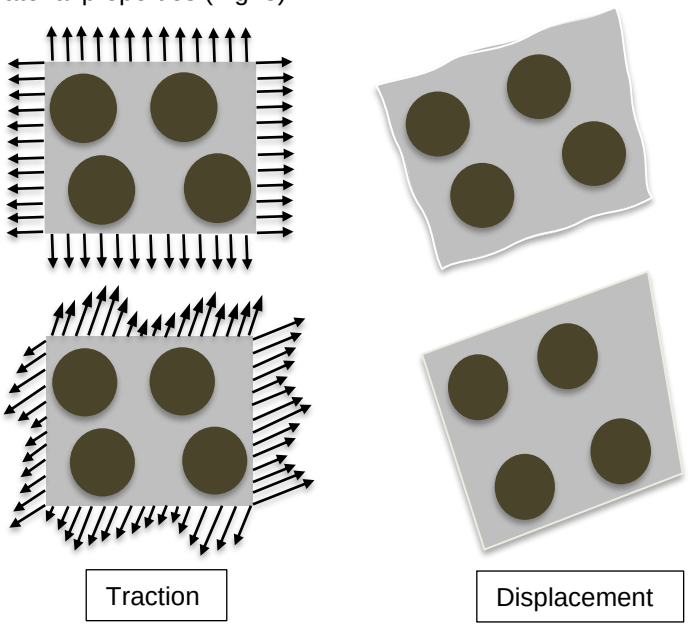

Figure 3: Effect of Traction-controlled Uniform Traction (top row) and Uniform Displacement (bottom row) Boundary Conditions.

Probabilistic Upscaling

For a fixed microstructure with measured effective energy E_{eff}, the effective material property κ_{eff} can be computed in a probabilistic setting using Bayes' Rule

$$f(\kappa_{eff}|E_{eff}) \propto f(\kappa_{eff})\, f(E_{eff}|\kappa_{eff})$$

where $f(\kappa_{eff})$ (Fig. 2) reflects the available expert knowledge on κ_{eff} (Prior) and $f(E_{eff}|\kappa_{eff})$ incorporates the experimental data of E_{eff} (Sensory Evidence). Hence, κ_{eff} is expressed as a probabilistic estimate $f(\kappa_{eff}|E_{eff})$, accounting for the available knowledge on the variables.

Conclusions & Future Work

Effective material property computed by Classical homogenisation theory & Bayes' Rule are same. Stochastic descriptions with Bayes' Rule can systematically incorporate the available knowledge and variations. The given Bayes' rule is to be further extended to incorporate random microstructures.

References

[1] ENLIGHTEN, Perspectief Project, NWO, 2020.
[2] Shivakumar I. Ranganathan, Martin Ostoja-Starzewski, Scaling function, anisotropy and the size of RVE in elastic random polycrystals, Journal of the Mechanics and Physics of Solids, 2008.
[3] B. Rosić, M. Sarfaraz, H. Matthias, Bayesian multiscale analysis of random structures, Conference Paper: The Proceedings in Applied Mathematics and Mechanics, 2017.

Towards a small-scale active anechoic chamber

R. Haasjes[1], A.P. Berkhoff[1,2]

[1]University of Twente ET-AMDA, Drienerlolaan 5, 7522 NB Eneschede (NL)

[2]TNO Acoustics and Sonar, Oude Waalsdorperweg 63, 2597 AK Den Haag (NL)

1. Introduction

Acoustic anechoic chambers (example in Fig. 1):
- Conduct measurements and experiments under free-field conditions;
- **Low-frequency reflections** due to limitations of the passive absorption measures [1].

Active noise control:
- **Effective at lower frequencies**;
- Requires separation of **inward-** and **outward-traveling** soundwaves.

Fig.1

2. Objective

- **Eliminate** all the **reflections** from the walls, while not disturbing the direct sound field;
- Mimic a real anechoic chamber with absorption material at the walls;
- Start simple, with a 2-dimensional sound field of dimensions $0.84\ m$ x $0.84\ m$, and a height of $0.2\ m$ (see Fig. 2);
- Apply real-time active noise control in the $\mathbf{20 - 500\ Hz}$ frequency range.

Fig.2

3. Idea

- Use **12 equidistant sensors** placed on a circle with radius $0.24\ m$;
- Each sensor has three pressure microphones (see Fig. 3):
  - p_2: measures the acoustic pressure;
  - $v_r = \frac{p_3 - p_1}{\delta x}$: measures the radial outward particle velocity.
- With the pressure (p_2) and particle velocity (v_r) at each sensor, the Kirchhoff-Helmholtz integral (KHI) can be computed:

$$p(\boldsymbol{R}) = \int_S \left(G(\boldsymbol{R}, \boldsymbol{r}) \nabla p(\boldsymbol{r}) - \nabla G(\boldsymbol{R}, \boldsymbol{r}) p(\boldsymbol{r}) \right) \cdot \boldsymbol{n}\, dS\ ,$$

which integrates over the sensors on the circle.

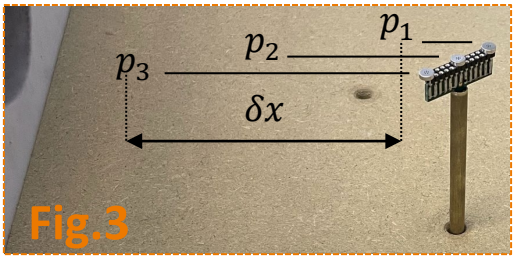

Fig.3

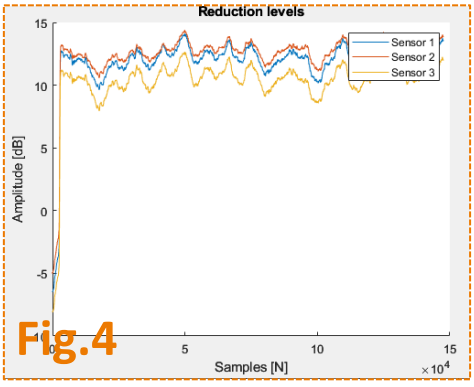

Fig.4

4. Preliminary results

- Real-time multi-channel performance with 3 error sensors, 12 secondary sources, 1 reference sensor and 1 primary source;
- An average **reduction** of **12 dB** over all 3 error sensors (see Fig. 4), the colours match with indicated microphones in Fig. 2.

5. Conclusion

- Sound field separation not implemented yet, multichannel control algorithm is working with a simple configuration;
- Testing needs to be done to verify whether the KHI is a good approximation of the inward-traveling sound field.

References [1] S. Schneider and C. Kern. "Acoustical Behavior of the Large Anechoic Chamber at the Laboratoire de Mécanique et d'Acoustique in the Low Frequency Range". In: Acta Acustica united with Acustica 94 (Jan. 2008), pp. 141-147.

Acknowledgements This research is funded by TNO. The support and funding of TNO are gratefully acknowledged.

Hybrid Modelling of Lateral Flow in Hot Rolling of Steel Strips

A. Hashemzadeh, A. Cometa, C. Soyarslan, T. van den Boogaard

Faculty of Engineering Technology, Nonlinear Solid Mechanics,
University of Twente

Introduction and Motivation

Hot rolling is one of the key forming methods for producing intermediate and end products such as plates, strips, and rods [1], in which the working material is heated beyond the recrystallization temperature. Hot strip rolling is one of the most common rolling setups in the industry and its mathematical modelling has numerous merits [2]; in doing so, numerous parameters effect the model outcome, including the large-strain thermo-mechanical behaviour of the strip, strain-rate and temperature dependency, the behaviour of the rollers, and the roller-strip contact and friction definitions. The exhaustive models that accurately account for the hot rolling process are not favoured in the industry because of their prolonged computations. On the other hand, the time-efficient models that suffer from lack of accounting for the true physics and accuracy.

The aim of this project is to provide a **fast high-fidelity data-driven** model that bridges between these techniques and contains corrections based on the experimental data for the single- and multi-stand rolling processes.

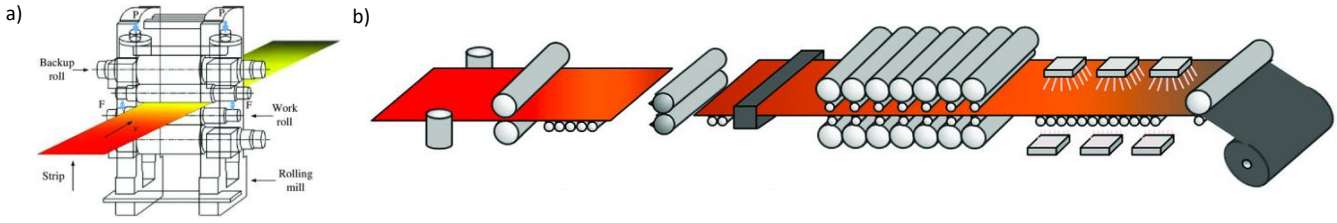

Figure 1. The schematic of a) single and b) multi stand strip rolling [3].

Project Description

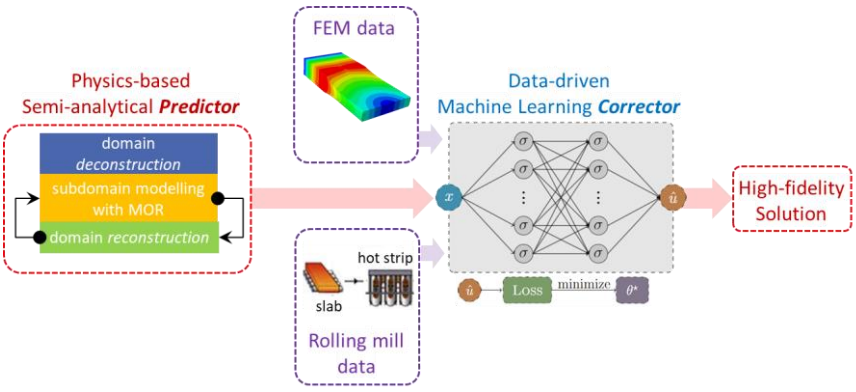

Figure 2. A visual depiction illustrating the various stages involved in the project.

Objective Breakdown and Methodology

- **Rolling simulation with FEM:**
  - ALE model set up for single/multi-stand rolling
  - Preparation of an offline database
- **Experiments:**
  - Mechanical material characterization
  - Conducting small-scale single-stand rolling tests at Tata Steel
  - Data curation from the actual rolling mills of Tata Steel
- **Physics-based semi-analytical prediction:**
  - Identifying the most suitable Reduced Order Modelling (ROM) strategies
  - Development/implementation of the ROM-based semi-analytical model for single/multi-stand rolling
- **Data-driven machine learning (ML) correction:**
  - Machine learning architecture with data integration from experiments as well as offline simulations (FEM)
  - Data-driven architecture to integrate the reduced order model into the high-fidelity model
- **Verification/validation studies**

Research Questions

- What is the physically meaningful way to account for the coupled thermo-mechanical behavior of steel, incorporating temperature and strain-rate dependency at large strains, compared to the experimental results?
- What are the meaningful assumptions to simplify the analysis via domain decomposition?
- How to formulate the coupled thermo-mechanical field equations to in the ALE setting to ward off the free boundary issue?
- What is the best reduced-order modelling technique to accurately represent the system properties?
- What should be the architecture of the machine learning training to result in the final high-fidelity model?

References

[1] Serajzadeh, S. (2014). Hot Rolling and Direct Cooling. Comprehensive Materials Processing, 3, 377–396.
[2] Hodgson, P.D., Mathematical Modelling of Recrystallisation Processes During the Hot Rolling of Steel. PhD Thesis, University of Queensland, Australia, 1993.
[3] Liu, Y., Wang, X., Sun, J., Liu, G., Li, H. and Ji, Y. (2023), Strip Thickness and Profile–Flatness Prediction in Tandem Hot Rolling Process Using Mechanism Model-Guided Machine Learning. steel research int., 94: 2200447.

Graph Neural Networks with Embedded Symmetries for Robust Computational Homogenization

Fleur Hendriks[1], Vlado Menkovski[1], Martin Doškář[2], Marc G. D. Geers[1], Ondřej Rokoš[1]

[1]*Eindhoven University of Technology*

[2]*Czech Technical University in Prague*

Introduction

Porous, flexible metamaterials are useful in soft robotics. To design these materials, the mechanical behavior needs to be modelled. Current computational homogenization of a periodic representative volume element (RVE) using the finite element method (FEM) is too slow to optimize the design. Therefore, a surrogate model, replacing FEM, is used to quickly simulate the mechanical behavior of the porous materials obtaining the stress $\mathbf{P}$ in the material and its stiffness $\mathbf{D}$, described by the deformation gradient $\mathbf{F}$. We create a newly developed surrogate model of the material behavior using graph neural networks (GNNs) [1], decreasing the simulation time with a factor 8.

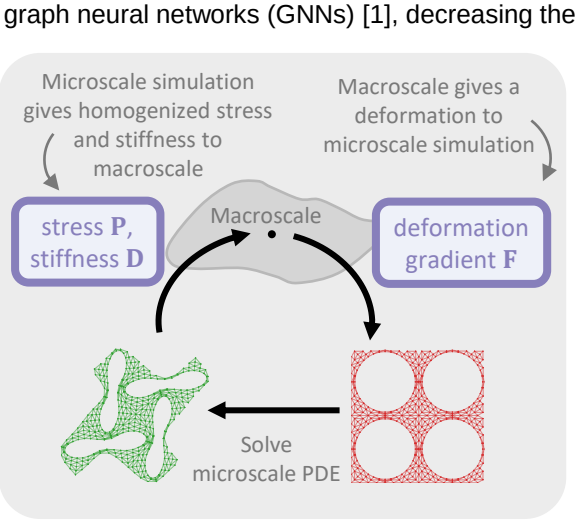

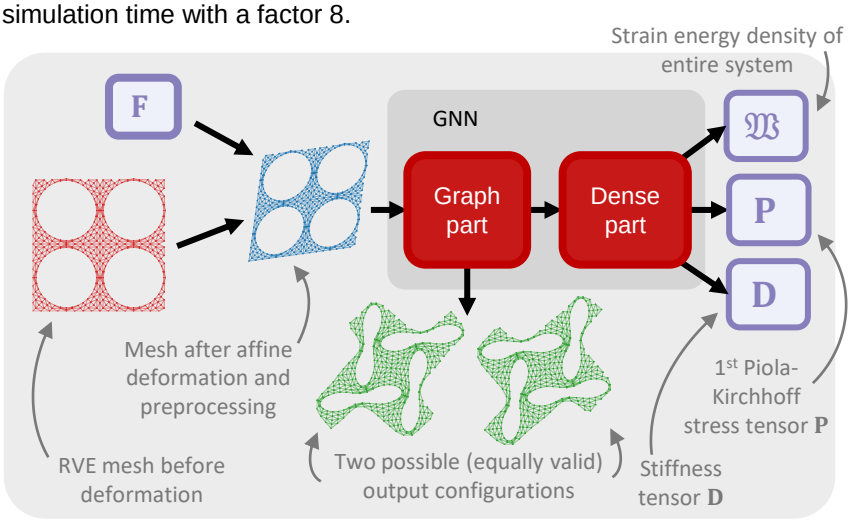

Incorporating symmetries

For optimal accuracy and efficiency, GNNs need to respect the right symmetries, such that the output transforms with the input in the correct way.

Results

Three models, with varying types of symmetries embedded, are compared. The model that respects all symmetries has the lowest mean squared error.

- **GNN**: periodicity
- **EGNN**: GNN plus rotation and reflection
- **SimEGNN**: EGNN plus scaling

Mean square error of the 3 different models

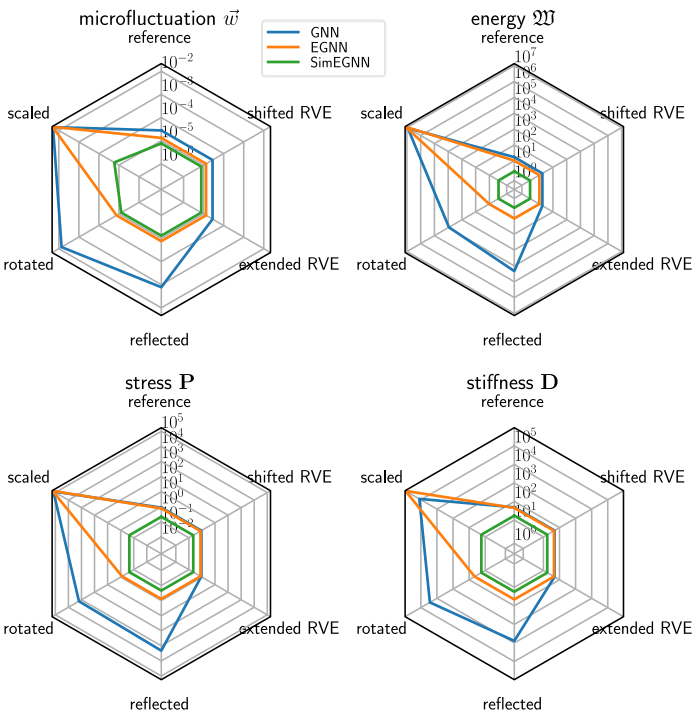

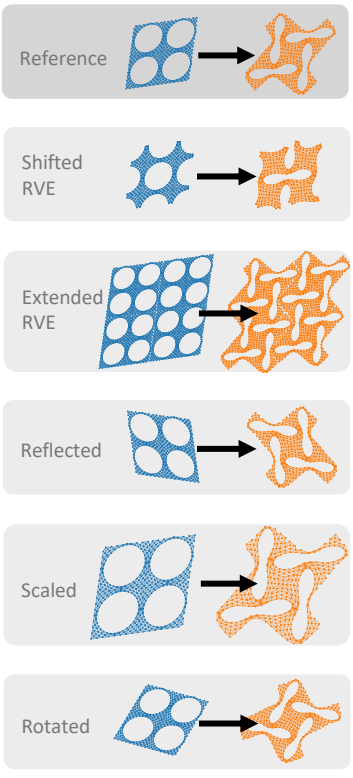

Future work

Often the material can buckle in several different ways. To ensure the model can predict all valid solutions, a generative model will be used. We are also looking at geometrical parametrization of the input.

References

[1] Satorras, Vıctor Garcia, Emiel Hoogeboom, and Max Welling. "$E(n)$ equivariant graph neural networks." International conference on machine learning. PMLR, 2021.

Computational Modeling of Fatigue Failure in Composite Laminates

P. Hofman, F. P. van der Meer, L. J. Sluys

Delft University of Technology

Introduction

The **ENLIGHTEN** (Enabling Integrated Lightweight Structures in High Volumes) seeks to increase the use of light-weight, high-performance **thermoplastic materials** within the aircraft and automotive industry, ultimately contributing to a more **environmentally sustainable economy**. It is the objective of this PhD project to develop **numerical tools** that are accurate, efficient and robust. With these virtual testing tools the high costs and time demands associated with traditional experimental procedures can be significantly reduced.

Methodology

A fatigue cohesive zone model that covers fatigue crack **initiation** and **propagation** [1] has been improved and embedded in a numerical framework for simulating progressive failure in composite laminates with **XFEM matrix cracks** and **interface delamination** [2]. A **cycle-jump approach** is used in order to account for the effect of **residual stresses** on the **local stress ratio** while maintaining computational efficiency in high-cycle fatigue loading (**Figure 1**).

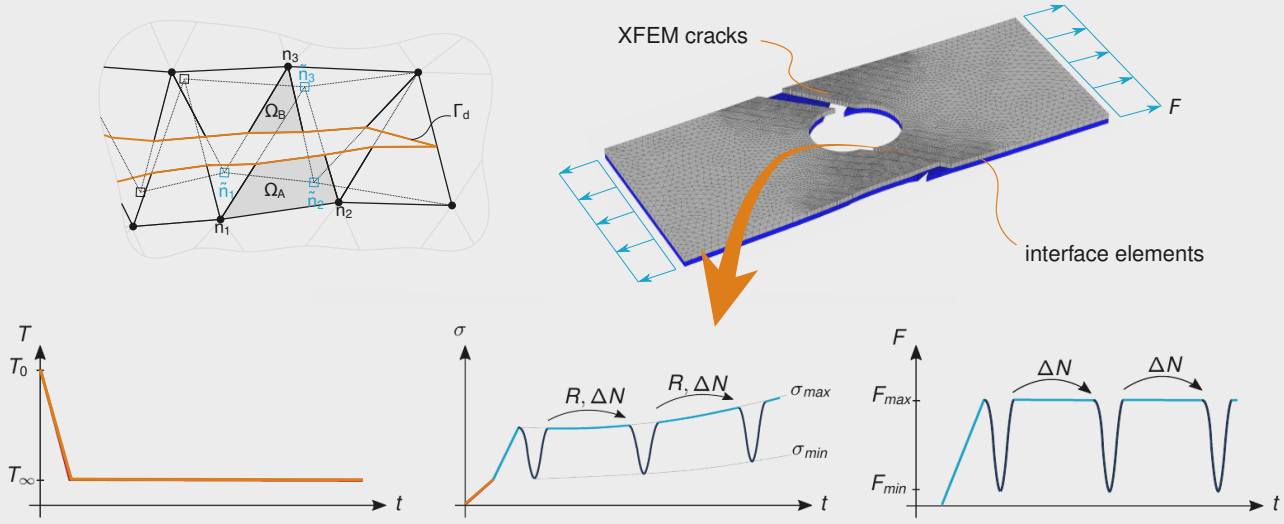

Figure 1: Meso-scale numerical framework for simulating progressive failure in composite laminates under high-cycle fatigue loading

Results

The numerical framework is capable of handling **multiple** transverse matrix cracks (**Figure 2A**). This allows for simulating the complete failure process from **distributed damage** to **localized failure**. The cycle-jump approach allows for capturing a varying **local stress ratio** in the cohesive zone (**Figure 2B**) in the presence of thermal residual stresses.

Summary

- ✓ Improved **fatigue cohesive zone model** for more **efficient** analyses
- ✓ XFEM fatigue crack **insertion criterion**
- ✓ **Open-hole [±45]-laminate** simulation with **multiple** matrix cracks
- ✓ **Adaptive cycle jumping** to account for **local stress ratio**

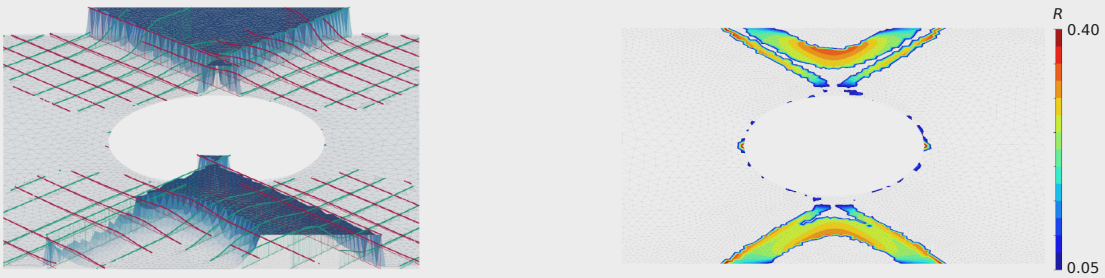

Figure 2: Results with open-hole [±45]-laminate **(A)** Damage evolution in XFEM cracks and interface. **(B)** Local stress ratio variations in the cohesive zone

References

[1] Dávila, C. G. "From S-N to the Paris law with a new mixed- mode cohesive fatigue model for delamination in composites". In: *Theoretical and Applied Fracture Mechanics* (2020).

[2] P. Hofman, F. P. van der Meer, L. J. Sluys. "A numerical framework for simulating progressive failure in composite laminates under high-cycle fatigue loading". In: *Engineering Fracture Mechanics* (2023). Submitted

Digital Twin of Interacting Medical Interventional Devices and Patient Tissues

R. van Hoof[1], O. van der Sluis[1,2], J.J.C. Remmers[1], C. Verhoosel[1]
[1] *Eindhoven University of Technology*
[2] *Philips Innovation and Strategy*

Background and motivation

This project is centred around endovascular treatments. Such a procedure involves manoeuvring of medical devices inside arteries, resulting in multiple interactions between the devices and the arterial wall, such as friction and damage. In order to get more insight into these interactions, a digital twin will be created. This is a virtual representation of the physical situation. A digital twin can assist a doctor in decision making by, for example, comparing different treatment options.

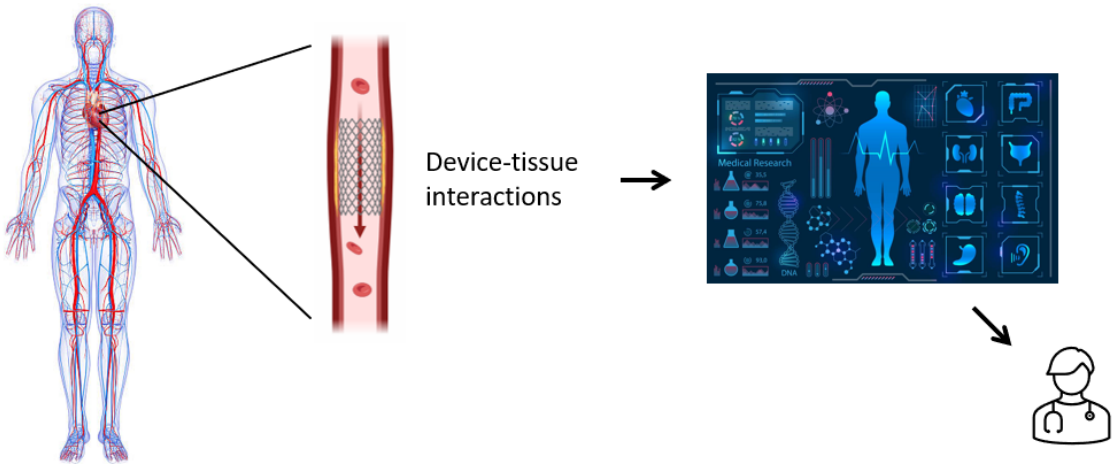

Figure 1: Schematic overview of creating a digital twin of the interactions between medical devices and the arterial wall.

Reduced Order Modelling (ROM)

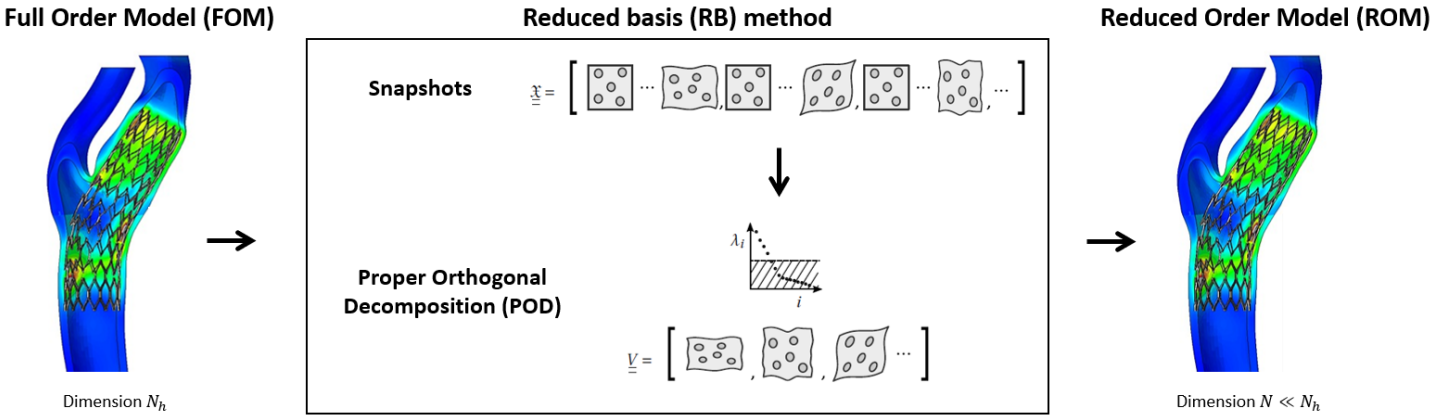

Figure 2: Schematic overview of Reduced Order Modelling based on [1] and [2].

Future work

- Finite Element Analysis of contact mechanics
- Reduced Order Modelling of contact mechanics
- Hyper-reduction

References

[1] Quarteroni et al. (2016). Reduced basis methods for partial differential equations. An introduction. `https://doi.org/10.1007/978-3-319-15431-2`

[2] Van Tuijl (2019). Wavelet based reduced order modelling for computational homogenisation

PhD progress: 1 | 2 | 3 | 4

Structural health monitoring of composite marine propellers using embedded piezoelectric sensors

A. Huijer[1], C. Kassapoglou[2], L. Pahlavan[1]

[1] *Delft University of Technology, Maritime and Transport Technology*
[2] *Delft University of Technology, Aerospace Engineering*
A.J.Huijer@tudelft.nl

Introduction

The implementation of an embedded piezoelectric sensor network inside a composite marine propeller can allow for measurement of damage-induced acoustic emissions (AE) that can give an indication of the nature, location and growth of damages inside the blades. These measurements can enable predictive maintenance of composite propellers and also allow for more detailed assessment of the models and assumptions that are used in the design process [2].

Measuring acoustic emissions

To test the ability to record AE using embedded piezoelectric sensors, standardised pencil lead breaks (PLB) were performed on different locations on the blade in submerged conditions (Figure 1). Responses were successfully measured throughout the blade (Figure 2).

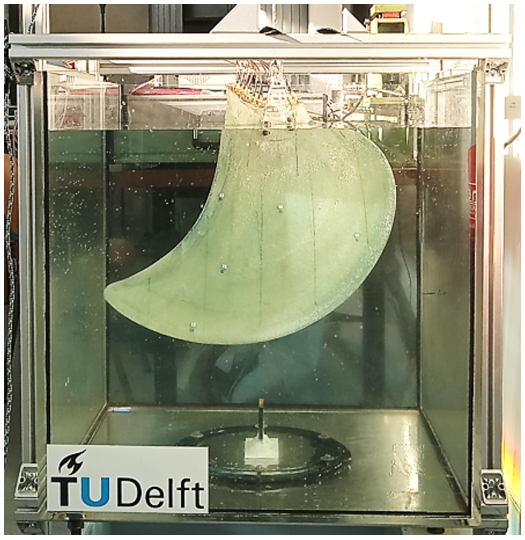

Figure 1: The submerged blade.

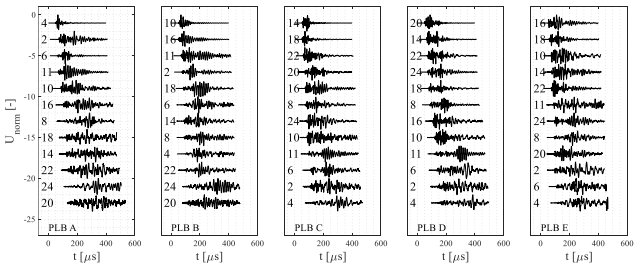

Figure 2: PLB signals from 5 locations recorded by multiple sensors.

Attenuation of acoustic emissions

For each PLB, amplitude drop over the blade was determined for various frequencies. Results are given in Figure 3 [1].

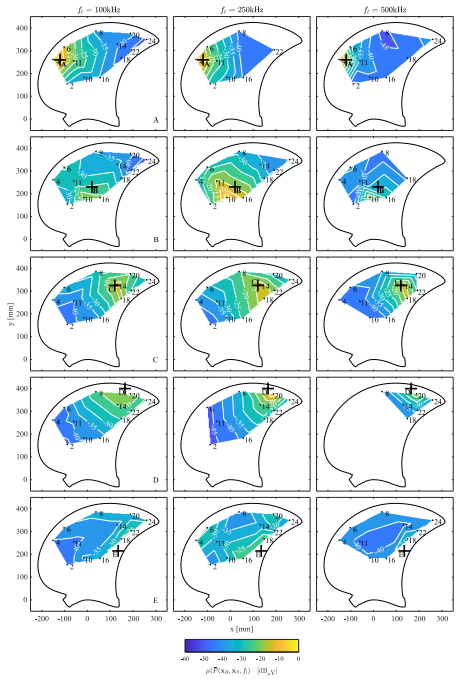

Figure 3: Amplitude drop from PLBs at 5 locations for three different frequencies.

From these results a maximum measurable distance was determined in different conditions regarding signal amplitude, frequency content and noise level. This is shown in Figure 4.

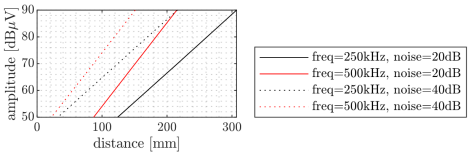

Figure 4: Measurable distance for different signal amplitudes, frequency content and noise level.

Conclusions

- Embedded piezoelectric sensors can measure AE throughout the submerged propeller blade;
- Sensor placement can be improved using knowledge on signal amplitude, frequency content and noise level.

Further development of the methodologies for damage and load monitoring using embedded sensors is carried out in the ECoProp project.

References

[1] A. Huijer, C. Kassapoglou, and L. Pahlavan, *Acoustic emission monitoring of composite marine propellers in submerged conditions using embedded piezoelectric sensors*, Marine Structures (Manuscript under review).

[2] A. Huijer, X. Zhang, C. Kassapoglou, and L. Pahlavan, *Feasibility evaluation for development of composite propellers with embedded piezoelectric sensors*, Marine Structures, (2022).

PhD progress

1 | 2 | 3 | 4

Studying the real area of contact to develop a friction model

F. Jalali Moghadas[1], M.B. de Rooij[1], A.H. van den Boogaard[1], J. Hazrati[1]

[1]University of Twente, Faculty of Engineering Technology

Objective

Friction model should provide **coefficient of friction** for each element, depending on its specific contact condition.

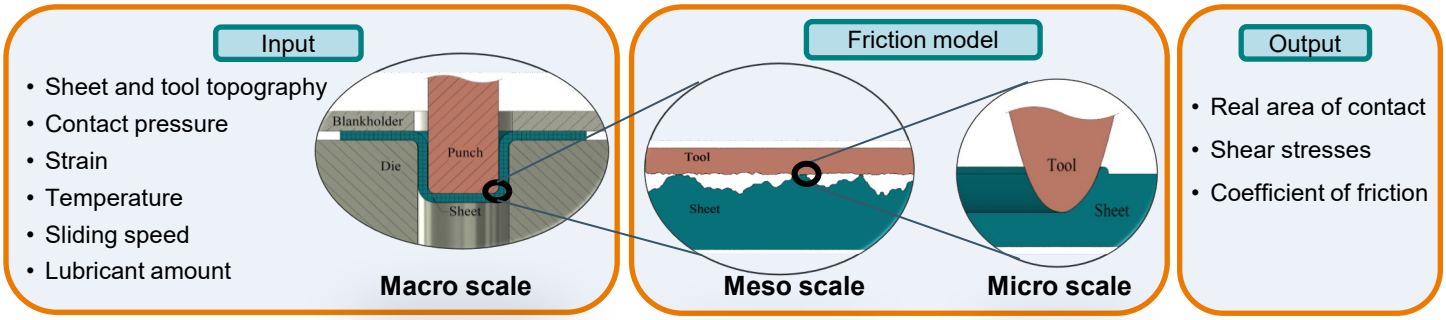

- Accurate estimation of **real area of contact** is required for the reliable friction model.
- Friction model should account for the effect of **normal load**, **bulk strain**, sliding and lubricant.

Effect of Normal Load and Bulk Strain on the Surface Topography

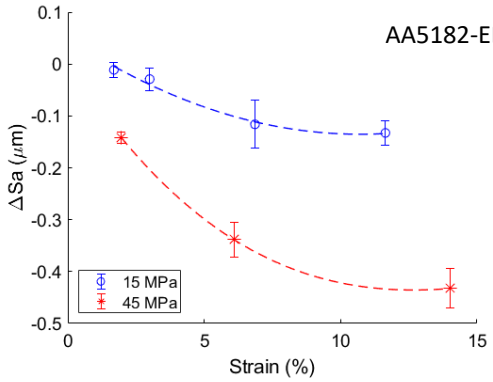

Surface roughness changes due to combined normal load and bulk strain

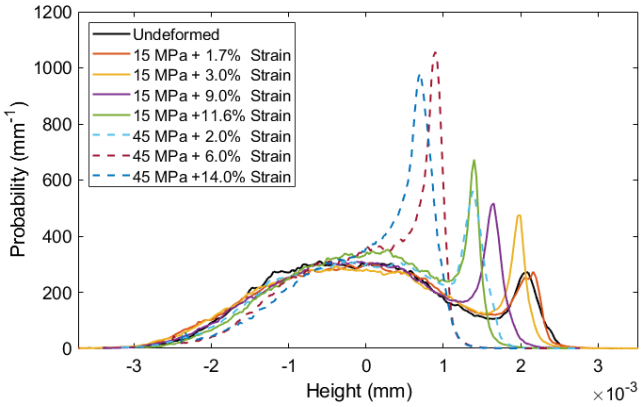

Height probability histogram of the samples after different loading conditions

To develop and validate the friction model, real area of contact should be **measured** precisely in the **experiments**.

A Hybrid Approach to Measure Real Area of Contact

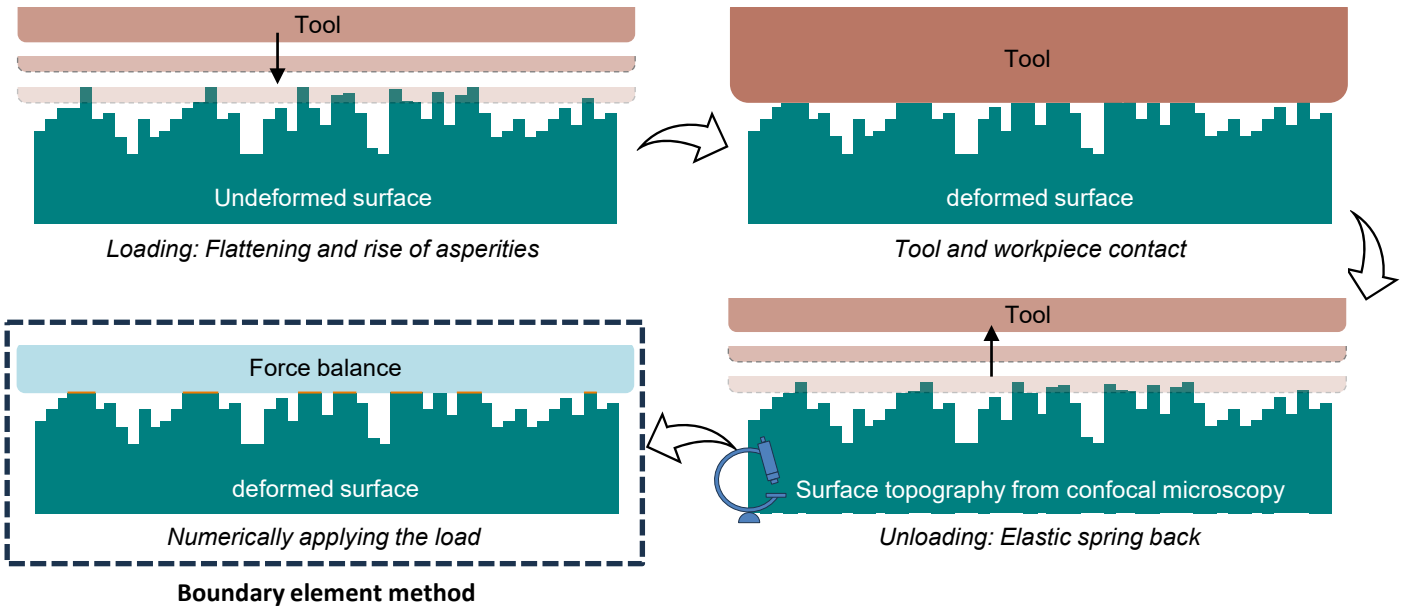

FORMALUB

This research was carried out as a part of the FORMALUB project.

Top-Down Component Requirements with Guaranteed Assembly Accuracy

L.A.L. Janssen[1], B. Besselink[2], R.H.B. Fey[1], D. Kostić[3], N. van de Wouw[1]

[1] *Dynamics & Control, Department of Mechanical Engineering, Eindhoven University of Technology*
[2] *Bernoulli Institute for Mathematics, Computer Science and Artificial Intelligence, University of Groningen*
[3] *ASMPT Center of Competency, Beuningen, The Netherlands*

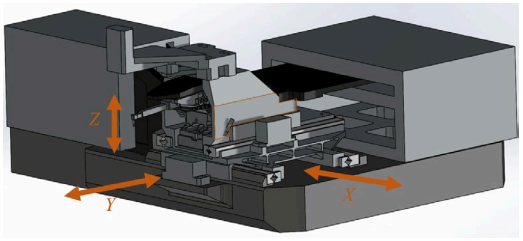

Figure 1. *ASMPT Industrial Wirebonder Model*

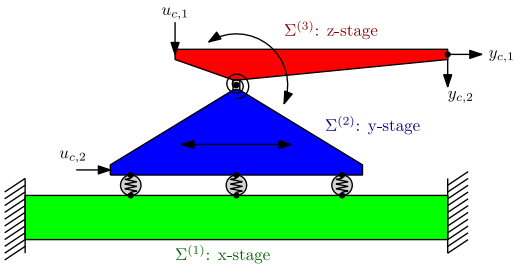

Figure 2. *(Simplified) 2D-Wirebonder model*

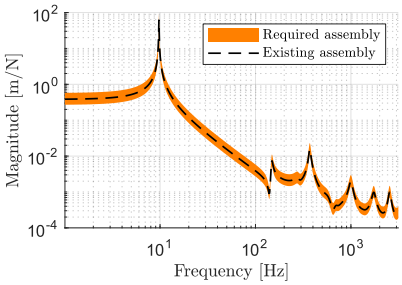

Figure 3. *Example of assembly requirements*

User-Defined Assembly Requirements

Complex mechatronic systems often involve assemblies of multiple components. To achieve high performance and precision, system engineers usually establish **design specifications at the assembly level**. We propose a top-down approach that **automatically determines requirements for each component** based on specifications for the overall assembly. This approach enables **modular redesign** to improve the system's performance, precision, reliability and reduce costs.

Assuming the availability of models for the system and its components, assembly requirements are defined in the frequency domain. From these, component requirements are derived, based on a **maximum allowed change in the dynamics** of the existing models. The component requirements are allocated in such a way that more freedom is available to redesign components with less impact on the overall assembly specifications.

Derived Requirements x-stage → **Verify** → **Modular Redesign**

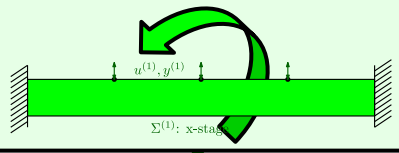

Example: Mass Reduction

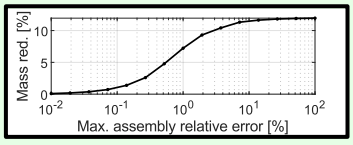

Figure 4. *Given required assembly accuracy, possible allowed mass reduction x-stage*

Derived Requirements y-stage → **Verify** → **Modular Redesign**

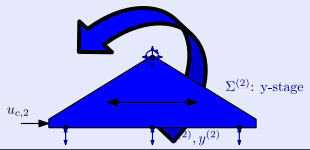

Example: Addition of Encoder Ruler

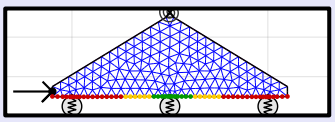

Figure 5. *Allowed locations of:*
- *Ruler 80 g,* *Ruler 40 g and,*
- *Neither ruler possible*

Derived Requirements z-stage → **Verify** → **Modular Redesign**

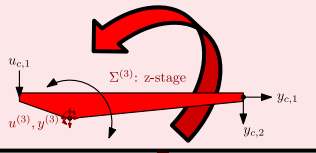

Example: Addition of Accelerometer

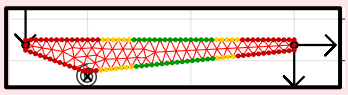

Figure 6. *Allowed locations of:*
- Accelerometer (ACC) *50 g,*
- ACC *25 g and,* *Neither* ACC *possible*

Guaranteed Satisfaction of Assembly Requirements

The top-down approach is based on previous work [1], where a model reduction problem was reformulated into a **robust performance analysis framework.** This framework enables the application of robust control tools, such as ***μ*-analysis**. By treating assembly specifications as robust performance criteria, the approach allows for determining maximum design modifications at the component level that satisfy the assembly criteria. Summarizing, if individual components meet their requirements, this approach **guarantees that the overall assembly specifications are also satisfied.**

References

[1] Janssen, Lars A.L., Besselink, Bart, Fey, Rob H.B., & van de Wouw, Nathan. "Modular Model Reduction of Interconnected Systems: A Top-Down Approach." *IFAC World Congress 2023, Yokohama*. 9-14 July 2023.

Continuous non-parametric density space for a data-driven solution approach

K. Karaca[1], R. H.J. Peerlings [2], M. G.D. Geers[3]

[1,2,3]*Eindhoven University of Technology*

Introduction

Classical solid mechanics solutions employ empirical constitutive relations that inherently feature model prediction error. Data-driven mechanics aims to bypass this error by directly using discrete data points in the problem solution procedure [1]. Yet, data points themselves are susceptible to experimental errors as well [2], and do not cover the true material state. These drawbacks can be answered by using a continuous density estimation of the material behavior.

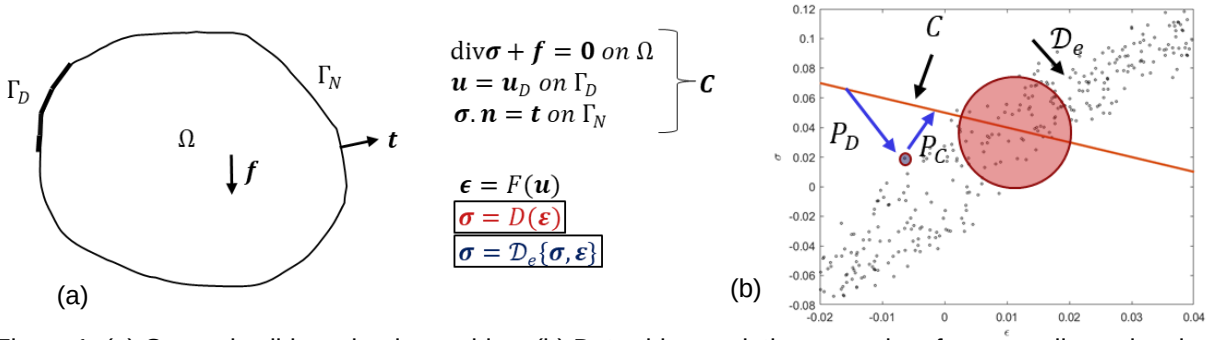

Figure 1: (a) General solid mechanics problem (b) Data-driven solution procedure for a one-dimensional problem

Data-driven solution procedure

The data-driven solution procedure works iteratively by solving a Lagrange multiplier problem to minimize the distance between the constraint and data states. In other words, successive states are obtained via closest point projection (P_D and P_C) to the constraint and data sets.

$$\min_{\boldsymbol{z}_C \in C} \min_{\boldsymbol{z}_D \in D_e} d(\boldsymbol{z}_C, \boldsymbol{z}_D)$$

Continuous density field

Based on experimental errors, the discrete space can be expanded to a continuous one via kernel density estimation by modeling each discrete data point with a Gaussian distribution using a covariance matrix. The resulting density field features multiple minima and is highly nonconvex.

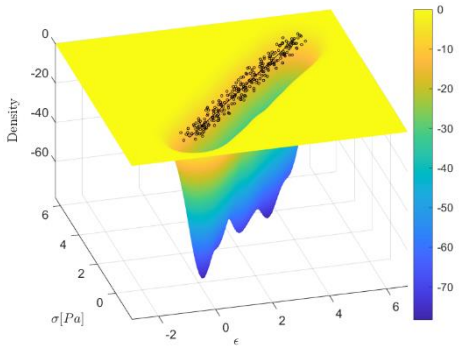

Figure 2: Continuous density field of discrete dataset

Finding the data state of a material point in the continuous space is handled via a nonlinear constrained optimization problem. The point with the highest density is targeted, yet this point has to be the true solution as well. Therefore, equilibrium and compatibility constraints are employed in projection that will result in a high density point that obeys the constraints as well.

Two-bar problem

The distance measure is still used in the projection in two distinct ways:

Weighted objective function:

$Objective\ function = a(density) + b(distance)$

Sequential optimization: find the closest data points first, then optimize density.

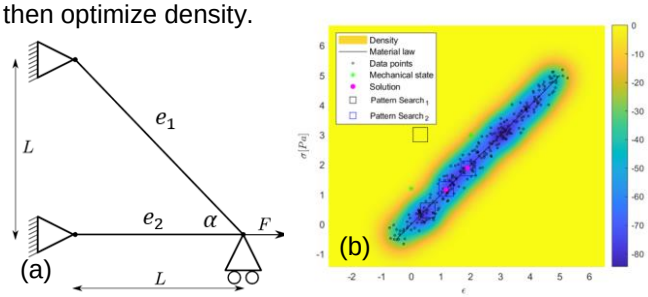

Figure 3: (a) Two-bar problem and (b) solution in data space

It is observed that the sequential optimization approach is able to capture the analytical solution, whereas the weighted objective function approach results in a solution state that misses the target region of the continuous field.

Conclusion and outlook

Although the optimization problem is solved successfully, it is computationally expensive thus a different projection method is required. The high nonconvexity of the continuous density field contributes to the computational cost of the projection as well and can be addressed in the future.

References

[1] Kirchdoerfer, Trenton, and Michael Ortiz. "Data-driven computational mechanics." *Computer Methods in Applied Mechanics and Engineering* 304 (2016): 81-101.

[2] Ayensa-Jiménez, Jacobo, et al. "A new reliability-based data-driven approach for noisy experimental data with physical constraints." *Computer Methods in Applied Mechanics and Engineering* 328 (2018): 752-774.

Multiscale analysis of reinforced elastomer-based composites

E. Karaseva, I. Gitman, T. Bor, A. Blume, D. Huang

University of Twente

Motivation and aim

Improving well-known and introducing new technologies requires the involvement of new efficient and durable materials, particularly elastomer-based composites. The project explores multiscale modelling of such materials for better prediction of their mechanical behaviour.

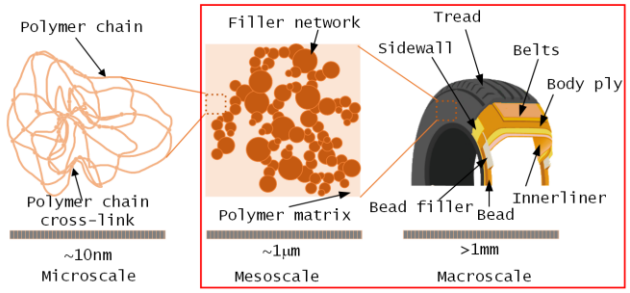

Figure 1: Material in focus scales of observation

Strain energy-based homogenisation

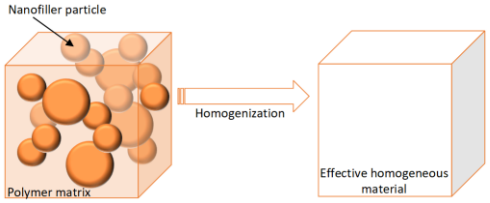

Figure 2: Homogenisation schematics

Computational modelling is a cost-effective alternative to full-scale experiments for analysing the mechanical behaviour of materials, especially in the case of complex elastomer-based composites consisting of a soft elastomer matrix and a hard filler. To homogenise non-linear and linear elastic material, the strain energy-based approach is used [1]:

$$W_{HM}^{macro} = \varphi_{matrix} W_{matrix}^{meso} + \varphi_{filler} W_{filler}^{meso} + \varphi_{interphase} W_{interphase}^{meso} + W_{Van\ der\ Waals}^{meso}$$

Filler modelling

Carbon Black is a reinforcement filler that is widely used in elastomer-based composites. The mechanical properties and fractal structure [2,3] of this filler were recreated to model the Carbon Black network in a soft elastomer matrix:

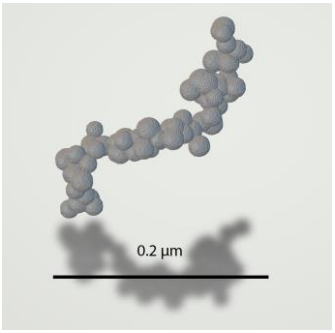

Figure 3: Carbon Black aggregate simulation example

$$n_p = k_f \left(\frac{R_g}{r_p}\right)^{D_f},$$

where n_p is a number of particles in the aggregate, r_p is an average particle radius R_g is a radius of gyration, D_f is a fractal dimension, k_f is a fractal pre-factor.

Matrix modelling

The soft elastomeric matrix of the composite, made of SBR, is modelled by hyperelastic constitutive laws, using experimental data

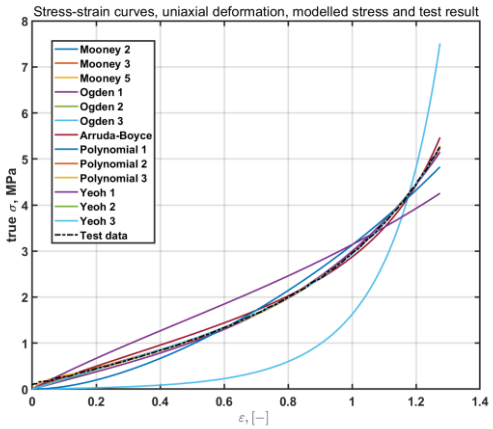

Figure 4: Elastomer matrix modelling

Results

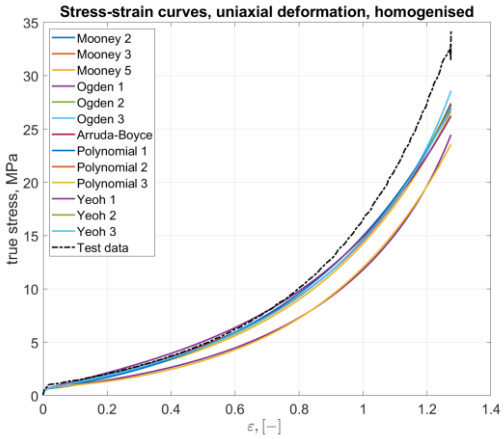

Figure 5: Stress-strain modelling results

Discussion

The results were validated by performing a tensile test on the filler material, the fraction of Carbon Black is 40 PHR. The average error in estimation is 16% for the models, which performed on a sufficient level for pure matrix modelling and 32% for 3rd-order Ogden and 1st-order Yeoh models. Along higher strains, the models tend to underestimate the stress in the material, which can be explained by the lack of matrix-filler bond qualification. This bond can be quantified through the free surface energy of both materials, which is considered to be the extension of the current approach.

References

[1] D. Sokołowski, M. Kamiński, Probabilistic homogenisation of hyper-elastic particulate composites with random interface

[2] M. Kluppel. The Role of Disorder in Filler Reinforcement of Elastomers on Various Length Scales

[3] L. Pascazio, et al. Mechanical Properties of Soot Particles

Fault Bond Graphs for Correct Prognostics

L.S. Keizers[1,2], R. Loendersloot[1], T. Tinga[1,2]

[1]University of Twente

[2]Netherlands Defence Academy

Motivation

- **Prognostics** are essential for **predictive maintenance**

- **Direct** condition **data** improve prognostics

- Typically, only **indirect data** are **available**

- **Relation** between **indirect <-> direct data** is needed

- **Damage models** can create this relation

Method

- **Bond graphs** are based on **energy conservation**

$$power = flow \cdot effort$$

- This makes them feasible for **multi-domain** models

- **Modularity** yields easy **extension** and **reuse**

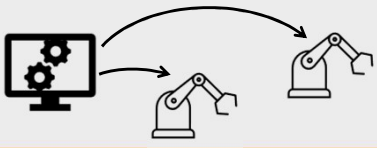

Model

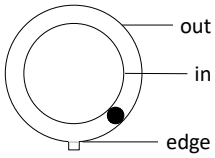

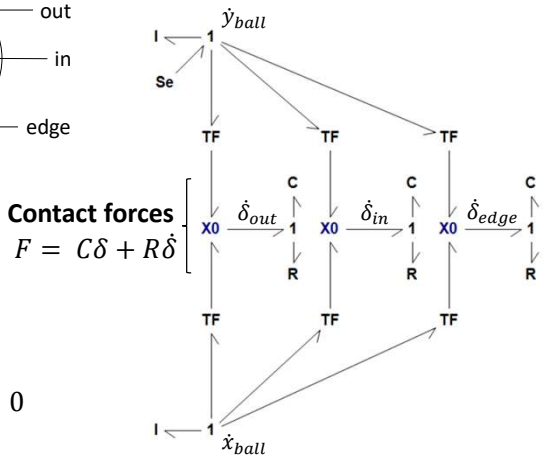

Contact forces

$$F = C\delta + R\dot{\delta}$$

1: $\sum$ efforts $= 0$

0: $\sum$ flows $= 0$

Damaged bearing and corresponding bond graph

Results

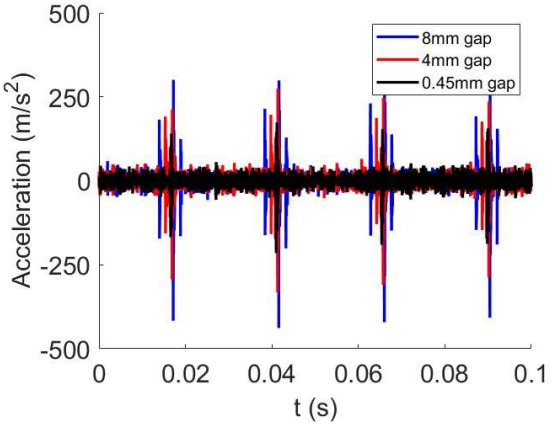

Outer race vibration responses from bearing simulations

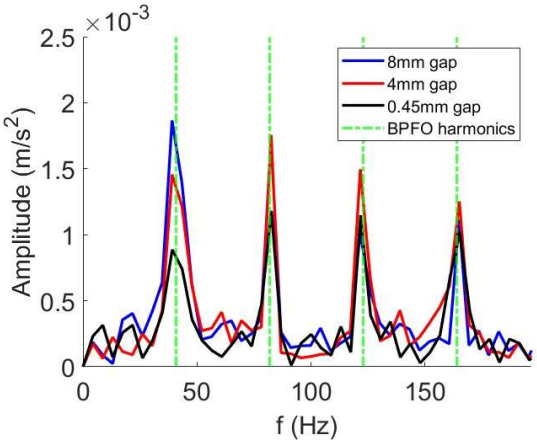

Frequency spectra of outer race acceleration from bearing simulations

Conclusion

- **Bond graphs can describe** damage dynamics
- **Characteristic frequency** outer race is **found**
- Time signal shows **difference** small – medium – large **gap**

Future work

- **Validation** on real data

- Include different **fault types**

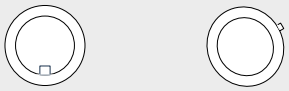

- **Integrate** in prognostic framework

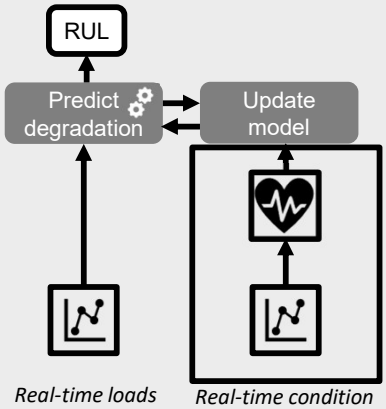

Real-time loads

*Real-time condition from **bond graphs***

Acknowledgements

This work is part of the **PrimaVera Project**, which is partly financed by the Dutch Research Council (**NWO**) under grant agreement **NWA.1160.18.238**.

Contact

l.s.keizers@utwente.nl

linkedin.com/in/luckeizers/

UNIVERSITY OF TWENTE.

PhD progress: 1 | 2 | 3 | 4

Ministerie van Defensie

PrimaVera

NWO

Model Parameter Updating for Digital Twins using Gaussian Process Regression as Inverse Mapping Model

B.M. Kessels, R.H.B. Fey, and N. van de Wouw

Eindhoven University of Technology,
Department of Mechanical Engineering, Dynamics and Control

Introduction

To ensure that a high-tech system digital twin is and remains an accurate representation of the physical system, model parameter updating can be applied. However, conventional methods for model updating, generally, do not simultaneously enable:

- real-time updating, e.g., to allow for structural health monitoring,
- updating of physically interpretable parameters, and
- updating of nonlinear dynamics models.

To meet these requirements, in this research, the Inverse Mapping Parameter Updating (IMPU) method is developed [1]. To improve performance of this updating method, we propose the use of Mutual Information (MI) based Feature Selection (FS) which selects the most informative information to be provided to the IMPU method. The IMPU method is illustrated on a (simulated) model of an ASMPT wirebonder, see Fig. 1.

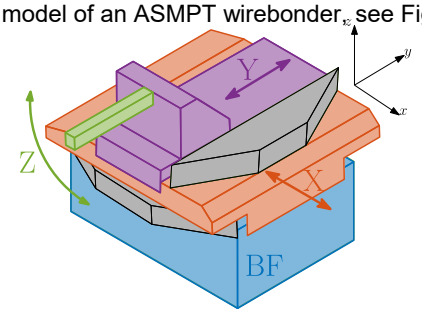

Figure 1: Multibody model of motion stage of ASMPT wire bonder.

Methodology

The IMPU method employs an Artificial Neural Network (ANN) to infer updating parameter values from a set of features of output responses. Here, the ANN is trained, offline, using simulated data, see Fig. 2. Afterwards, in the online phase, measured features are used as input to the ANN yielding, with little computational cost, parameter value estimates.

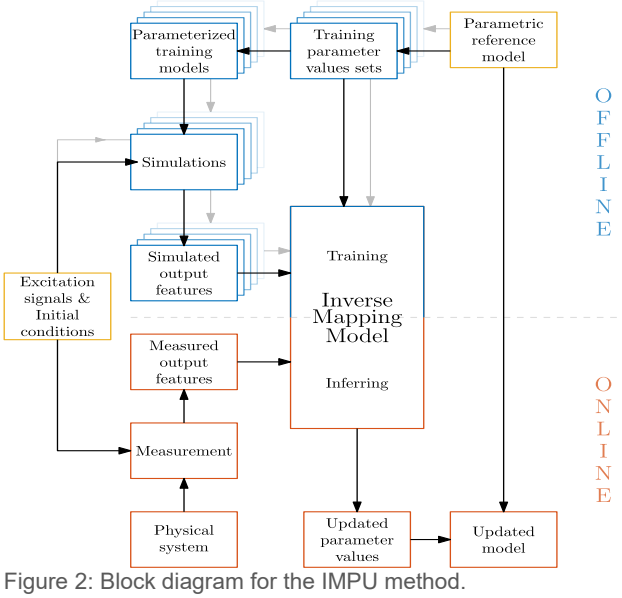

Figure 2: Block diagram for the IMPU method.

As shown in Fig. 3, not all features may be affected by a change in parameter value (compare the high dependency at the left side and low dependency at the right side of the plot), and, therefore, also do not provide any information about the parameter value. Hence, for each feature that is extracted from the simulated response data, a score for the MI with respect to a parameter to be updated is determined from the training data. Then, the features with the highest scores are selected and used to train the ANN and infer parameter values. Note that when multiple parameters are updated simultaneously, the unique union of selected features per parameter is used.

Table 1: Parameter error with and without FS and different ANNs.

FS	# features	ANN architecture	Average rel. parameter error
No FS	1500	250/100/50	3.71 %
With FS	32	250/100/50	3.14 %
With FS	32	40/20/15	3.17 %

Results

The IMPU method is illustrated by updating eight parameters of the ASMPT wirebonder motion stage. Motions in the X, Y, and Z-direction are measurable and controlled via feedforward and feedback control. From each of the three measured tracking error signals (here obtained via simulation), 500 time samples for each signal are extracted, serving as features. Then, four features are selected per parameter using MI-based FS. As shown in Tab. 1, employing FS decreases the parameter error and allows for a smaller ANN, decreasing training and inference time (in our case up to a factor of 6). Furthermore, Fig. 4 shows that the updated model more accurately resembles the measurement.

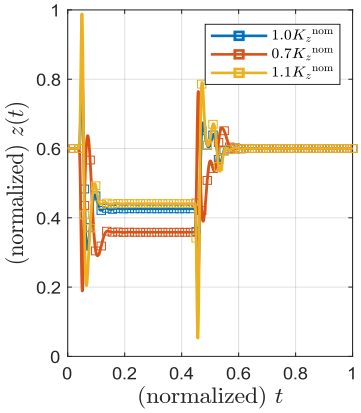

Figure 3: Example of difference in dependencies of multiple features on parameter values.

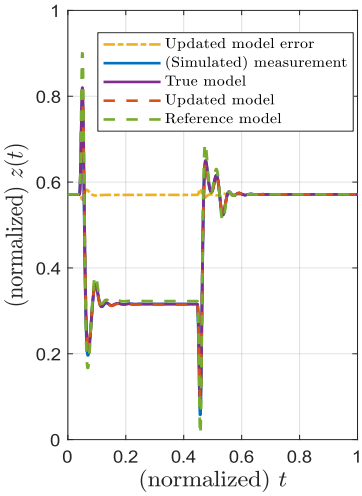

Figure 4: Simulated responses before and after updating parameter values

Conclusions and future work

The NNUM enables (near) real-time interpretable updating of nonlinear models. Feature selection improves parameter estimate accuracy and offline and online computation speed. Additional work involves hyperparameter tuning and an application to real measurement data of a physical wirebonder.

Acknowledgements

This publication is part of the project Digital Twin project 2 with project number P18-03 of the research programme Perspectief which is (mainly) financed by the Dutch Research Council (NWO).

References

[1] Kessels, B.M., Fey, R.H.B., and van de Wouw, N. "Real-time parameter updating for nonlinear digital twins using inverse mapping models and transient-based features". In: *Nonlinear Dynamics*. 111, 11, 10255-10285.

Physically Recurrent Neural Networks for Cohesive Homogenization of Composite Materials

N. Kovacs, M.A. Maia, I.B.C.M. Rocha, F.P. van der Meer

Delft University of Technology

A new surrogate model architecture

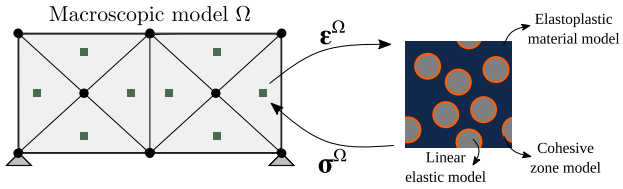

Most of the existing surrogate modeling techniques that address the computational bottleneck of FE^2 method require an extensive dataset, leaving the fracture mechanics field largely unexplored. The goal of this research is to extend a recent surrogate that requires less data, Physically Recurrent Neural Networks (PRNNs)[1], to include the effect of debonding at the fiber-matrix interface.

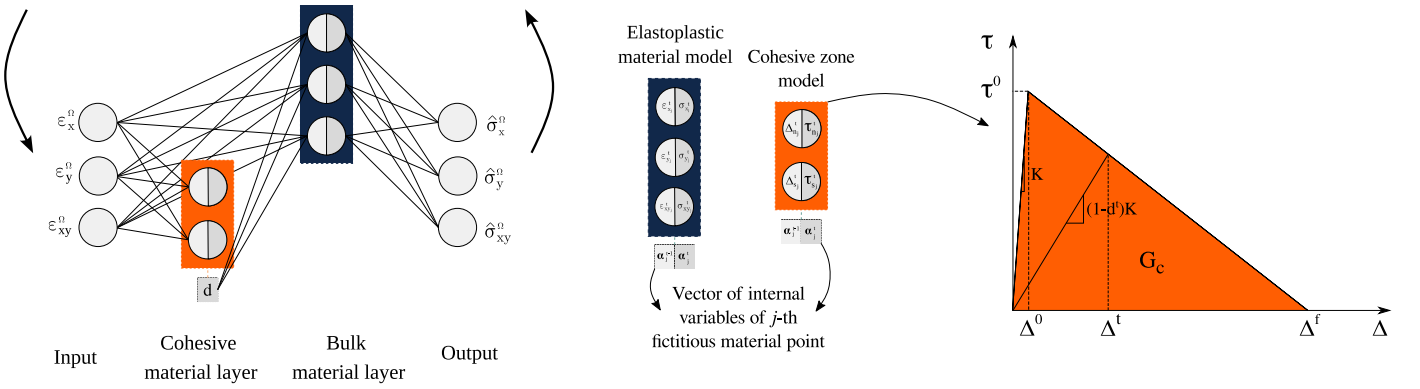

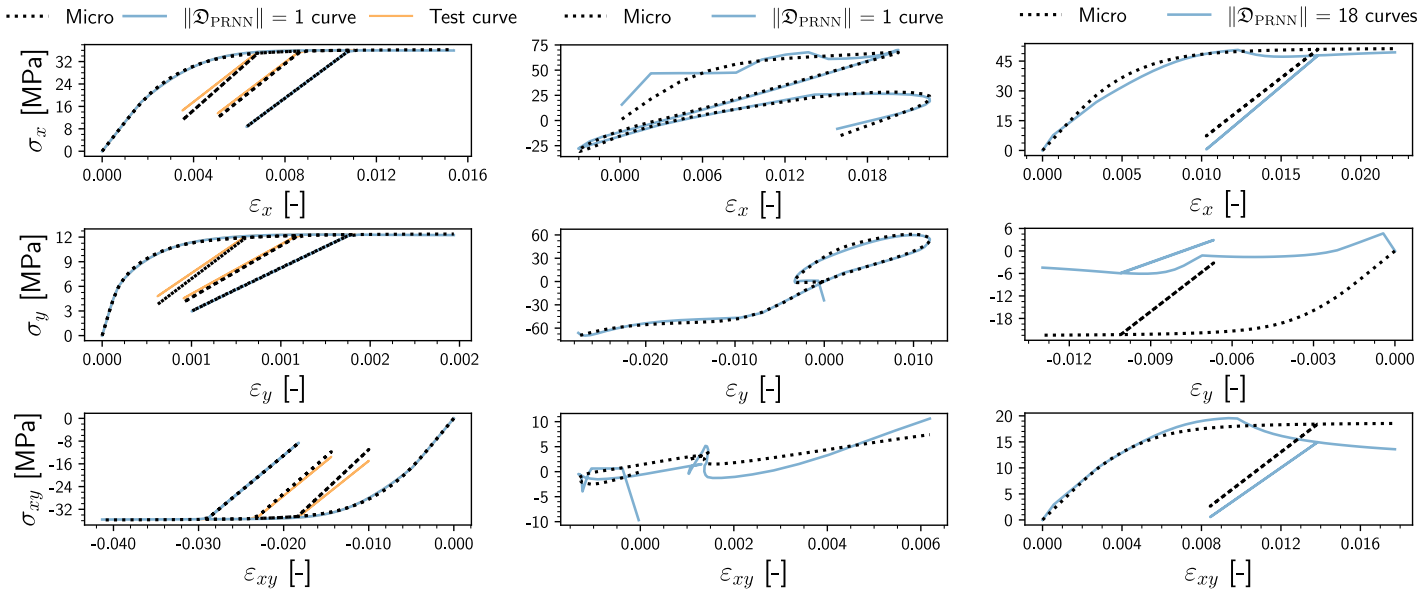

(a) PRNN with 1 bulk and cohesive point (b) PRNN with 3 bulk and cohesive points (c) PRNN with 2 bulk and 3 cohesive points

Figure 1: Prediction of PRNNs trained on different non-monotonic curves

Main takeaways

- A new architecture is required to accurately represent stress homogenization
- There exists a need to account for nonlinearity in the macrostrain to displacement jump relation
- Increasing the size of training data and material points is a necessary step forward

References

[1] M.A. Maia, I.B.C.M. Rocha, F.P. van der Meer. Physically recurrent neural networks for path-dependent heterogeneous materials: Embedding constitutive models in a data-driven surrogate. CMAME, 2023.

MSc progress

1 | 2

Design of a gradient locally resonant acoustic metasurface for negative reflection

X. Kuci, M.G.D. Geers, V.G. Kouznetsova

Eindhoven University of Technology

Introduction

Standard medical devices often pose challenges in ultrasound imaging, increasing the risk during medical interventions due to poor needle visibility. Coating the needle for improved reflection shows promise, yet further enhancements are required. New visualization solutions are vital for precision in needle procedures.

Proposed solution: explore a novel coating type - locally resonant metamaterial (LRAM) to enhance reflection and redirect the reflected wave back to the probe.

Needle visualization *(www.philips.nl)*

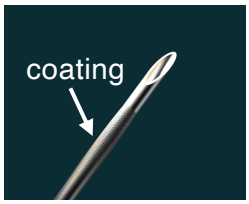

Coated needle for enhanced visibility *(www.encapson.eu)*

LRAM Coating Design

LRAM unit cell:

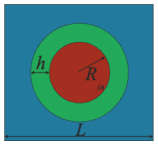

Polyethylene (stiff)
Rubber (soft)
Tungsten (heavy)

- operate in subwavelength regime
- band gap formation (waves cannot propagate)
- waves reflect back to the source

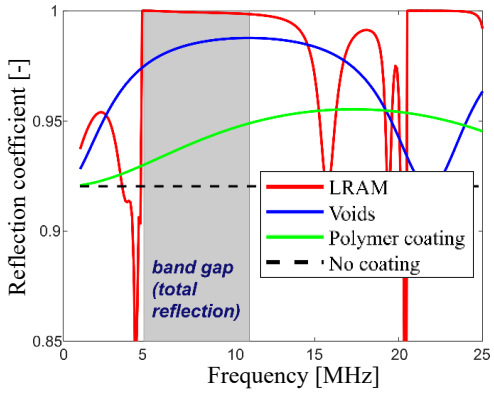

1) Enhanced reflection by LRAM coating:

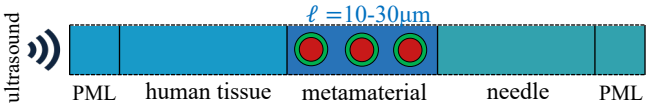

→ Improved reflection (visibility of needle) by LRAM coating compared to alternatives, for frequencies inside the band gap

2) Redirection of reflected wave by gradient LRAM coating:

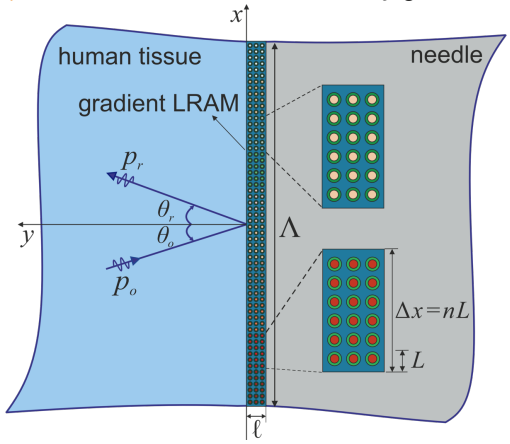

a) Calculate meta-atom size Δx based on the generalized law of reflection:

$$\sin\theta_r = \sin\theta_i + m\frac{\lambda_1}{2\pi}\frac{d\phi(x)}{dx}$$

reflected · incident · diffraction order → phase variation along the surface (discrete steps within the 2π range)

b) Achieve required phase gradient through suitable change of LRAM parameters:

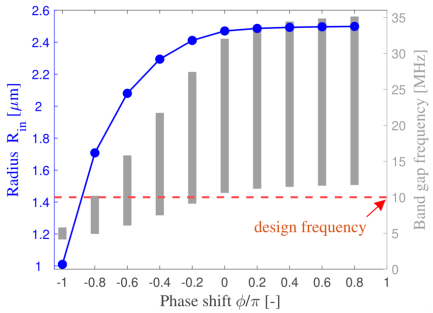

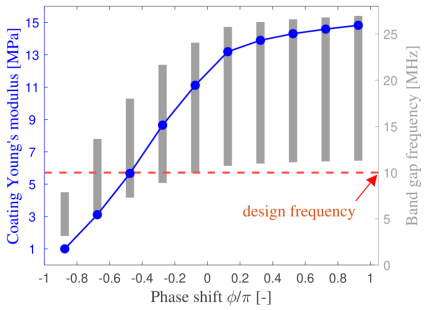

Results

1) Negative reflection:

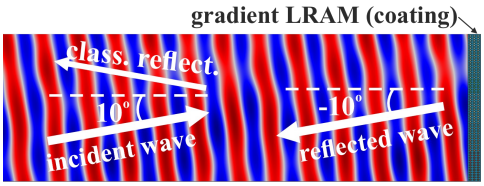

- Robust design w.r.t small variations in angle of incidence
- Good performance for a frequency band of 17% from the design frequency
- Negative angle preserved when incorporating material damping

2) Reflected energy distribution over diffracted order m:

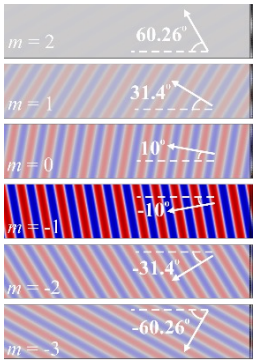

- Gradient LRAM metasurface diffracts energy into different directions
- Highest energy is reflected in the designed negative direction ($m = -1$)

PhD progress: 1 2 3 4

Structure and mobility of twin boundaries in Ni-Ti Shape-Memory Alloys revealed by atomistic simulations

L. La Rosa[1], F. Maresca[1]

[1] *Computational Mechanical and Materials Engineering, Engineering and Technology Institute, University of Groningen*

Abstract

In this study, **atomistic simulations** were conducted to examine the structure and gliding of **Type II twin boundaries** in Ni-Ti. Molecular static simulations confirmed a **terraced geometry**, consistent with experiments [1], and revealed that twin-interface movement is controlled by **twinning disconnections gliding on the terrace planes** at low stresses. Our work thus suggests a **novel selection mechanism** for twin systems in SMAs, whereby interface mobility plays a key role.

Research Questions & Methods

Despite being known for a long time, the shape-memory effect (SME) is still poorly understood, being an emergent property resulting from interactions of mechanisms that take place at different length scales. **Reversible twinning** is the key to unravelling the SME. However, state-of-the-art theories (e.g., EMT) [2] cannot solve the following issues:

1. The atomistic structure of the Type II twins is still debated due to the twin plane orientation's **irrationality** at the continuum scale;
2. It is unclear why the Type II twins are **more observed** in experiments than the other type of twins in Ni-Ti.

A multiscale approach is therefore needed (Fig.1).

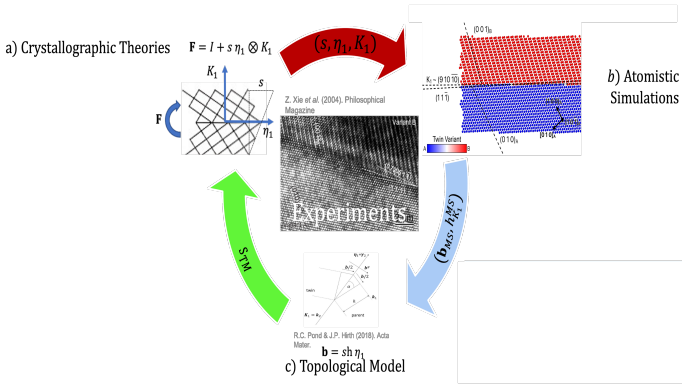

Figure 1: Twin systems (b) have been constructed based on EMT equations (a) [2]. The structures of the relaxed atomic interfaces are then compared with available HRTEM images [1] and the topological model (c) [3].

Results & Conclusions

In Fig.2, the Type II atomic structure can be appreciated.

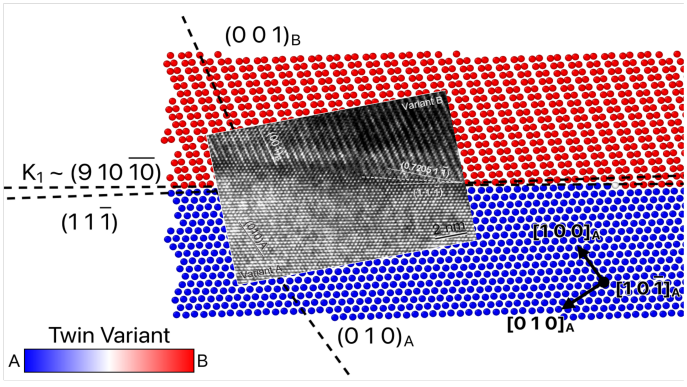

Figure 2: The relaxed twin interfaced has a **terraced structure**. The simulation agrees with the crystallography shown in the attached HRTEM image [1].

In Fig.3, the inverse of the **observation frequency** f_x scales with the twin gliding activation stress τ_{TS}. Therefore, **our analysis suggests that twinning systems with low τ_{TS} will be favoured during martensitic transformations**.

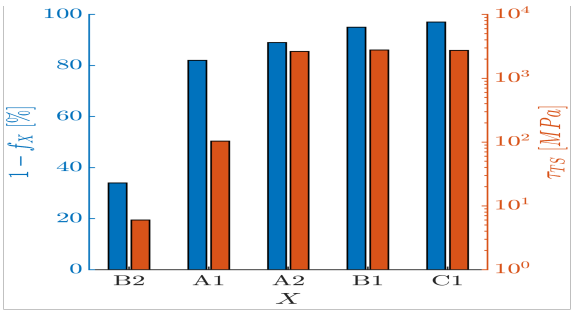

Figure 3: Type II twins (labelled as B2), the most observed twinning system in Ni-Ti, have the **lowest** twinning stress.

References

[1] Xie, *et al.*; Philos. Mag., 2004.

[2] Ball, *et al.*; Arch. Ration. Mech. Anal., 1987.

[3] Pond, *et al.*; Philos. Mag., 2019.

Sound insulation performance of labyrinthine metamaterial described by enriched homogenized continuum

R. Liupekevicius [1], J. A. W. van Dommelen [1], M. G. D. Geers [1], V. G. Kouznetsova [1]

[1]Eindhoven University of Technology

Introduction

Sound insulation at the low audible frequencies can be achieved with sparse arrays of metamaterials [1]. They are a promising candidate to replace classic acoustic treatments that typically use high-density materials. An efficient equivalent continuum is proposed for computing the dynamic response of such labyrinthine domains.

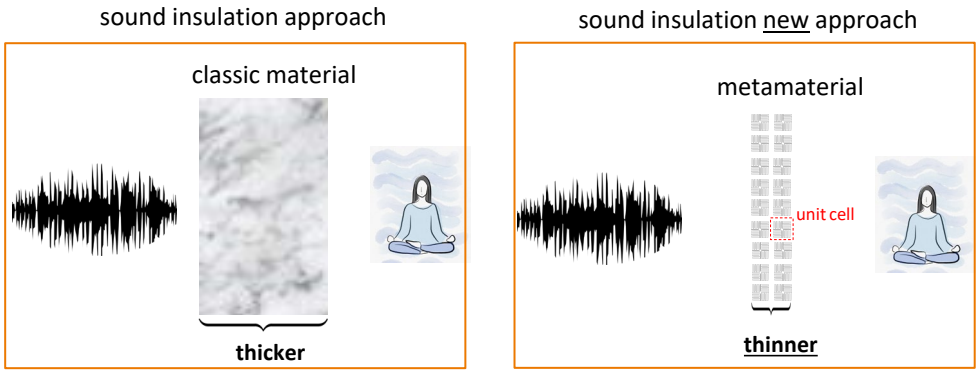

Multi-scale model

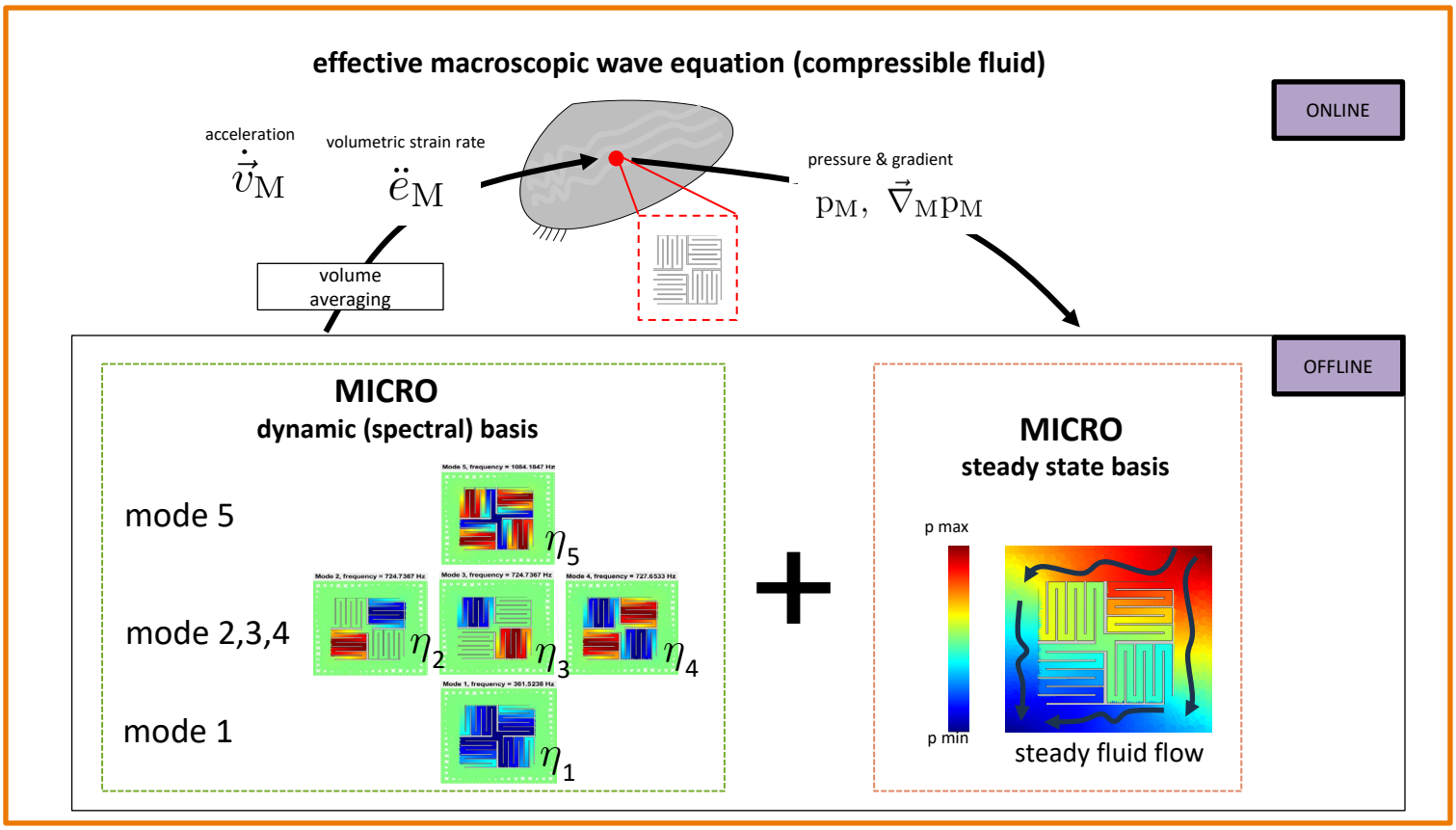

Results

The *mode amplitudes* η are additional dependent variables in the system of equations. The continuum can be solved in a $(p, \eta_1, \eta_2 ...)$-formulation. The effective continuum satisfies the modified constitutive relations below. It is a combination of the frameworks developed in [2] and [3].

$$\phi \ddot{e}_M = -\frac{1}{(K_f)_M}\ \ddot{p}_M + \frac{1}{V}\sum_s c_s\ \ddot{\eta}_s$$

$$\phi \ddot{\vec{v}}_M = -\frac{1}{(\rho_f)_M}\cdot \vec{\nabla} p_M + \frac{1}{V}\sum_s \vec{d}_s\ \ddot{\eta}_s$$

dispersion curve

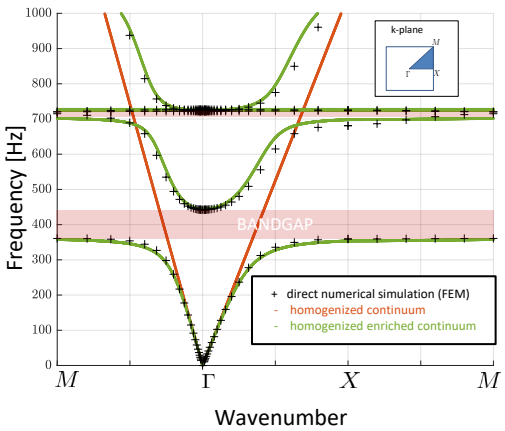

5-unit cell thickness layer

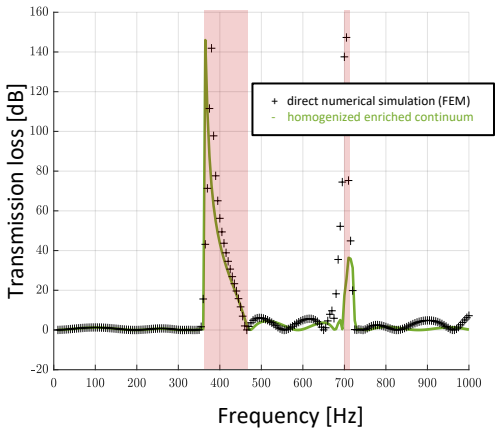

References

[1] Cheng, Y., et al. Nature materials, (2015); **[2]** A. Sridhar. PhD thesis, 2019; **[3]** K. Gao. PhD Thesis, 2016.

PhD progress: 1 | 2 | 3 | 4

Kinematic-based Mathematical and Numerical Formulation for Soft Tissues Growth and Remodeling accounting for Multiple Constituents

Ludovica Maga[1,2] Lise Noël[2] Mathias Peirlinck[1]

1. Department of BioMechanical Engineering
2. Department of Precision and Microsystems Engineering
Delft University of Technology

Soft Tissue G&R

Living tissues have the ability to **growth and remodel** (G&R) as an adaptive response to pathological or physiological changes in the bio-environment.

G&R is the manifestation of sub-processes that occur at the microscale involving **multiple constituents** that are present in the tissue.

Understanding how local changes in the microstructure translate into global adaptation of soft tissues is crucial to predict disease onset and progression.

Aim of the work

Developing a novel **mathematical and numerical framework** able to correlate local changes in volume and density of multi-constituents to global geometrical and functional alteration at the tissue level by using kinematic-based approach.

.

Modeling Approaches for G&R

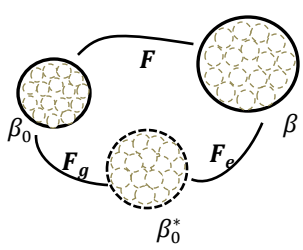

$$F = F_e F_g$$

Kinematic growth (KG)

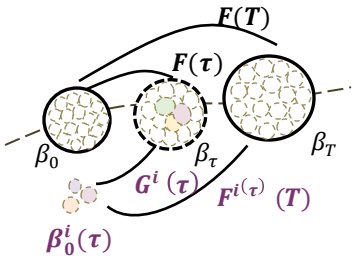

$$F^{i(\tau)} = F(T)\,F(\tau)^{-1}\,G^i$$

Constrained mixture growth (CMG)

In classical KG formulation the tissue is modeled as a single-constituent that experience **volumetric changes** due to alteration in **mechanical stress/strain** state of the material. According to CM, different tissue constituents deposit and remove continuously and are bound to deform within a single continuum.

Although *microstructurally* informed, CM is intrinsically more complex compared to KG and computationally highly demanding. Furthermore, its validation against experimental data presents significant challenges.

KG-based Multi-Constituent Formulation

1. Soft tissues are modeled as mixture of constituents that are simultaneously present at a material point at *affine* deformations.

$$F = F_e F_g$$
$$F^g = \hat{v}^{\frac{1}{3}} I \quad \textit{Isotropic growth}$$

2. Individual mass change of each constituent can occur due to an alteration in **volume** or **density** and sum up to changes in mass of the whole tissue

$$\hat{v} = \sum_{\zeta=1}^{N} \hat{v}_1 \varphi_{0,1} + \hat{v}_2 \varphi_{0,2}$$
$$\hat{\rho}_\zeta = \hat{m}_\zeta \cdot \frac{1}{\hat{v}}$$

Numerically, local mass and volume changes are treated as *internal variables* that are iteratively determined via Newton-Rapson iteration procedure.

KG-based Growth: Numerical Result

Stress-driven growth in a 3D single-constituent cubical tissue sample. Volume growth is induced by applying *n=5* loading steps.

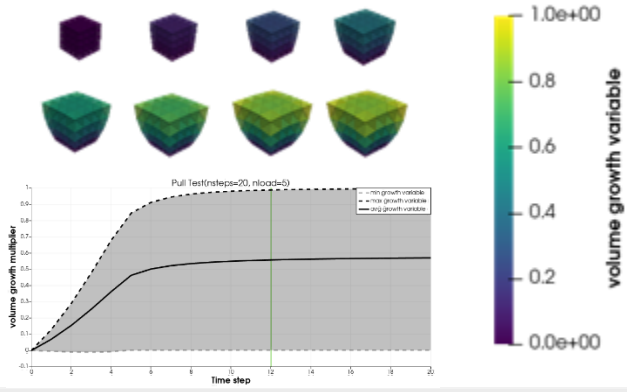

Conclusions

A novel formulation has been introduced, which integrates key aspects from KG theory and CM theory, to model growth and remodeling processes in soft tissues. Such formulation allows to link changes in the micro-structure to global alteration at the tissue level. Future work will be devoted in testing and validating the formulation to assess its capabilities in predicting tissue maladaptive G&R.

References

1. Cyron, C.J., Humphrey, J.D. Growth and remodeling of load-bearing biological soft tissues. *Meccanica* 52, 645–664 (2017).
2. Yifan, G., Mohammad, RKM., Tepole, A. On modeling the multiscale mechanobiology of soft tissues: Challenges and progress. *Bioph. Rev.* 3.3 (2022).

Physically Recurrent Neural Network (PRNN) for rate and path-dependent heterogeneous materials

M.A. Maia, I.B.C.M. Rocha, F.P. van der Meer

Delft University of Technology

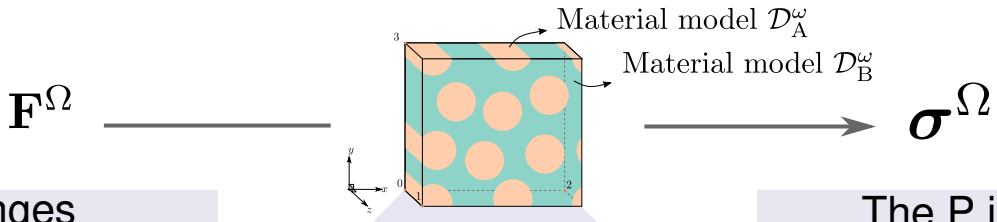

Challenges

Feed-forward Neural Networks (NNs) can learn a mapping from strains to stresses as a surrogate for a micromodel. However, such setting cannot reproduce path and rate-dependency.

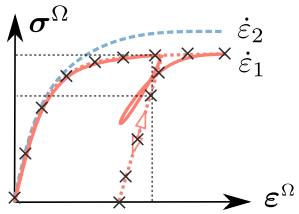

For that, Recurrent NNs (and more complex variations such as LSTMs and GRUs) are often used to account for the history-dependence. In LSTMs, the cell and hidden states play the role of the history variables.

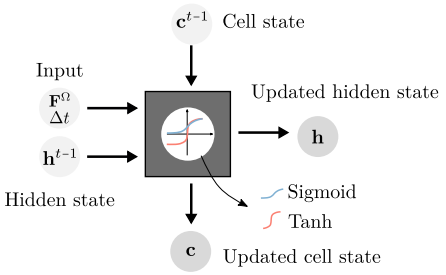

However, the black-box nature of these mechanisms still poses many challenges (e.g. data-hungriness, poor extrapolation, etc.).

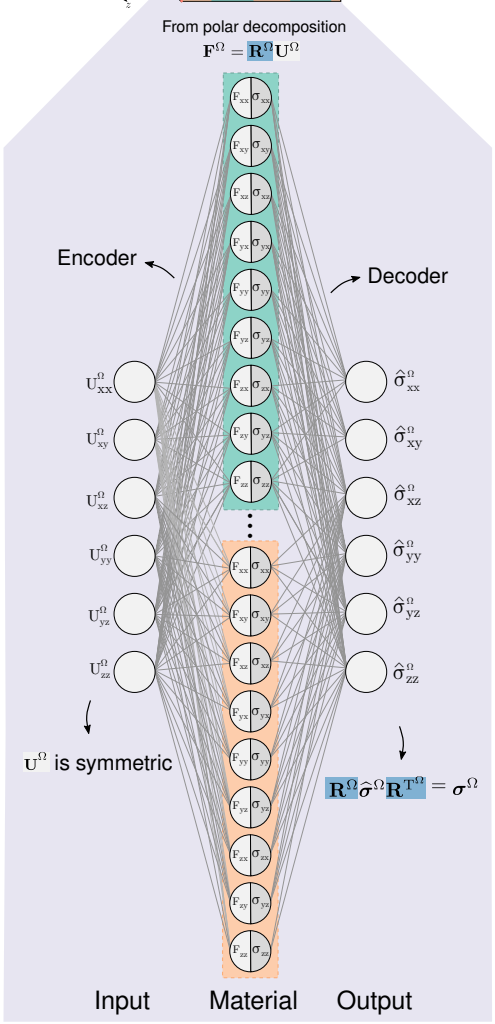

The P in PRNN

A Material layer is introduced with the same physics-based material models as in the micromodel. This way, rate and path-dependency arises naturally since each material point keeps track of its own (local) internal variables.

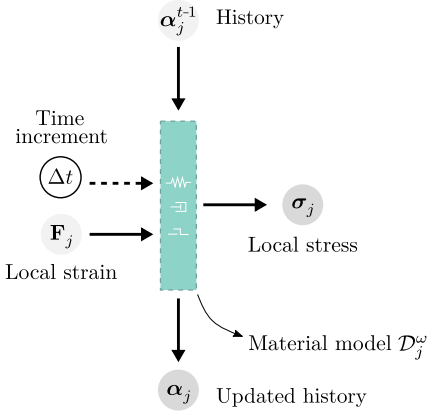

The encoder learns how to dehomogenize the macro strain into local strains and the decoder learns how to homogenize the local stresses into macro stress.

Here, a network with 4 points of each material model is used:

$\mathcal{D}^\omega_\mathrm{A}(\mathbf{F})$ → Hyperelastic transversely isotropic

$\mathcal{D}^\omega_\mathrm{B}(\mathbf{F}, \Delta t, \boldsymbol{\alpha})$ → Elasto-viscoplastic

Results

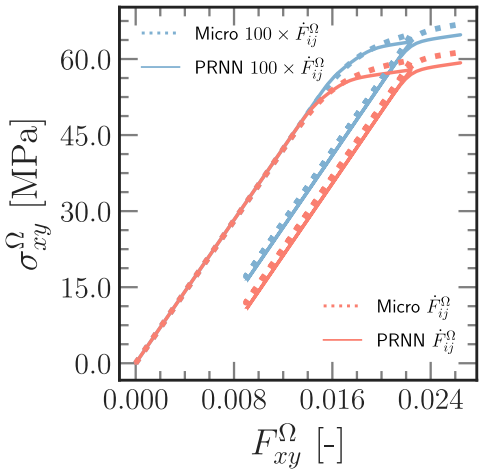

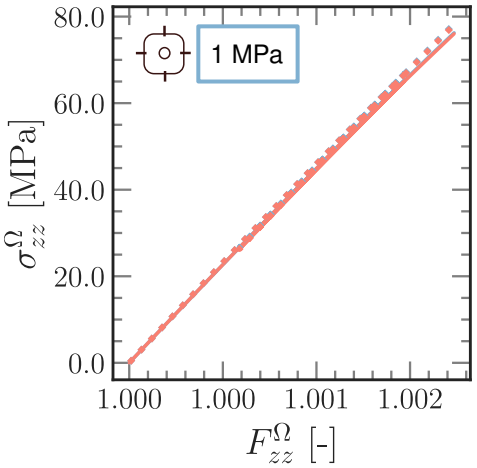

- ✓ Extrapolation to unloading behavior based only on monotonic data
- ✓ Time and path-dependency are incorporated through the use of rate and path-dependent material models
- ✓ The orthotropic behavior of the micromodel shows in the unloading in the xy component vs the z component (fiber direction)

References

M.A. Maia, I.B.C.M. Rocha, P. Kerfriden, F.P. van der Meer. CMAME, 2023.

PhD progress

1 | 2 | 3 | 4

Quantum Computing for Machine Learning Interatomic Potentials

Koen Mesman

Aerospace Structures and Computational Mechanics,
Delft University of Technology

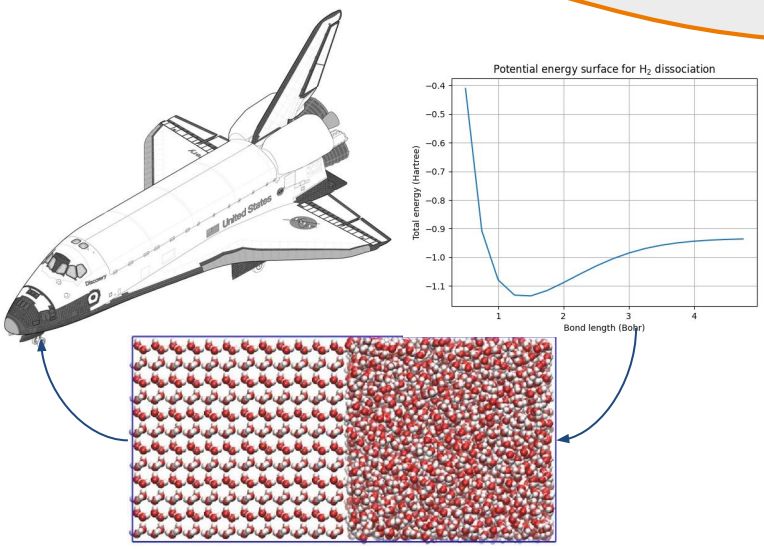

Molecular dynamics simulation by Y. Xiong et al. [3]

Background

An important but challenging field within aerospace materials is the development of **heat shields**. Heat shields must have the properties of having a low thermal conductivity or high melting temperature and high durability[1]. Since in-situ experiments on potential materials is an expensive solution that does not scale, simulations are used to approximate the material properties. For this reason, accurate simulations are required to provide a suitable surrogate. To simulate these challenging materials and dynamics, **molecular dynamics** (MD) are needed: a simulation of classical effects aimed at a larger structure in the order of nm. To facilitate MD simulations, forces derived from interatomic potentials (IAP) are required. The data for the IP are generated through **ab-initio** methods, such as Density Functional Theory (DFT) simulations. This method is, however, too computationally expensive for MD[2]. Instead, machine learning IAP (MLIAP) models are used as a faster but less accurate method.

Quantum computing

Quantum computers, as opposed to conventional computers, use quantum bits (qubits) to store information. This allows the processing of quantum data such as entangled quantum mechanical states to be prepared and processed. As quantum computers can efficiently simulate materials in the ab-initio regime [3], it naturally is a candidate to accelerate the simulation and possibly improve machine learning of ab-initio potentials. The conventional method to compute IAP using quantum computing algorithm is the variational quantum eigensolver (**VQE**) as shown in the Figure, right [4]. This method uses a parameterized circuit and a classical optimizer to train its parameters. However, this process is slow with large engineering challenges.

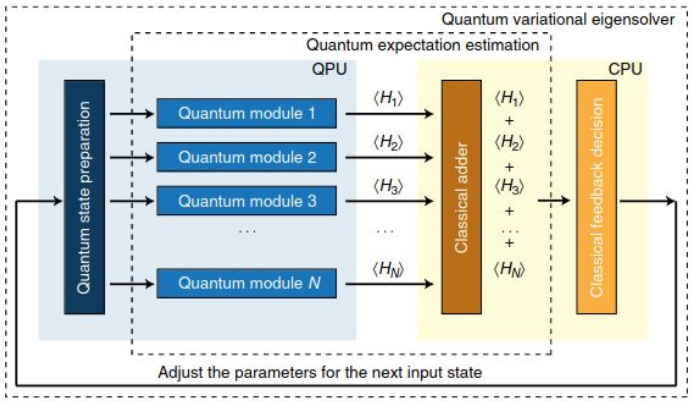

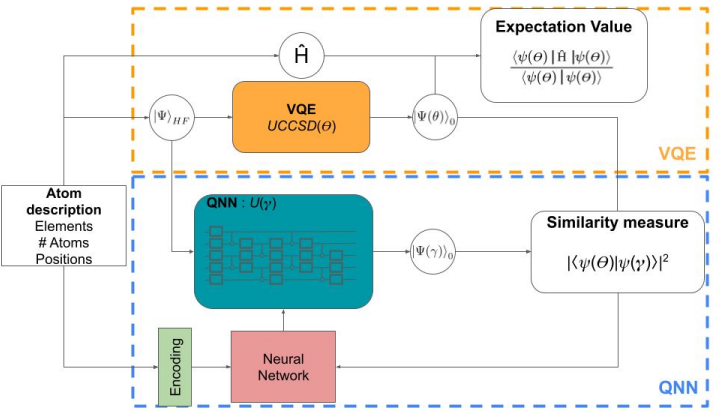

Current status

The proposed method of improving MLIAP using quantum computing is to use quantum machine learning (**QML**). In this method, quantum computing models are used to learn quantum mechanical processes, such as the stabilization of a system to a ground state. The proposed model learns the quantum state it needs to construct based on the atom descriptions given. The model receives its feedback from a similarity test for **supervised learning**. Quantum supervised learning was shown to give an advantage over classical learning with respect to training data requirements [4]. Currently, a basic *TwoDesign* model [5] has been used for the QML model. The model needs to be verified that the search space of the model can capture the quantum mechanical process, and improvements are required for the required accuracy.

Future work

Currently, a very basic implementation of the QML model has been implemented. Results need to be examined and used to improve upon the model. The direction of improving the model using graph based networks will also be taken into consideration. Furthermore, challenges in qubit efficiency in **encoding** and model **generalization** will be addressed. To this end, quantum autoencoding will be explored, but could give challenges in the form of nonphysical solutions. Furthermore, making the model **physically informed** is required to make the model accurate and generalizable.

Citations

[1] S. Loehle, T. Hermann, and F. Zander, "Experimental assessment of the performance of ablative heat shield materials from plasma wind tunnel testing," CEAS Space journal, vol. 10, pp. 203–211, 2018.
[2] M. R. Gilbert, et al., "Perspectives on multiscale modelling and experiments to accelerate materials development for fusion," Journal of Nuclear Materials, vol. 554, p. 153113, 2021.
[3] Y. Xiong, P. S. Shabane, and A. V. Onufriev, "Melting points of opc and opc3 water models," ACS Omega, vol. 5, no. 39, pp. 25087–25094, 2020. PMID: 33043187.
[3] R. P. Feynman et al., "Simulating physics with computers," Int. j. Theor. phys, vol. 21, no. 6/7, 2018.
[4] A. Peruzzo et al., "A variational eigenvalue solver on a photonic quantum processor," Nature communications, vol. 5, no. 1, pp. 1–7, 2014.
[5] M. Cerezo, et al. "Cost function dependent barren plateaus in shallow parametrized quantum circuits," Nature Communications, vol. 12, Mar. 2021. DOI: 10.1038/s41467-021-21728-w

TU Delft

PhD progress

1	2	3	4

QAIMS

Time-dependent Anisotropic Behavior of Continuous Fibre Reinforced Thermoplastics.

S.N.R. Mudunuru, J.A.W. van Dommelen, L.E. Govaert

Eindhoven University of Technology

1. Introduction

As part of the Enlighten program, this project aims to provide a methodology that links microstructural information, such as matrix morphology, and fibre distribution, to macroscopic laminate performance.

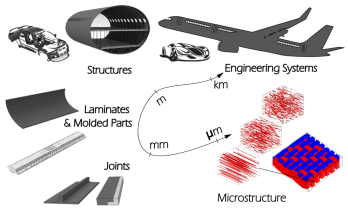

2. Methodology & Materials

While micromechanical simulations provide the means to include relevant deformation mechanisms and orientation-dependent complexities, they are computationally expensive for full-scale models of structures. The goal is to develop a continuum model based on the data gathered using micromechanical simulations.

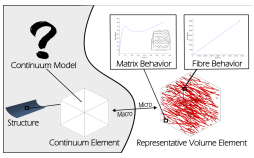

The methodology will be validated by characterizing the mechanical behavior of two Fibre Reinforced Thermoplastic Composite (FR-TPC) systems:

1. Glass fibres in PA410 matrix
2. Carbon fibres in LM-PEAK matrix

3. Research Objectives

1. **Micromechanical simulation of the FR-TPC.**
2. **Characterization of polymers and composites.**
3. **Model the continuum behavior of FR-TPC.**

4. Results

Statistically Equivalent Representative Volume Element (SERVE)

1000μm micrograph [a]

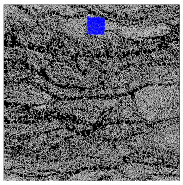

Voronoi diagram

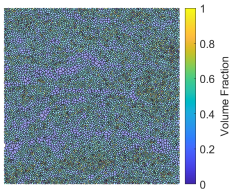

Area fraction distribution

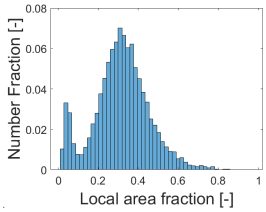

Area fraction from 100 μm windows

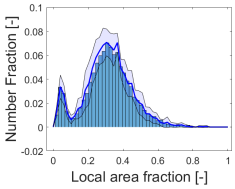

100 μm window

Test geometry

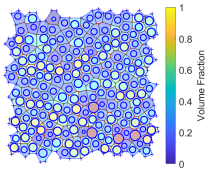

Area fraction distribution

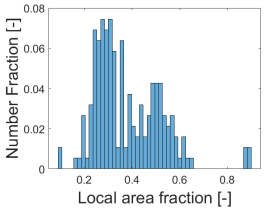

Deformed geometry

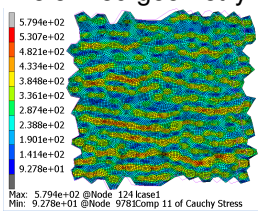

Transverse loading

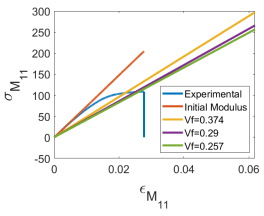

[a] Microscopy image from B.K. Sundararajan, University of Twente

4. Future Work

1. Survey for material properties of fibers and the matrix in the elastic regime.
2. Refine fibre detection procedure.
3. Use appropriate constitutive models for FR-TPC systems of interest.
4. Develop continuum models.

PhD progress

1	2	3	4

Comparison of artificial neural network and physics-informed neural network applied to finite deformation

F. Munzone[1], J. Hazrati[1], W.B.J. Hakvoort[2], T. van den Boogaard[1]
[1]University of Twente, Faculty of Engineering Technology, Nonlinear Solid Mechanics
[2]University of Twente, Faculty of Engineering Technology, Precision Engineering

1 Motivation and methods

Surrogate models are employed as a substitute for physics-based models to obtain cheap predictions. **Physics-informed neural networks** (PINN) are a type of surrogate model, heavily based on neural networks, capable of solving PDEs while respecting the governing equations of the system [2]. Metal forming processes are subject to **finite** (large) **strain** and **non-proportional loading**. Moreover, design space exploration is expensive if perused with expensive tools (i.e., FEM). The **simple shear** problems are subject to non-proportional loading [1], which makes them a good candidate for evaluating the potential of PINN. The **uniaxial tension** is applied to add complexity to the problem.

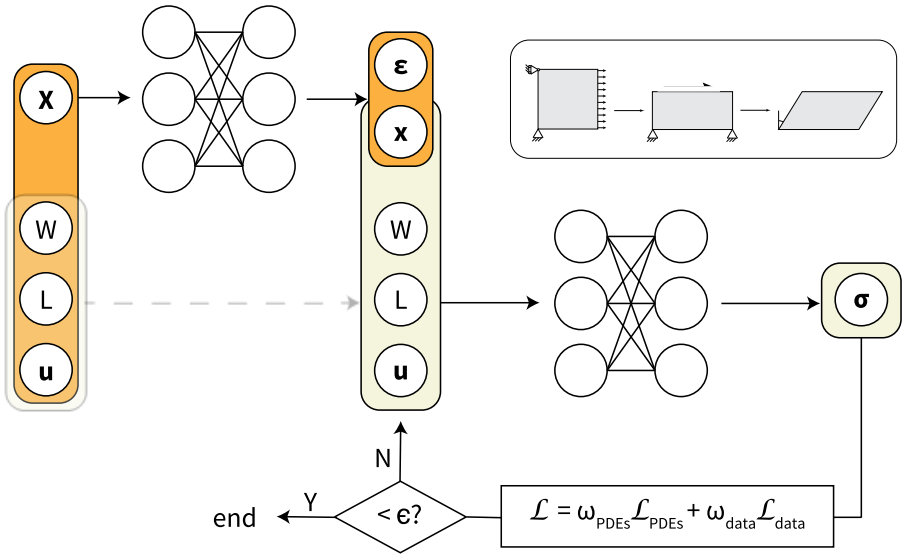

Figure 1: PINN architecture employed to study the tension-simple shear problem.

2 Results

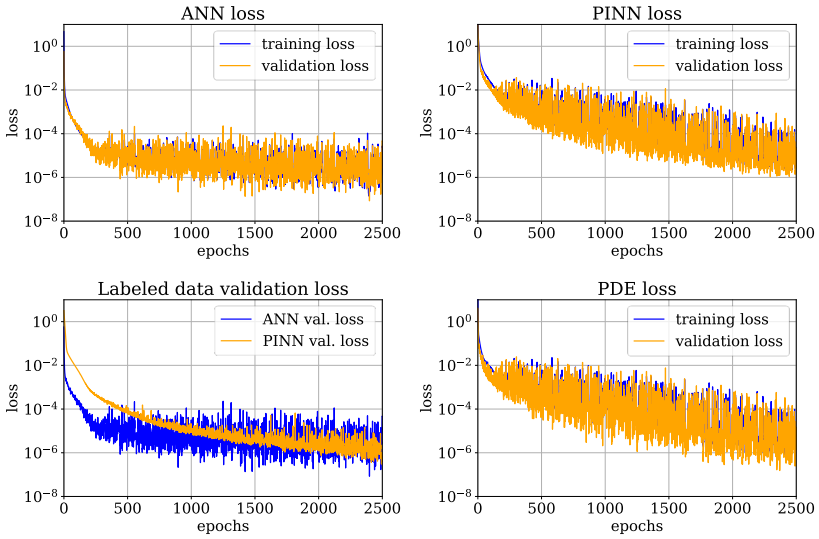

Figure 2: Comparison of ANN and PINN losses.

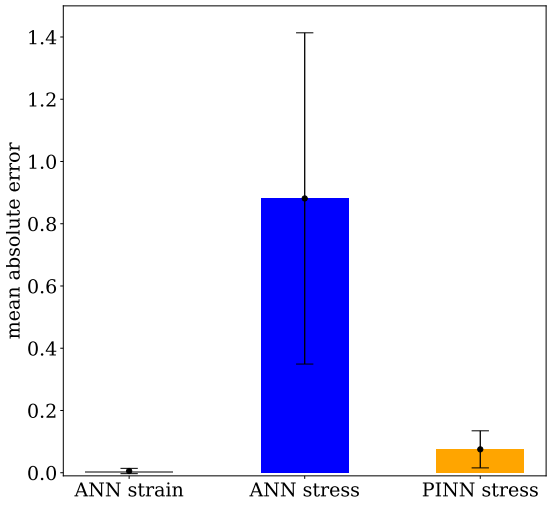

Figure 3: Mean absolute error and standard deviation of different quantities.

3 Conclusion and outlook

- The ANN performs better than the PINN regarding the minimization of the loss. However, the physics equations act as a regulator leading to better predictions (labeled data loss). Furthermore, the mean absolute error and the standard deviation of the absolute error prove that the PINN predictions are of higher quality;
- Even better predictions are expected with the implementation of **time steps** and **constitutive equations**.

References

[1] C. Butcher, A. Abedini, Shear confusion: Identification of the appropriate equivalent strain in simple shear using the logarithmic strain measure, Int. J. Mech. Sci. 134 (2017) 273–283
[2] M. Raissi, P. Perdikaris, G. E. Karniadakis, Physics-informed neural networks: A deep learning framework for solving forward and inverse problems involving nonlinear partial differential equations, J. Comput. Phys. 378 (2019) 686–707

Modelling of Recycled Fibre-Reinforced Polymer Composites

N. Nazemzadeh[1,*], I. Gitman[1] , F. Liu[1], R. Akkerman[2]

[1]University of Twente, Computational Design of Structural Materials
[2]University of Twente, Production Technology
*n.nazemzadeh@utwente.nl

SCAN ME

Introduction and problem statement

Fibre-reinforced polymer (FRP) composites are engineered materials used in many industries, including aerospace, automobile, sports and healthcare, due to their excellent strength-to-weight and stiffness-to-weight ratios. Due to their wide usage, these materials unfortunately produce industrial scraps. Recycling and reusing composites' scraps could potentially reduce disposal expenses, the demand for new materials and the negative effects on the environment.

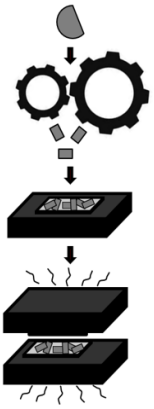

Figure 1: Recycling and remanufacturing processes

Project Aim

•Develop understanding and predict the behavior of recycled fiber reinforced polymers through a comprehensive multi-scale modeling approach.
•Investigate the impact of different geometric arrangements (periodic, aperiodic, and random) on specific applications and loading conditions.

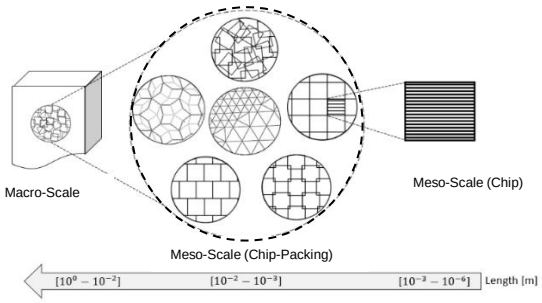

Figure 2: Multiscale modelling strategy

Method

Boundary condition & loading

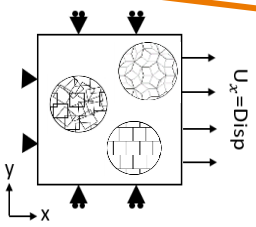

Figure 3: Tensile loading & Boundary condition

Material properties

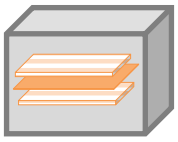

Figure 4: Materials

C/PEEK flake: Transversely isotropic

Interface: cohesive interface

PEEK resin: Isotropic

Geometry

Periodic

Simple Tiling

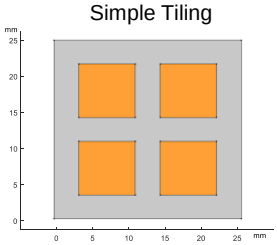

Shifted Tiling

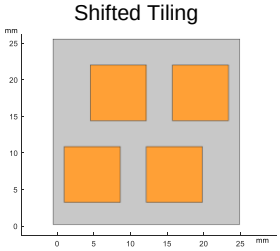

In simple tiling, *the distance between centers is equal in both the x and y directions. However, in* ***shifted tiling,*** *the distance in the y-direction is twice that in the x-direction.*

Aperiodic

Penrose

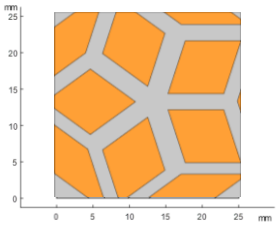

Penrose algorithm *consists of two triangular flakes, with apex angle of 36° and 108°. There is another vertex (P), which is called golden ration, equals to* $\frac{1+\sqrt{5}}{2}$.

Random

2D Random

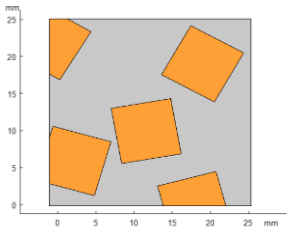

3D Random In-plane Orientation

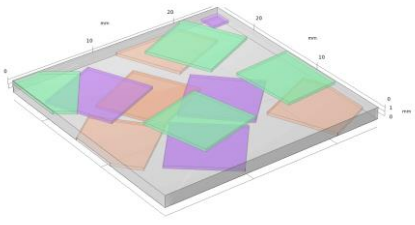

3D Random Out-of-plane Orientation

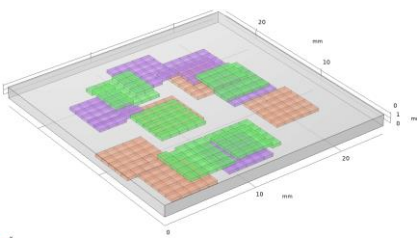

2D Random *creates based on non-overlapping algorithm between flakes. at higher volume fraction, 2D models tend to overpredict the ultimate tensile stress (UTS).* ***3D in-plane orientation*** *created based on random sequential adsorption algorithm. In-plane model limited by lower volume fraction, lacks resin-rich areas.* ***3D out-of-plane orientation*** *is based on Voxel-based framework.*

Resin
3rd Layer
2nd Layer
1st Layer

Conclusions and future work

Investigate the impact of different geometric arrangements (periodic, aperiodic, and random) under tensile loading condition, aiming to develop tailored composite materials with superior performance.

References

[1] M. I. A. Rasheed., "Compression molding of chopped woven thermoplastic composite flakes." (2016).

UNIVERSITY OF TWENTE.

PhD progress

1	2	3	4

Production Technology
ADVANCED MATERIALS ENGINEERING

A new view on the solution of rate-independent crystal plasticity models

B. Nijhuis✉, E.S. Perdahcioğlu, A.H. van den Boogaard

Chair of Nonlinear Solid Mechanics, University of Twente

✉ b.nijhuis@utwente.nl

1. Background

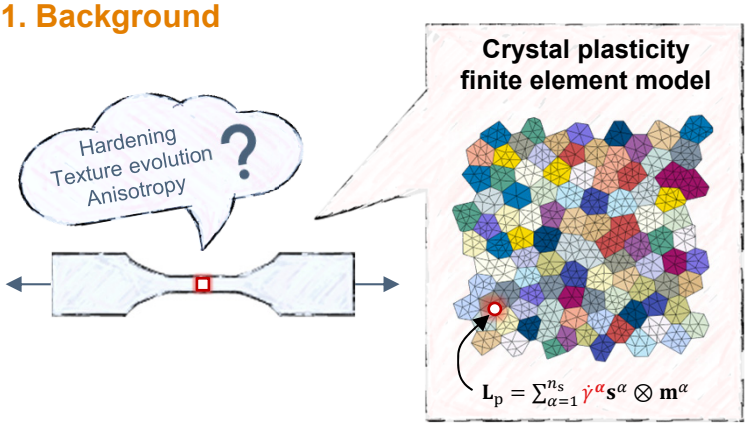

2. Common crystal plasticity models

- **Rate-dependent:** $\dot{\gamma}^\alpha = \dot{\gamma}_0 \left(\frac{|\tau_\mathrm{R}^\alpha|}{\tau_\mathrm{f}^\alpha} \right)^\mathrm{p} \mathrm{sign}(\tau_\mathrm{R}^\alpha)$

  All slip systems active

  × ↳ Small amount of slip even if $|\tau_\mathrm{R}^\alpha| < \tau_\mathrm{f}^\alpha$

  × Instable in rate-independent limit $p \to \infty$, $\dot{\gamma}_0 \to 0$

- **Rate-independent:** $\boldsymbol{\sigma} = \arg\max_{\tilde{\boldsymbol{\sigma}} \in \mathcal{F}} (\tilde{\boldsymbol{\sigma}} : \mathbf{D}_\mathrm{p})$

  $\mathcal{F} = \{ \boldsymbol{\sigma} \mid |\tau_\mathrm{R}^\alpha| - \tau_\mathrm{f}^\alpha \leq 0 \quad \forall \alpha \}$

  Subset of slip systems active

  ✓ ↳ No slip if $|\tau_\mathrm{R}^\alpha| < \tau_\mathrm{f}^\alpha$

  × Active set may be instable

3. A new view on the problem

Function monotonically non-increasing in γ^α — Plane in n_s dimensions

$$\hat{r}^\alpha = \tau_\mathrm{tr}^\alpha - \hat{g}^\alpha(|\boldsymbol{\gamma}|) - \sum_{\beta=1}^{n_\mathrm{s}} \mathbf{P}^\alpha : \mathbb{C}_\mathrm{e} : \mathbf{P}^\beta \Delta\gamma^\beta = 0 \quad \forall \alpha$$

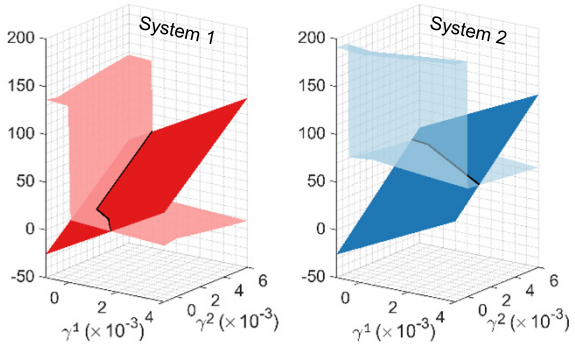

4. Fixed-point iteration-based stress update algorithm

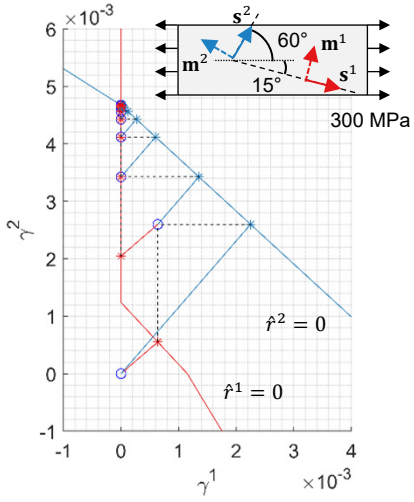

$\Delta\boldsymbol{\gamma} \leftarrow \Delta\boldsymbol{\gamma}_0$, $n \leftarrow 0$

until convergence do:

- for $i = 1, 2 \ldots, k$:
  - $n \leftarrow n + 1$
  - for $\alpha = 1, 2 \ldots, n_\mathrm{s}$:
    - **Line search:**
      - find intersection point $\Delta\hat{\boldsymbol{\gamma}}$
      - between line $\Delta\boldsymbol{\gamma}_{n-1} + t^\alpha \mathbf{d}^\alpha$
      - and hypersurface $\hat{r}^\alpha = 0$
    - $\Delta\gamma_n^\alpha \leftarrow \Delta\hat{\gamma}^\alpha$
- **Acceleration:**

  Update estimate $\Delta\boldsymbol{\gamma}_n$ based on previous k estimates

5. Results

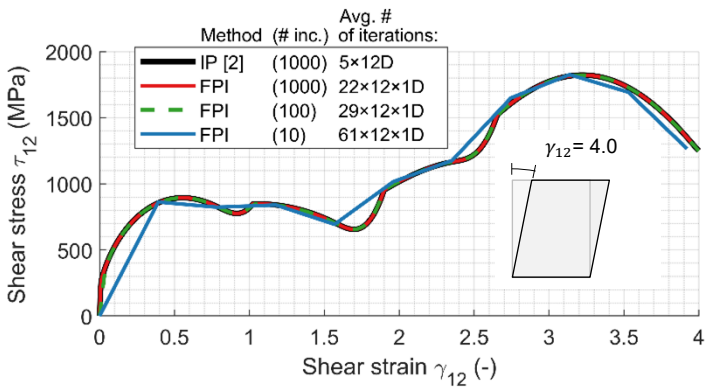

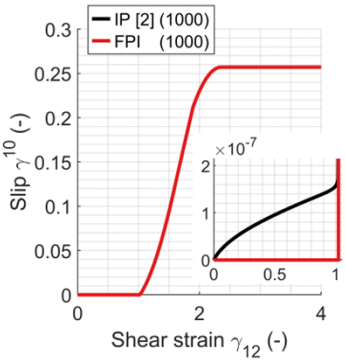

Material properties

Aluminium - FCC crystal

$\tau_\mathrm{f}^\alpha = \tau_0 + Gb\sqrt{\sum_{\beta=1}^{n_\mathrm{s}} Q^{\alpha\beta}\rho^\beta}$

G = 27.7 GPa

τ_0 = 18 MPa

b = 2.87× 10^{-7} mm

$Q^{\alpha\beta}$ = 1.0 if $\alpha = \beta$, else 1.4

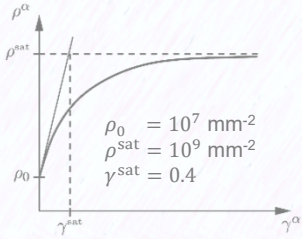

ρ_0 = 10^7 mm^{-2}

ρ^sat = 10^9 mm^{-2}

γ^sat = 0.4

6. Conclusions and outlook

The novel stress update algorithm based on fixed-point iterations (FPI) automatically identifies active slip systems without introducing spurious slips on inactive systems.

It will be further improved by combining mathematical accelerations methods for FPI with knowledge about the physics of the problem.

References

[1] Miehe and Schröder (2001) Int. J. Numer. Meth. Eng. **50**:273-298.

[2] Perdahcioğlu (2023) *A rate-independent crystal plasticity algorithm based on the interior point method*. Under review.

Gaps and Overlaps in Automated Fiber Placement (AFP) Composites. WHY DO THEY OCCUR?

Siddharth Pantoji[1], Dr. Daniël Peeters[1], Dr. Christos Kassapoglou[1]

[1]Delft University of Technology

Sources of Gaps & Overlaps

Gap and overlap defects slow down AFP composites production because they need to be detected, checked for allowable magnitude and repaired if necessary. These gaps and overlaps are caused due to incorrect tape position and/or incorrect tape geometry caused due to various manufacturing process variations. Such defects cannot be predicted before manufacturing.

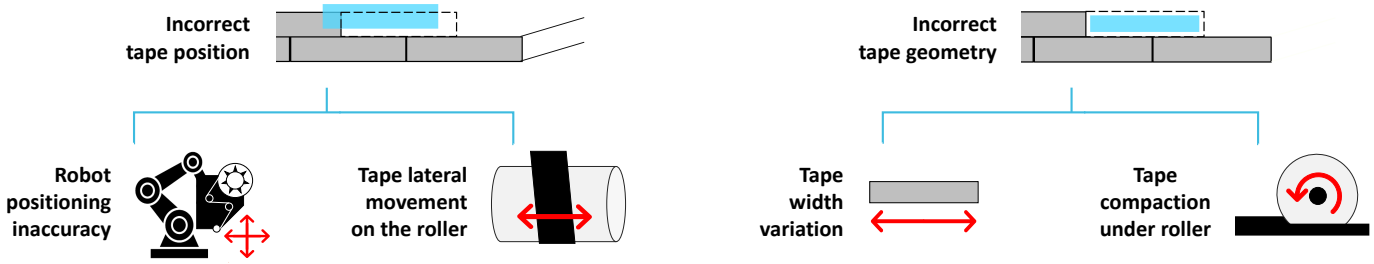

Experimental Setup

Four sources of manufacturing process variations were measured using various sensors mounted on an AFP head. A laser tracker measured robot positioning inaccuracy while a camera measured tape lateral movement on the roller. Two laser line scanners measured the width of the tape, before and after layup.

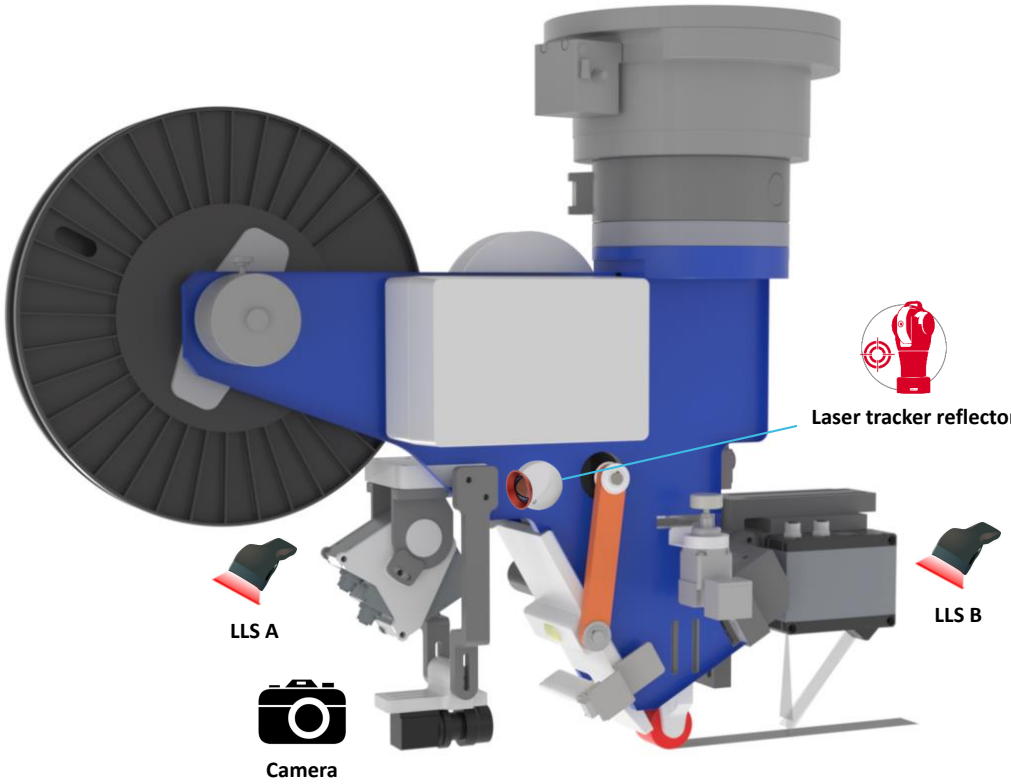

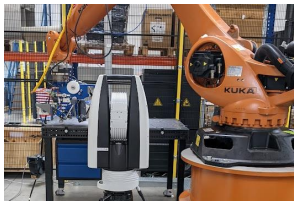

Laser Tracker

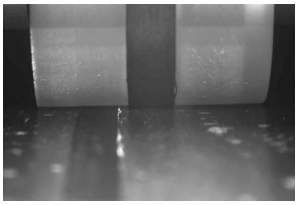

Tape measured by camera

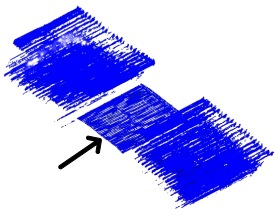

Tape measured by LLS

Results

Resulting probability density functions from the experimental layup are shown below. These distributions illustrate the relative significance of the sources of defects. These can help in prioritizing future AFP technology enhancements, improving process control and predicting the frequency and magnitude of gap and overlap defects in a composite part.

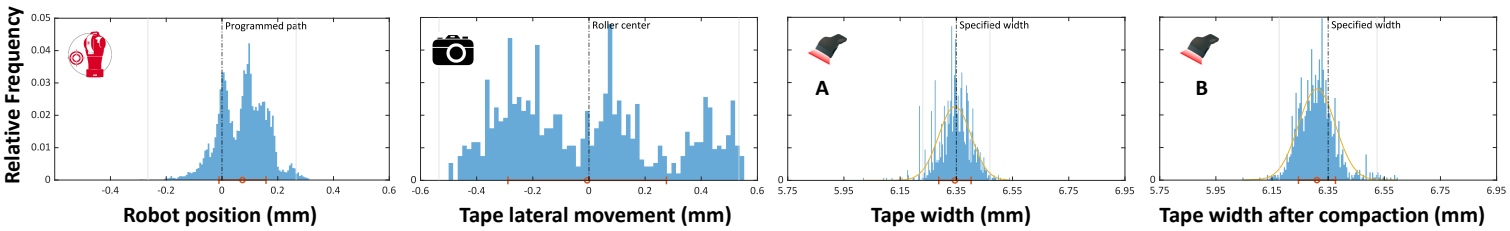

A multi-scale approach for chemo-mechanical degradation of paper: insights into the governing factors

A. Parsa Sadr[1], E. Bosco[1], A.S.J. Suiker[1]

[1]*Eindhoven University of Technology*

Department of the Built Environment

Introduction

Paper degradation results from complex physical and chemical processes over time. Chemical degradation reduces the cellulose molecular weight and has consequences on the mechanical strength of fibers. Moisture-induced fiber expansion and inter-fiber bond stresses can further affect the paper integrity. Our research examines the impact of the micro-structural features of paper, as well as the influence of time-dependent acidity and moisture content on the paper degradation process. We employ a multi-scale, multi-physics approach to gain insights into the aging process of historical paper artifacts.

Method:

The decrease of fiber mechanical properties is associated with the cellulose degree of polymerization (DP) [1]. The rate of this chemical reaction depends on paper moisture content, temperature (T), and pH level. As paper ages, volatile compounds increase acidity, accelerating chemical degradation [2] (Fig. 1). Furthermore, during the degradation process the cellulose capacity to absorb moisture progressively decreases [2, 3] (Fig. 2).

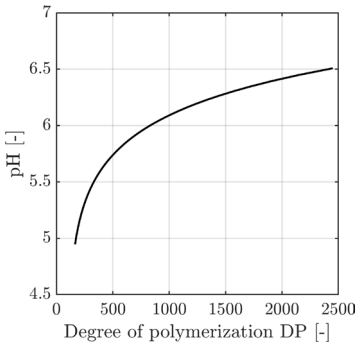

Fig 1. pH variation as a function of degree of polymerization.

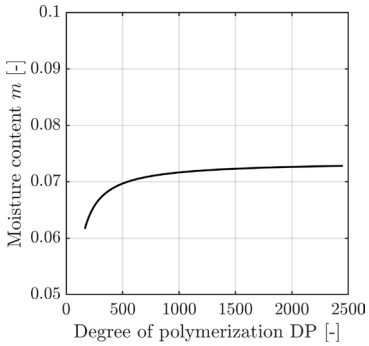

Fig 2. Moisture content variation as a function of degree of polymerization.

Different fiber orientations at inter-fiber regions trigger interactions between hygroscopic and mechanical phenomena, causing internal stresses in paper. To account for the impact of fiber orientation on paper degradation, we use a wrapped Cauchy orientation distribution for generating the fibrous network, in which a parameter q defines the degree of anisotropy. Asymptotic homogenization is employed to obtain the internal stresses within the fibrous network and the homogenized hygro-elastic paper properties. When the local fiber stress reaches its age-dependent tensile strength, brittle failure occurs. The homogenized mechanical properties are evaluated based on the updated, degraded microstructure. Figure 3 illustrates the evolving microstructure and stress distribution within a unit cell due to chemo-mechanical paper degradation at pH = 6, under storage conditions T = 20°C and RH = 50%.

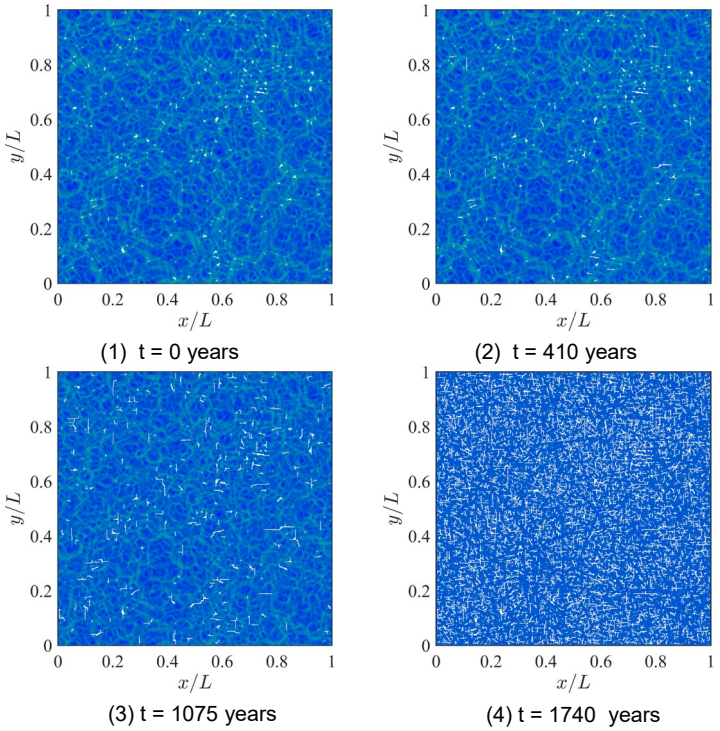

Figure 3. Time-dependent degradation of the micro-structure

Results

Figures 4 and 5 depict the impact of microstructural features (fiber orientation and the fiber's elastic modulus) on the stiffness degradation of paper, respectively.

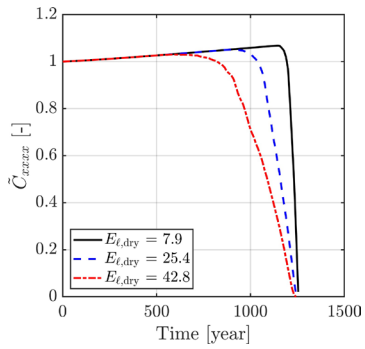

Figure 4. Normalized stiffness degradation of paper with different Young's modulus.

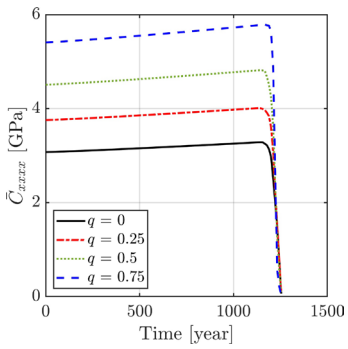

Figure 5. Stiffness degradation of paper with different degree of anisotropy.

Figures 6 and 7 illustrate paper stiffness degradation under constant conditions (RH = 50%, T = 20°C, pH = 6.5). In Figure 6, the red dashed-dotted line represents constant moisture content, while Figure 7 has a blue dashed line representing constant pH. In both figures, the black solid line depicts simulations where moisture content and pH evolve with polymerization (Figs. 1 and 2).

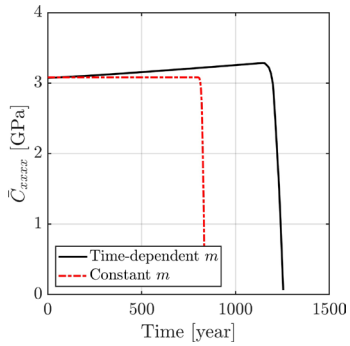

Figure 6. Influence of time-dependent moisture content on stiffness degradation.

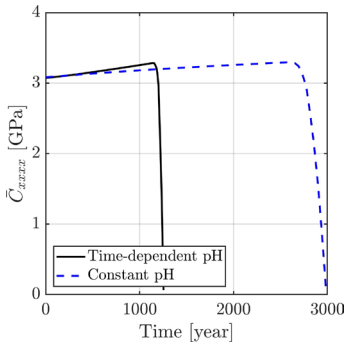

Figure 7. Influence of time-dependent acidity on stiffness degradation.

References

[1] Parsa Sadr A, Bosco E, and Suiker ASJ. "Multi-scale model for time-dependent degradation of historic paper artifacts". In: *International Journal of Solids and Structures* 248 (2022), 111609.

[2] Tetreault J, Begin P, Paris-Lacombe S, and Dupont A-L. "Modelling considerations for the degradation of cellulosic paper". In: *Cellulose* 26 (3) (2019), pp. 2013–2033.

[3] Nissan AH. "H-bond dissociation in hydrogen bond dominated solids". In: *Macromolecules* 9 (5) (1976), pp. 840–850.

TU/e EINDHOVEN UNIVERSITY OF TECHNOLOGY

COLL ECTION CARE

PhD progress

European Union's Horizon 2020 research and innovation programme under grant agreement No 814624

Numerical and Experimental Study of a Butt-Joint Thermoplastic Composite Multi-Stringer Panel Under Compression

A.M. Pereira[1], S. Turteltaub[1], C. Kassapoglou[1]

[1]*Delft University of Technology*

Introduction

Thermoplastic composites allow for cost-effective structural designs, such as butt-joint fuselage structures, which are usually not achievable when utilizing thermoset composites.

Goal

Develop a methodology for monitoring the growth of skin-stringer delaminations in post-buckled butt-joint multi-stringer panels quasi-statically loaded in compression.

Methods

Skin-stringer delamination growth is to be monitored by capturing localized strain phenomena at skin-stringer delamination fronts using Digital Image Correlation (DIC).

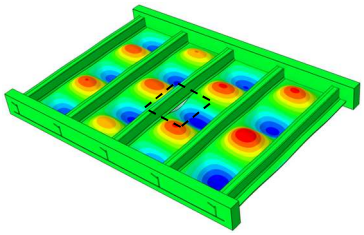

- 5-stringer panel.
- Compressively loaded.
- Damage model: VCCT.

- Minimum principal strains on the outer mold line side of the panel.
- Damage morphology:
  → Intact skin-stringer interface in dark grey.

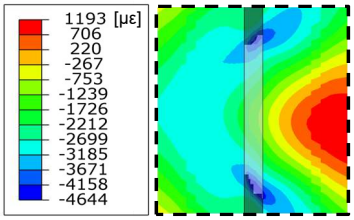

A "global" DIC captures post-buckling deformations across the panel, while a "local" DIC captures strain concentrations at the skin-stringer delamination's fronts. The higher spatial resolution of the local DIC requires a smaller speckle size:

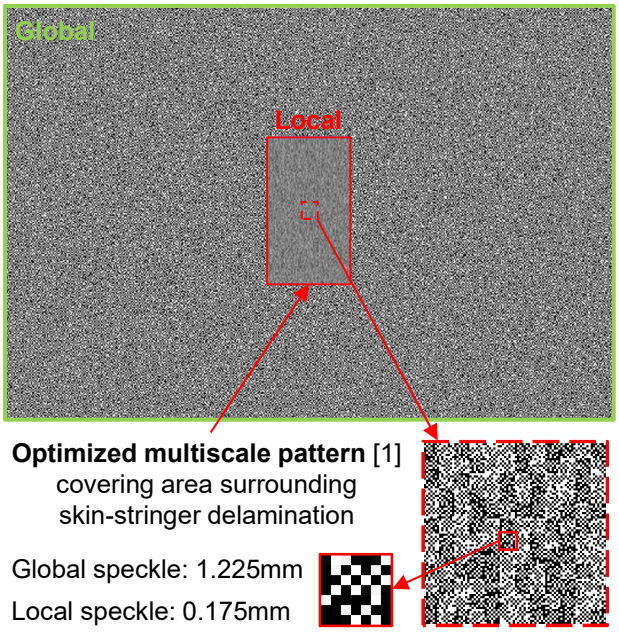

Optimized multiscale pattern [1] covering area surrounding skin-stringer delamination

Global speckle: 1.225mm

Local speckle: 0.175mm

Experimental Test

Pristine butt-joint 5-stringer panel is quasi-statically tested in compression up to failure, implementing global/local DIC.

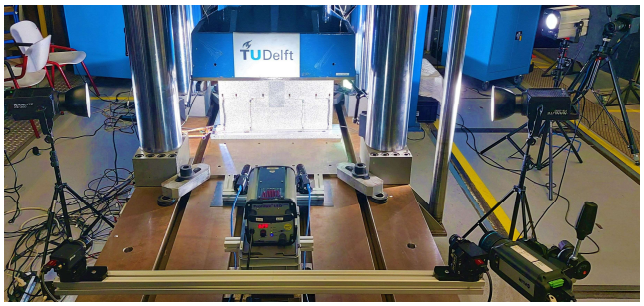

Global vs. Local DIC Strain Analysis

Comparison of maximum principal strains captured at the optimized multiscale pattern's location:

Global (VSG: 35mm)

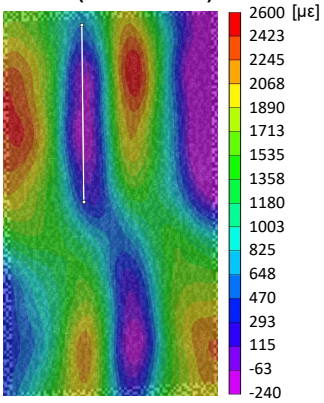

Local (VSG: 13mm)

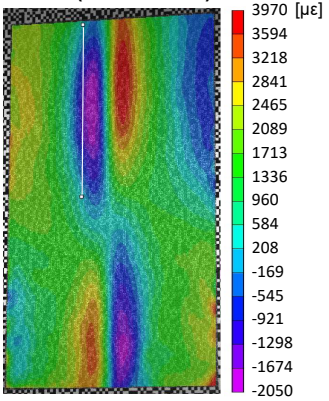

- Smallest virtual strain gauge (VSG) size for acceptable noise levels:
  → Global DIC: 35mm
  → Local DIC: 13mm
- Amplitude increase indicates non-converged strain results.

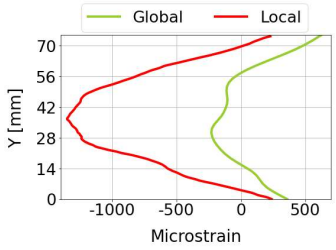

Conclusions & Future Work

- A global/local DIC technique has been successfully implemented and verified through the physical testing of a pristine butt-joint 5-stringer panel.
- A butt-joint 5-stringer panel with an artificial skin-stringer delamination will be physically tested, implementing the global/local DIC to monitor delamination growth.

References

[1] G. F. Bomarito, J. D. Hochhalter, and T. J. Ruggles, "Development of optimal multiscale patterns for digital image correlation via local grayscale variation," Experimental Mechanics, vol. 58, no. 7, Sep. 2018.

A New Setup to Measure Friction of Thermoplastic Composite Tape in Melt

E.R. Pierik[1,2], S. Benou[1], W.J.B. Grouve[1], S. Wijskamp[2], R. Akkerman[1,2]

[1]*University of Twente, Enschede, The Netherlands*
[2]*ThermoPlastic composite Research Center (TPRC) Enschede, The Netherlands*

Hot Press Forming & Process Simulations for First-Time-Right Manufacturing of TPC Parts

Accurate **forming predictions** require **accurate characterization** of the material behavior, classified in several **deformation mechanisms**. We developed a **new setup** to characterize one of these mechanisms: **inter-ply slip**.

1 *Conceptual design*

Slippage between adjacent plies (ply-ply friction):

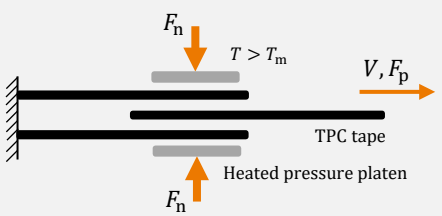

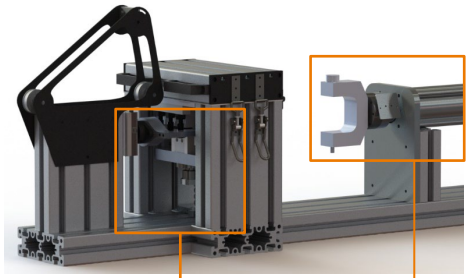

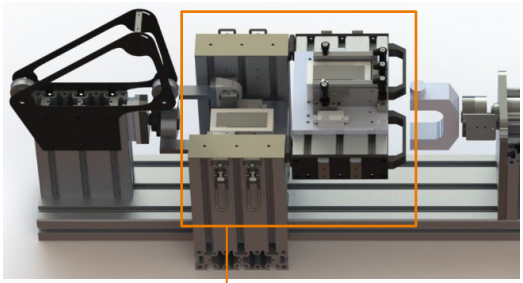

2 *Features*

Guiding system for 3 DoF of lower platen to obtain a **uniform pressure distribution**.

Multiple heating cartridges to obtain **uniform temperature distribution**.

LabVIEW-controlled **air bellow** for constant **normal force** (3 load cells).

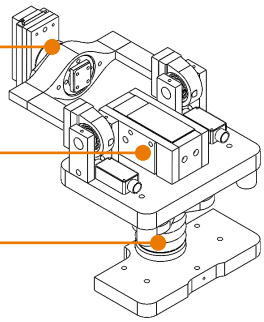

Open workspace to easily mount a specimen with **good alignment** in fast clamping system (different fiber orientations possible).

Controlled actuator for both **rate- and stress-controlled** friction tests. Data logging via LabVIEW.

3 *Realization*

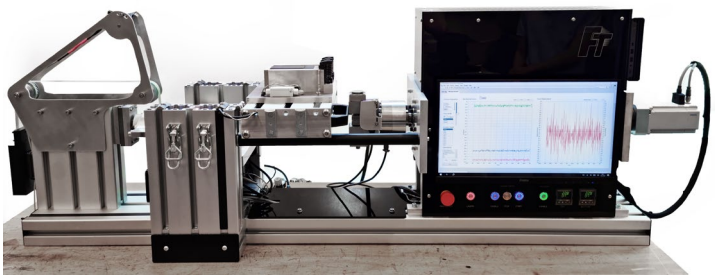

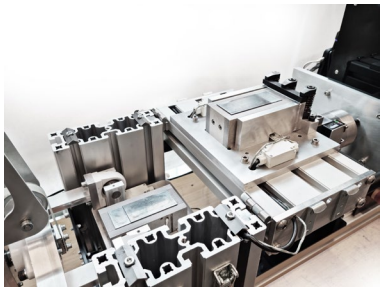

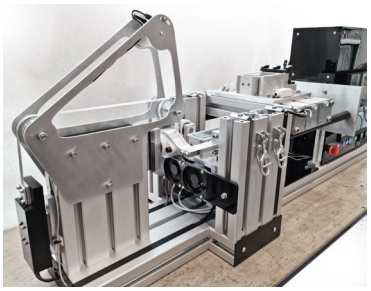

4 *Characterization*

Future work:

- Compare results from new friction tester with current one for different TPC tapes.
- Include new friction tester in ongoing worldwide benchmark exercise.
- Perform new tests to further investigate the underlying mechanisms for inter-ply friction of TPC tapes in melt.

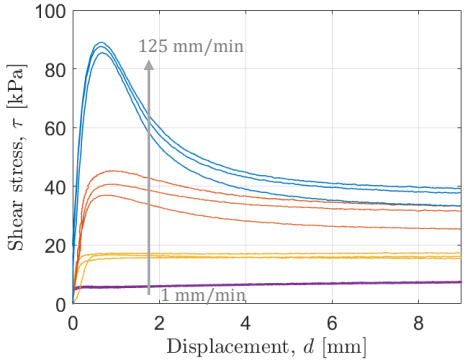

First ply-ply friction experiments for UD C/PEEK tape in melt.

Rate-controlled at 1, 5, 25, and 125 mm/min with 15 kPa normal pressure and a temperature of 385 °C in triplicate.

UNIVERSITY OF TWENTE.

PhD progress: 1 | 2 | 3 | 4

TPRC THERMOPLASTIC COMPOSITES RESEARCH CENTER

NWO

Multi-Scale Study of Fiber Orientation Effect on Mechanical Behavior of Fiber-Reinforced Concrete

P. Pirmoradi[1], P. Poorsolhjouy[1], A.S.J. Suiker[1]

[1]*Chair of Applied Mechanics, Department of the Built Environment, Eindhoven University of Technology*

Introduction

Plain concrete is a brittle material with a low tensile strength and deformation capacity. An appealing solution for enhancing the mechanical properties of concrete is through the inclusion of high strength, short fibers.

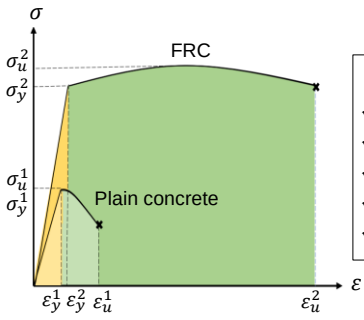

Advantages of FRCs

- ✓ Higher stiffness
- ✓ Higher yield strength
- ✓ Higher ultimate strength
- ✓ Higher deformation capacity
- ✓ Higher toughness

Anisotropic behavior of FRCs

Geometrical alignment of the fibers in a 3D-printed-FRC structure [1]

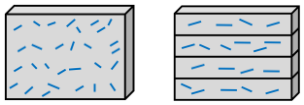

Mold cast FRC | 3D-printed FRC

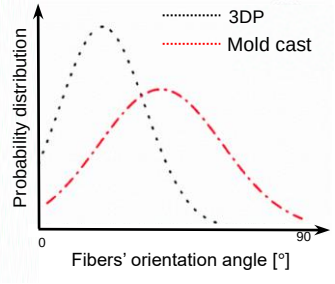

Model Description

A multi-scale model based on Granular Micromechanics Approach (GMA) [2,3] is developed for the analysis of FRCs.

ε_{kl} → Kinematic assumption → δ_k → Constitutive equations → f_i → Principle of virtual work → σ_{ij}

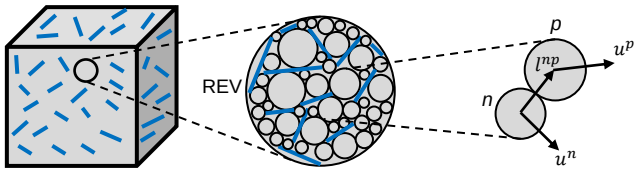

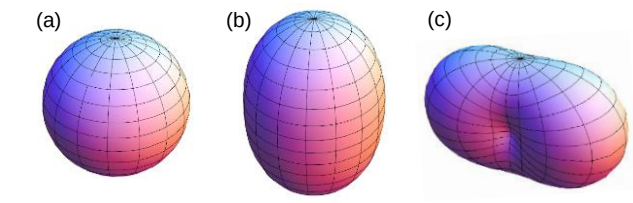

$$\xi(\theta,\phi)=\frac{1}{4\pi}\left[1+\sum_{k=2}^{\infty}{}'\left[a_{k0}P_k(\cos\theta)+\sum_{m=2}^{\infty}{}'P_k^m(\cos\theta)\left[a_{km}\cos m\phi\right]\right]\right]$$

Distribution function facilitating incorporation of microstructure directionality for a) isotropic, b) transversely isotropic, and c) orthotropic fiber-reinforced materials

Numerical Results

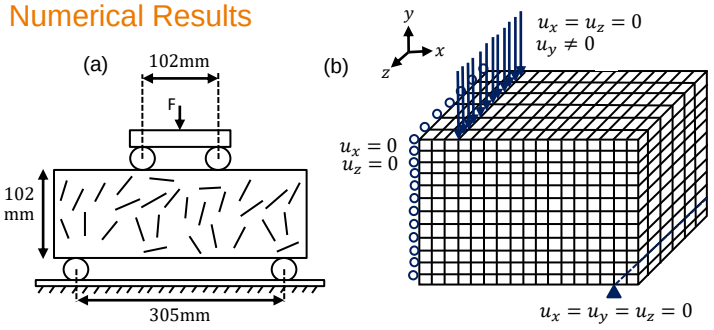

(a) 2D diagram of bending test. [4] b) The boundary condition of the bending test simulation (because of symmetry half of structure is simulated)

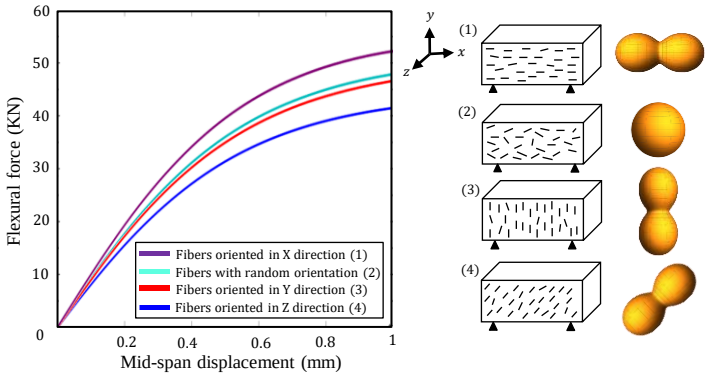

Numerical results of flexural force-displacement relationships for FRC with 4.5% of acrylic fibers with different orientations

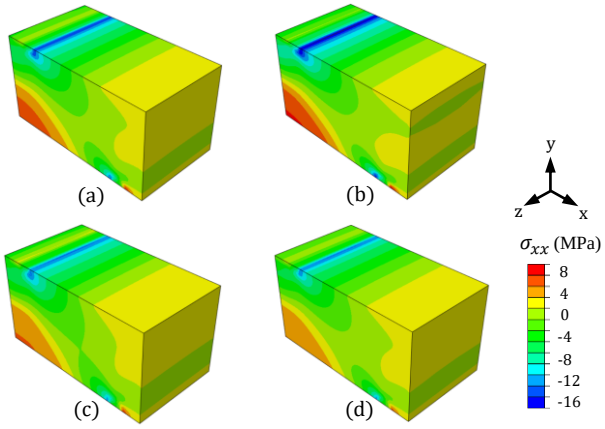

Stress distributions in bending test when the mid-span displacement reaches 1mm for a) fibers with random orientation, b) fibers oriented in X direction, c) fibers oriented in Y direction, d) fibers oriented in Z direction.

References

[1] Bos, F, et al., "Additive manufacturing of concrete in construction: potentials and challenges of 3D concrete printing." *Virtual and physical prototyping,* 11 (2016): 209-225.

[2] Suiker, A.S.J., et al., "Micro-mechanical modelling of granular material. Part 1. Derivation of a second-gradient micro-polar constitutive theory." *Acta Mechanica,* 149 (2001): 161–180.

[3] Poorsolhjouy, P, and Misra, A,. "Effect of intermediate principal stress and loading-path on failure of cementitious materials using granular micromechanics." *International Journal of Solids and Structures,* 108 (2017): 139-152.

[4] Wang, Y, et al., "An experimental study of synthetic fiber reinforced cementitious composites." *Journal of materials science,* 22 (1987): 4281-4291.

Reduction of Interconnected System Models: Extending Computational Limits with Abstractions

L. Poort[1], R.H.B. Fey[1], B. Besselink[2], N. van de Wouw[1]

[1] *Eindhoven University of Technology, Dept. of Mechanical Engineering, D&C group*
[2] *University of Groningen, Bernoulli Institute*

Introduction

Complex systems Σ_c often consist of several interconnected components Σ_j (Figure 1). Model reduction is required to achieve low-order, yet high-fidelity models for tasks such as simulation and model-based control. Two approaches are:

- Reduce Σ_j to $\hat{\Sigma}_j$, constituting $\hat{\Sigma}_C$:
  $\rightarrow$ resulting $\hat{\Sigma}_C$ is generally not accurate
- Reduce Σ_C to $\hat{\Sigma}_C$, preserving its structure, [1]:
  $\rightarrow$ not computationally tractable

We therefore present the framework of abstracted reduction to reduce each Σ_j while connected to an *abstraction* of its environment E. This significantly reduces computational costs, while ensuring that $\hat{\Sigma}_C$ accurately approximates Σ_C.

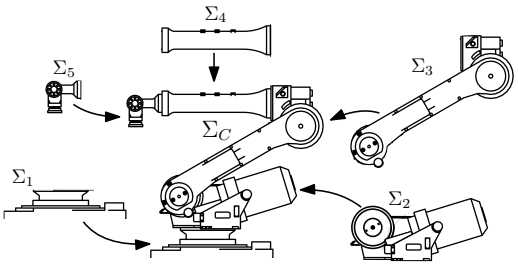

Figure 1: An example of an interconnected system, [2].

Method

We will employ Interconnected Systems Balanced Reduction (ISBR) of [1] to reduce Σ_C to $\hat{\Sigma}_C$, while preserving its interconnection structure. However, instead of a reduction of each Σ_j, as shown in red in Figure 2, we take the blue path:

1. For every Σ_j, split Σ_C in Σ_j and its environment E_j.
2. Reduce E_j to $\hat{E}_j$ using a 'cheap' reduction method.
3. Reduce Σ_j in interconnection with $\hat{E}_j$ with ISBR to $\hat{\Sigma}_j$.
4. Substitute the original environment E_j.

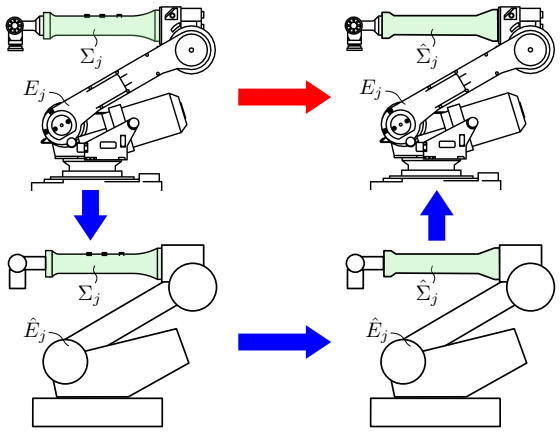

Figure 2: Reduction of subsystem Σ_j to $\hat{\Sigma}_j$ by reduction using E_j (red) and by abstract reduction using $\hat{E}_j$ (blue), [2].

By taking this *abstracted* environment $\hat{E}_j$ into account we ensure that the reduced $\hat{\Sigma}_j$ is relevant in the scope of the overall structure. Yet by only considering $\hat{E}_j$ instead of E_j, computational costs are significantly diminished.

Results

Our AISBR approach using abstractions with ISBR is compared to direct ISBR and subsystem balanced reduction (ssBR) when applied the interconnected system in Figure 3. Component models consist of 152 to 1038 states (2136 in total) and each component model is reduced to 20 states. For AISBR, each E_j is reduced to 20 states using a CMS method [3]. The resulting frequency responses and their errors with respect to the full order model (FOM) are shown in Figure 4.

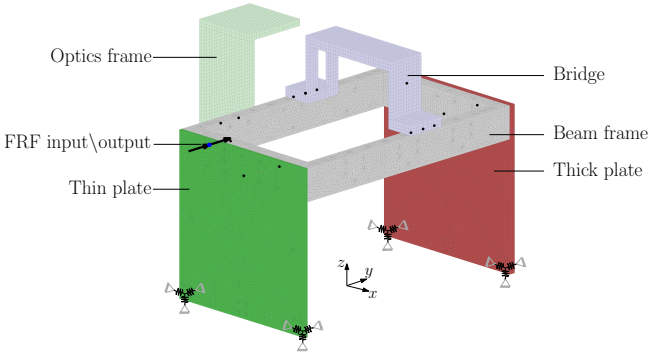

Figure 3: Benchmark model with 5 components.

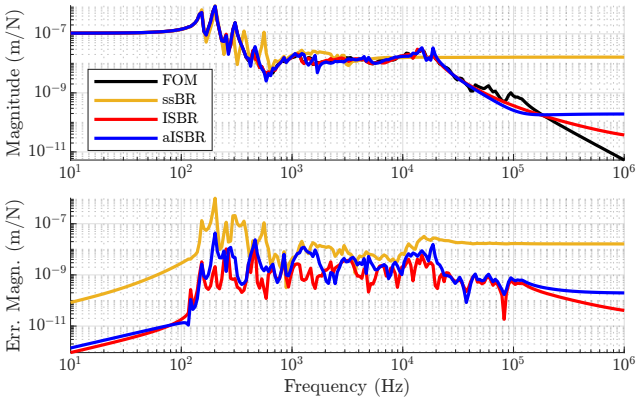

Figure 4: Frequency response magnitude of the FOM and differently reduced models, and their error magnitudes.

Computation times for the reduction are: ssBR (17 s), ISBR (216 s) and AISBR (34 s). As shown in Figure 4, AISBR outperforms ssBR in terms of accuracy, while saving significant computational costs with respect to ISBR.

Conclusion

Our novel approach of abstracted reduction saves computational costs for otherwise computationally intractable methods for the reduction of interconnected systems.

References

[1] A. Vandendorpe, P. van Dooren (2008). Model Reduction of Interconnected Systems. In *Model Order Reduction: Theory, Research Aspects and Applications*.
[2] L. Iborra, *Robotic Arm*. www.NounProject.com
[3] D. Herting (1985). A general purpose, multi-stage, component modal synthesis method. *Finite Elements in Analysis and Design*, **1**: pp. 153-164.

TU/e EINDHOVEN UNIVERSITY OF TECHNOLOGY

PhD progress: 1 | 2 | 3 | 4

ASML

Structural integration of a full-composite, double-walled, vacuum-insulated, cryo-compressed tank

V.K. Poorte, J.M.J.F. van Campen, O.K. Bergsma, and R.C. Alderliesten

Delft University of Technology
Aerospace Structures and Materials

Introduction

Hydrogen is seen as a potential energy carrier to sustain the energy transition of the aviation industry. **Hydrogen's** low volumetric energy density lead to **storage challenges**. To limit the aerodynamic penalty, hydrogen can be stored in the **cryo-compressed state**, 300 - 1000 bar and 33 - 100 K. A **full composite vacuum** insulation is envisioned, to limit heat ingress, and achieve high gravimetric efficiency.

The structure provides the **opportunity to carry additional loads**, other than the pressure differences. It is unclear which of the two shells is more suitable to carry the additional loads. The aim of this study is to establish **which of the two composite shells is more suited** for this.

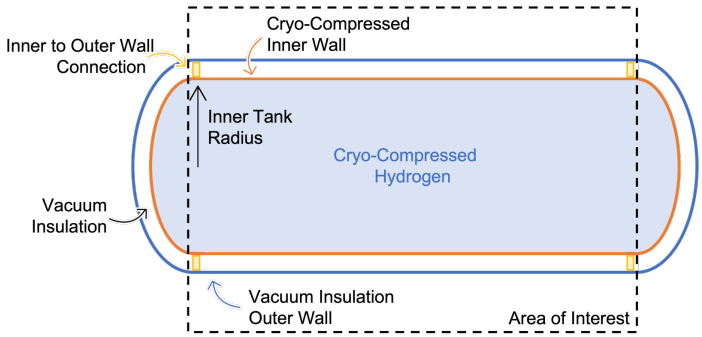

Methods

An analytical method is set-up to capture the strain state of the composite cylinder. This is combined with analytical methods to define the buckling of shells. These methods are used as boundary conditions for the optimisation.

Analytical Model

The analytical model is based on the work of M. Xia at al. (2001). This work is further developed to enable the analysis of a thick-walled composite cylinder, subjected to thermo-mechanical loading. A deformation $u^{(k)}$ is assumed for each layer k, with unknowns, $D^{(k)}$ and $E^{(k)}$ per layer, and ε_0 and γ_0 unknown constants for the entire tube.

$$u_r^{(k)} = D^{(k)} r^{\beta^{(k)}} + E^{(k)} r^{-\beta^{(k)}} + \alpha_1^{(k)} \varepsilon_0 r + \alpha_2^{(k)} \gamma_0 r^2 + \frac{\eta^{(k)} \Delta T}{1 - (\beta^{(k)})^2} r$$

$$\varepsilon_z^{(k)} = \varepsilon_0$$

$$\varepsilon_\theta^{(k)} = \frac{u_r^{(k)}}{r}$$

$$\varepsilon_r^{(k)} = \frac{\mathrm{d}u_r^{(k)}}{\mathrm{d}r}$$

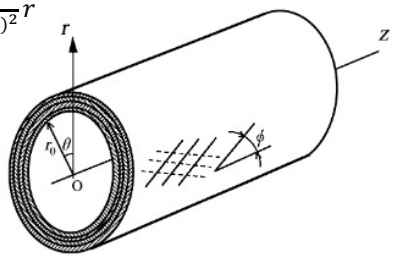

With stress and displacement continuity assumptions at the interface, in combination with axial equilibrium, the unknowns can be determined.

Non-Linearisation

The analytical model is non-linearised using a **full Newton-Raphson method**, which **minimises the residual**, to account for the non-linear loading. The system of equations is derived from the boundary conditions. The loading stiffness matrix is derived from the loading, accounting for the change in loading, due the change in vessel radius.

Inner Radius

$$r_{i+1} = r_0(1 + \varepsilon_{\theta,i})$$

Layer Thickness

$$t_{i+1} = t_0(1 + \varepsilon_{r,i})$$

Layer Winding Angle

$$\tan\theta_{i+1} = \tan\theta_0 \left(\frac{1 + \varepsilon_\theta}{1 + \varepsilon_z}\right)$$

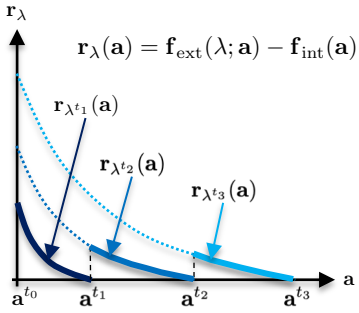

Idealization of incremental loading

The **analytical** method enables quick computation of the **stiffness matrices**. The low number of layers, leads to few degrees of freedom and thus **straight forward inversion of the stiffness matrix**. This leads to **short computation times**.

Optimisation

A **mass based objective function** is chosen, to maximise the gravimetric efficiency of the system. Design **variables** are the **layer thicknesses and winding angles**. The number of layers is yet to be determined. The **constraints** are the strain states of the vessel's layers, which are combined with **failure criteria** to avoid material failure. **Buckling** is also considered, which is deemed problematic for the external shell.

Objective

$$f(\boldsymbol{x}) = \sum t_i \rho_i$$

Objective function is mass based

Variables

$$x = \begin{bmatrix} \theta_i \\ t_i \end{bmatrix}$$

Winding angles and thicknesses of layers are varied

Constraints

- Material failure
- Structural instability

It is expected that the inner shell is more suited to carry the additional loads. The optimisation shall confirm or deny this hypothesis, by indicating which solution is more lightweight.

References

M. Xia, H. Takayanagi, and K. Kemmochi, Analysis of multi-layered filament-wound composite pipes under internal pressure, Composite Structures, 2001.

PhD progress

1	2	3	4

A Bayesian Approach to Modeling Finite Element Discretization Error

A. Poot[1], I.B.C.M. Rocha[1], P. Kerfriden[2], F.P. van der Meer[1]

[1] 3MD, CiTG, Delft University of Technology
[2] SIMS, MAT, Mines Paris – PSL

Introduction

In this work, we try to model the discretization error of the finite element method from a Bayesian point of view. There are three elements to our setup:

1. *A PDE-informed choice of prior.* Usually a zero-mean Gaussian process with Green's function appearing in the covariance function $k(\boldsymbol{x}, \boldsymbol{x}')$
2. *A fine discretization of the prior.* By approximating the continuous prior, we avoid needing to know the Green's function of the PDE.
3. *A coarse discretization for forcing term observations.* By observing the forcing term only on a coarse mesh, we leave uncertainty in the posterior.

This remaining uncertainty can be indicative of the discretization error $\boldsymbol{u_f} - \boldsymbol{u_c}$. Because we now have a probabilistic description of this error, we can propagate it in inverse problems, multiscale models and data assimilation contexts.

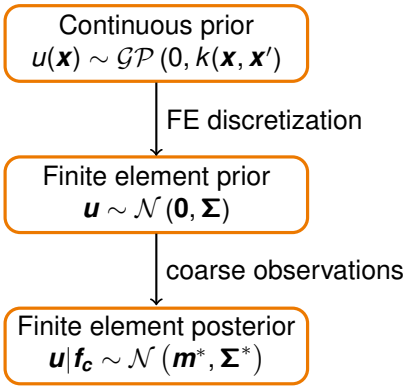

Right-hand side perturbation prior

We perturb the solution with a white noise forcing term:

$$k(\boldsymbol{x}, \boldsymbol{x}') = \int_\Omega \int_\Omega G(\boldsymbol{x}, \boldsymbol{z}) G(\boldsymbol{x}', \boldsymbol{z}') \delta(\boldsymbol{z} - \boldsymbol{z}') \, \mathrm{d}\boldsymbol{z} \, \mathrm{d}\boldsymbol{z}'$$

This implies a prior covariance of the FE solution:

$$\boldsymbol{u} \sim \mathcal{N}\left(\boldsymbol{0}, \boldsymbol{K}^{-1} \boldsymbol{M} \boldsymbol{K}^{-1}\right)$$

We get a great posterior mean, but a covariance that is not very informative about $\boldsymbol{u_f} - \boldsymbol{u_c}$ (especially in 2D):

$\boldsymbol{m}^* \approx \boldsymbol{u_f}$ $\qquad$ $\boldsymbol{\Sigma}^* \approx \boldsymbol{0}$

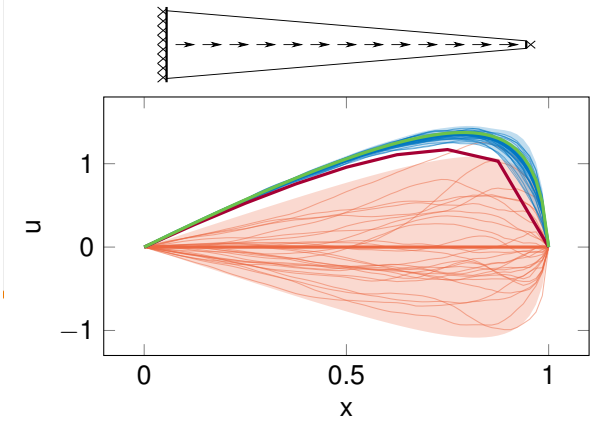

Figure 1: 1D tapered bar with RHS perturbation prior

Green's function prior

We assume the prior covariance to be Green's function:

$$k(\boldsymbol{x}, \boldsymbol{x}') = G(\boldsymbol{x}, \boldsymbol{x})$$

Which implies a prior covariance of the FE solution:

$$\boldsymbol{u} \sim \mathcal{N}\left(\boldsymbol{0}, \boldsymbol{K}^{-1}\right)$$

Now, our posterior mean is no better than $\boldsymbol{u_c}$, but our covariance captures the error:

$\boldsymbol{m}^* = \boldsymbol{u_c}$ $\qquad$ $\boldsymbol{\Sigma}^* \boldsymbol{f_f} = \boldsymbol{u_f} - \boldsymbol{u_c}$

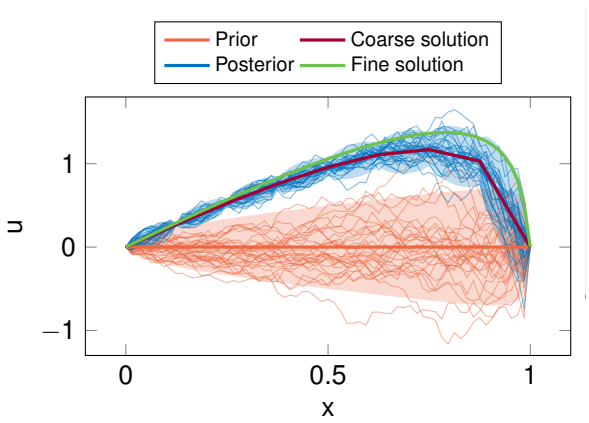

Figure 2: 1D tapered bar with Green's function prior

Conclusions

We can see a trade-off between posterior mean and covariance, which gives us a choice:

- good posterior mean, but uninformative covariance; or
- coarse-scale posterior mean, but useful covariance

For our present objective of modeling discretization error, option 2 is ideal.

Future works

Next topics we are planning to investigate:

- Sampling non-Gaussian quantities of interest
- Improving the computational efficiency
- Extending the method to non-linear PDEs
- Applying the method to inverse problems

We have only begun to scratch the surface!

Melting-Free Metal Production: Solid-State Additive Manufacturing of an Al-Mg-Si Alloy Using FSEAM

S.S. Rezaeinejad[1*], T.C. Bor[1], M. Luckabauer[1], R. Akkerman[1]

[1]*University of Twente, Production Technology*

** s.rezaei@utwente.nl*

1. Additive Manufacturing (3D Printing)

Process of creating objects layer by layer using CAD or 3D scanning technology

Features:

- Layer-wise fabrication: complex, customized designs & lightweight structures
- Material diversity: using various materials from polymers to metals
- Waste reduction: environmental impact and green technology
- On-demand production: enables just-in-time manufacturing

Amsterdam bridge (MX3D Co.)

Ship propeller (m2i Co.)

Body implants (ConMet Co.)

Fusion-based Additive manufacturing issues:

- Melting and re-solidification
- Hot cracking
- Porosity
- Evaporation of alloying elements
- High residual stresses
- Preferred orientation
- Intergranular micro-segregation

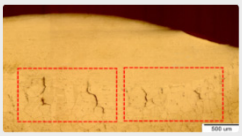

Solidification Cracking

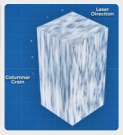

Cellular structure

Solid-state Additive manufacturing:

- Building without melting
- Free from above issues

2. Friction Screw Extrusion Additive Manufacturing (FSEAM)

- Based on the principle of Friction Stir Welding (FSW)
- Using a screw-like rotating tool
- Generating heat through Friction and Severe Plastic Deformation (SPD)
- Multi-purposes: Extrusion or Additive Manufacturing

Masselink, Friction Screw Extrusion, University of Twente, 2021

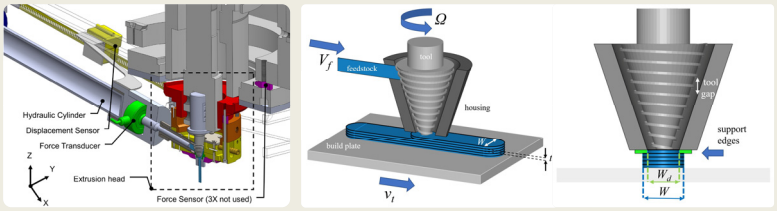

Schematic outline of FSE(AM) setup and printhead

FSEAM of AA6060 T6 builds:

- Rotational speed: 400 RPM
- Feed ratio: 1.3
- Tool gap: 3.2 mm
- Number of layers: 50
- Table velocity:100-500 mm/min (variable parameter)

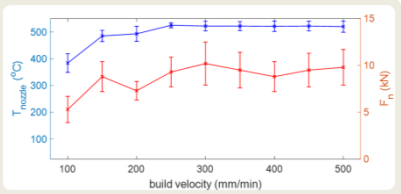

Build appearance

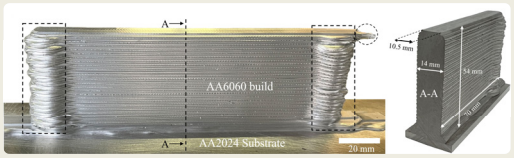

Macroscopic view of an AA6060 build manufactured by FSEAM

3. Microstructure and Mechanical properties

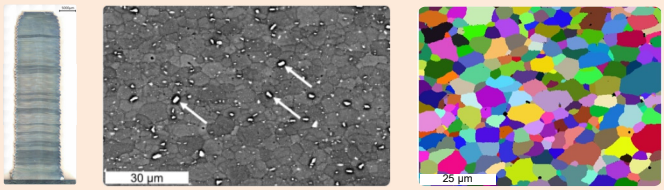

Microstructure evaluation of manufactured AA6060 build through OM, SEM, and EBSD

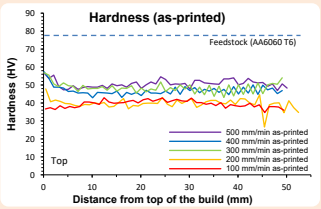

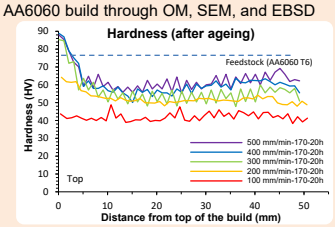

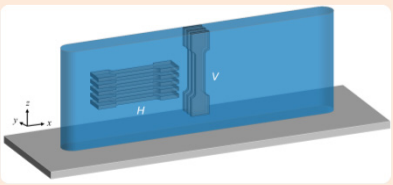

Extracting location of tensile samples

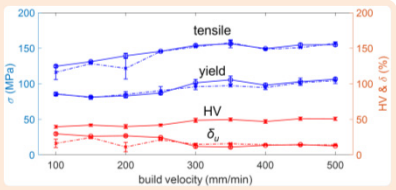

Overview of mechanical properties

Fracture behavior

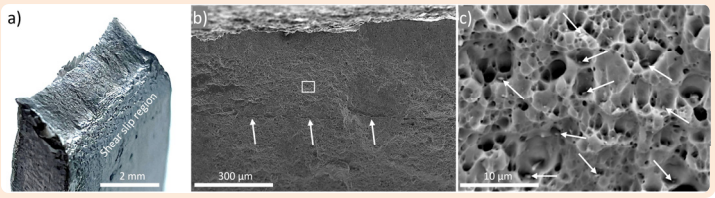

4. Thermal process description for FSEAM

- In-situ heat treatment cycle during FSEAM
- Higher aging temperatures than what is required
- Optimizing mechanical properties with post-deposition cooling

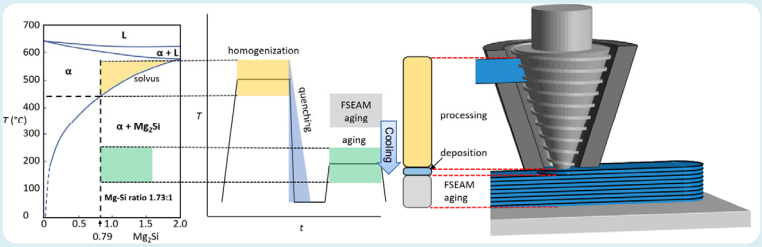

5. Summary and References

- FSEAM is capable of manufacturing defect-free AA6060 builds by applying enough force at elevated temperatures.
- Fine equiaxed grains (2–4 µm) were formed without crystallographic texture.
- Promising tensile test results in horizontal & vertical (building) directions.
- Hardness was affected by the thermo-mechanical nature of the FSEAM process.
- Improved hardness through post-manufacturing heat treatment if the initial temperature was high enough to dissolve the precipitates.
- Dominant ductile fracture characteristics with dimple-rich patterns.

References:

- Rezaeinejad, S.S., et al., *Solid-state additive manufacturing of AA6060 employing friction screw extrusion additive manufacturing*, JOM 75, (2023).
- Bor, T.C., et al., *A feasibility study on friction screw extrusion additive manufacturing of AA6060*, Friction Stir Welding & Processing XII, TMS 2023 (2023).
- Bor, T.C., et al., *Friction screw extrusion additive manufacturing of an Al-Mg-Si alloy*, Additive Manufacturing, (2023).

UNIVERSITY OF TWENTE.

PhD progress: 1 | 2 | 3 | 4

Production Technology
ADVANCED MATERIALS ENGINEERING

Gold Decorated Carbon Nanotube for Molecular Hydrogen Storage- A First-Principles Study

Shima Rezaie[1,2] , Azahara Luna-Triguero[1,2]

[1]Eindhoven University of Technology

[2]Graduate School Engineering Mechanics

Introduction

The permanent use of fossil fuels has many consequences, including depletion of energy resources and negative environmental impacts [1,2]. In this context, hydrogen has been introduced as a promising substitute for declining the dependence on fossil fuels [3]. However, using hydrogen as a fuel requires finding a convenient and cost-effective way to produce, store and deliver it [1]. In this regard, carbon nanostructures have aroused the interest of researchers due to their high surface area, good chemical stability, low mass density, and rich pore volume [4]. Despite these pros, bare carbon nanostructures have represented low hydrogen storage capacity at ambient temperature [4]. Resulting in surface modification (such as decorating or adding doping) can be a significant step to increase hydrogen adsorption capacity. This work investigates the properties of several modified CNTs using density functional theory. We analyze the binding and formation energies of the uniformed Au-doped CNTs and assess their adsorption capability.

Simulation Results

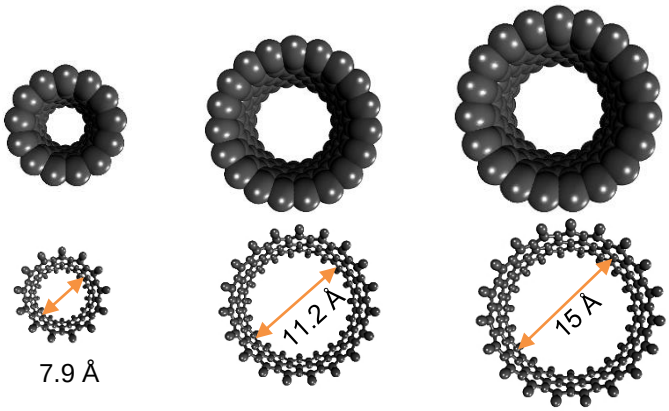

Figure 1. Schematic representation of three zigzag CNT nanostructures.

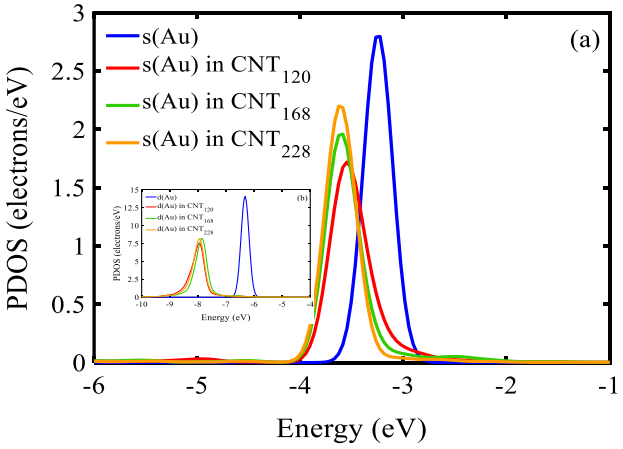

Figure 2: PDOS of (a) s and (b) d-orbitals of the pure Au atom and Au atom on the surface of the CNTs.

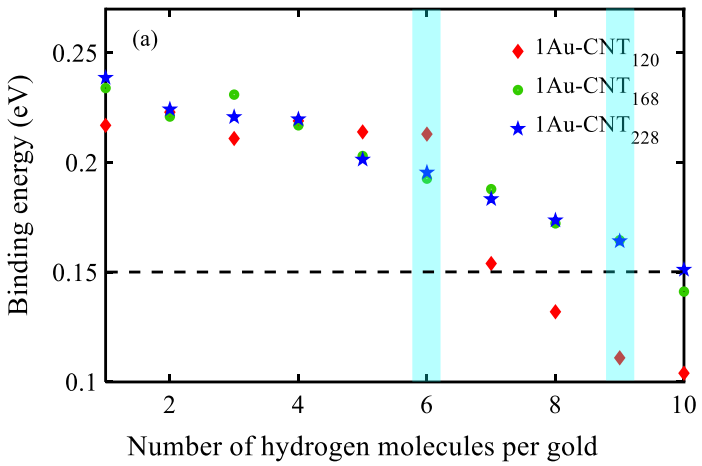

Figure 3. Binding energy between hydrogen molecules and the surface of 1Au-CNTs (dashed line: the lower boundary of binding energy as defined by DOE).

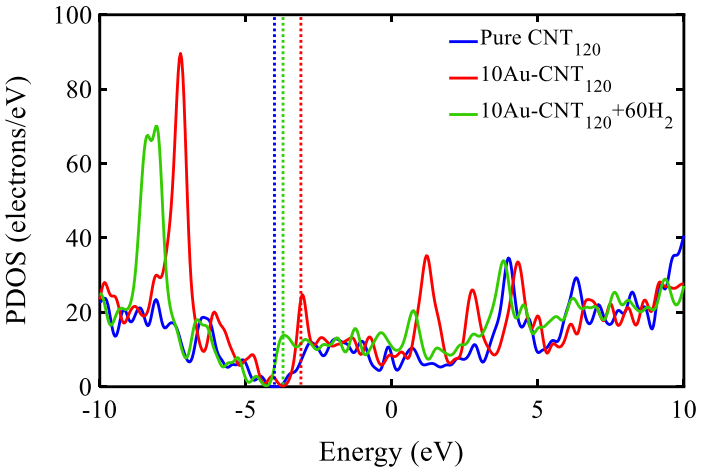

Figure 4. PDOS of carbon nanotube, pristine (blue), saturated with gold (red), after hydrogen adsorption in the saturated structure (green). Dashed lines indicate the Fermi Energy (E_F) per configuration.

References

[1] S. ullah Rather. "Preparation, characterization and hydrogen storage studies of carbon nanotubes and their composites: A review." *Int. J. Hydrog*, 45, no. 7 (2020): 4653-4672.

[2] H. G. Shiraz, et al. "Palladium nanoparticle and decorated carbon nanotube for electrochemical hydrogen storage." *Int. J. Hydrog*, 42, no. 16 (2017): 11528-11533.

[3] R. S. Rajaura, et al. "Structural and surface modification of carbon nanotubes for enhanced hydrogen storage density." *Nano-Structures & Nano-Objects* 14 (2018): 57-65.

[4] Li. Bi, et al. "DFT study of hydrogen sorption on light metal (Li, Be, and Na) decorated novel fullerene-CNTs networks." Applied Surface Science, 569 (2021): 151000.

Unravelling air entrapment during polymer thin film lamination: A two-scale model

V. Rezazadeh[1] , J.A.W. van Dommelen[1] & M.G.D. Geers[1]

[1]*Mechanics of Materials, Eindhoven University of Technology*

v.rezazadeh@tue.nl

1. Introduction: Film lamination

To produce polymer coated packaging steel, the metal substrate is pre-heated, and passed between two rubber coated laminator rolls together with the PET polymer film.

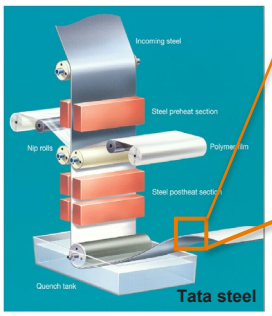

PET film lamination process

2. Introduction: Air entrapment

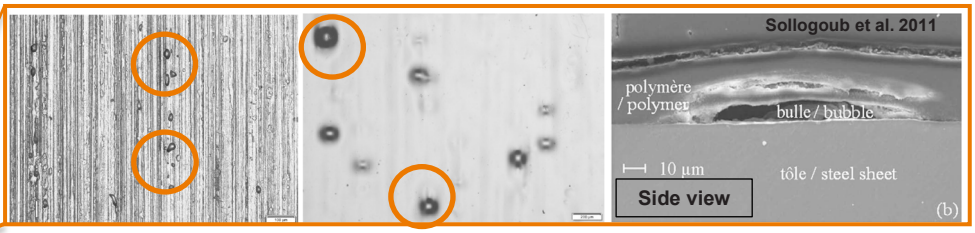

- Air entrapment phenomena are known to exist in many coating systems.
- The defect density of air bubbles depends on the processing conditions; such as the line speed, the pre-heat temperature or the laminator roll pressure.
- To ensure the quality of polymer-coated packaging steel and to enable high production speeds, air entrapment needs to be reduced or eliminated.

3. Hypothesis: Mechanism of air entrapment

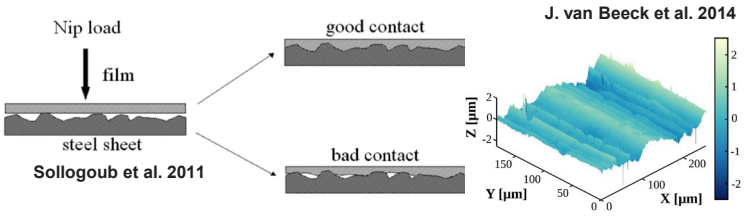

- Left: Entrapped air in the metal substrate roughness due to bad contact.
- Right: surface roughness profile of the substrate steel used by Tata steel.

4. Approach: A two-scale model

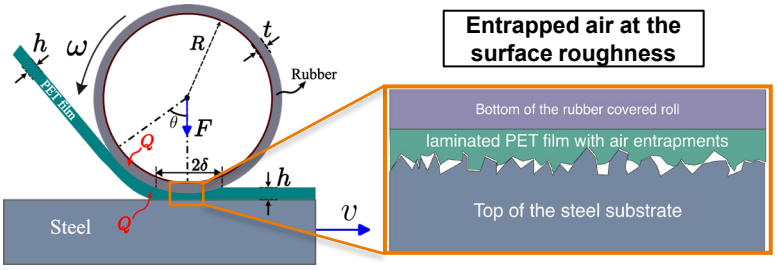

Macro-scale: actual lamination process at the meter-scale

Micro-scale: cavity filling at the micron-scale (surface roughness)

5. FEM simulation setup

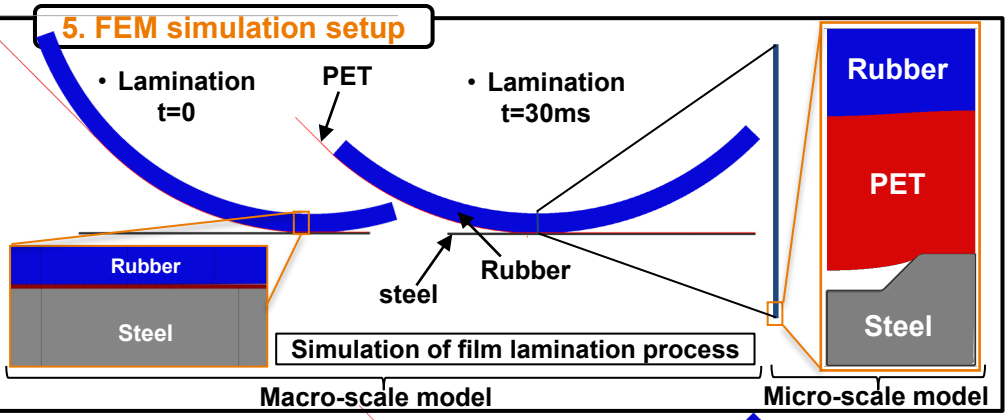

6.Eindhoven Glassy Polymer (EGP)

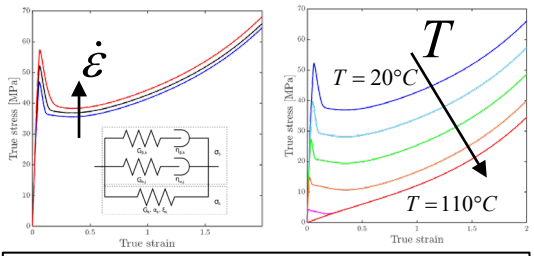

- The stress and temperature dependency of the model is based on the Eyring theory.
- To model PET behavior at the micro-scale, the EGP model is used.

7. Numerical results

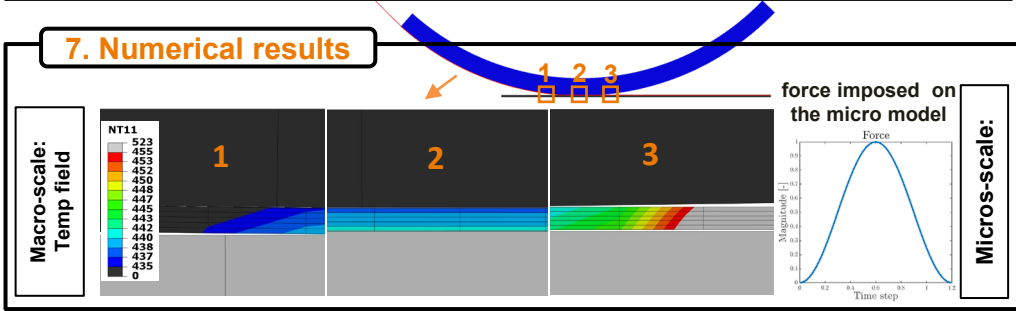

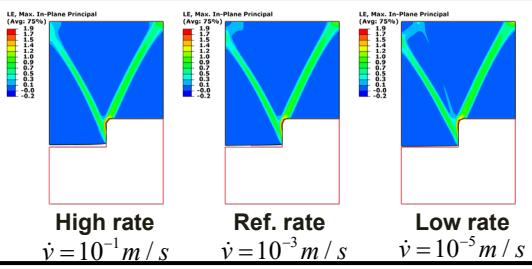

8. Conclusion & future work

- By coupling these models, direct relations can be established between the main processing parameters and the air entrapment phenomenon.
- To obtain reliable results, temperature/rate-dependent behavior of PET and rubber need to be calibrated.
- Contact conductance properties between interfaces of rubber-PET and PET-steel must be obtained through experimental-numerical methods.

Dynamics-based impact identification method for composite structures

N.R. Marinho[1], R. Loendersloot[1], T. Tinga[1], and F. Grooteman[2]

[1] Dynamics Based Maintenance Group, University of Twente, P.O. Box 217, 7500AE Enschede, The Netherlands
[2] National Aerospace Laboratory (NLR), P.O. Box 153, 8300AD Emmeloord, The Netherlands

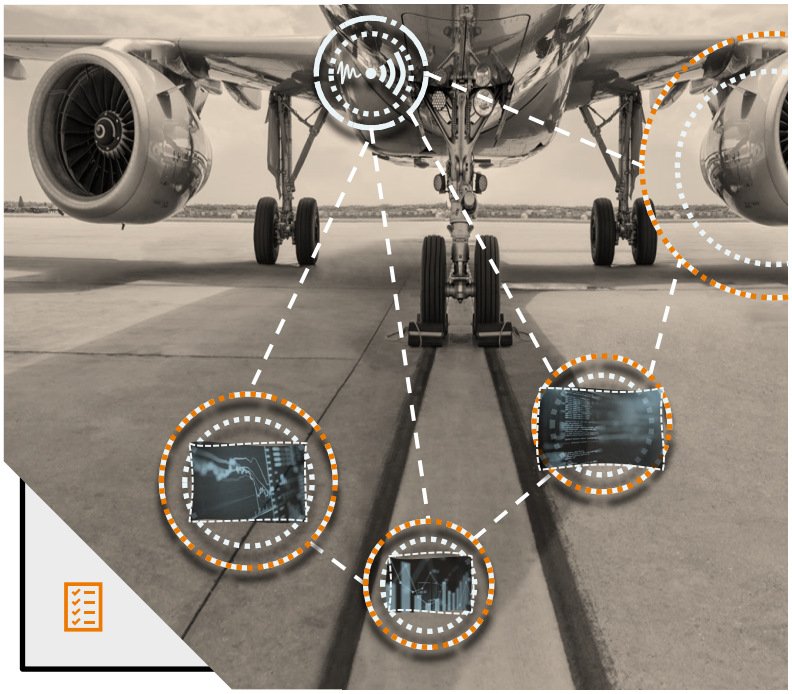

MOTIVATION & BACKGROUND

We're changing aerospace composite design and optimising maintenance efforts through STRUCTURAL HEALTH MONITORING

Impacts pose a significant threat to composite aerospace structures due to the risk of introduce barely visible impact damage (BVID). Therefore, Structural Health Monitoring (SHM) is used to:

- better assess the impact energy in different aircraft sections;
- provide information for prognostics.

As a result, we can move away from time-based inspection intervals and ground and repair aircraft only when an impact causes damage.

OBJECTIVE

Impact energy estimation on aerospace composites

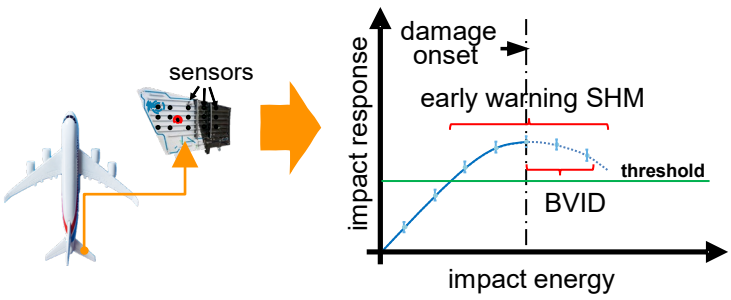

EXPERIMENTAL WORK

Intermediate-mass impacts on square (1x1 m) composite plate at 13 different locations (I1 to I13) and various impact energy levels.

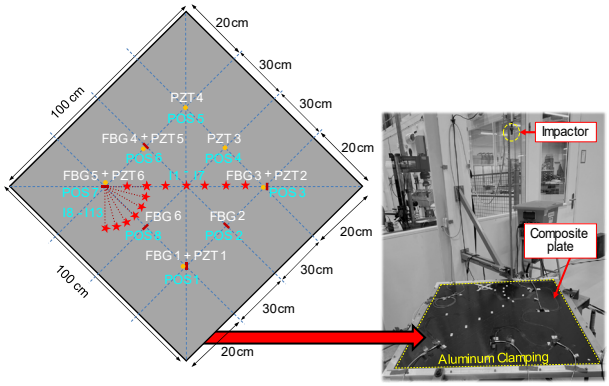

DISCUSSION & RESULTS

Signal feature:
TRANSMITTED ENERGY : $E = \int_{t=0}^{t_{end}} |y(t)|^2 dt$

Observations:

- PZT and FBG show similar sensitivity to transmitted energy;
- Uneven distribution of transmitted energy;

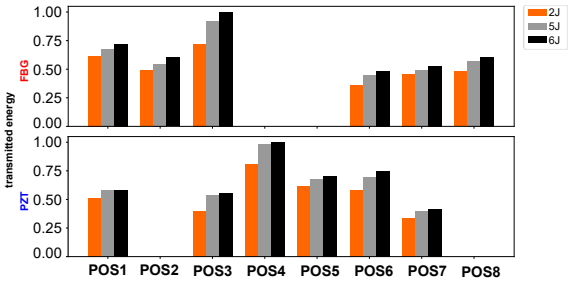

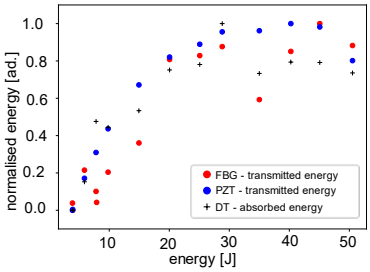

- Linear behaviour at low energy levels;
- Decrease in impact response due to damage;
- Transmitted energy behaves similarly to the absorbed energy;

- Signal decay with increasing distance;
- Low standard deviation for varying incident angle.

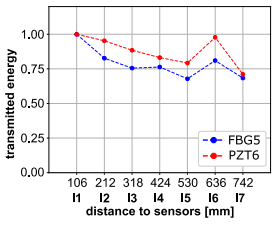

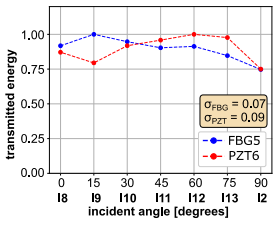

Non-Contact Acoustic Emission Monitoring of Corrosion-Fatigue Damage in Mooring Chain Links

F.Riccioli*, L. Pahlavan

Maritime and Transport technology
Delft University of Technology
**F.Riccioli@tudelft.nl*

Introduction

Corrosion-fatigue is regarded as one of the main degradation mechanisms affecting the structural integrity of mooring chains. Detailed inspection of these structures can be challenging due to difficult access, surface conditions (Figure 1) waves, and weather conditions. Additionally, the presence of marine growth on the surface of the chain links often requires the need of surface cleaning to obtain a detailed assessment of the structural integrity.

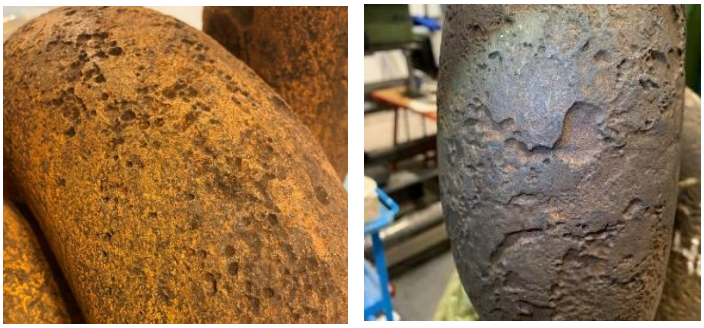

Figure 1: Mooring chains surface condition due to corrosion

Objective

To assess the feasibility of detection, localization, and monitoring of corrosion-fatigue damage in mooring chain links by means of underwater non-contact Acoustic Emission (AE).

Experimental investigation

A 5-links mooring chain segment was subjected to cyclic loading while submerged in artificial seawater. Ultrasound signals were measured using fixed and moving arrays of AE transducers on two perpendicular planes.

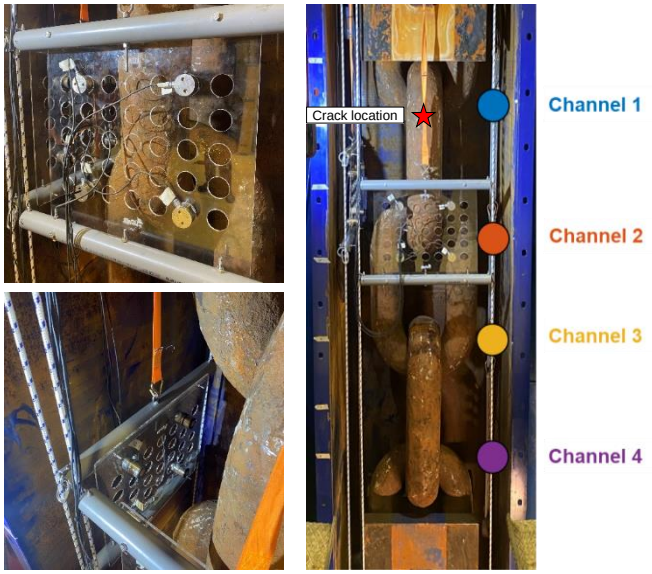

Figure 2: Instrumented test rig

AE monitoring of corrosion-fatigue damage

Parametrization of the AE signals measured by the vertical array of sensors (Figure 2) was used to detect and monitor the initiation and growth of the corrosion-fatigue damage. AE sources were localized using triangulation of the AE signals measured by the arrays of AE transducers. The results of the AE source localization projected on the 3D geometry of the chain links are shown in Figure 3.

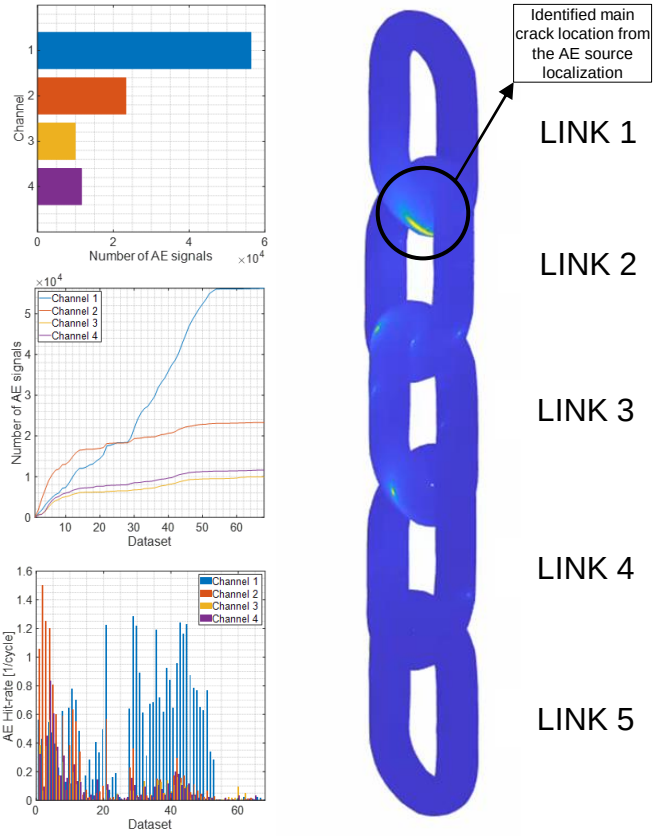

Figure 3: AE monitoring and localization of damage

Conclusions

- Growth of corrosion-fatigue damage in mooring chains was successfully detected and localized using underwater non-contact AE.
- Good agreement between the measurement results and the observed crack was obtained.
- Further data processing may provide the basis for damage characterization and prognosis in mooring chain links.

Figure 4: Main fracture in lower crown of LINK 1

PhD progress

1	2	3	4

Bayesian Machine Learning for Multiscale Modeling of 3D-printed Materials

L.F. Riccius, I.B.C.M. Rocha, F.P. van der Meer

Delft University of Technology, Faculty of Civil Engineering and Geosciences

Introduction

Inferring spatial distributions of material properties in large structures is a common exercise in a structural health monitoring workflow. A Bayesian analysis is a potent tool to solve these problems. It does, however, require a large number of costly finite element model (FEM) runs, that might involve complex materials with expensive constitutive laws. The runtime of the inference can be reduced by replacing computationally demanding routines of the statistical model. Two possible tasks to be replaced are considered.

Surrogate for likelihood function

The first choice is to replace the likelihood function with a metamodel, and train it with a small amount of FEM evaluations.

$$\log(p(\mathcal{D}|\theta)) = \mathcal{L}(\theta) \approx \mathcal{GP}_{\mathcal{L}}(\theta)$$

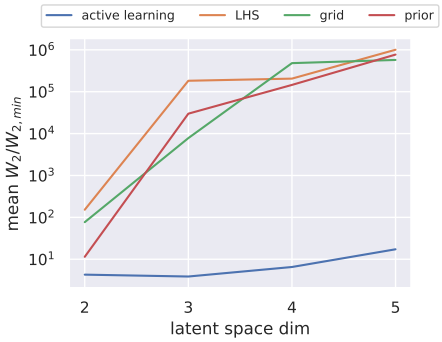

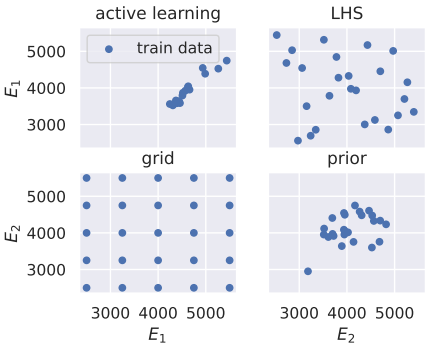

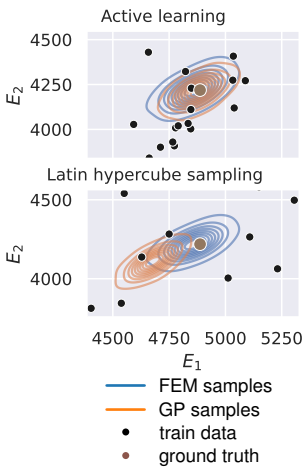

Different strategies to assimilate training data for the Gaussian process were investigated. For latin hypercube (LHS), grid, and prior sampling, the datasets are obtained *a priori*. In the active learning approach, the full model is called whenever the surrogate's uncertainty violates a threshold.

- Comparable results for all *a prior* strategies.
- Their performance quickly deteriorates with dimensionality.
- Active learning prevails in all settings with equal dataset sizes.

Effective data assimilation is crucial for surrogate model's accuracy.

Surrogate for material model

The other choice is to go to a lower level of the FEM simulator and replace the material model.

$$\sigma(\epsilon, \theta) \approx \mathcal{GP}_{\sigma}(\epsilon, \theta)$$

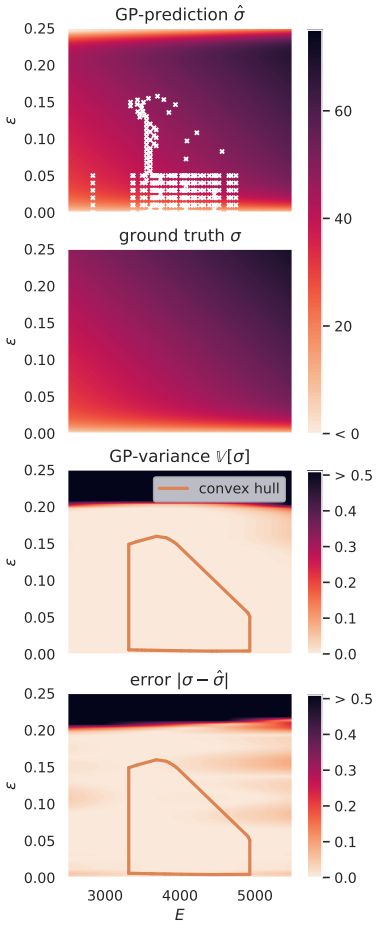

The Gaussian process emulates the material's behaviour after observing a limited number of material model evaluations.

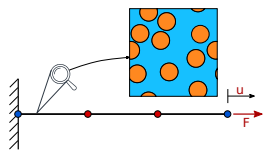

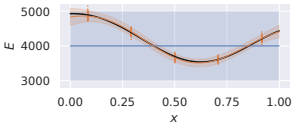

Conlusions

- The surrogate for the material model is independent of the latent space dimension, the surrogate for the likelihood is not.
- For low-dimensional inference, replacing the likelihood is preferred.
- In high-dimensional settings, emulating the material model's response instead is recommended.
- The choice of MCMC algorithm has no influence on accuracy.

Beyond plain performance, the application can determine the surrogate modeling choice. The FEM can be treated as a black box for the likelihood approach, but does not allow further propagation of the obtained parameter distributions. The surrogate model for the constitutive law can seamlessly be integrated into further analysis.

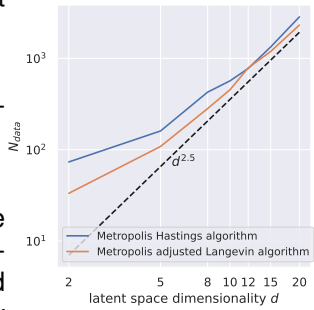

PhD progress

1	2	3	4	5

Computational modelling of moisture transport in paper sheets through a multi-phase flow approach

C.A. Rojas Vega[1],
R.H.J. Peerlings[1], M.G.D. Geers[1]
[1] *Eindhoven University of Technology*

Introduction

When water based ink is used for digital printing, absorption of the water may induce out of plane deformations of the paper sheet due to hygroexpansion. If the printing process is not properly controlled unacceptable deformations may result. In this work, we address the moisture transport process within the paper, which is a relevant aspect to understand the deformations due to swelling. Paper sheets are modelled as a multi-phase material, by means of the hybrid mixture theory [1]. This methodology incorporates some characteristics of the mixture theory and averaging procedures. Balance equations are presented at the microscale level, and by means of an averaging procedure the corresponding balances at the macroscale are obtained. Constitutive relations are obtained by using the Coleman-Noll procedure. Mass balance equations are derived in terms of the chemical potential, which is taken as the driving force for water movement.

Balance equations for multi-phase systems

A multi-phase material is composed of phases and a phase is composed of constituents. The constituents within the phases are assumed to be miscible, while the phases are not. The mass balance equations for the phase α and the constituent j within the same phase can be generalized as:

$$\frac{\partial}{\partial t}\left(n_\alpha \rho_\alpha\right) + \nabla \cdot \left(n_\alpha \rho_\alpha \vec{v}_\alpha\right) = \sum_{\beta \neq \alpha} \hat{e}_\alpha^\beta \,, \tag{1a}$$

$$\frac{\partial}{\partial t}\left(n_\alpha \rho_{\alpha_j}\right) + \nabla \cdot \left(n_\alpha \rho_{\alpha_j} \vec{v}_{\alpha_j}\right) = \sum_{\beta \neq \alpha} \hat{e}_{\alpha_j}^\beta + \hat{r}_{\alpha_j} \,, \tag{1b}$$

where n_α is the volume fraction of the phase, ρ_α and ρ_{α_j} are the densities of the phase and the constituent, $\vec{v}_\alpha$ and $\vec{v}_{\alpha_j}$ are the velocities, $\hat{e}_\alpha^\beta$ and $\hat{e}_{\alpha_j}^\beta$ are related to the mass exchange and $\hat{r}_{\alpha_j}$ is asociated to chemical reactions.

Paper as a two phase material

In order to apply the hybrid mixture theory framework a simple example is introduced. An illustration of the model is shown in Figure 1.a. Moreover, a typical high speed digital inkjet printer is shown in Figure 1.b. Paper is modelled by means of two phases: solid (s) and liquid (l). The solid phase is composed of dry fibers (s_s) and intra fiber water (s_w). The dry fibers are assumed undeformable. Liquid progressively fills the pores of the material. The amount of water within the pores is described by means of the saturation S, while in the fibers it is described with the fiber moisture ratio ω. A mass exchange term is considered, allowing water to enter fibers from the pores. It is dependent on the difference between the chemical potentials, canceling out under equilibrium conditions. Chemical reactions are neglected.

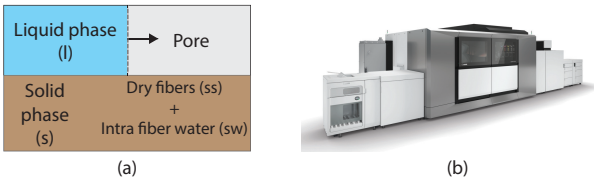

Figure 1: (a) Paper represented as a two phase medium. (b) Digital inkjet printer developed by Canon Production Printing.

Under these assumptions, the mass balance of inter fiber liquid water (l) reads

$$\varphi \frac{\partial (S(\mu_l)\rho_l)}{\partial t} + \vec{\nabla} \cdot (R_l \cdot \vec{\nabla}\mu_l) + \zeta_l^s(\mu_l - \mu_{sw}) = 0 \,, \tag{2a}$$

while the mass balance of intra fiber liquid water (s_w) is given by

$$(1-\varphi)\frac{\partial (\rho_{s_s}\omega(\mu_{sw}))}{\partial t} + \vec{\nabla} \cdot (R_{sw} \cdot \vec{\nabla}\mu_{sw}) - \zeta_l^s(\mu_l - \mu_{sw}) = 0 \,, \tag{2b}$$

where ρ_l and ρ_{s_s} are densities, φ is the porosity, R_l and R_{sw} are tensors related to the inter and intra fiber water flux, ζ_l^s is related to the mass exchange between both phases.

Results

Figure 2 shows the solution of the above equations. The boundary conditions represent an immersion test, with half the thickness of the paper sheet normalized to 1. Pores are initially dry. Water enters the pores first, initiating the filling process during the simulation. Some of the water in the pores enters the fibers through the mass exchange term. By the end of the simulation, both pores and fibers are fully saturated. Next steps in the research involve incorporating the gas phase into the multi-phase system. Following this, we will introduce the momentum equations to analyze the deformations of the paper sheet caused by swelling.

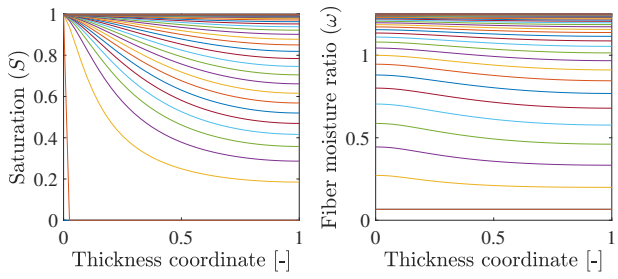

Figure 2: Immersion test modelling results.

References

[1] Bennethum, L. S., Cushman, J. H. (1996). Multiscale, hybrid mixture theory for swelling systems—I: balance laws. International Journal of Engineering Science, 34(2), 125-145.

PhD progress: 1 | 2 | 3 | 4

Acoustic Emission Sensing for Informed Maintenance of Ship Structures

C. Saccone*, L. Pahlavan

Maritime and Transport Technology
Delft University of Technology
** C.Saccone@tudelft.nl*

Introduction

Naval vessels are valuable national assets. Predictive maintenance is essential to enhance their efficiency and extend their service life. Advanced sensor systems feeding data into digital twin models can enable real-time structural monitoring of naval vessels (Figure 1). Fatigue is regarded as one of the main degradation mechanisms affecting the structural integrity of ship structures (Figure 2). Detection of fatigue cracks is challenging due to the layout of stiffeners and other structural elements (Figure 3). Accurate detection and localization of the damage can reduce the uncertainty in the estimation of the fatigue life of the vessels.

Figure 1: Navy vessel.

Figure 2: Fatigue crack on stiffener [1].

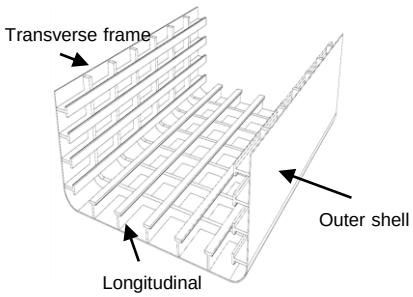

Figure 3: Internal ship structural frame.

Scope of the research

This research aims at detection, localization, and characterization of fatigue-induced damage in ship structures by means of acoustic emission (AE) propagating as ultrasonic guided waves.

Approach

In this research, the approach encompasses:

- Investigating interactions of ultrasonic guided waves with structural components (stiffeners and longitudinal frames), considering phenomena such as dispersion, scattering, reflection, and multimodality
- Classifying ultrasound signatures associated with damage.
- Locating AE sources and assessing the probability of damage detection (PoD)
- Optimizing sensor placement for detecting and monitoring fatigue and corrosion-induced cracks

Research progress

Experimental measurement and spectral finite element (SEM) simulations have been performed to assess the behavior of ultrasound waves in ship hulls and decks in the presence of structural elements, such as stiffeners and longitudinal/transversal frames. The ultrasound guided waves transmission through these structures is investigated, and its dependency on source frequency and angle of impact is characterized.

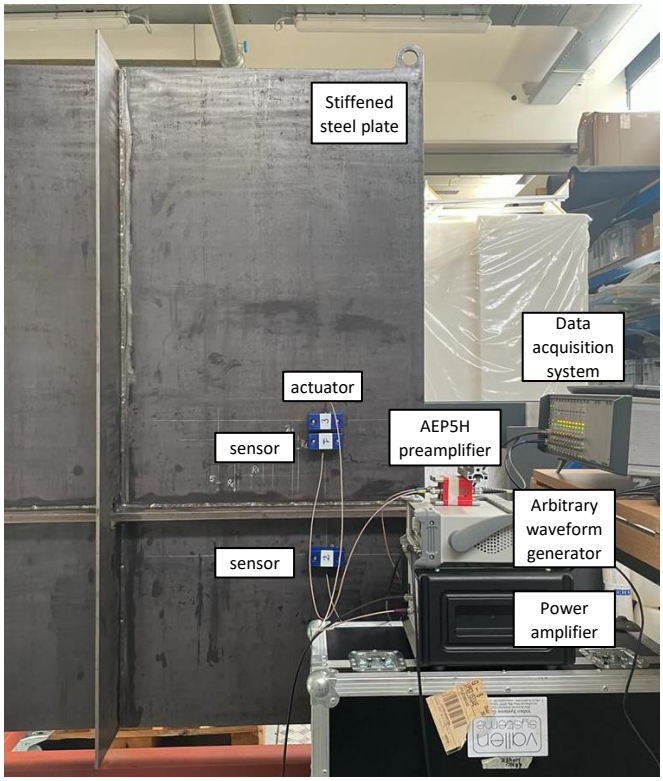

Figure 4: Instrumented steel plate

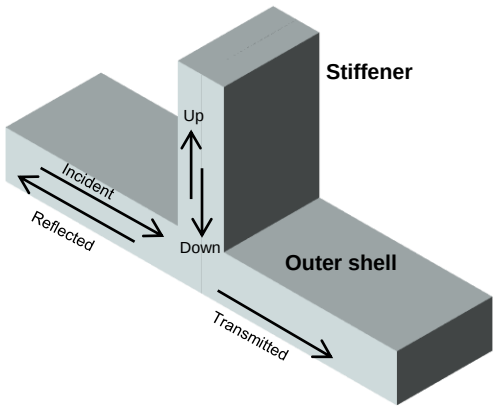

Figure 5: The geometry used for assessing the wave propagation behavior in the presence of stiffener.

References

[1] Storhaug G. Experimental investigation of wave induced vibrations and their effect on the fatigue loading of ships. PhD Thesis, NTNU, 2007.

PhD progress: 1 | 2 | 3 | 4

Acoustic Emission Bearing Condition Monitoring in Practice: Laboratory to Field

B. Scheeren[1,2], L. Pahlavan[1]

[1] *Delft University of Technology, Department of Maritime & Transport Technology*
[2] *b.scheeren@tudelft.nl*

Introduction

The reliability of low-speed roller bearings is essential to the safe operation of several offshore installations, such as heavy-lifting cranes, single-point-mooring systems, and wind turbines. Condition monitoring of such systems is still an unresolved challenge. This study presents a laboratory and a field implementation of a monitoring methodology based on acoustic emissions (AE). AE are transient elastic stress waves generated by the material as it degrades (Figure 1).

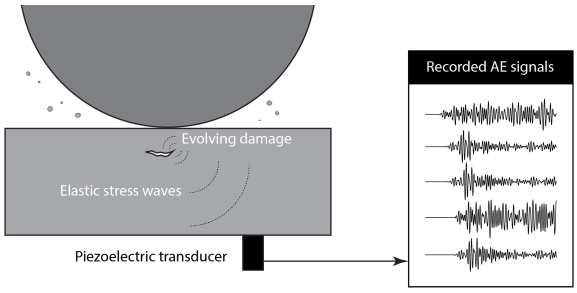

Figure 1: Illustration of the acoustic emission phenomenon.

Methodology

A bearing condition index is defined which infers the state of the bearing from source mechanism clustered AE signals in multiple frequency bands:

$$C_B = \frac{1}{1 + \sum_{q=1}^{Q} \sum_{k=1}^{K} \alpha_q \alpha_k \frac{dc_{k,q}}{dN}}. \quad (1)$$

This formulation collects the load-cycle normalised AE activity of the different measurement frequencies (Q) and identified source clusters (K) in a single index, which equals 1 for a healthy bearing and approaches 0 for a severely degraded bearing.

To assess the bearing condition index, laboratory and field experiments are performed on bogie wheels of the topside lift system of Allseas' Pioneering Spirit.

Figure 2: Picture of laboratory measurement of bogie wheel.

Laboratory Experiment

In a frame (Figure 2), the bogie wheel is pressed against a test wheel using a hydraulic cylinder. The wheel is densely instrumented with piezoelectric AE sensors and tested up to 80% of the dynamic rating lifetime at 60 rpm.

Field Experiment

On-board Pioneering Spirit (Figure 3), the four wheels that support y-movement of a lifting beam are instrumented with piezoelectric AE sensors. The beam is cycled between the slot and outboard position, introducing a rotational speed of 6 rpm. A total of 64 wheels supporting the 16 lifting beams have been tested.

Figure 3: Pictures of "Pioneering Spirit" measurement, showing; (a) an overview of several starboard beams of the topside lift system, and (b) instrumentation of the outboard support.

Results & Conclusions

The bearing condition indices obtained in these experiments may be used to support asset management and operational decisions. In addition:

- Short-term measurements seem viable to infer bearing condition.
- Contamination of the grease is a major source of AE activity.
- The ultrasonic background noise in the field is less harsh than in the laboratory.

References

[1] B. Scheeren, M.L. Kaminski, and L. Pahlavan. (2022). "Evaluation of Ultrasonic Stress Wave Transmission in Cylindrical Roller Bearings for Acoustic Emission Condition Monitoring," in *Sensors 22(4), 1500.*

[2] B. Scheeren, M.L. Kaminski, and L. Pahlavan. (2023). "Acoustic Emission Monitoring of Naturally Developed Damage in Large-scale Low-speed Roller Bearings," in *Structural Health Monitoring, OnlineFirst.*

SOFEC bluewater Huisman Allseas

TU Delft Delft University of Technology · HiTeAM · THI Maritiem Nederland Maritiem Land

PostDoc progress 1 2

TotalEnergies · Marine Contractors · SBM Offshore

Life prediction of composite materials

Creating a digital-twin framework

J.C. Schönthaler[1], B. Rosic[1], D. Di Maio[1]

[1]University of Twente

Introduction

In the transition to a climate-neutral economy, composite materials can play a big role due to their high strength-to-weight ratio. However, reliable fatigue evaluation methods must be found to ensure long-term integrity of the designs. In aid, a digital-twin framework will be built to predict the residual lifetime of composite materials subjected to vibration fatigue.

Background

Previous research [1, 2] has shown applications of **near-resonance fatigue testing**. This shows a phase degradation up to a critical event, causing a sudden stiffness drop, see Figure 1.

The phase degradation is used for two important parameters:

- the **crack propagation** up to point (a),
- a **failure criterion** between (a) and (b).

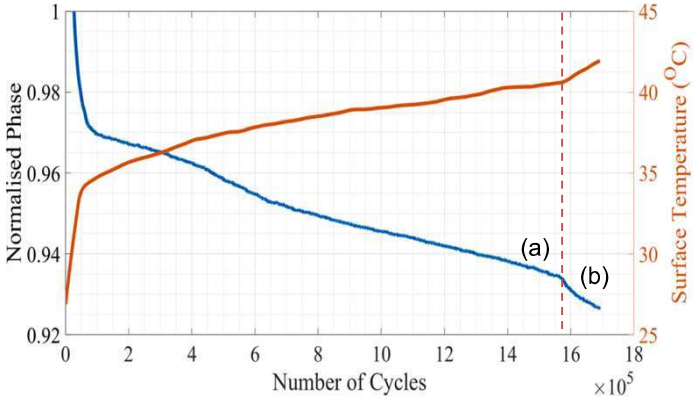

Figure 1 The phase decay and critical event [1].

The crack propagation is used to identify **Paris' Law**, shown in equation 1, containing material parameters C and m.

$$\frac{da}{dN} = C(\Delta K)^m \qquad (1)$$

This can be combined with the critical event between point (a) and (b) in Figure 1 to create an **SN-curve** for the material, where rapid delamination after point (b) indicates failure.

Method

Experimental results from the experimental setup shown in Figure 2 will be combined with the simulation framework. The analysis steps for the framework can be seen in Figure 3.

Conclusion

A **digital-twin framework** will be created to predict the **residual life** of composite materials that are subjected to **vibration fatigue**. This can significantly **speed up** conventional fatigue testing methods for composite materials.

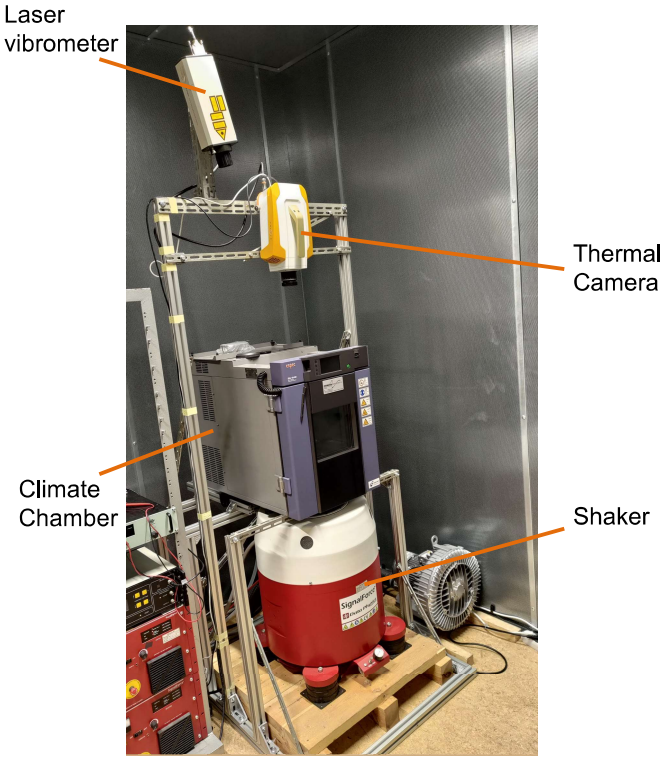

Figure 2 The experimental setup that will be used for high-frequency fatigue testing.

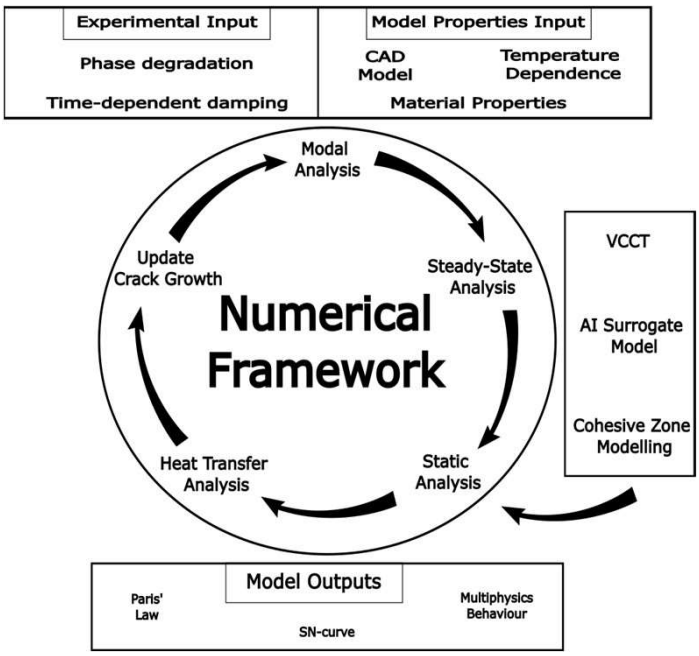

Figure 3 Different analysis steps to create the digital-twin framework.

References

[1] Magi et al., Composites Sci. & Tech., 132 (2016) 47-56.
[2] Di Maio et al., I. J. Fatigue, 155(2022)106617.

ROBUST PROCESS CONTROL FOR THE INDUCTION WELDING OF THERMOPLASTIC COMPOSITES

Wouter J. Schuttert, M.I. Abdul Rasheed, B. Rosic

University of Twente

Chair of Applied Mechanics and Data Analysis

Thermoplastic Composites

Lightweight alternative to metals for transportation industry

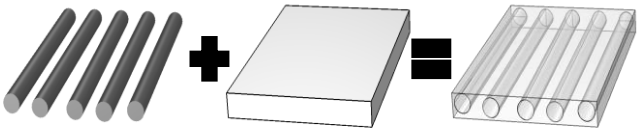

Consists of a fiber material and matrix material
Example: Carbon fiber reinforced PEEK

Material Parameters

Macro properties like electrical/heat conductivity and heat capacity tensors

Experimental data

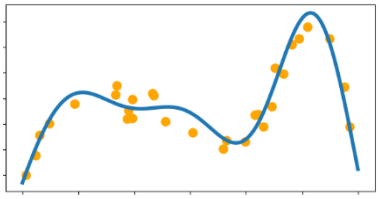

Identification is challenging
and outcomes have a high variance

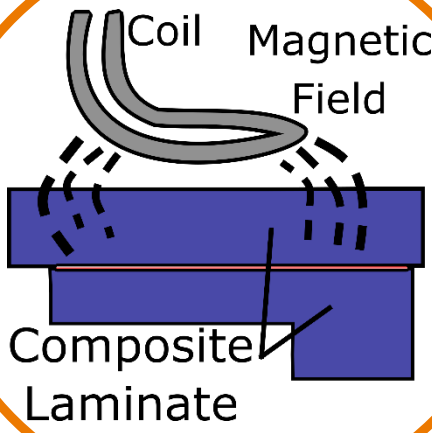

Multi-physics Process Model

Induction welding is a highly nonlinear, strongly coupled physics-based problem

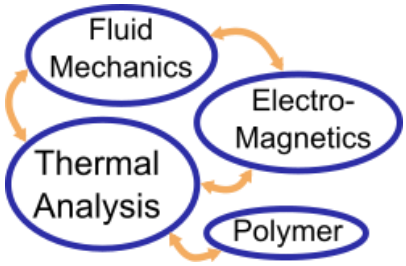

Control and Optimization

Minimize production time and maximize weld quality

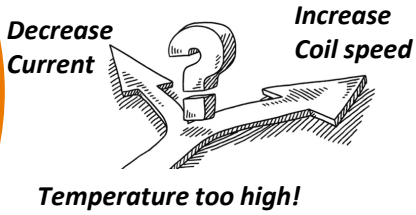

1000s of model evaluation are required for sensitivity analysis and inline control

Stochastic Modelling of Tensors

Material parameters are collected in tensors which vary in space for thermoplastic composites. An example is a random field of a zeroth order tensor,

Random field

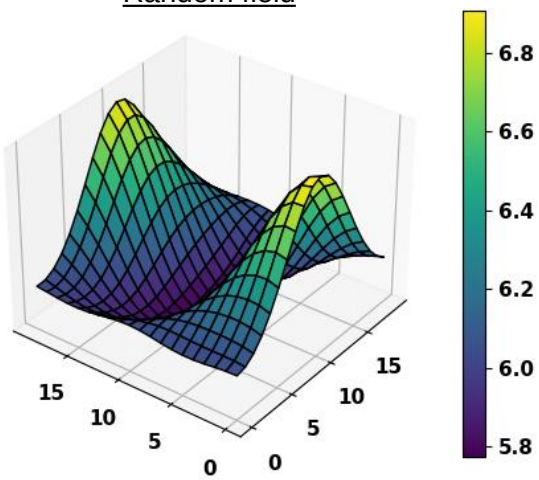

A random field uses a mean, variance and correlation length to describe the spatially varying parameter

Surrogate modelling

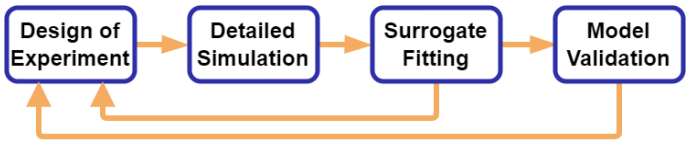

Polynomial Chaos Expansion

Uncertainty described by a deterministic set of equations with a stochastic basis

$$Y = \sum_{i \in \mathbb{N}} c_i \Psi_i(\mathbf{X})$$

Basis functions — *Coefficients* — *Random variables*

Bayesian Neural Networks

Mixture of Bayesian methodology and deep learning

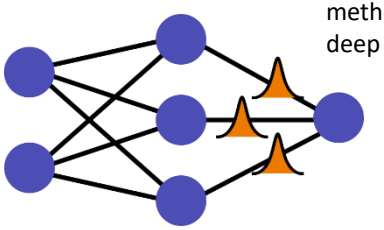

Contact

THE BRAIN EXTRACELLULAR MATRIX: A MULTISCALE COMPUTATIONAL STUDY

Saber Shakibi*, Patrick Onck, Erik Van der Giessen

Zernike Institute for Advanced Materials, University of Groningen, The Netherlands

Brain Cancer

Glioblastoma (GBM) is the most common and malignant brain tumor. Similar to solid tumors the stiffness of the brain tumor is observed to increase with, the grade of cancer [1]. This increase in stiffness is associated with remodelling of the extracellular matrix (ECM) of the brain shown in figure 1, where many of the ECM components are overexpressed.

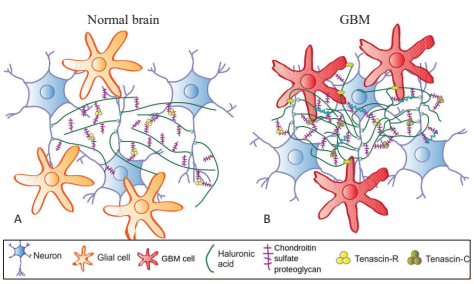

Figure 1: ECM Remodelling from (A) normal brain to (B) GBM (edited from Ref. [1]).

Brain ECM

Perineuronal nets (PNNs) shown in figure 2 are one of the compartments of the brain ECM. Hyaluronic acid (also known as hyaluronan) serves as the bachbone of the PNNs. Chondroitin sulfate proteoglycans are attached to hyaluronic acid, and tenascins serve as crosslinkers of this network. We regard PNNs as a simplified model of the brain ECM.

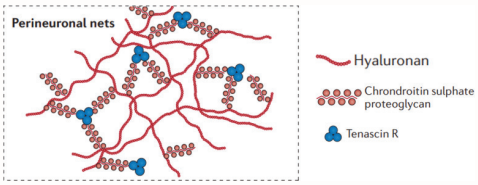

Figure 2: Perineuronal net and its constituents [2].

Glycosaminoglycans and Proteoglycans

Hyaluronic acid (HA) and Chodroitin sulfates (CS) that serve as the side chains of chodroitin sulfates proteoglycans, are two types of glycosaminoglycans. CS Proteoglycans, shown in figure 3b, are a family of brush-type biopolymers that are composed of a core protein to which a number of CS chains are attached. Aggrecan is a well-known proteoglycan that is also found in cartilage, however, neurocan and brevican are among the most dominant proteoglycans in the brain [3].

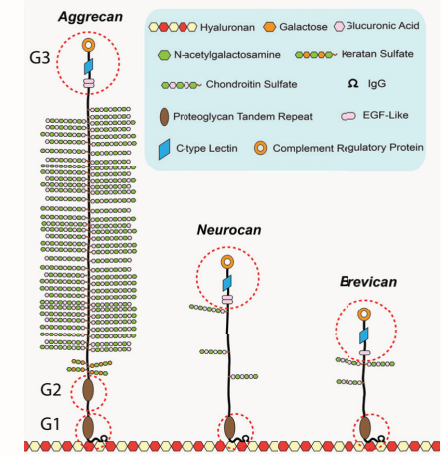

Figure 3: Proteoglycans present in the brain (edited from: Ref. [4]).

The 1BPS model

We have coarse-grained an existing three-bead-per-saccharide model of HA and CS chains [5] to develop a one-bead-per-saccharide (1BPS) model [6] as illustrated in figure 4.

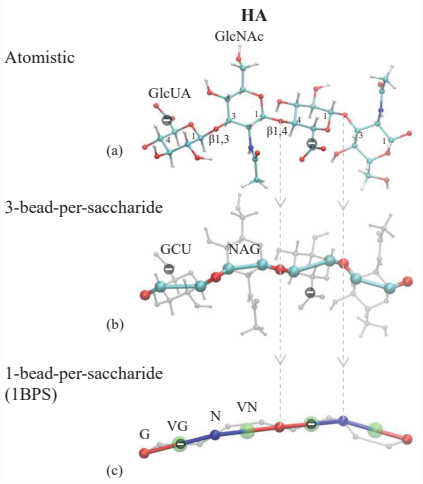

Figure 4: Definition of coarse grained beads in the 1BPS model.

In this model we are treating the solvent implicitly and use the Debye-Hückel potential for electrostatic interactions. Despite being 'super' coarse-grained, the 1BPS model still makes predictions that match experimental observations without any fitting parameter (figure 5).

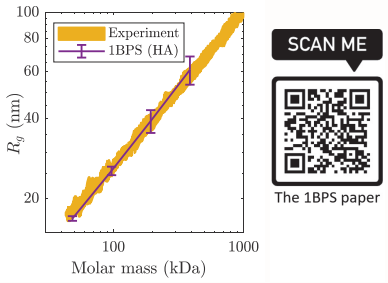

Figure 5: Radius of gyration vs molar mass for HA the longest simulated chain has 2048 monosaccharides [6].

Proteoglycans

We modelled proteoglycans by combining the 1BPS model for CS chains with the one-bead-per-aminoacid (1BPA) model previously developed in our group [7] for the unfolded regions of the core protein and an elastic network model for the folded regions of the core protein. Encouraged by the results for aggrecan shown in figure 6, we proceeded by using the model to study other brain-specific proteoglycans in terms of radius of gyration as shown in figure 7.

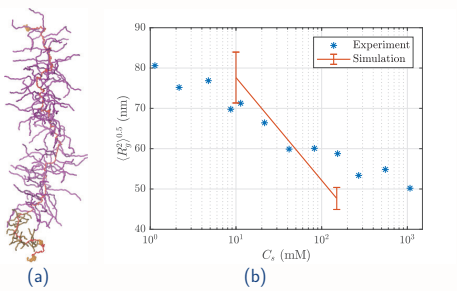

Figure 6: Results of simulating an aggrecan with a molecular weight of 1.60 MDa. (a) A characteristic screenshot; (b) Dependence of root-mean-squared radius of gyration on salt concentration: simulation vs experimental data from Ref. [8].

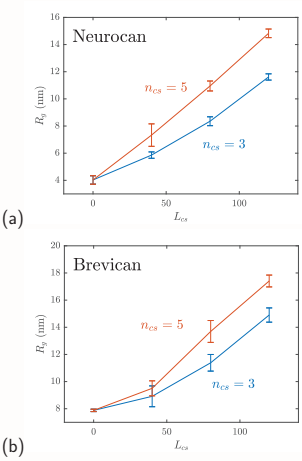

Figure 7: Radius of gyration of (a) neurocan and (b) brevican as a function of number of side chains, n_{cs}, and number of monosaccharides of the side chains, L_{cs}, at biological salt concentration ($C_s = 150$ mM).

Methacrylated HA gel

Methacrylated HA (MeHA) gels are hydrogels made out of crosslinked HA chains. These gels are a further simplified versions of PNNs. We modelled these gels as a periodic network of chains modelled using 1BPS model (shown in Figure 8a) and performed simple shear simulations. Fig. 8b compares the predicted storage modulus to experimental observations.

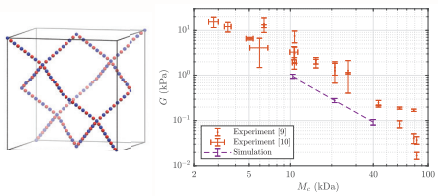

Figure 8: Methacrylated HA gel: (a) initial configuration of the periodic cell; (b) Comparison between simulations and experimental observations [9, 10] for the storage modulus, G, as a function of the molecular mass between crosslinks, M_c. Simulation error bars indicate 95% confidence interval of fitting the slope of the stress–strain curve.

Outlook

The network model for MeHA will be extended by including proteoglycans and a coarse-grained model of tenascins. This more complex model will be used to predict the stiffness of perineuronal nets as a function of the concentration of its components. This will allow us to study the relationship between expression of ECM components with its stiffness in healthy and cancerous state.

References

[1] J. M. Barnes et al. *J. Cell Sci.*, vol. 130, pp. 71 – 82, 1 2017.

[2] L. W. Lau et al. *Nat. Rev. Neurosci.*, vol. 14, no. 10, pp. 722–729, 2013.

[3] D. R. Zimmermann and M. T. Dours-Zimmermann *Histochem. Cell Biol.*, vol. 130, no. 4, pp. 635–653, 2008.

[4] R. V. Iozzo and L. Schaefer *Matrix Biol.*, vol. 42, pp. 11–55, 2015.

[5] M. Bathe et al. *Biophys. J.*, vol. 88, pp. 3870–3887, 6 2005.

[6] S. Shakibi et al. *J. Chem. Theory Comput.*, 2023. DOI: 10.1021/acs.jctc.3c00238.

[7] A. Ghavami et al. *Biophys. J.*, vol. 107, pp. 1393–1402, 9 2014.

[8] X. Li and W. F. Reed *J. Chem. Phys.*, vol. 94, pp. 4568–4580, 3 1991.

[9] C. Credi et al. *J. Mech. Behav. Biomed. Mater.*, vol. 29, pp. 309–316, 2014.

[10] E. Tsanaktsidou et al. *Eur. Polym. J.*, vol. 114, pp. 47–56, 2019.

* ✉ S.Shakibi@rug.nl

Experimental characterization of Acoustic Metasurface and Metafoams

S.K. Sikundalapuram Ramesh[1], X. Kuci, R. Liupekevicius, M.G.D. Geers, V.G. Kouznetsova

Eindhoven University of Technology

Email: s.k.sikundalapuram.ramesh@tue.nl

Goals

Experimentally demonstrate the implementation of novel coating types (locally resonant metamaterials) to enhance the sound absorption, or to enhance reflection and redirect the reflected wave back to the probe.

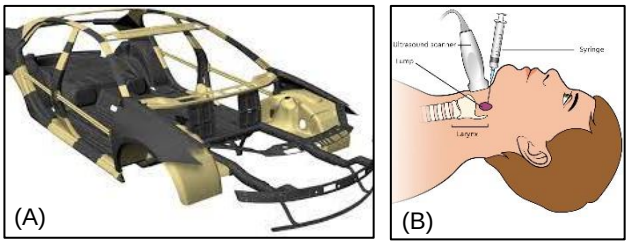

Figure 1: (A) Acoustic Foams placed over the car body for sound absorption(https://www.dow.com/). (B) Ultrasound needle inspection (https://www.macmillan.org.uk/)

Acoustic Metafoams

A new generation of acoustic foam is designed by combining standard acoustic foams with the Locally Resonant Acoustic Metamaterial (LRAM) features.

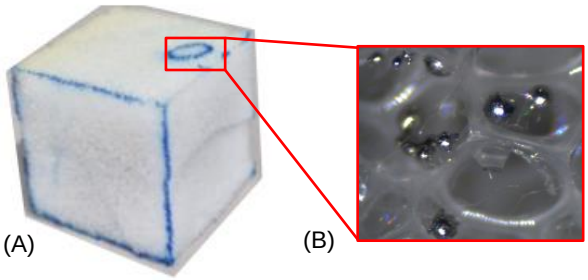

Figure 2: (A) Metafoam sample manufactured within METAFOAM project (ERC-PoC, PI M. Geers) (B) Image from the light microscope of the sample with steel particles embedded in a foam material[4]

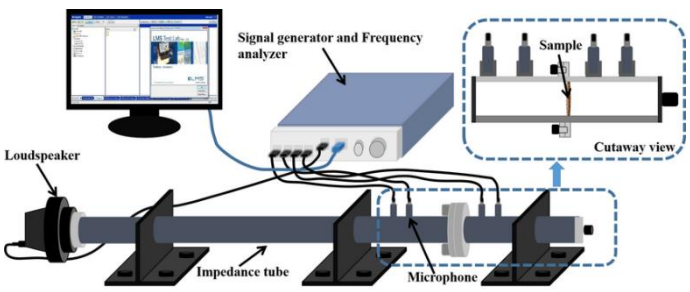

Figure 3: Schematic of Transmission Impedance Tube setup for Acoustic Metafoam Experiments[3]

Redirection of waves by Gradient Acoustic Metasurface

Locally resonant acoustic metamaterials (LRAM) based coating are developed to enhance the needle visualization in medical devices[5]

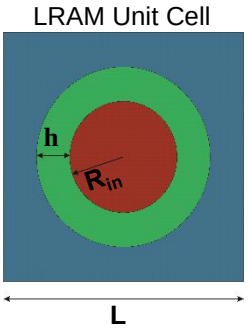

Redirection based on Generalized Snell's Law of reflection:

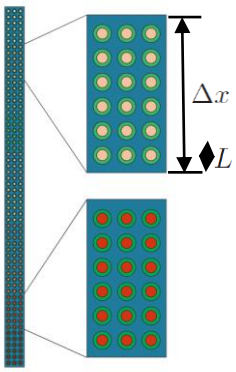

$$\sin\theta_r = \sin\theta_i + m\frac{\lambda_1}{2\pi}\frac{d\phi(x)}{dx}$$

θ_r - reflected angle

θ_i - incident angle

m - diffraction order

$\frac{d\phi(x)}{dx}$ - variation of phase along the surface

take k subdivisions

$$\Delta\phi = \frac{2\pi}{k}$$

$$\Delta x = \frac{m\lambda_1}{k(\sin(\theta_r) - \sin(\theta_i))}$$

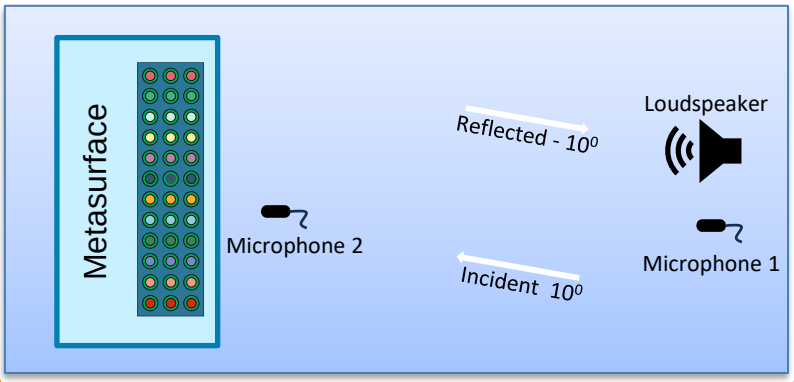

Figure 4: Schematic of Acoustic Metasurface Experiments in an Anechoic Room

References

[1] M. A. Lewinska. PhD Thesis, 2019.
[2] K. Gao. PhD Thesis, 2016.
[3] Chen etal, Cellulose 29, 355–365, 2022.
[4] Koen van der Velde MSc Thesis, 2023.
[5] X. Kuci, M.G.D. Geers, V.G. Kouznetsova, Towards design of a gradient locally resonant acoustic metasurface for negative reflection[under preparation]

Bayesian estimation and uncertainty quantification of a temperature-dependent thermal conductivity

R.L.S. Silva, C.V. Verhoosel, E. Quaeghebeur

Eindhoven University of Technology

Introduction

The thermal conductivity is the proportionality constant in Fourier's law [1]. This constitutive model relates the heat flux to the gradient of the temperature [1]. While it can be often assumed a linear relation between the heat flux and the gradient of temperature, there are many engineering problems where the thermal conductivity varies significantly with the temperature.

Different techniques have been used for estimating a temperature-dependent thermal conductivity, and most of them are limited to point estimates. The goal of this work resides in creating a Bayesian framework to provide not only the estimation, but also the uncertainty quantification of a temperature-dependent thermal conductivity.

Transient heat conduction problem

We consider a 1-D transient heat conduction problem in which a slab of length L is heated on one edge by a constant heat flux and cooled on the other by a constant temperature ambient medium (see Figure 1). Initially, the temperature in the slab is equal to the medium temperature. We aim at estimating and quantifying the uncertainties of the temperature-dependent thermal conductivity *k(T)*.

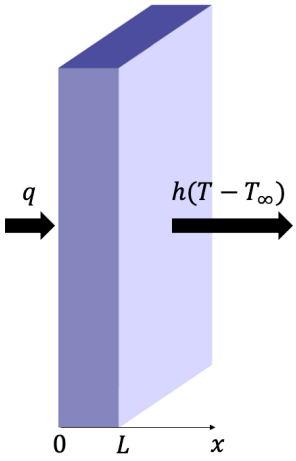

Figure 1: Illustration of the heat conduction problem

Bayesian framework

We start by defining **D** as the vector with data. This data consists in temperature measurements obtained from sensors located at both edges of the slab. We also define **P** as the vector with $N = 100$ discretized values of the function *k(T)* between the minimum and maximum measured temperatures. We then consider Bayes' theorem as follows:

$$p(\mathbf{P}|\mathbf{D}) \propto p(\mathbf{P})p(\mathbf{D}|\mathbf{P})$$

The likelihood $p(\mathbf{P}|\mathbf{D})$ is modeled as a multivariate normal distribution. This distribution is given in terms of the measurement errors, and admit null mean and constant standard deviation equal to 1% of the maximum measured temperature. The prior $p(\mathbf{P})$ is modeled by a Gaussian Markov Random Field (GMRF) [2, 3] as follows:

$$p(\mathbf{P}) \propto \exp\left[-\frac{1}{2\gamma^2}(\mathbf{P}-\overline{\mathbf{P}})^T\mathbf{D}^T\mathbf{D}(\mathbf{P}-\overline{\mathbf{P}})\right],$$

where γ is a parameter associated to the uncertainties in **P**, $\overline{\mathbf{P}}$ is a reference value for **P** and

$$\mathbf{D} = \begin{bmatrix} -1 & 1 & 0 & \cdots & 0 \\ 0 & -1 & 1 & \cdots & 0 \\ \vdots & \ddots & \ddots & \ddots & \vdots \\ 0 & \cdots & 0 & -1 & 1 \end{bmatrix}_{(N-1)\times N}$$

Results and discussions

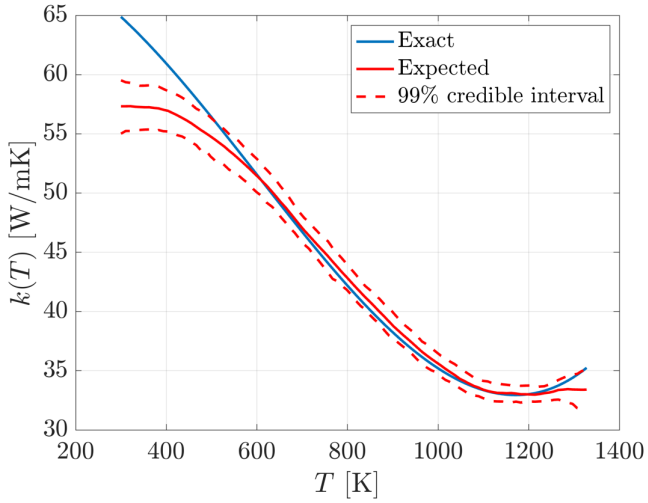

Figure 2: Estimation and uncertainty quantification of *k(T)*

Figure 2 shows the results obtained for $\overline{\mathbf{P}} = 0$ and $\gamma = 0.01$. The GMRF prior allows us to simultaneously estimate all the discretized values of the function *k(T)*. The uncertainty quantification is given in terms the 99% credible interval. We notice general a good agreement between the estimated and exact values. This agreement can be improved for values of *T* around 400 K by setting different values of $\overline{\mathbf{P}}$ and γ.

References

[1] Ozisik, M.N. *Heat Conduction*. John Wiley & Sons, 1993.
[2] Ozisik, M.N. *Inverse heat transfer: fundamentals and applications*. Routledge, 1993.
[3] Kaipio, J. and Somersalo, E. *Statistical and computational inverse problems. Vol. 160.* Springer Science & Business Media, 2006.

A Microstructure-based Graph Neural Network for Accelerating Multiscale Simulations

J. Storm, I.B.C.M. Rocha, F.P. van der Meer

Delft University of Technology

Introduction

We develop a graph neural network (GNN) surrogate for multiscale modelling with plasticity. The GNN predicts the full-field microscopic solution based on macroscale loading and microscale geometry. By obtaining all relevant microscopic fields (displacements, state variables), the model is interchangeable with FE simulations at any timestep.

Periodicity in graph creation & features

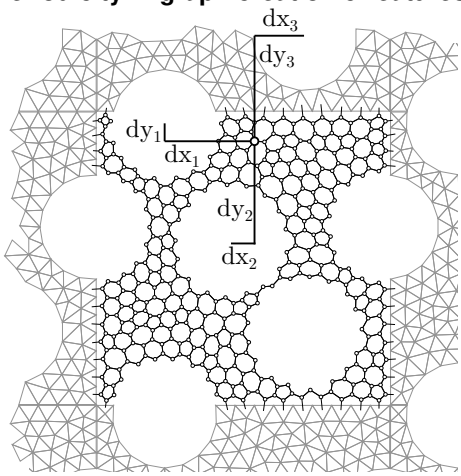

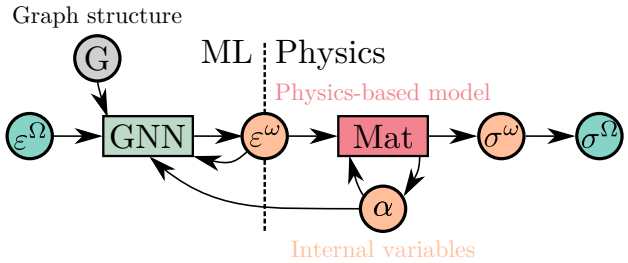

Motivation

Most surrogates essentially transform a multiscale problem back to a single-scale one with a learned macroscopic constitutive model. When such a model expresses an unacceptable uncertainty in its prediction, there is no history available to use FE instead for that timestep. Our surrogate replaces only the most expensive part of the multiscale simulation, namely solving the microscopic boundary-value problem, while still keeping the problem multiscale in nature. This allows the model to be interchangeable with FEM for any timestep.

Methodology

Based on any mesh, initial state, and input loading, a graph is created for which the GNN predicts the full-field microscopic strain. The physics-based microscopic elasto-plastic material model is used to compute the stresses (which can then be homogenized) and to track internal variables. These internal variables are used by the GNN for the next timestep. The GNN parameters are updated based on the differences between the predicted and true strain fields for all timesteps. Automatic differentiation is used to propagate these errors through the material model.

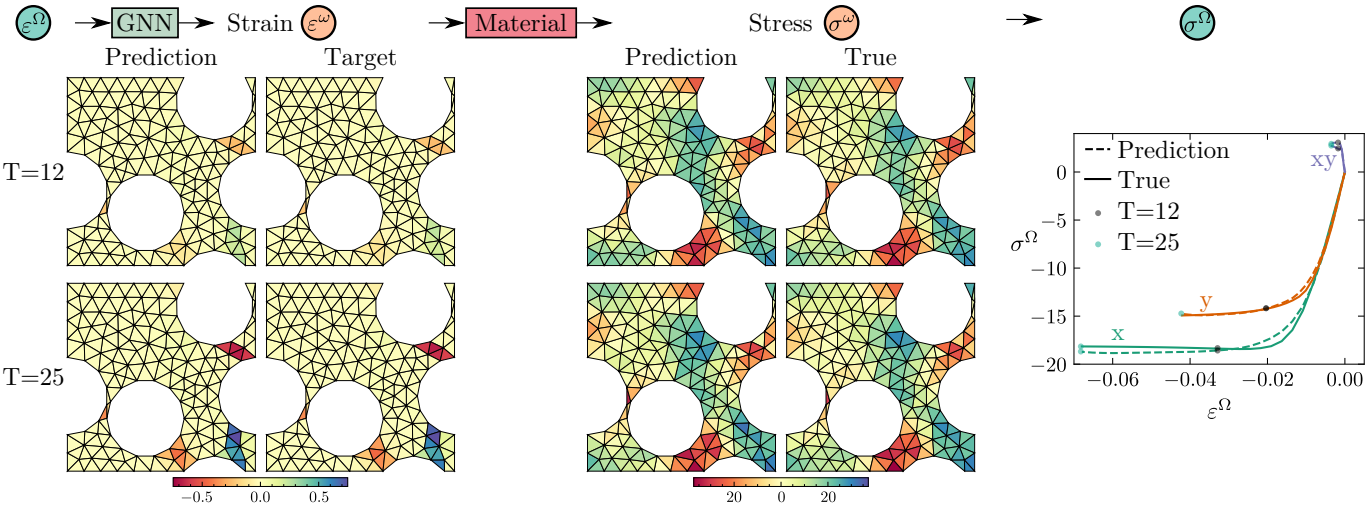

Findings

- The GNN is 10x faster than using FEM.
- Capturing unloading and reloading is challenging, even when training on non-monotonic samples and with the material model.
- The homogenized stress predictions can be improved by including it in the loss function, however this comes at the cost of full-field accuracy.
- A single model can handle various mesh densities.

Future work

- Adjust the training data to improve model accuracy, e.g. by including a larger fraction of unloading/reloading steps.
- Get probabilistic outputs to quantify prediction uncertainty.
- Implement fibers instead of voids.
- Transfer learning to a model with different material parameters.

PhD progress

1 | 2 | 3 | 4 | 5

Vibration-Induced Friction Force Modulation

E. Sulollari[1], A. Cabboi[1], K. van Dalen[1]

[1]Facutly of Civil Engineering and Geosciences,
Delft University of Technology

Introduction

Relevant applications

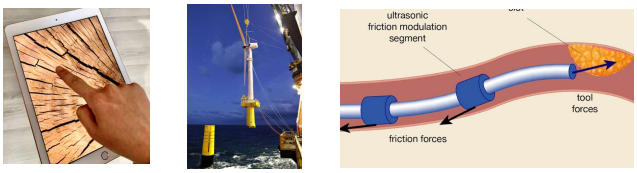

Figure 1: From left to right : surface haptics, slip joint installation/ decommission, catheter development

What is our goal concerning the presence of friction

Control friction forces

Ex: using lubricants

Figure 2: Lubricated gears

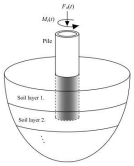

Ex: using external vibrations

Figure 3: Normal and torsional vibrations in Gentle Pile Driving [1]

Research gap and goal

Current models lack the effect of a general frequency of excitation, interaction of different loads, the influence of interface properties etc.

Quantify the effect of excitation on friction by increasing model complexity including:

- General frequency range
- Micro- and macrostructure
- Local and global dynamics

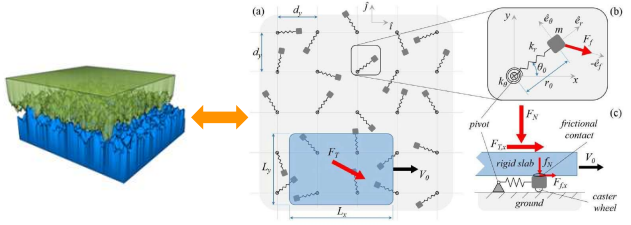

Figure 4: Example of modelling micro-structure and its dynamics [2]

Current results

Friction modulation expression:

$$\bar{\mu}(V_r) = \mu_s \langle sgn(V(t) - V_b) \rangle = \begin{cases} \mu_s\left(1 - \frac{2}{\pi}\arccos\left(\frac{V_b}{\hat{V}}\right)\right) & for \ |V_b| \le \hat{V} \\ \mu_s sgn(V_b) & for \ |V_b| \ge \hat{V} \end{cases}$$

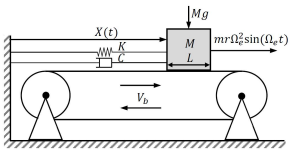

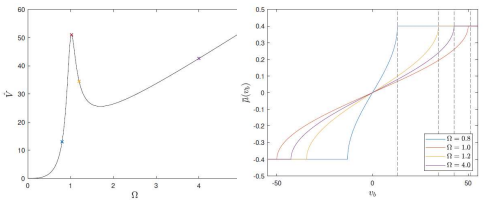

Applicable for:

- ✓ general freq.
- ✓ SDOF/MDOF
- ✓ defining stick-slip region

Figure 5: Friction modulation for SDOF

Depends on:

- ✓ Load directions and combinations
- ✓ Normal contact force formulation

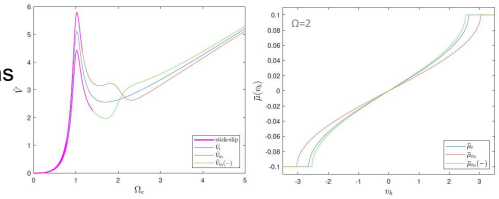

Figure 6: Friction modulation when contact force depends on stiffness/damping

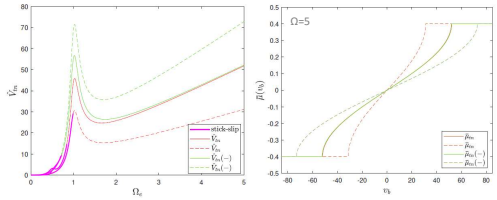

Figure 7: Friction modulation when contact force depends on inertia

- ✓ Nonlinear contact properties that cause instability

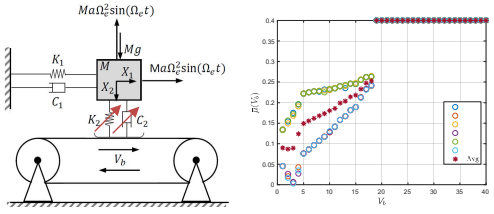

Figure 8: Effect of nonlinear contact properties on friction modulation

Main conclusions

- Velocity response function quantifies vibration-induced effect on friction
- Directions /combinations of dynamic loads influence friction modulation
- Choice of normal contact force expression effects friction modulation
- Nonlinear contact properties can lead to both stability or instability

References

[1] A. Tsetas, A. Tsouvalas, A.Metrikine. The mechanics of the Gentle Driving of Piles. Int J Solids Struct, 282:112466, 2023.

[2] N. Menga, F. Bottiglione, and G. Carbone. Dynamically induced friction reduction in microstructured interfaces. Nature, 11(1):171–184, 2021.

PhD progress

1	2	3	4

TU Delft Delft University of Technology

Mimicking Living Bones To Optimise Hierarchical, Multimaterial, 3D Printed Auxetic Metamaterials

E. Tay[1,3], M.C. Saldivar[1,3], H. Pahlavani[1,3], E.L. Doubrovski[2,3], M.J. Mirzaali[1,3], A.A. Zadpoor[1,3]

[1] *Department of Biomechanical Engineering, Faculty of 3ME*
[2] *Faculty of Industrial Design Engineering (IDE)*
[3] *Delft University of Technology (TU Delft)*

Introduction

Architectured celllular lattices are an essential tool in engineering design but their mechanical performance is intrinsically linked to, and limited by, their geometry [1-4]. We developed a bioinspired bone remodelling-like algorithm to hierarchically arrange composite (hard/soft) materials within a unit cell [5-6]. We demonstrate a decoupling of properties and expansion of design space.

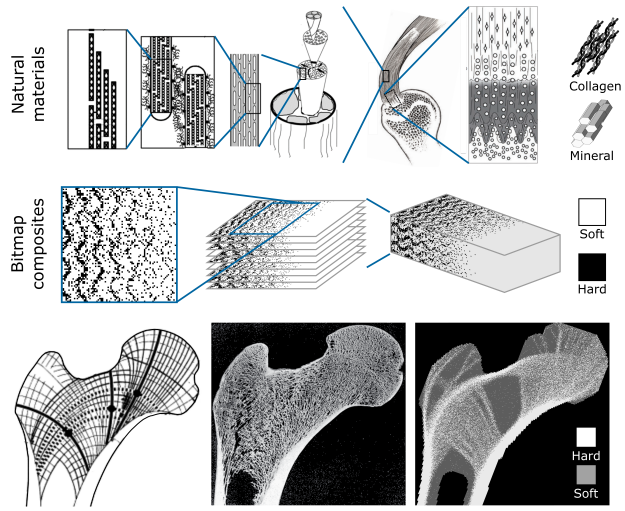

Remodelling algorithm

Our remodelling algorithm is based on a principle of a weighted relative strain energy density (SED). Voxels with the highest effective SED are replace with hard material, whilst voxels with the lowest are replaced with soft material.

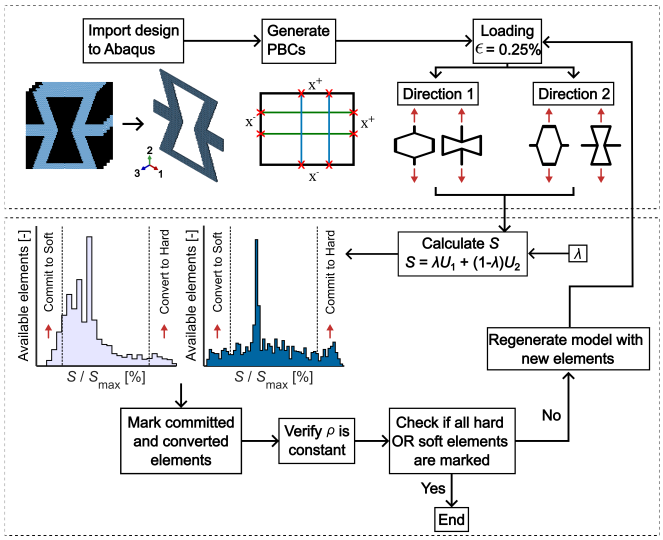

Expansion of design space

Our results demonstrate the capacity to greatly expand the range of achievable mechanical properties for fixed unit cell designs, simply by modifying hierarchical material placement. We are also able to anisotropically tune properties for specific stiffnesses, whilst retaining auxeticity.

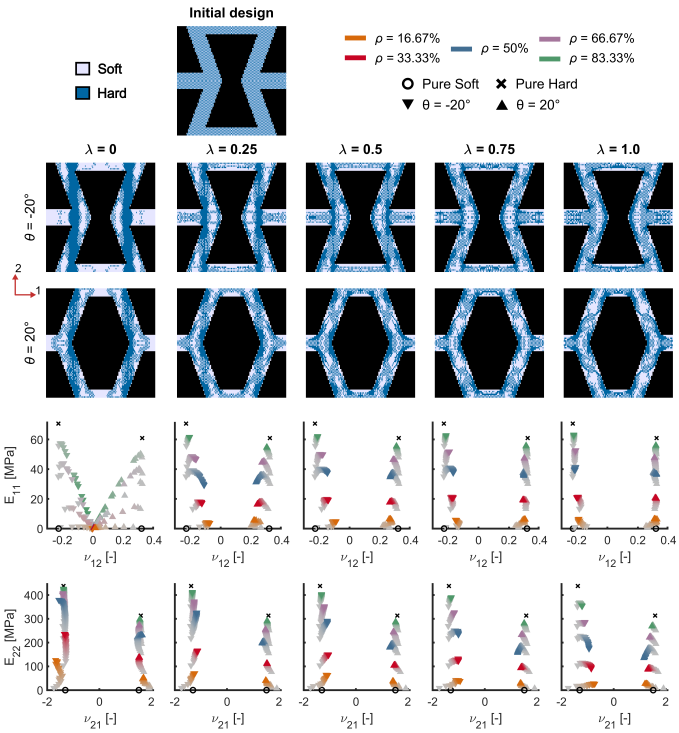

Mechanical validation

We 3D printed our samples and mechanically tested them with digital image correlation. We also carried out a mesh convergence test. Our results demonstrate our FEM simulations are accurate and valid.

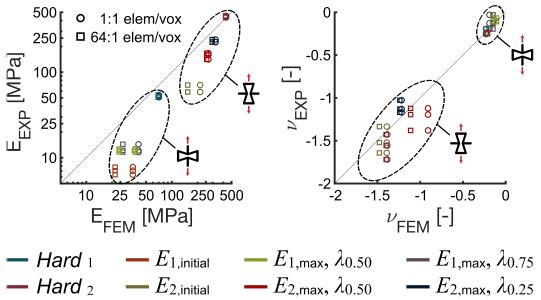

References

1. M. Ashby, Phil. Trans. R. Soc. A 364 (2006) 15-30
2. H.N. Wadley, Phil. Trans. R. Soc. A 364 (2005) 31-68
3. M.N. Andersen et al., Mat. & Des. 198 (2021) 109356.
4. Y. Brechet et al. Scr. Mat. 68 (2013) 1-3.
5. U.G.K. Wegst et al. Nat. Mater. 14 (2014) 23-36.
6. J.W. Dunlop et al., Ann. Rev. Mater. Res. 40 (2010) 1–24

PhD progress

1	2	3	4

Full publication

Forced vibrations of system assemblies: An unsolved challenge

J. van Tiggelen[1], M.H.M. Ellenbroek[1], B. Rosic[1], D. Di Maio[2]

[1]University of Twente, Chair of Applied Mechanics and Data Analysis
[2]University of Twente, Chair of Dynamics Based Maintenance

Introduction

Being able to predict the forced vibration response of assembled systems is paramount for creating reliable structures that can survive in dynamic environments. However, stress predictions of system assemblies under dynamic loads are still lacking due to the nonlinear behaviour at the mechanical interfaces between components. For efficient computation of the nonlinear forced vibrations, a quasi-static nonlinear modal analysis method is proposed.

Nonlinear behaviour of joints

The forced vibration response depends on the vibration amplitude because of the nonlinear interaction laws at the joints.

Joints nonlinearities

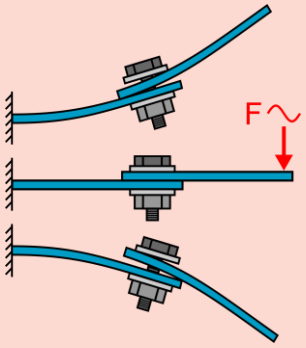

Non-constant **normal load** due to reduction of the applied preload.

Nonlinear **contact stiffness** due to stick-slip-separation of the contact surfaces

Nonlinear **friction laws** that lead to stick-slip motion or nonlinear energy dissipation.

Why do we care?

The **reliability** of our structures is compromised by inaccurate stress calculations. Whereas our linear models may predict a certain margin of safety, the real stress can be beyond critical levels.

Linear models predict

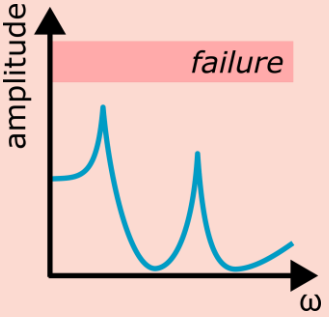

Vibration tests show

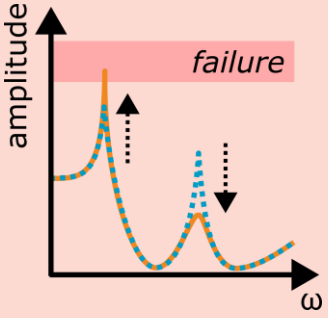

Contact

✉ j.vantiggelen@utwente.nl
jip-van-tiggelen

Forced vibrations

The equation of motion of a system with nonlinear internal forces

$$\boldsymbol{M\ddot{x} + C\dot{x} + Kx + F_{NL}(x, \dot{x}, \ldots) = f(t),}$$

can be solved using **time-domain methods**, but this is **computationally expensive**. For linear systems, the computational effort can be reduced by assuming steady-state harmonic excitation and response,

$$(-\omega^2 \boldsymbol{M} + i\omega \boldsymbol{C} + \boldsymbol{K})\bar{\boldsymbol{X}} = \boldsymbol{F}.$$

which can be solved using **frequency-domain methods**. For solving the forced response of nonlinear systems in the frequency domain, **harmonic balance methods** [1] have been developed, but those are still very expensive for models with more than a few nonlinear elements.

Quasi-static nonlinear modal analysis

Building upon quasi-static modal analysis [2], a numerical framework is envisioned by which the **stress analysis** can be **expanded over the frequency domain**. From a linear steady-state dynamics model, the forced vibration response of a structure is determined. The obtained deflection shapes are used as boundary condition on a nonlinear meta-model, that provides updated dynamic properties to the linear model, based on a quasi-static stress analysis.

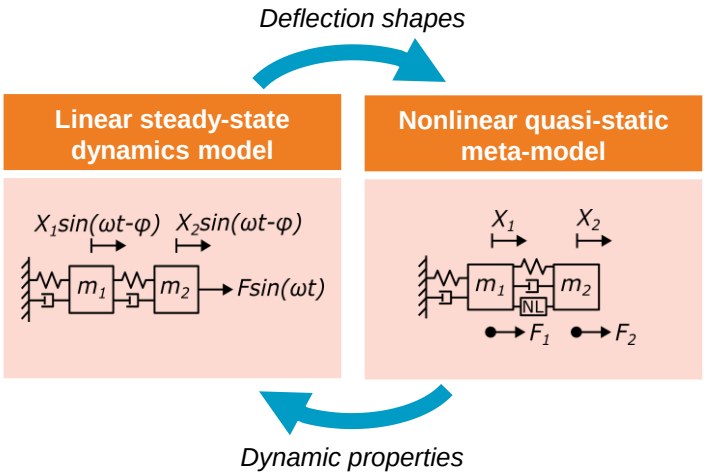

References

[1] M. Krack, J. Gross. Harmonic Balance for Nonlinear Vibration Problems. Mathematical Engineering. Cham: Springer International Publishing; 2019.
[2] M.S. Allen, R.N. Lacayo, M.R.W. Brake. Quasi-Static Modal Analysis based on Implicit Condensation for Structures with Nonlinear Joints. In: International Conference on Noise and Vibration Engineering, Leuven, Belgium; September 2016.

Substructures as classifiers: predicting composites failure with classical and quantum kernel methods

G. Tosti Balducci[1], B. Chen[1], M. Möller[3], M. Gerritsma[2], R. de Breuker[1]

[1] *TU Delft, Aerospace Structures and Materials*
[2] *TU Delft, Flow Physics and Technology*
[3] *TU Delft, Applied Mathematics*

Motivation

Full-scale finite element analyses capturing different physics at different scales are computationally expensive, if not unviable. A typical technique used to obviate to this problem is substructure homogenisation. This consists in replacing sections of a larger model with smaller higher-fidelity models, while setting the right internal boundary conditions. In recent times, data-trained machine learning models have been used as substructures [1], allowing to capture complex material behaviour with the extreme local numerical efficiency of simply querying a nonlinear function.

The grand majority of substructuring techniques focuses on material homogenisation. For data-based approaches, this means that the sub-model is generally a regressor and most often some kind of neural network. However, situations where we want to identify the occurrence of an event and possibly its location, such as damage onset in the larger structure, intuitively suggest to treat the local substructures as classifiers.

Binary classification

The aim is to train a composite substructure to classify loading conditions that lead to structural failure from those that do not. If $\varepsilon^{(m)}$ is a homogenized strain loading sample, we label it as $y^{(m)} = \pm 1$, if there is/is not associated failure. We get the following *binary classification problem*:

Given $\left\{\varepsilon^{(m)}, y^{(m)}\right\}$, $m = 1, \ldots, M$, *find the function* f *that correctly labels unseen loading states.*

SVM, kernels and alignment

We use the support vector machine (SVM) algorithm to train the classifying substructure. This consists in the following optimization problem (in dual form):

$$\begin{aligned} \max_{\alpha_1,\ldots,\alpha_M} \quad & \sum_{m=1}^{M} \alpha_m - \frac{1}{2} \sum_{m,m'=1}^{M} \alpha_m \alpha_{m'} y^{(m)} y^{(m')} \kappa\left(\varepsilon^{(m)}, \varepsilon^{(m')}\right) \\ \text{s.t.} \quad & \alpha_m \geq 0, \quad m = 1, \ldots M \\ & \sum_{i=1}^{M} \alpha_m y^{(m)} = 0. \end{aligned}$$

The function $\kappa\left(x, x'\right)$ is known as *kernel* and defines a measure of similarity between different samples. The kernel function par excellence is the *Gaussian kernel*

$$\kappa\left(x, x'\right) = \exp\left(-\gamma \left\| x - x' \right\|^2\right),$$

but recently *quantum* kernels [2] (either simulatred or quantum-computed) have been proposed which can potentially better separate the two classes.

Also, we can fine-tune the free parameters of kernel functions (s.a. γ for the Gaussian kernel) by doing *kernel-target alignment* optimization:

$$\theta^* \longrightarrow \max_{\theta} \frac{\mathbf{y}^\top \mathbf{K} \mathbf{y}}{M \|\mathbf{K}\|_F}.$$

Test case

As a prototypical substructure, we consider an open-hole composite plate (OHCP) with Hashin damage, which is subject to homogenized strain loading in the two in-plane directions and shear. The substructure is considered failed (label +1), after ultimate strength has been reached.

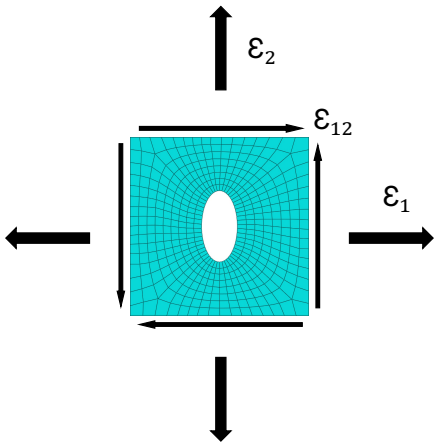

Results

Before aligning the kernel parameters, SVM with quantum kernels scores similarly to the classical RBF kernel with $\gamma = 1$. Furthermore, for low constraint penalty, quantum kernels are close to random guessing.

However, kernel-target alignment improves the mean test accuracy of all quantum kernels both for low and for high constraint strenght, suggesting learning of the OHCP ultimate strength envelope. For higher number of quantum bits (qek0608), quantum kernels show better generalization than classical RBF with optimized γ.

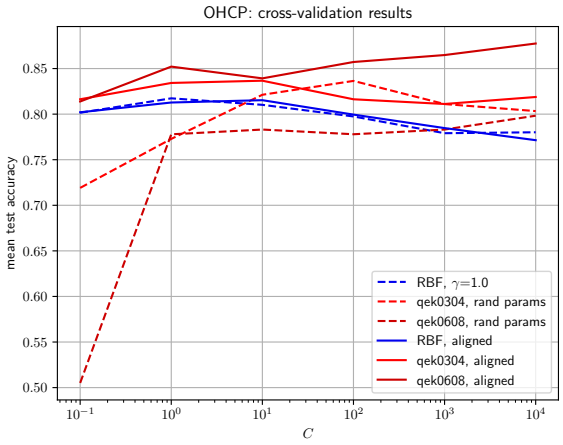

References

[1] T. Gullikers, *An Integrated Machine Learning and Finite Element Analysis Framework, applied to Composite Substructures including Damage*, 2018, MSc thesis, TU Delft, Aerospace Structures and Materials.

[2] V. Havlíček *et al.*, *Supervised Learning with Quantum-Enhanced Feature Spaces*, 2019, Nature.

Friction stir welded joints in steel maritime structures: micro-material scale characteristic fatigue properties

N.C.H. Troost[1], J.H. den Besten[1]

[1]*Delft University of Technology*

Introduction

Fatigue is a governing limit state for steel maritime structures. Conventional arc-welded joints are considered to be a limiting factor in that respect because of welding induced micro- and mesoscopic stress concentrations at material scale and macroscopic stress concentrations – hot spots – at maritime structural scale. Since the friction stir welding process does not involve material melting, the welding induced defect sensitivity significantly decreases [1]. Heating and subsequent cooling of the welded material generally results in a grain structure similar to that of the parent metal, although refined and with different material zones still present [2]. At the same time, no filler material is added, meaning hardly any weld reinforcement induced macro-structural stress concentrations are introduced (Figure 1). Accordingly, crack initiation governing parameters like steel phase and grain size at micro-scale, as well as weld surface roughness, defect size (Figure 2) and undercut suggest the material properties are in charge.

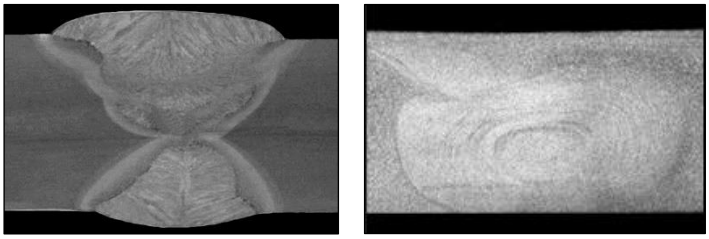

Figure 1: An arc welded butt joint (left) and a FSW butt joint (right) showing FSW joints contain significantly reduced macroscopic stress concentrations.

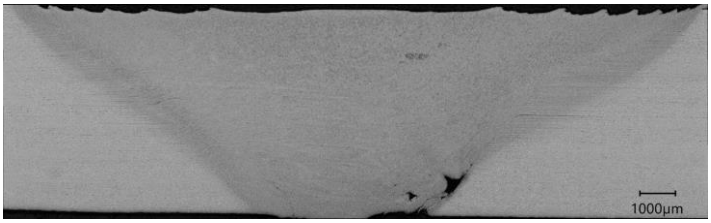

Figure 2: A friction stir welded butt joint in steel showing a tunnel defect at the lower advancing side.

Objective

To develop a friction stir welding characteristic fatigue damage criterion in the mid-cycle and high-cycle fatigue region, taking the micro- and mesocale characteristics like defect size, surface roughness and microstructural properties explicitly into account.

Experimental work

Friction stir welds made with various combinations of welding speed and tool rotation speed, the two main parameters controlling the weld properties, are subjected to cyclic loading, principally until fatigue induced failure is reached.

Figure 3: A friction stir welded specimen showing fatigue induced failure.

Preliminary conclusions

- When present, the defect size dominates the fatigue performance, reducing the fatigue strength and increasing the lifetime scatter.
- The resistance curve slope significantly increases from $m = 5$ for defect free welds to $m = 9$ for welds that contain a defect, in contradiction to the typical behaviour of growth dominated fatigue life for welded joints.
- When no defects are present, the fatigue performance is constant for a large range of welding parameters.
- Defect free welds show fatigue strength exceeding that of base material at similar slope. Fatigue strength of welds that contain defect often exceeds that of similar arc welded joints. However, the significantly larger slope of defect containing friction stir welded joints means that the fatigue performance at a small number of cycles is much worse.

References

[1] Cater, S. (2014). *Fundamentals of friction stir welding.* Cambridge: TWI Ltd.

[2] Fujii, H., Cui, L., Tsuji, N., Maeda, M., Nakata, K., & Nogi, K. (2006, August). Friction stir welding of carbon steels. *Materials Science and Engineering: A, 429*, 50–57. doi:10.1016/j.msea.2006.04.118

Design Optimization of Acoustic/Elastic Metamaterial-Based Structures for Underwater Noise Mitigation

A.C.A. Vasconcelos

Delft University of Technology

A meta-interface for underwater noise reduction during offshore monopiles installation

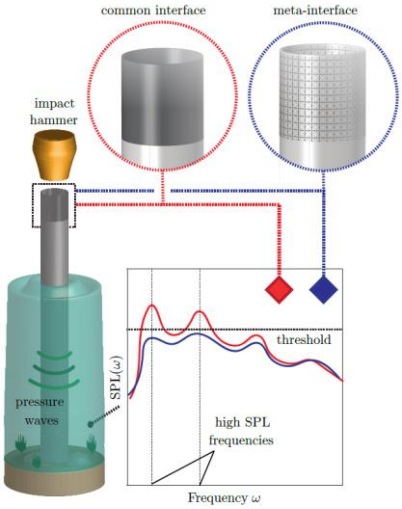

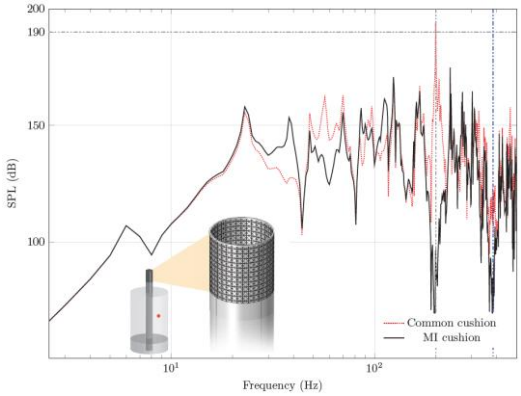

How to increase bandwidth of noise attenuation and improve mechanical performance?

Dynamic Effective Properties

Effective Mass Density

Mechanical Performance

Equivalent Static Analysis

Multi-Objective Optimization via Genetic Algorithms

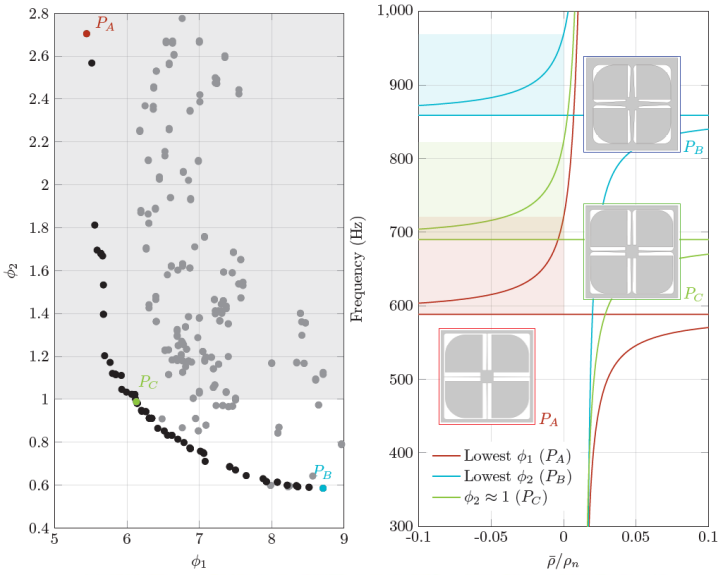

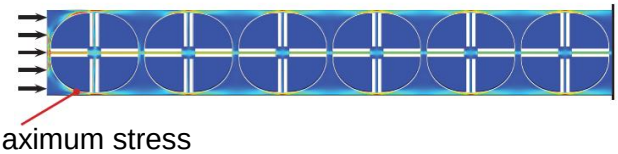

Maximum stress

First experimental study: noise reduction functionality

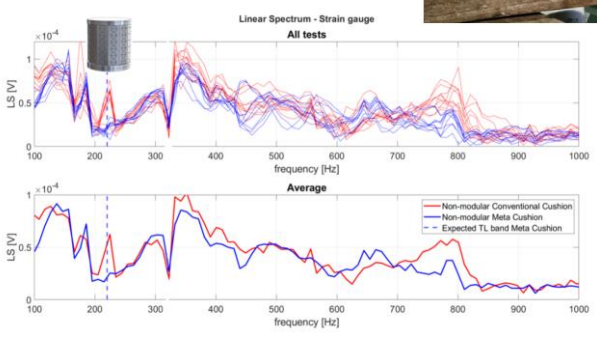

Conclusions and next steps

- Meta-cushion efficiency improved by multi-objective optimization
- Design of a new meta-cushion and experimental study in a lab-scale setup
- Pile driveability analysis: feasibility of meta-cushion in real application

TU Delft

PhD progress

1 | 2 | 3 | 4

Tension-Field Theory for General Hyperelastic Materials in Isogeometric Analysis

H.M. Verhelst[1,2], M. Möller[1], J.H. Den Besten[2]

[1] *Maritime Transport and Technology, 3mE, TU Delft*
[2] *Delft Institute of Applied Mathematics, EEMCS, TU Delft*

Introduction

Wrinkling of thin membranes is omnipresent in the world around us. Wrinkles occur in our skin or in our cloths, and are relevant in various engineering disciplines, e.g. for the design of **airbags**, **parachutes** or **offshore solar platforms**. When modelling wrinkling patterns **explicitly** with **shell elements**, mesh-sizes hence computational costs increase with decreasing wave lengths. A remedy for this problem is to use **membrane elements** with **implicit wrinkling models**, modelling the **influence of wrinkling** on the **global structural response**. This poster highlights a **tension field theory**-based wrinkling model for **hyperelastic membranes**.

Methodology

The presented wrinkling model is based on a modification of the stress and material tensors, $\mathbf{S}$ and $\mathbb{C}$ based on the **tension field** ϕ, defined through **principal stresses** $S_1^p \leq S_2^p$ and **principal strains** $E_1^p \leq E_2^p$:

$$\phi = \begin{cases} \text{Taut} & S_1^p > 0 \\ \text{Slack} & E_2^p \leq 0 \\ \text{Wrinkled} & \text{else} \end{cases} \implies (\mathbf{S}, \mathbb{C}) = \begin{cases} (\mathbf{S}, \mathbb{C}) & \text{Taut} \\ (\mathbf{0}, 0) & \text{Slack} \\ (\mathbf{S}', \mathbb{C}') & \text{Wrinkled} \end{cases}$$

The modified stress and strain tensors $\mathbf{S}'$ and $\mathbb{C}'$ are derived from the assumption that the deformation gradient contains a contribution orthogonal to the wrinkling direction [2, 3, 4]

$$\mathbf{F}' = (\mathbf{I} + \boldsymbol{w} \otimes \boldsymbol{w}) \cdot \mathbf{F} \implies \mathbf{E}' = \mathbf{E} + \frac{1}{2} b(b+2) \hat{\boldsymbol{w}} \otimes \hat{\boldsymbol{w}} = \mathbf{E} + \mathbf{E}_W \quad (1)$$

with $b > 0$ a measure for *wrinkliness* and $\hat{\boldsymbol{w}} = \boldsymbol{w} \cdot \mathbf{F}$ the unit-vector orthogonal to the wrinkles. Assuming a **uniaxial tension state** [1], $\mathbf{S}' \cdot \boldsymbol{w} = 0$, the vector $\boldsymbol{w}$ can be computed. Here, the modified stress tensor becomes

$$\mathbf{S}' = S(\mathbf{E}') \approx \mathbf{S}(\mathbf{E}) + \mathbb{C}(\mathbf{E}) : \mathbf{E}_W, \quad (2)$$

and the modified material tensor $\mathbb{C}'$ is obtained via

$$\delta \mathbf{S}'(\mathbf{E}) = \frac{\mathrm{d}\mathbf{S}'}{\mathrm{d}\mathbf{E}} : \delta \mathbf{E} = \mathbb{C}' : \delta \mathbf{E}. \quad (3)$$

From these derivations, it follows that $\mathbb{C}'$ depends on $\frac{\partial \mathbb{C}}{\partial \mathbf{E}}$. This **sixth-order tensor** only appears for hyperelastic materials, and is zero in the linear elastic case [3]. The derivative $\frac{\partial \mathbb{C}}{\partial \mathbf{E}}$ is obtained **analytically** for the **statically condensated incompressible** material models, and **numerically** for the **statically condensated compressible** material models. Moreover, it should be noted that **the variation of ϕ is not taken into account in the definition of $\mathbb{C}$**.

Results

The model is verified with a number of benchmark problems. Here, the combined stretch and twist of a hyperelastic cylinder is presented, see fig. 1. The cylinder is modelled using **isogeometric hyperelastic Kirchhoff-Love shell** elements for comparison, and with the novel **isogeometric hyperelastic membrane wrinkling element**.

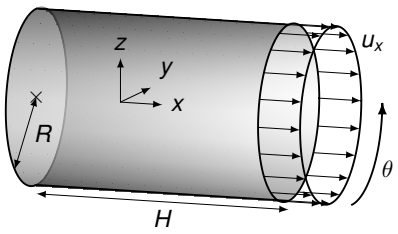

Geometry		
R	250	[mm]
L	1.0	[m]
t	0.05	[mm]
Material	*Incompressible Neo-Hookean*	
E	1.0	[GPa]
ν	0.5	[−]
Boundary Conditions		
θ	$\pi/2$	[rad]
u_x	1.0	[m]

Figure 1: Problem setup

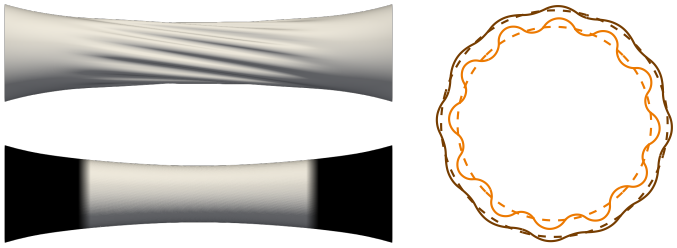

Figure 2: Shell result (left, top), membrane result with taut and wrinkled regions in black and white, resp. (left, bottom), contour lines of the deformation for the shell model (solid) and the membrane model (dashed) at the middle and 75% of the length (right).

The results in fig. 2 show that the membrane model approximates the mid-plane of the solution obtained by the shell model. This is in line with the assumptions of the original model developed by [1].

Conclusions & Future Work

This poster presents a modification scheme for membrane elements using tension field theory. The original theory developed by [1] and implemented by [2, 3, 4] is extended for hyperelastic materials. This extension yields the derivative of the material tensor $\mathbb{C}$ with respect to the strain tensor $\mathbf{E}$, which is zero in the original model. In future work, a **fully variational model using a level-set model or comparable** will be used to define $\mathbb{C}'$.

Paper & Code availability

The paper related to this poster is available on arXiv () and the code of this project is open-source and will be published in the Geometry + Simulation modules (G+Smo).

References

[1] Roddeman (1987), *J. Appl. Mech.*
[2] Lu et al. (2001), *Int. J. Numer. Methods Eng.*
[3] Nakashino & Natori (2005), *AIAA Journal*
[4] Nakashino et al. (2020), *Comput. & Struct.*

Geometry+Simulation Modules
https://github.com/gismo
Licensed under the MPL 2.0

OptimiseD matrix and fIbre treatmeNt for recycling composites

F. F. Visser[1,2], M. van Drongelen[1], V. Marinosci[2] and L. E. Govaert[1,3]
[1]Production technology, University of Twente
[2]Thermoplastic composites research center
[3]Processing and Performance, Eindhoven University of Technology

Use of composite materials has increased, leading to an increase of the amount of material in circulation. However, reuse has been complicated due to costs and uncertainty about performance. Consequently, waste is accumulating, for example on a municipal landfill in Casper Wyoming (Bloomberg 2020).

RECYCLE ROUTE & OBJECTIVE

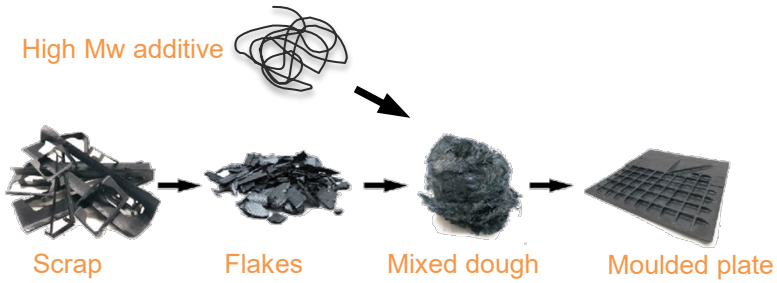

Shredded scrap is mixed with a high molecular weight polymer, which is subsequently compression moulded. Studying the effect of molecular weight on the mechanical properties of composite materials.

MATERIALS & METHOD

Injection moulded bars in ISO 527-1A specification were kindly provided by Sabic. Three different grades were produced in polypropylene with 30w% short glass fibers. The reference PP G3230A at 45 MFI, a low flow grade at 5.7 MFI and a high flow grade at 110 MFI. Tests were performed in a Zwick Z05 Retroline with a 10KN loadcell. DSC test were performed on a TA DSC 250 with a sample mass of 6-6.5 mg. Melting enthalpy is measured form the first heating at 10 °C/min

RESULTS

		MFI	Mw [Kg/mol]	Xc [%]
Low flow	○	5.7	320	47
PP G3230A	○	45	185	50
High flow	○	110	120	55

Current results in the short-term time domain show an increase in strength for the high flow grade. At elevated temperatures, these results converge in the domain where only one failure mechanism is present. This difference stems from the difference in crystallinity.

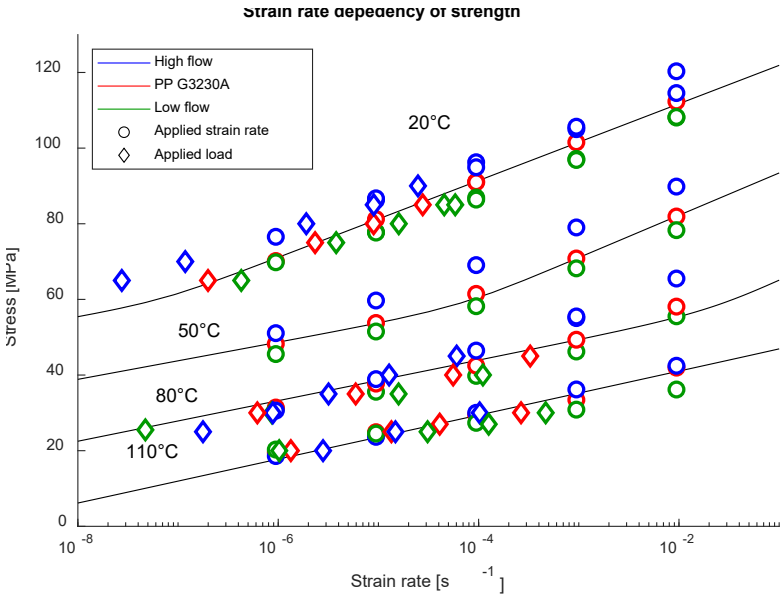

OUTLOOK

Further investigation will be focused on fatigue testing to elucidate the effect of molecular weight on crack growth resistance, where crystallinity is expected to contribute less to the strength.

Nest investigation steps include:

- Fatigue testing on injection moulded bars
- Mixing trials with scrap material

TPRC

DPI Shaping polymer innovation

PhD progress

1	2	3	4

UNIVERSITY OF TWENTE.

Fluid-conveying pipes in the floating frame of reference formulation

Karlijn van Voorthuizen, M.I. Abdul Rasheed , J.P. Schilder, B. Rosić

Chair of Applied Mechanics & Data Analysis, University of Twente

Objective

Computationally efficient modelling of flexible multibody systems through the floating frame of reference formulation.

+

Modelling of the effect of fluid flowing through flexible tubes.

⇨

Computationally efficient modelling of dynamic systems including fluid-conveying pipes.

[1]

Approach

The pipe acts as control volume within which the material points of the fluid undergo axial movement.

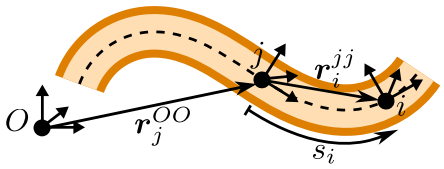

Position: $\boldsymbol{r}_i^{OO} = \boldsymbol{r}_j^{OO} + \boldsymbol{R}_j^O \boldsymbol{r}_i^{jj}$

Derivative with respect to time:

- Pipe: $\frac{d\boldsymbol{r}_i^{OO}}{dt} = \frac{\partial \boldsymbol{r}_i^{OO}}{\partial t}$
- Fluid: $\frac{d\boldsymbol{r}_i^{OO}}{dt} = \frac{\partial \boldsymbol{r}_i^{OO}}{\partial t} + \frac{\partial \boldsymbol{r}_i^{OO}}{\partial s}\frac{\partial s}{\partial t}$

Derivation of the equations of motion by:

- derivation of the kinematics and
- the principle of virtual work.

Discretization by:

- shape functions $\boldsymbol{N}(\boldsymbol{x})$ and
- reduction by a basis $\boldsymbol{\Psi}$ yields:

$$[\hat{\boldsymbol{R}}_j^O]\left(\boldsymbol{\Phi}^T\boldsymbol{M}_p\boldsymbol{\Phi}[\hat{\boldsymbol{R}}_O^j]\ddot{\boldsymbol{q}} + \boldsymbol{\Phi}_0^T\boldsymbol{M}_f\boldsymbol{\Phi}_{M_f}\begin{bmatrix}[\hat{\boldsymbol{R}}_O^j] & 0\\ 0 & 1\end{bmatrix}\begin{bmatrix}\ddot{\boldsymbol{q}}\\ \ddot{s}\end{bmatrix}\right)$$
$$+ [\hat{\boldsymbol{R}}_j^O]\left(\boldsymbol{\Phi}^T\boldsymbol{D}_p\boldsymbol{\Phi}_{\mathrm{D_p}}[\hat{\boldsymbol{R}}_O^j]\dot{\boldsymbol{q}} + \boldsymbol{\Phi}_0^T\boldsymbol{M}_f\boldsymbol{\Phi}_{D_f}\begin{bmatrix}[\hat{\boldsymbol{R}}_O^j] & 0\\ 0 & 1\end{bmatrix}\begin{bmatrix}\dot{\boldsymbol{q}}\\ \dot{s}\end{bmatrix}\right) + \boldsymbol{\Phi}^T\boldsymbol{K}_p\boldsymbol{\Phi}\boldsymbol{q} = \boldsymbol{Q}^O$$

which can be implemented when combined with algebraic kinematic constraints $C(\boldsymbol{q}) = \boldsymbol{0}$.

Assumptions:

- Incompressible fluid: $\frac{\partial s}{\partial t}$ and $\frac{\partial^2 s}{\partial t^2}$ do not depend on s.
- Fully developed turbulent flow.

O - Origin
j - Floating frame
i - Material point
$[\cdot]_m^{kl}$ - Vector from l to m expressed in k
$\boldsymbol{q}$ - Vector of generalized coordinates
s - Position along the centreline
$\boldsymbol{R}_l^k$ - Rotation matrix from k to l
$\boldsymbol{M}_k$ - Mass matrix
$\boldsymbol{D}_k$ - Quadratic velocity matrix
$\boldsymbol{K}_k$ - Stiffness matrix
$\boldsymbol{Q}^O$ - Vector of forces
$\boldsymbol{\Phi}_k$ - A matrix consisting of rigid body modes, $\boldsymbol{\Psi}$, nodal displacements and velocities and flow speed.

Validation

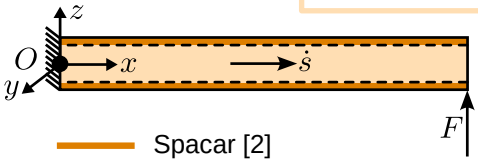

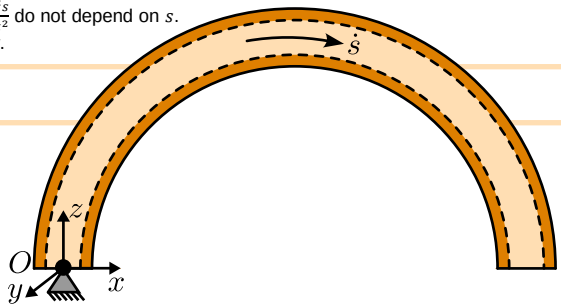

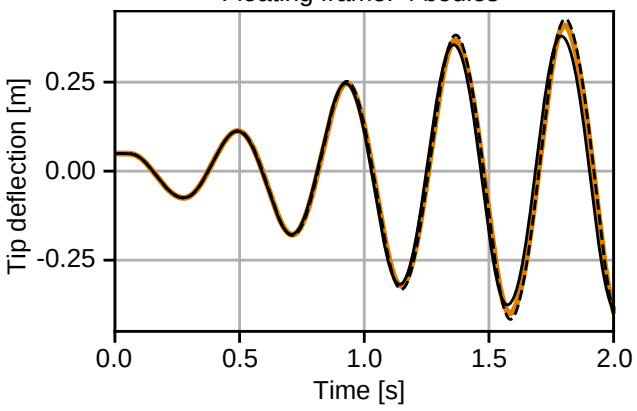

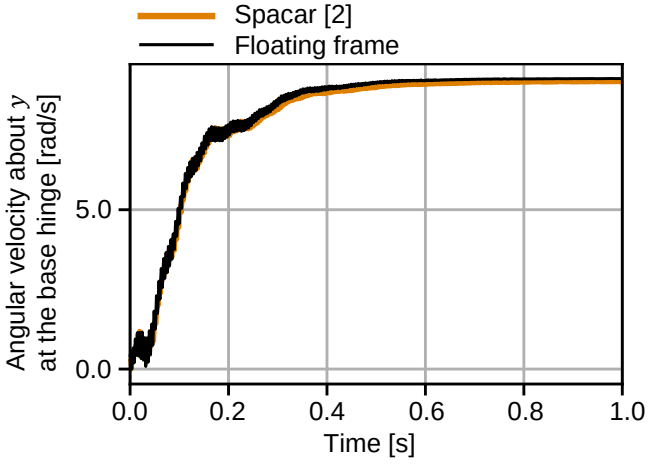

The results of the implementation of the fluid-conveying pipes within the floating frame of reference formulation closely resemble the results obtained using Spacar [2].

Contact information

k.l.vanvoorthuizen@utwente.nl
www.linkedin.com/in/karlijn-van-voorthuizen

References

[1] https://worldarchitecture.org/architecture-news/epghg/a-high-res-explanation-into-3d-printing-concrete.html
[2] J. P. Meijaard, "Fluid-conveying flexible pipes modeled by large-deflection finite elements in multibody systems," Journal of Computational and Nonlinear Dynamics, vol. 9, pp. 1555–1415, 2014.

UNIVERSITY OF TWENTE.

PhD progress

1	2	3	4

An isogeometric analysis framework for ventricular cardiac mechanics

R. Willems[1], C.V. Verhoosel[1], O. van der Sluis[1,2]

[1]Eindhoven University of Technology

[2]Philips Innovation and Strategy

Patient-specific cardiac analysis

Computer simulations provide information that can be used by clinicians to support decision-making regarding the treatment of **cardiac diseases.** Advanced discretization techniques might improve to overall efficiency and robustness of these models, which is desired for clinical integration. The **isogeometric analysis** (IGA) [1] is considered due to the curved biomedical application(s) involving sparse geometric data.

Research steps

IGA framework cardiac mechanics [2]:

1) B-spline **surface fitting algorithm** for sparse 3D data.
2) IGA-based cardiac mechanics model.
3) Model verification with established FEA solvers.
4) Reduced order model.

References

[1] Hughes, T. J. R. et al. (2005). Isogeometric analysis: CAD, finite elements, NURBS, exact geometry and mesh refinement, CMAME.

[2] Willems, R. et al. (2023). An isogeometric analysis framework for ventricular cardiac mechanics, CM.

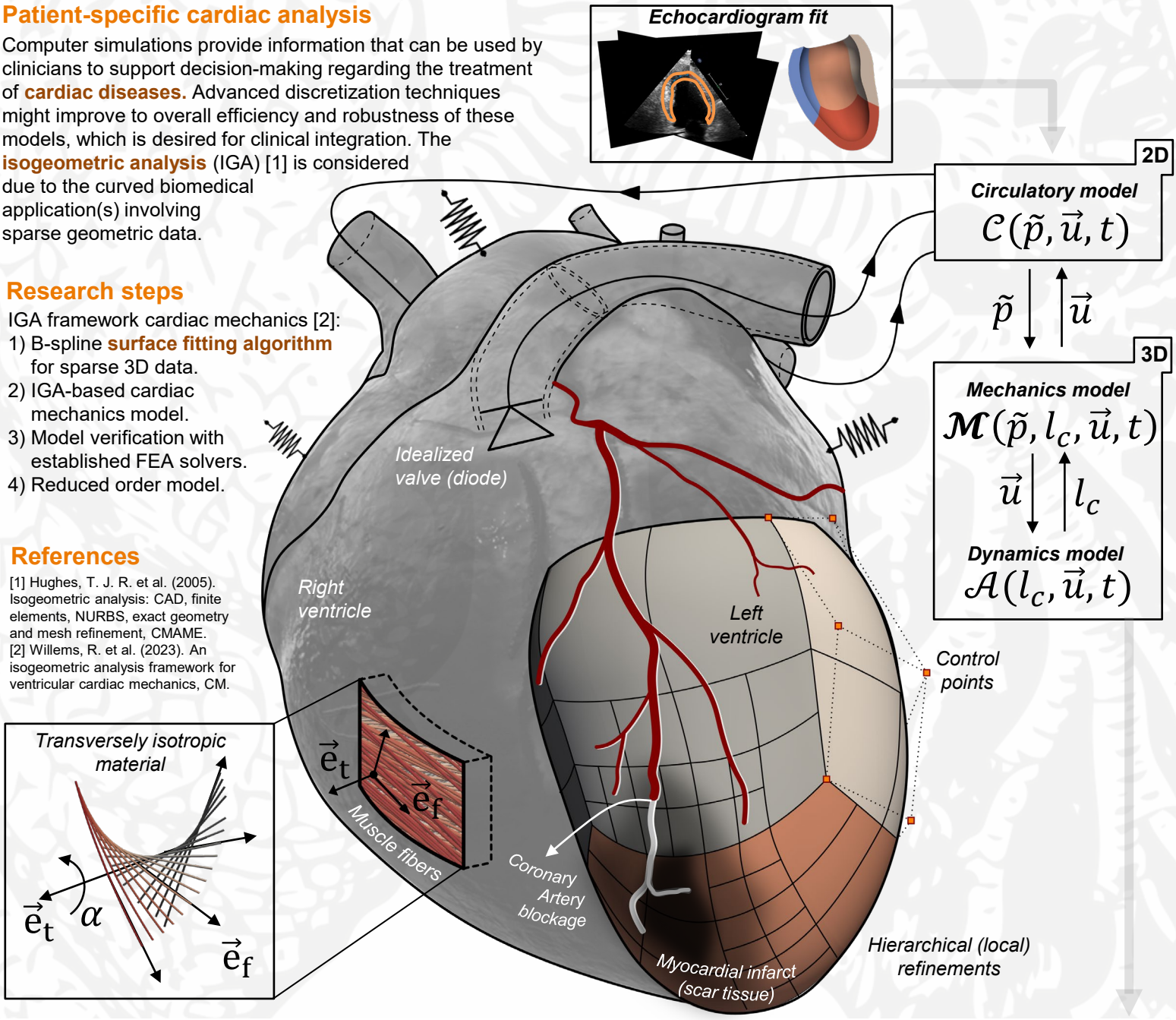

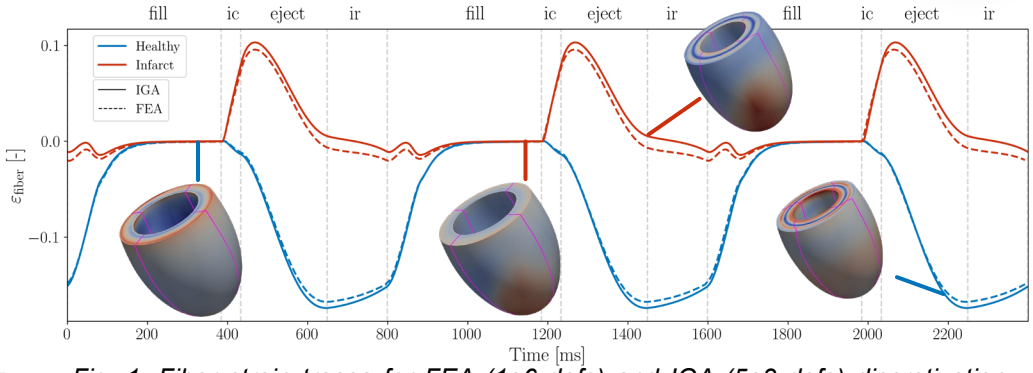

Fig. 1: Fiber strain traces for FEA (1e6 dofs) and IGA (5e3 dofs) discretization comparing both healthy and diseased tissue response.

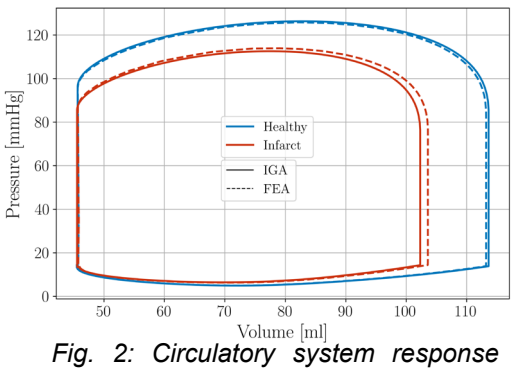

Fig. 2: Circulatory system response between cavity pressure and volume

Relating strain hardening, ductility and impact energy to ductile fracture toughness for steels

W.J. Wong, C.L. Walters

Department of Maritime and Transport Technology

Delft University of Technology

Introduction

Strain hardening and ductility in terms of the yield-to-tensile strength ratio σ_y/σ_u and the fracture elongation A respectively are often used in design as part of a substitute upper-shelf toughness criterion [1]. However, the relationship between strain hardening, ductility and fracture toughness is still not well understood [1], while the existing substitute criterion presents a restriction on the use of high-strength steels [2], which inherently have less strain hardening reserve. Strain hardening and ductility are usually assessed using uncracked specimens, while the fracture toughness is assessed using cracked specimens. This work attempts to correlate the two using damage mechanics. A numerical approach with experimental validation (Figs. 2 & 3) is adopted.

Method

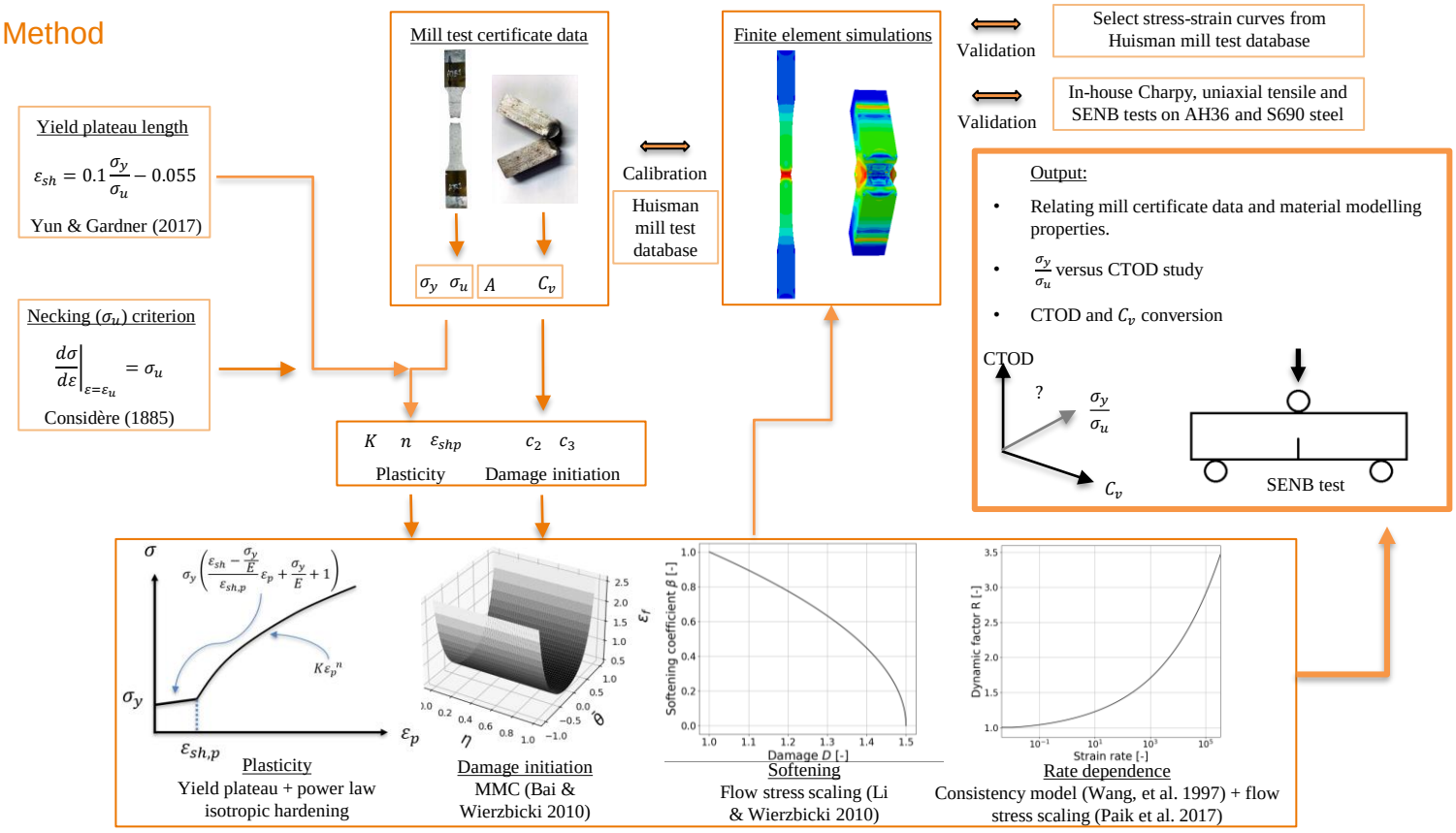

Fig. 1: Approach for relating mill test certificate data to ductile fracture toughness.

Ductile fracture FE – Consistency model for viscoplasticity with damage softening

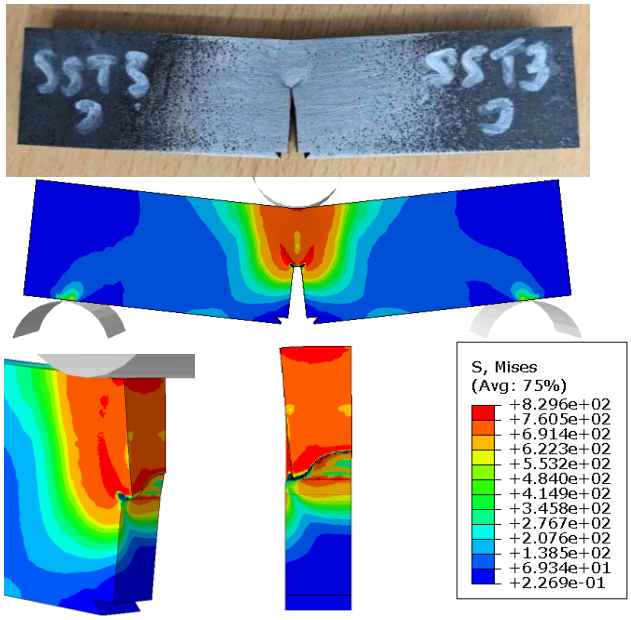

Fig. 2: Ductile fracture mechanism with shear lips in SENB test.

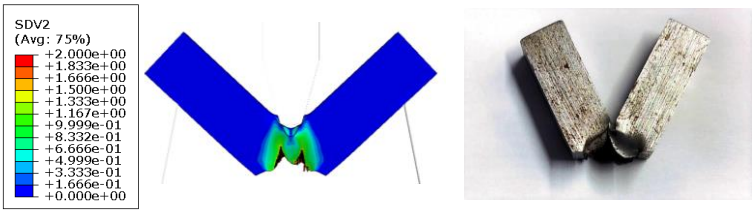

Fig. 3: Ductile fracture mechanism with shear lips in Charpy testing.

Final objectives (work in-progress):

1. Finding how strain hardening, ductility and impact energy are correlated with damage modelling parameters.

2. Improved correlations between fracture toughness $CTOD$ or J and C_v, and how this is affected by hardening in terms of σ_y/σ_u.

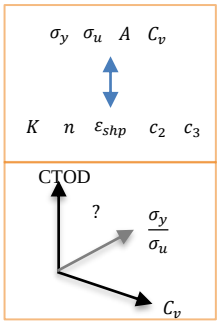

References

[1] Feldmann, M., et al. (2020). Draft: Background document to Eurocode 3 EN 1993 – Part 1-10: Material toughness - Approach for upper-shelf toughness requirements for the design of steel structures based on damage mechanics.

[2], W. J. and C. L. Walters (2021). In: ASME 2021 40th International Conference on Ocean, Offshore and Arctic Engineering (OMAE), June 21-30, 2021, Virtual, Online. ASME (The American Society of Mechanical Engineers).

Part of this work has been presented at the International Conference of Fracture in June 2023 at Atlanta, Georgia.

PhD progress

1 | 2 | 3 | 4

Simulation of PIR pyrolysis in self-supporting sandwich panels under fire

Qingfeng Xu[1], Hèrm Hofmeyer[1], Johan Maljaars[1,2], Ruud A.P. van Herpen[1,3]

[1] *Eindhoven University of Technology, Eindhoven*
[2] *TNO, Delft*
[3] *Peutz Consulting Engineers, Mook*

Introduction

A self-supporting sandwich panel façade system sees several challenging aspects for numerical simulation, related to different components on multiple scales, e.g. connections such as bolts and screws, columns, thin-walled plates, and insulation (Fig.1). Additionally, the inclusion of PIR (polyisocyanurate) insulation makes the system even more complex, as under fire its pyrolysis behaviour may affect the heat transfer analysis and the subsequent structural response. Moreover, following structural failures can significantly influence the fire's development, which must also be carefully considered. Therefore, here a methodology is introduced to enable the simulation of PIR pyrolysis within fire-structure simulations, as shown in Fig. 2.

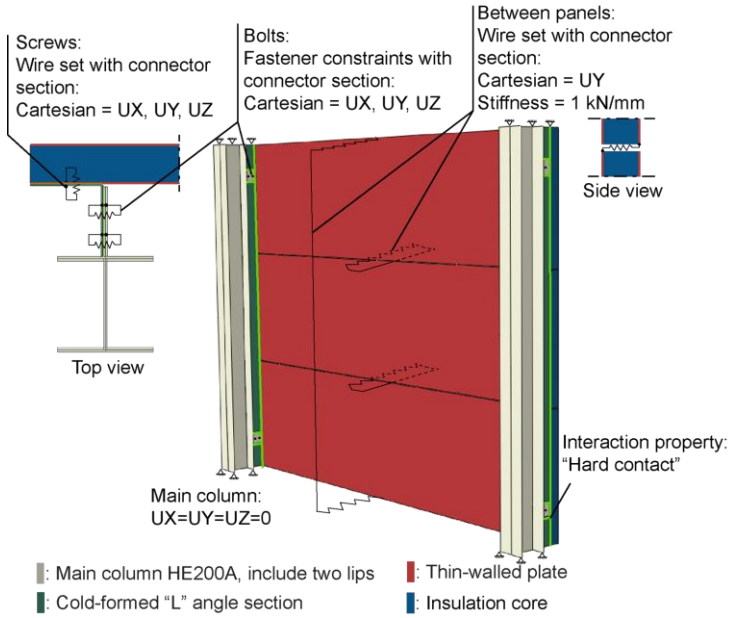

Fig.1 Modelling of a self-supported sandwich panel façade system

Methodology

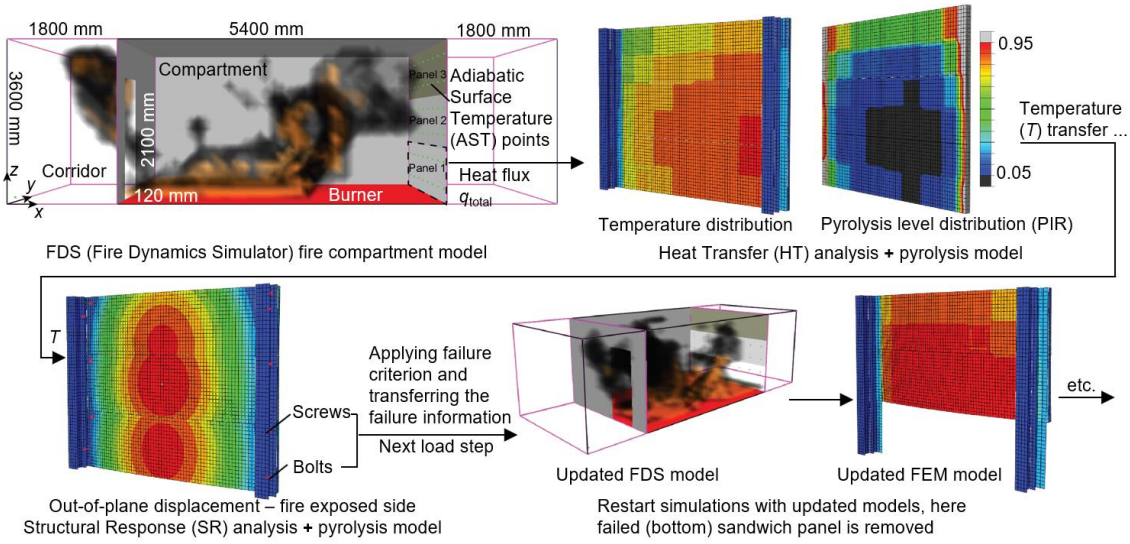

Fig.2 Methodology to enable simulation of PIR pyrolysis within fire-structure simulations

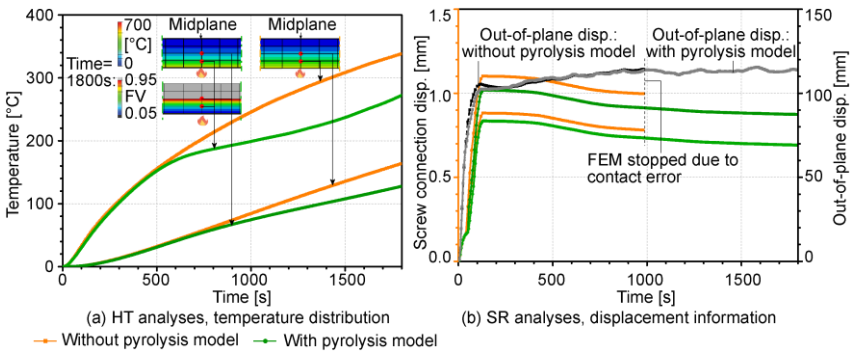

Fig.3 Results for a one-way coupled simulation, bottom sandwich panel shown

Results & Future work

The pyrolysis reaction dissipates heat, resulting in lower temperatures (Fig. 3a).

Structural responses of the sandwich panel are not significantly affected by pyrolysis, due to their direct fire exposure (Fig. 3b).

More complex thermo-chemical properties should be considered for PIR, such as expansion, viscoelasticity, and delamination.

Poisson's ratio-driven bone cell growth in meta-biomaterials

E. Yarali[1,2,*], A. A. Zadpoor[1], M. Klimopoulou[1], U. Staufer[2], K. David[3], P. E. Boukany[3], L. E. Fratila-Apachitei[1], A. Accardo[2,*], M. J. Mirzaali[1,*]

[1]Departments of Biomechanical Engineering, [2]Precision and Microsystems Engineering & [3]Chemical Engineering, Delft University of Technology (TU Delft)

Why and what?

The Poisson's ratio and elastic modulus (or stiffness) are two parameters determining the elastic behavior of biomaterials[1,2]. However, very little is known regarding the effects of Poisson's ratio on cell response in meta-biomaterials with negative Poisson's ratios (=auxeticity) as compared to those with positive values.

How?

Decoupling the **Poisson's ratio** from porosity, pore size, and stiffness via computational mechanics

Fabrication of the meta-biomaterials via **two-photon polymerization (2PP)** and their characterization

Metabolic activity and **adhesion** of preosteoblast cells (MC3T3-E1)

Differentiation of the preosteoblasts (Runx2 marker and mineralization marker, ARS)

Design of the meta-biomaterials

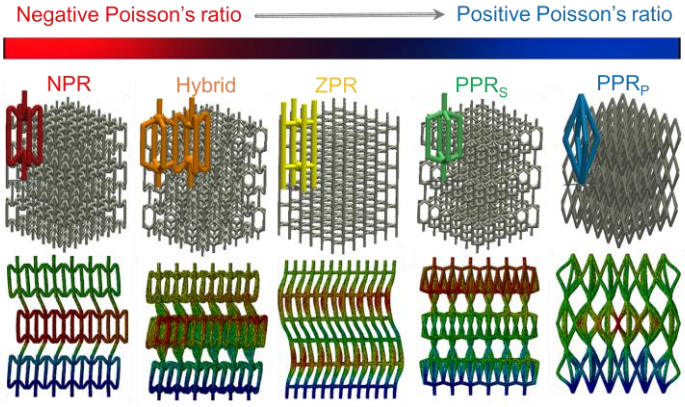

Fabrication and mechanical characterization

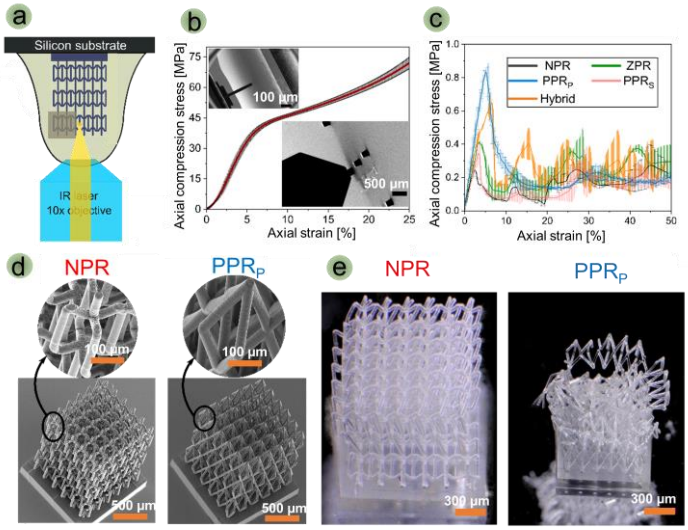

Metabolic activity and adhesion of the preosteoblasts

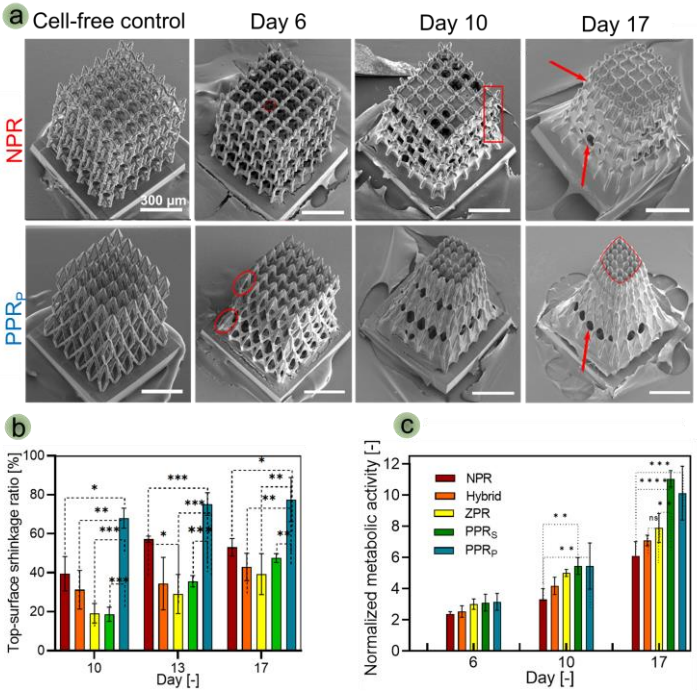

Differentiation of the preosteoblasts

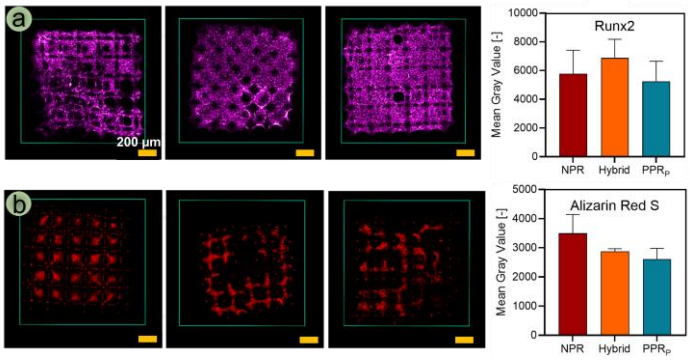

Conclusion

Meta-biomaterials with positive Poisson's ratio exhibit higher metabolic activity than those with negative values. A deformation due to cell-generated forces was observed via SEM. The osteogenic differentiation and matrix mineralization indicated the significant potential of these meta-biomaterials for 3D bone tissue models, paving the way for the development of advanced bone meta-implants.

References

[1]. E. Yarali et al., 10.1021/acsabm.3c00145
[2]. G. Flamourakis et al., 10.1002/mame.202000238

Ebrahim Yarali (e.yarali@tudelft.nl)

Efficient, Accurate, and Transferable ML Potentials: Application to Dislocation and Cracks in Iron

Lei Zhang[1], Gábor Csányi[2], Erik van der Giessen[1] and Francesco Maresca[1]

[1]University of Groningen
[2]University of Cambridge

1. *Introduction*

- **Fracture/plasticity** → Multi-scale phenomena → **atomic-scale** (Fig. 1)
- Limited **accuracy** and **transferability** of classical potentials
- Various ML-IAPs reach RMSE ~1 meV/atom at different **computational speed** [1,2]
- Fracture DFT database developed by GAP + Active learning (Fig. 2) [3,4]
- Research **goal**:
  - *Systematic training and accuracy analysis of various state-of-the-art ML-IAPs*
  - *Validating ML-IAPs by benchmarking to different physical properties*
  - *Provide a batch of ready-to-use ML-IAPs*
  - *Reveal **fracture mechanism** and **dislocation properties** of bcc iron*

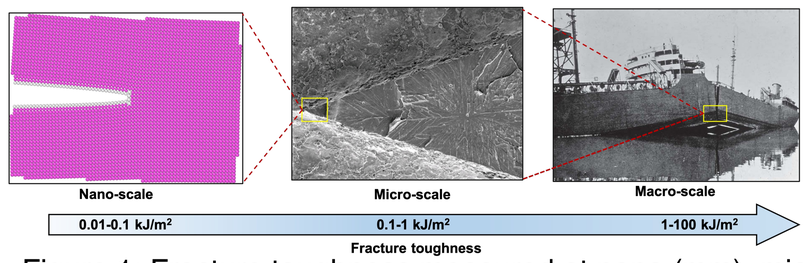

Figure 1: Fracture toughness measured at nano (mm), micro (μm) and macro (nm) scales.[3]

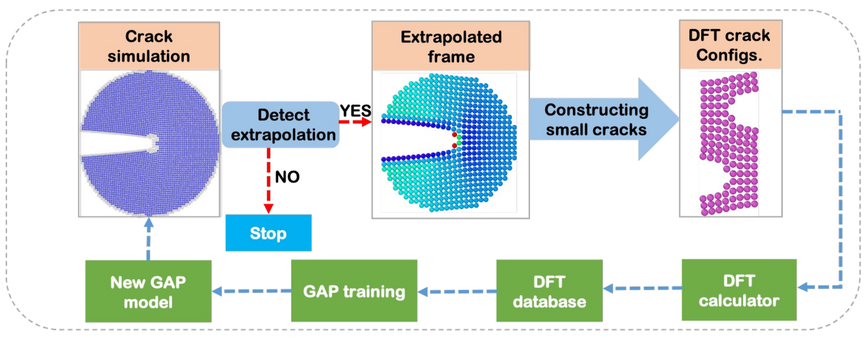

Fig. 2 Active learning workflow [4]

2. *Training of ML-IAPs*

- ML-IAPs
  - Atomic cluster expansion (*Julia* and *PACEMAKER*)
  - Gaussian approximation potential (*QUIP*)
  - Moment tensor potential (*MLIP-2*)
  - Neural network potential (*n2p2*)
- Optimization of ML-IAPs
  - Basis functions
  - Energy/Force Weights

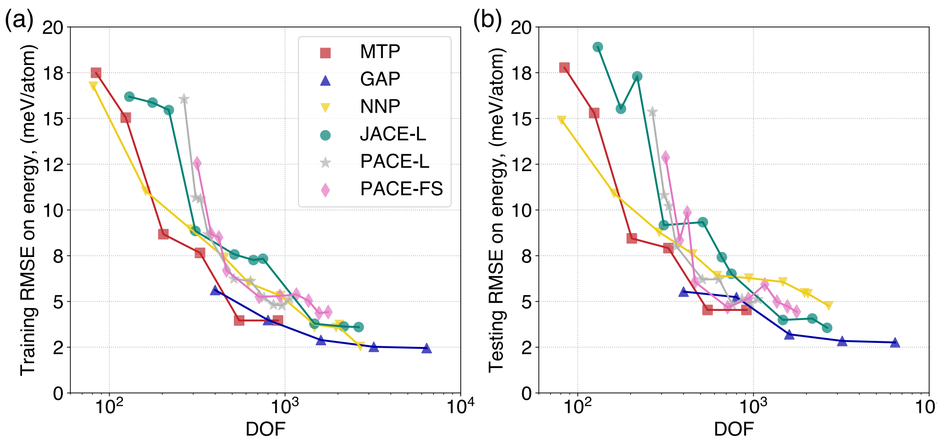

Fig. 3: (a) Training and (b) Testing energy RMSE as a function of DOF for all ML-IAPs

3. *Computational speed*

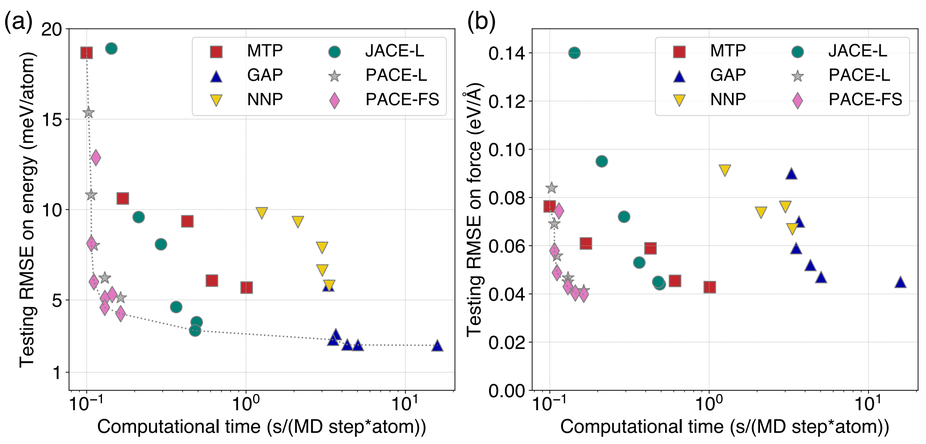

Fig. 4: (a) Energy and (b) force RMSE versus computational cost of different ML-IAPs.

- All ML-IAP can reach RMSE ~ 5 meV/atom
- RMSE can be converged by increasing DOF
- PACE-FS is the most efficient among all ML-IAPs

4. *Dislocation structure and mobility*

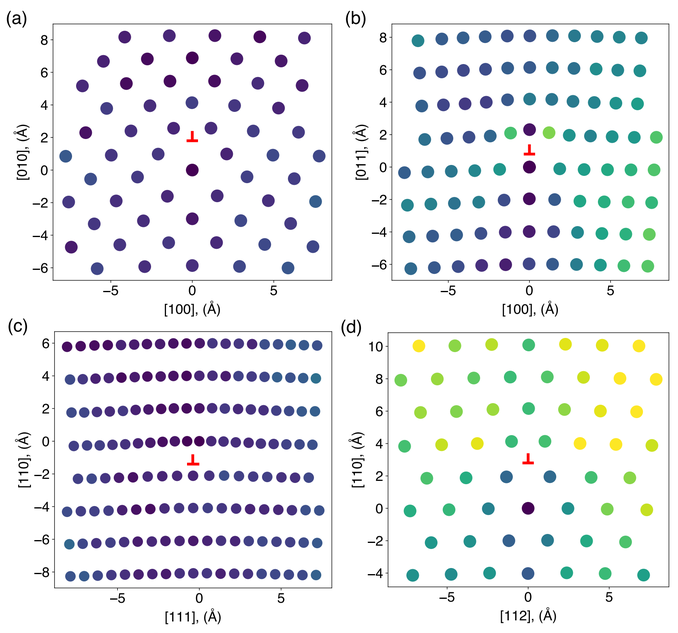

Fig. 5: (a) GAP-predicted core structures: (a) [100](010) edge, (b) [100](011) edge, (c) [111](110) edge, and (d) M111 dislocations. Atoms are coloured by the displacement difference relative to DFT predictions [5].

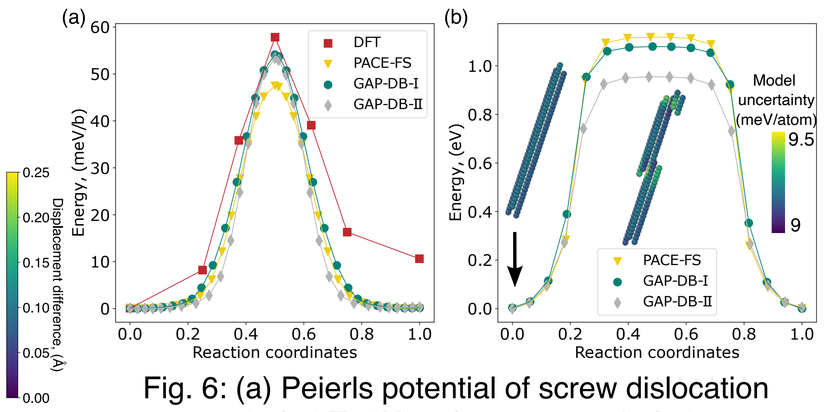

Fig. 6: (a) Peierls potential of screw dislocation computed at T=0K under zero applied stress. (b) The energy barrier for the kink-nucleation process.

- Core structures agree with **DFT**
- Converged **model uncertainty**
- Peierls barrier of screw dislocation
- Kink-pair formation/nucleation

5. *Atomistic fracture mechanism*

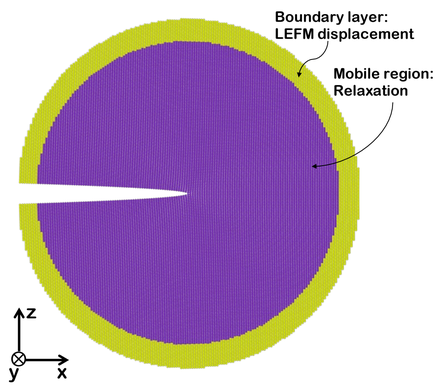

Fig. 7: K-test simulation setup

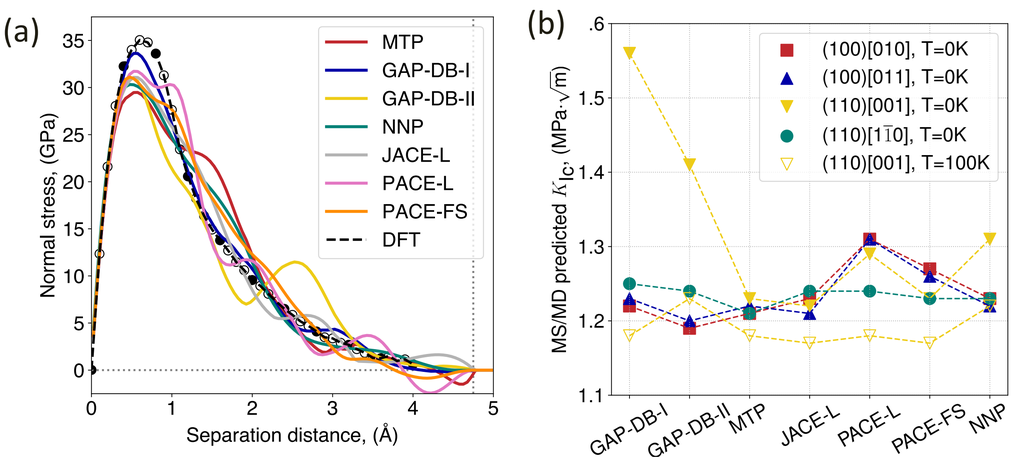

Fig. 8: (a) T-S curves of (100) plane predicted by all ML-IAPs in bcc iron. (b) Critical K_{Ic} at T=0K for four crack systems and T=100K for crack (110)[010].

- Cleavage is independent of DFT database
- Traction-separation (T-S) curves
- Convergence of critical stress intensity factor (K_{Ic})

References:

[1] Y. Zuo, et. *al*, The Journal of Physical Chemistry A, (2020), 4, 731.
[2] Y. Lysogorskiy et. *al*, npj computational materials, (2021), 7, 1.
[3] D. Dragoni et al., 2018, Physical Review Materials, (2018), 2, 013808.
[4] L. Zhang *et. al,* ARXIV.2208.05912, (2022).
[5] M. R. Fellinger, *et. al*, Physical Review Materials, (2017), 2, 113605.

university of groningen / ENTEG / CmME

PhD progress

1 | 2 | 3 | 4

Scaling Law between 3D-printed Polymer Yield Strength and Printing Parameters

X. Zhang[1], M. Lesueur[1], L.J. Sluys[1]

[1]Delft University of Technology
Faculty of Civil Engineering and Geosciences

From micro to macro

Additive manufacturing is undoubtedly a revolution in numerous disciplines. Yet fundamental aspects of mechanical properties of 3D-printed material are unclear as uncertainties exit during printing.

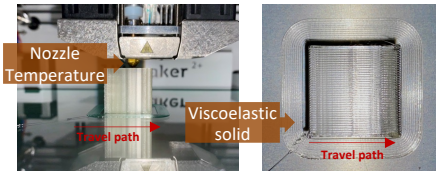

Fig.1. Printing features related to temperature and flow

- FDM parameters determine the internal structure.
- Properties of filaments are related to **printing temperature** and **material flow** (*Fig.1*) .

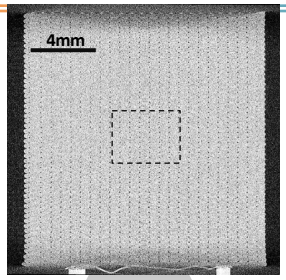

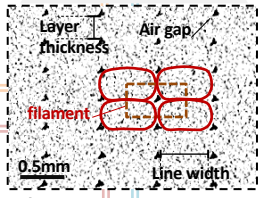

Extrusion multiplier

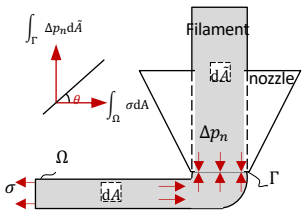

Fig.2. Pressure in nozzle

Mishra et al. (2022) [1]:

➢ Material flow is correlated to printing temperature and extrusion rate in the nozzle.

Real weight of a 3D-printed part:

$$m_{real} = \beta e^{-\alpha(T-T_0)} + m_0\phi$$

With $\alpha = 0.048\ ^\circ\mathrm{C}^{-1}$ for PLA [2] .

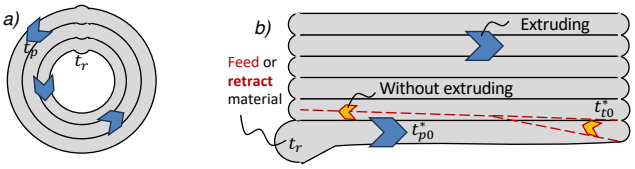

Fig.3. Travelling path for: a) cylindrical walls and b) lines infill

Printing parameters

Fig.4. Extrusion multiplier computed based on a) real weight of a part is used to computed b) the critical printing temperature

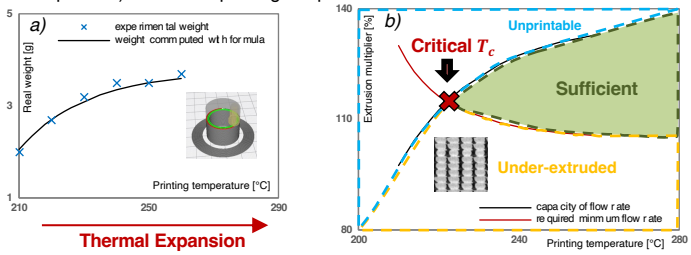

Tab.1. Overview of samples with correlated printing parameters

Cubes	TW0	M-II	M-III	L-III	S-I	M-I	M-IV
Parameters β, ϕ [-, %]	(-1.27, 80)	(-0.87, 80)	(-0.87, 80)	(-1.27, 80)	(-0.11, 80)	(-0.22, 80)	(-0.22, 80)
Thickness t [mm]	0.4	0.3	0.3	0.4	0.15	0.3	0.3
Length scale l [-]	60	60	80	80	100	50	100
Temperature T [°C]	Var	234	234	234	234	234	234
Diameter of nozzle D_n [mm]	0.8	0.8	0.8	0.8	0.4	0.4	0.4

Morphological results

Compared to the external structure, the internal structure is not visualizable. Therefore, a μ-CT scanner is used to characterize if the microstructure is formed as designed.

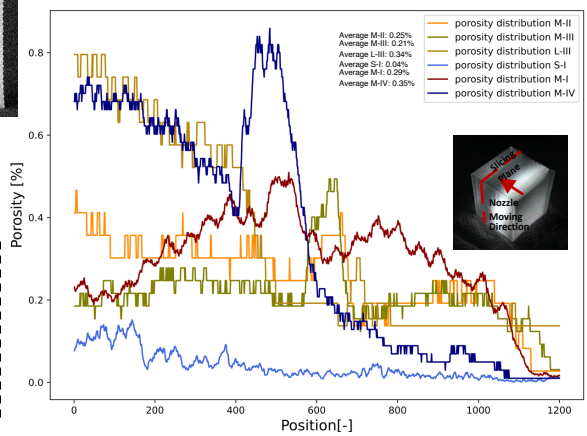

- The average porosity of 6 samples are identical (*Fig.5*):
  ➢ Geometry of air gaps inside these samples are scaled by scaling the printing parameters.
- Air gaps characterize the 3D-printed polymer as **porous material**.

Mechanical tests

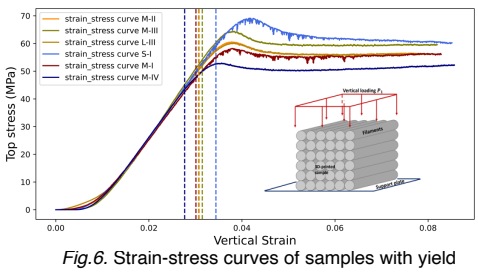

Fig.6. Strain-stress curves of samples with yield strength of each sample

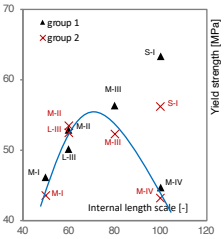

Fig.7. yield strength versus internal length scale

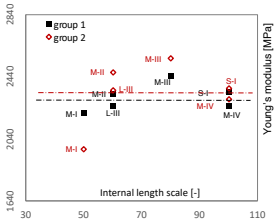

Fig.8. Young's modulus versus internal length scale

The strength of a sample increases first until a limit value then decreases with an increasing ratio between sample size and layer thickness.

➢ Bell (2018) [3] is verified.

- 3D-printed polymer behaves like a ductile material.
- Young's modulus is a constant if the porosity is fixed.
- Yield strength varies through **length scale**.

Conclusion

The yield strength of 3D-printed polymer **varies** with the **length scale** of the external and internal structure if the porosity is fixed. However, there may be a limit length scale above which the dominant imperfections of 3D-printed polymer are changed, making this law is not satisfied anymore.

Using homogenization theory, the next step will be upscaling for the strength of 3D printed materials modelled as a periodic porous unit cell (composed of filament and airgap).

➢ Combined with this work, the objective is to find more exact scaling laws considering layer-by-layer interfaces together with air gaps.

References

[1] A. A. Mishra, A. Momin, M. Strano, K. Rane, Implementation of viscosity and density models for improved numerical analysis of melt flow dynamics in the nozzle during extrusion-based additive manufacturing, Progress in Additive Manufacturing 7 (2022) 41–54.
[2] C. B. Luna, E. S. Ferreira, F. M. Sousa, E. P. Nascimento, E. M. Araújo, D. D. Souza, E. B. Bezerra, R. M. Welle, Determination of the Viscosity Temperature coefficient (β) and Pseudoplastic Index (n) of Polyacid Acid (PLA), Momento 2022 (2022) 25–38.
[3] Bell, D., & Siegmund, T. (2018). 3D-printed polymers exhibit a strength size effect. Additive Manufacturing, 21, 658-665

PhD progress: 1 | 2 | 3 | 4

Stevin Laboratory
Micro2Macro

Structural nonlinearities in marine hydroelasticity: A frequency-domain method for efficient numerical modelling

C.M. Van Zijl, A. Grammatikopoulos, J. Jovanova, C.L. Walters

Department of Maritime and Transport Technology
Delft University of Technology

Coupled interactions between large, flexible marine structures and ocean waves result in **hydroelastic** responses. This research investigates **two** methods to reduce the computational cost of models of offshore structures, including structural nonlinearities.

1

Typically, the finite element (FE) method is used to model the structure. An undesirable tradeoff often emerges in the selection of efficient beam versus more accurate shell elements. **Can this tradeoff be circumvented by using a different type of element?**

The Finite Strip Method

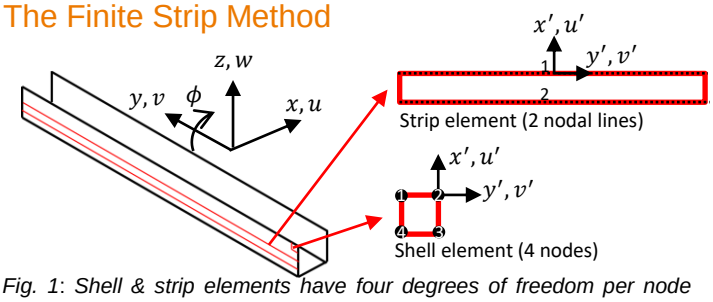

Fig. 1: Shell & strip elements have four degrees of freedom per node corresponding to membrane (u & v) and bending deformations (w & ϕ).

The finite strip method [1] uses the same interpolation functions as a shell elements in FEA for the $x-$ & $z-$ directions (Fig. 2).

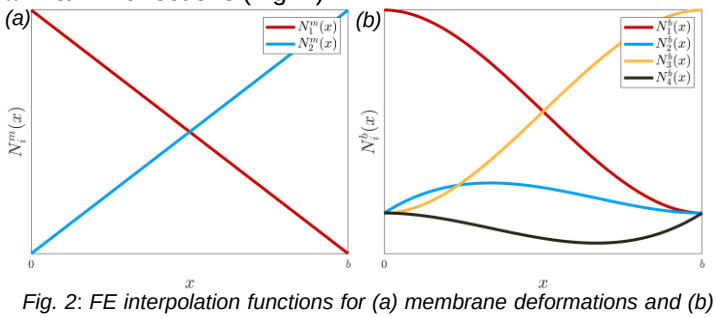

Fig. 2: FE interpolation functions for (a) membrane deformations and (b) bending deformations.

Analytical beam equations are used to describe deformation in the longitudinal $y-$ direction in the semi-analytical finite strip (SAFS) method, while spline functions are used in spline finite strip (SFS) method.

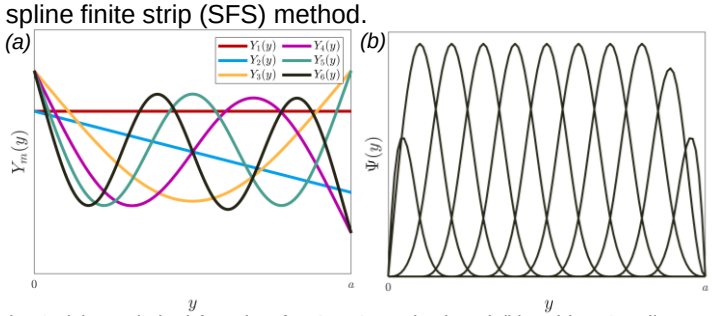

Fig. 3: (a) Analytical function for SFAS method and (b) cubic B3 spline interpolation functions for SFS method.

FEA versus SAFS

In order to compare SFAS against the FE method, a single strip element was modelled using both methods. A FE shell model was developed in ANSYS. The natural frequencies and mode shapes of the two-node vertical bending (2nVB), three-node vertical bending (3nVB) and four-node vertical bending (4nVB) modes were compared. Small differences were observed in both natural frequencies and mode shapes.

Tab. 1: Comparison of natural frequencies

	FE	SFAS	% error
2n	1.3	1.3	0.087
3n	3.6	3.7	1.7
4n	7.1	7.0	0.72

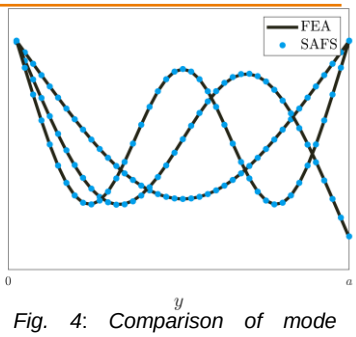

Fig. 4: Comparison of mode shapes

2

Studies on nonlinearities in the structure are limited to specific types of nonlinearities and relatively simple geometries. **Are there more general methods to model structural nonlinearities for structures with complex geometries?**

Alternating frequency-time (AFT) harmonic balance method (HBM)

One potential approach to predict the steady-state solution of a nonlinear dynamic system is to use the alternating frequency-time (AFT) harmonic balance method (HBM) [2], Fig. 5.

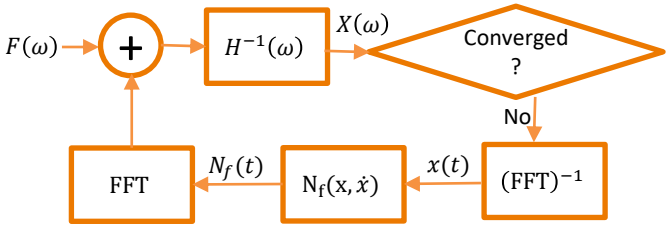

Fig. 5: AFT HBM algorithm [2]. A periodic input, $F(\omega)$ is mapped to the output, $X(\omega)$ by the frequency response function, $H(\omega)$. The nonlinear force, $N_f(t)$ is calculated in the time-domain and transformed back to the frequency-domain by FFT.

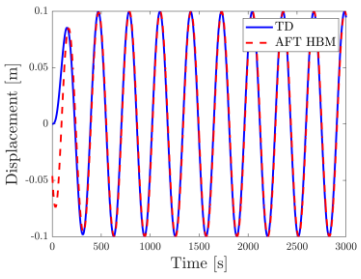

Fig. 6: TD vs AFT HBM

The response of a SDOF system with cubic stiffness was predicted using time-domain integration (TD) and the AFT HBM algorithm, Fig. 6. The AFT HBM algorithm was ≈ 3x faster and steady-state r.m.s error was ≈ 0.0042 m.

Next steps

1. Develop and validate finite strip ship model.
2. Couple the ship finite strip model with an open-source potential flow solver using the preCICE coupling library.

References

[1] Cheung, Y.K., & Tham, L.G. (1997). The Finite Strip Method (1st ed.). CRC Press. https://doi.org/10.1201/9781003068709
[2] Cameron, T.M. & J.H. Griffin. An Alternating Frequency/Time Domain Method for Calculating the Steady-State Response of Nonlinear Dynamic Systems. Journal of Applied Mechanics, 1989, 56 (1), pp.149-154. 10.1115/1.3176036. hal-01333697

PhD progress

1 | 2 | 3 | 4

Finding the Evolution law of Representative Elementary Volume Convergence

S. Zwarts[1], M. Lesueur[1]

[1]Delft University of Technology, department of 3MD

Introduction

- The Representative Elementary Volume (REV) is the smallest volume that accurately describes the mean constitutive response for larger scales.
- Determining the REV is a fundamental exercise in Digital Rock Physics.
- Yet, remains a challenging task, due to many and large simulations which are computational expensive.

➢ Determining the evolution law will simplify exercise.

Generic evolution law of convergence

By tracing the convergence of permeability in idealized rock microstructures, specifically random packings, the characteristics of the REV convergence are analysed to determine the generic evolution law.

Characteristics of the convergence:

- The evolution REV convergence is in the shape of an asymmetric cone.
- The cone is statistically described with a log-normal distribution, composed of a variance (σ) and mean (μ)
- Samples can be split into subsamples, which correlates the different distributions, depending on the volume (V).

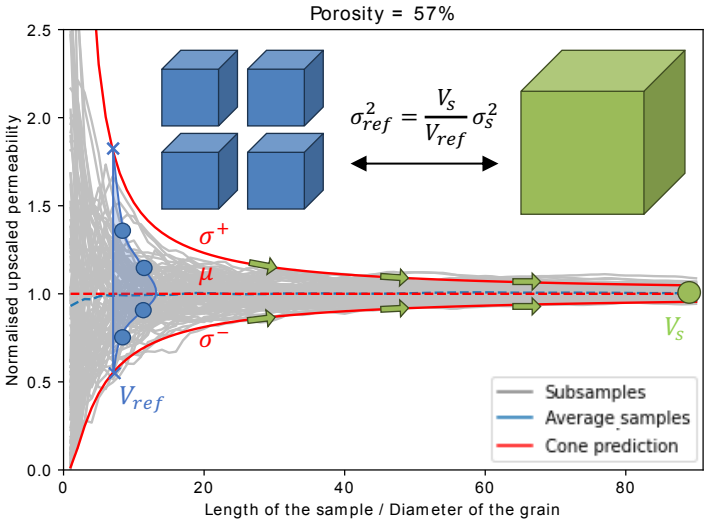

Therefore, the evolution law is described as follows:

$$y = \mu \cdot \exp\left(\pm 2 \frac{\sqrt{V_{ref}}}{\sqrt{V_s}} \sigma_{ref}\right)$$

References

[1] S. Zwarts and M. Lesueur, Homogenisation Method Based on Energy Conservation and Independent of Boundary Conditions, 2023, Advances in Water Science

Application on real samples

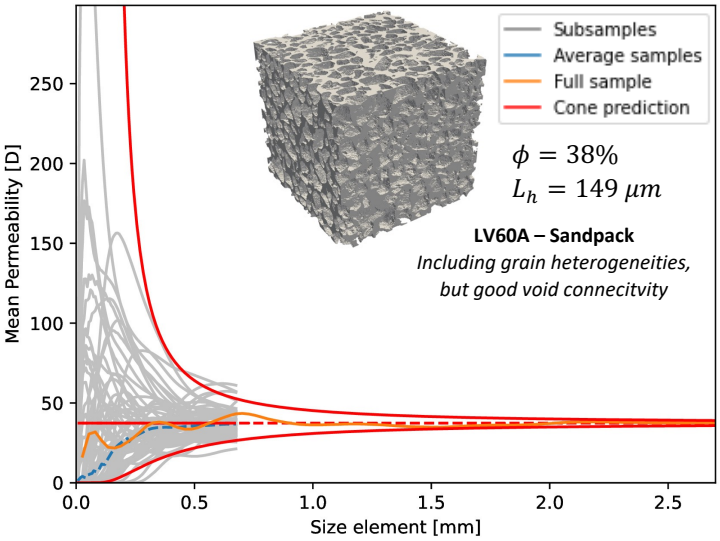

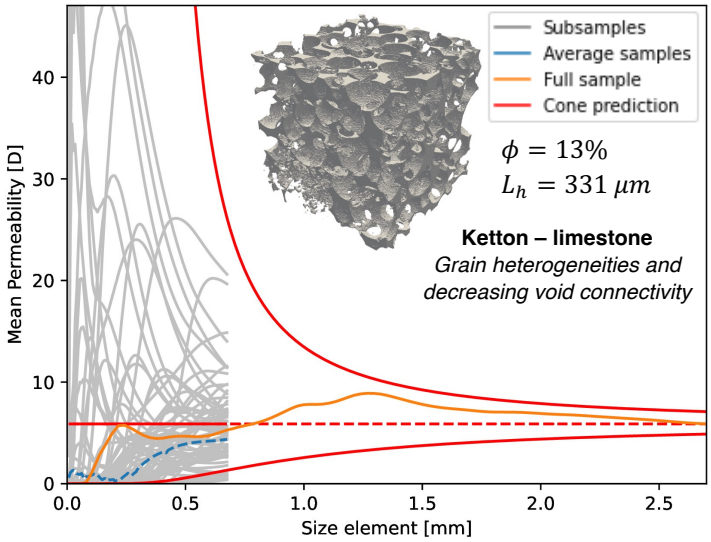

Findings

- The determined evolution law is applicable for different types of microstructures.
- Splitting into subsamples unlocks working with high resolution samples.
- The evolution law provides information about error within the homogenized parameter and REV size.

Recommendations

- Identify the required characteristics for the subsamples, such as the percolation threshold.
- Run the simulations in parallel to save computational resources.

➢ For example, utilizing the law on the sandpack reduced the simulation time with a factor of 231.

Prevention of enclosed voids in topology optimization

J.M. van der Zwet[1], A. Delissen[1], C. Ayas[1], M. Langelaar[1]

[1]*Delft University of Technology*

Introduction

- Topology optimization is a computational design technique that aims to find the optimal material distribution for a given engineering problem.
- It generates complex geometries that do not necessarily conform to manufacturing restrictions.
- One such a restriction for powder-based additive manufacturing is the absence of enclosed voids.
- We present a flood fill filter that eliminates enclosed voids during the optimization.

Method

- The flood fill filter works by cumulatively summing each element encountered from the outside surfaces
- Any summed value larger than one is subsequently reduced to one using a smooth minimum projection
- This forces the optimization process to either completely fill the void, or to generate a pathway towards it.

1	1	1	1	1	1	1	1	0	0
0	0	1	1	0	0	1	1	1	0
0	0	0	0	1	1	0	0	1	1
0	0	1	1	0	0	1	1	1	0
1	1	1	1	1	1	1	1	0	0

(a) Input design

1	1	1	1	1	1	1	1	0	0
0	0	1	1	1	1	2	2	1	0
0	0	0	0	1	2	2	2	2	1
0	0	1	1	1	1	2	2	1	0
1	1	1	1	1	1	1	1	0	0

(b) Design after cumulative sum

1	1	1	1	1	1	1	1	0	0
0	0	1	1	1	1	1	1	1	0
0	0	0	0	1	1	1	1	1	1
0	0	1	1	1	1	1	1	1	0
1	1	1	1	1	1	1	1	0	0

(c) Design after smooth minimum

Figure 1: Visual representation of the two main filter steps.

2D example

We first consider a cantilever beam case in 2D where we aim to maximize stiffness.

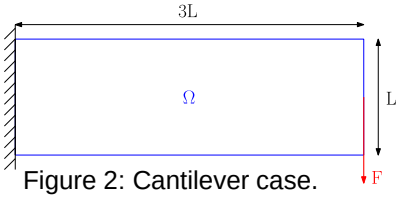

Figure 2: Cantilever case.

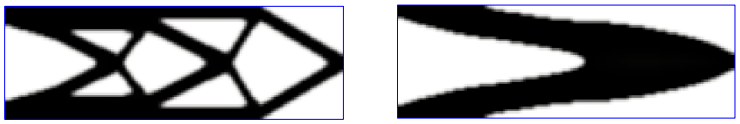

(a) Without flood fill filter. (b) With flood fill filter.

Figure 3: Resulting optimized designs for cantilever case

3D example

In 3D we consider a torsion beam case, again aiming to maximize stiffness.

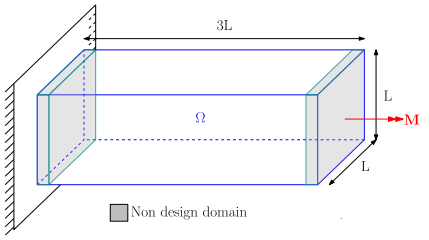

Figure 4: Torsion beam case.

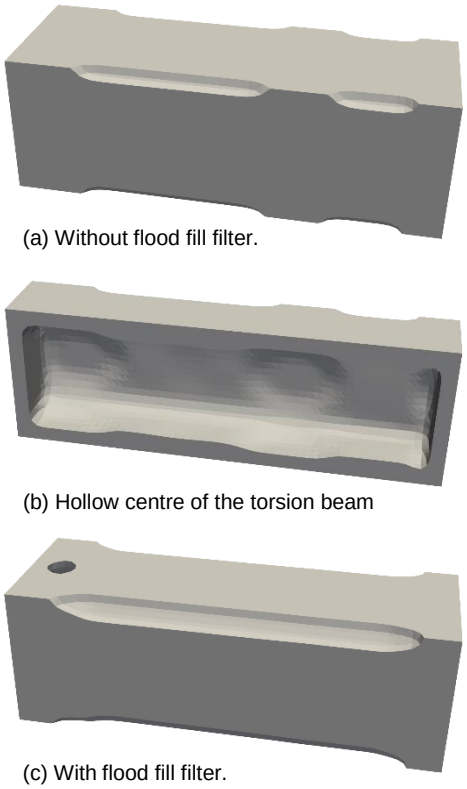

(a) Without flood fill filter.

(b) Hollow centre of the torsion beam

(c) With flood fill filter.

Figure 5: Resulting optimized designs for torsion beam case.

Conclusion

- The flood fill filter successfully prevents enclosed voids in topology optimization.
- It does so with a minimal impact on the design compared to unflooded results.